รายงานวิจัยฉบับสมบูรณ์

โครงการการออกแบบและสังเคราะห์สารเตรียมอนุพันธ์ไครัลชนิดใหม่

Design and Synthesis of New Chiral Derivatizing Agents

ผศ.ดร.เทียนทอง ทองพันชั่ง

มกราคม 2553

สัญญาเลขที่ RMU4980021

รายงานวิจัยฉบับสมบูรณ์

โครงการการออกแบบและสังเคราะห์สารเตรียมอนุพันธ์ไครัลชนิดใหม่

Design and Synthesis of New Chiral Derivatizing Agents

ผศ.ดร.เทียนทอง ทองพันชั่ง

มหาวิทยาลัยมหิดล

สนับสนุนโดยสำนักงานคณะกรรมการการอุดมศึกษา

และสำนักงานกองทุนสนับสนุนการวิจัย

บทคัดย่อ

โครงการวิจัยนี้ เป็นการออกแบบ สังเคราะห์และพัฒนาสารอนุพันธ์ไครัลชนิดใหม่ (THENA) เพื่อใช้ศึกษาคอน-ฟิกุเรชันสัมบูรณ์ของสารไครัลอัลกอฮอล์อย่างมีประสิทธิภาพและมีความถูกต้องแม่นยำในการแปลผล ซึ่งการออกแบบโครงสร้างของสารอนุพันธ์ไครัลชนิดใหม่นั้น จำลองจากการจัดตัวของเอสเทอร์ของกรดแมนเดลิก ซึ่งจัดให้ RO-C-C_a-C(O)-O-C*-H อยู่ในระนาบเดียวกันแบบ *syn*-periplanar โดยในสารอนุพันธ์ไครัลชนิดใหม่นี้ จะมีระนาบดังกล่าวเป็นส่วนหนึ่งของระบบไบไซคลิก ซึ่งจะยึดให้วงอะโรมาติกไม่สามารถหมุนได้ เมื่อประกอบกับการที่มีโปรตอนอ้างอิง (H_{ref}) ภายในโมเลกุลเพื่อช่วยในการเปรียบเทียบสเปกตรัมแล้ว การระบุค่าความต่างของ ^{1}H NMR chemical shift จะมีความแม่นยำ ทำให้การระบุค่าคอนฟิกุเรชันสัมบูรณ์มีความถูกต้องยิ่งขึ้น

สารอนุพันธ์ไครัลชนิดใหม่นี้ เมื่อนำมาทำปฏิกิริยากับสารไครัลอัลกอฮอล์ที่สนใจก็จะได้สารประกอบที่เป็นคู่อิแนนทิโอเมอร์ซึ่งจะให้สเปกตรัมของ ^{1}H NMR ที่ต่างกัน ซึ่งเมื่อนำผลต่างของค่า chemical shifts ดังกล่าวมาวิเคราะห์คู่กับแบบจำลองความสัมพันธ์ระหว่างค่าความแตกต่างของ chemical shifts กับค่าคอนฟิกุเรชันสัมบูรณ์ ก็สามารถบอกค่าคอนฟิกุเรชันสัมบูรณ์ของสารไครัลอัลกอฮอล์ชนิดทุติยภูมิได้อย่างถูกต้องและมีประสิทธิภาพ นอกจากนี้ สารอนุพันธ์ไครัลที่เตรียมขึ้นสามารถใช้ในการแยกเรโซลูชันของสารในกลุ่มไบแนพธอลได้อย่างมีประสิทธิภาพอีกด้วย

การปรับปรุงโครงสร้างของสารอนุพันธ์ไครัล (THENA) โดยการขยายวงอะโรมาติกให้ยาวขึ้นเพื่อเพิ่มผลของ anisotropic effect และการเติมหมู่อิพอกไซด์เข้าไปเพื่อลดความซับซ้อนของการอ่านสเปกตรัมของ ^{1}H NMR ทำให้การใช้สารอนุพันธ์ไครัลดังกล่าวในการระบุค่าคอนฟิกุเรชันสัมบูรณ์ทำได้สะดวกมากขึ้น

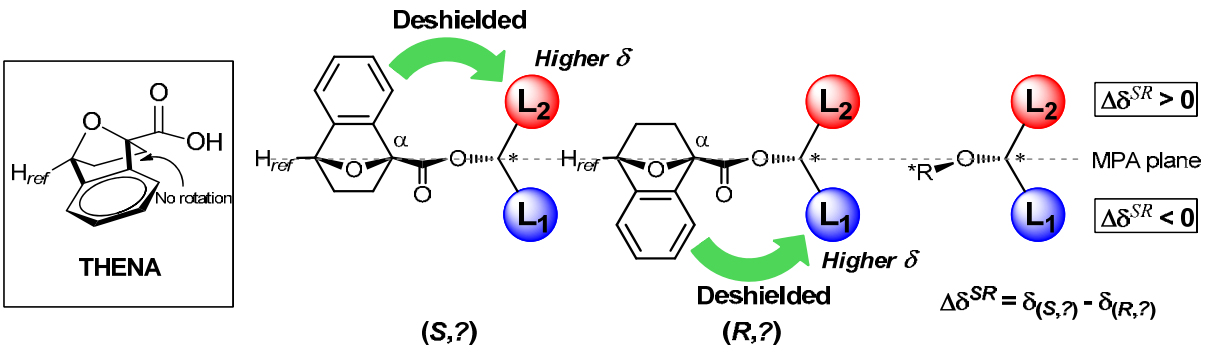

Abstract

This research focuses on the design, synthesis and development of a new chiral derivatizing agent (THENA) for the determination of the absolute configuration of chiral secondary alcohols, with high efficiency and reliable accuracy. The design was based on the preferred conformation of the mandelate ester with the *syn*-periplanar orientation of RO-C-C_a-C(O)-O-C*-H. This plane now becomes a part of the bicyclic system in order to constrain the rotational degree of freedom of the aromatic group. With the presence of an internal reference proton (H_{ref}) which can facilitate the spectral alignment, the determination of the chemical shift difference could be done unambiguously, leading to an accurate absolute configuration.

A diastereomeric pair from the reaction between the new chiral derivatizing agents and the chiral alcohol of interest would give ^{1}H NMR spectra with different chemical shifts. The correlation between the model derived from the chemical shift differences and the absolute configuration of the compound of interest would then lead to the absolute configuration of the chiral alcohol. In addition, it was found that THENA could also be used to resolved binaphthol derivatives.

Modification of THENA by extending the aromatic group as well as by installing an epoxide subunit led to a less complicated ^{1}H NMR spectra, making the determination of the absolute configuration more convenient.

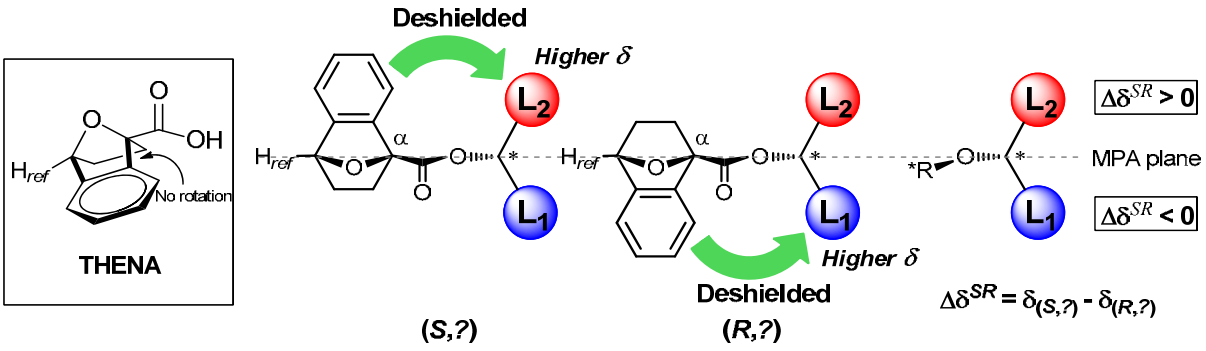

Executive summary

Research in the field of bioactive natural products, especially those with chiral centers, is of great significance since it can provide new potential pharmaceutical leads. Accordingly the simple and efficient tools to determine the absolute configuration of the chiral molecules are in high demand and this has led to the development of chiral derivatizing agents and the NMR shift difference method.

This research focuses on the development of a new chiral derivatizing agent (THENA) for the determination of the absolute configuration of chiral alcohols. The key features of THENA design include *i)* the analogous MPA plane as a part of bicyclic system, to limit the rotational degree of freedom of the aromatic moiety *ii)* the observed anisotropic deshielding effect on the substituents, due to the bicyclic tether *iii)* the presence of an internal reference proton (H_{ref}) to facilitate the spectra alignment *iv)* readily accessible at low cost *via* a straightforward synthesis.

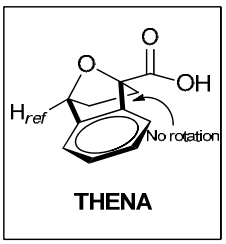

THENA

Enantiomers of THENA were synthesized and then applied to determine the absolute configuration of chiral secondary alcohols with known absolute configuration. The correlation between the model derived from the chemical shift differences and the absolute configuration of the compound of interest was constructed. In all cases, the absolute configurations derived from the experimental data were satisfactorily in good agreement with the known configuration. The application of THENA in the resolution of binaphthol derivatives was also realized.

Modification of THENA by extending the aromatic moiety as well as an addition of an epoxide subunit onto the bicyclic skeleton provided a new chiral derivatizing agent with much less complicated ^{1}H NMR spectra. This modified THENA could also be used successfully in the determination of the absolute configuration of the chiral alcohols.

At present, almost all of the chiral derivatizing agents being used in Thailand are imported. The success of this work thus provided an opportunity to implement the domestic

research and development through collaboration with natural product chemists who are interested to use this chiral derivatizing agent in their research.

Design and Synthesis of New Chiral Derivatizing Agents

Part I. Design of new chiral derivatizing agent THENA

Introduction

Research on the complex bioactive natural products which requires structure elucidation and the emerging of asymmetric synthesis in chemical and pharmaceutical areas have stimulated the development of simple, reliable and inexpensive methods to determine the absolute configuration of chiral centers.[1]

At present, there are several methods for determining the absolute configuration of a chiral compound. The most widely known is X-ray crystallography[2] which can be used to assign the absolute configuration of an optically pure compound and is often used to confirm the hypotheses used for stereochemical assignment. However, there are some inconveniences and limitations. Related to the equipment, the technique is very specific to the method and requires special training for operation. Related to the sample, the X-ray diffraction analysis (XRD) requires single crystals of good quality which is frequently not obtainable. The other methods, such as optical rotation study,[3] have also been applied with great convenience. However, the technique which is based on the rotation of plane-polarized light by the sample can be reliable only if the rotation of the pure compound is accurately known. This is impractical for a newly prepared material or a newly discovered natural product.

The utility of NMR spectroscopy then becomes the solution as one of the most convenient ways of detecting and analyzing the diastereomeric products. As exemplified in Figure 1, the difference in NMR spectra can be observed as a result of the difference in the physical properties of diastereomers derived from the covalent or noncovalent complex formation between the chiral molecules with unknown configurational chiral center and another chiral reagent with known absolute stereochemistry, the chiral derivatizing agents (CDAs).[4] The changes in the chemical shifts of the substituents of the asymmetric carbon of the substrate (L_1 and L_2) in the two derivatives can then be considered. These differences in the chemical shifts are represented by $\Delta\delta$, and the sign of this parameter (+ or –) provides the information about the configuration. For a particular substituent (e.g., L_1), $\Delta\delta$ is defined as the difference of chemical shifts of a given signal of the substituent (δL_1) in the two spectra

under consideration. The sign of the chemical shift differences of the substituents attached to the asymmetric carbon can then be correlated with the absolute configuration by using an empirical model.

a)

b)

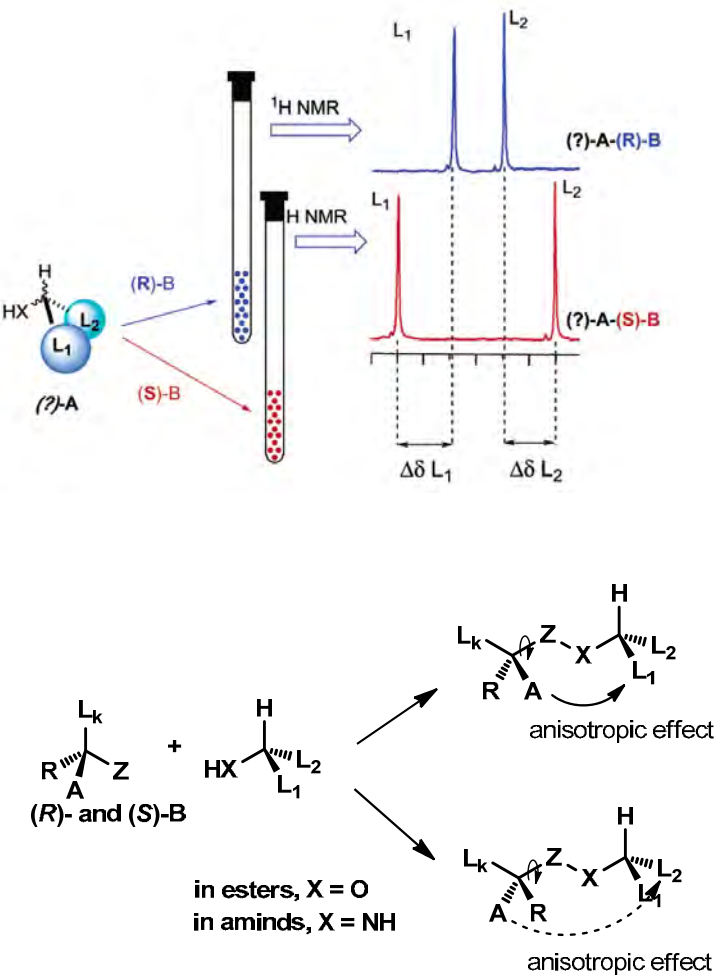

Figure 1. a) Representative protocol for the CDA-NMR shift difference method.[4]; b) General structure of CDA and the anisotropic effect of the corresponding esters.

Furthermore, the difference in the physical properties of the diastereomers provides the basis of chemical and physical separation processes. The process of the resolution is the separation of a diastereomeric mixture produced by the reaction of a racemic mixture with a pure enantiomer of a second reagent, the resolving agent. Since the two resulting products will be diastereomers, they can be separated. The separated diastereomers can then be converted to the pure enantiomers by reversing the initial chemical transformation, *i.e.* the hydrolysis reaction.

1.1. Procedure

The procedure to correlate the NMR chemical shift differences with the absolute configuration assignment can be described comprehensibly as follows. The chiral substrate (*i.e.* a secondary alcohol or amine) of unknown absolute stereochemistry (*?*)-A is separately esterified with the (*R*)- and (*S*)- enantiomers of an auxiliary reagent B of which the molecule possesses an aromatic functional group (*e.g.* a phenyl group) to provide the anisotropic effect. The NMR spectra of the two resulting diastereomers (*?*)-A-(*R*)-B and (*?*)-A-(*S*)-B are compared (Figure 1). The different anisotropic influence from the phenyl group of the chiral auxiliary on the substituents in each diastereoisomer then causes of chemical shift differences and thus the two spectra should be different and the assignment of configuration is based on the existence of a certain association between the absolute stereochemistry at the chiral centre of the auxiliary reagent B, and the chemical shifts of L_1/L_2 in the two derivatives.

For this relationship to exist, some characteristics and conditions of CDA have to be fulfilled:

a) have a polar or bulky group (L_k) (*e.g.* OMe) to fix a particular conformation which should be the same in the two diasteroisomeric derivatives and independent of the nature of substituents L_1 and L_2 of A.
b) have a functional group (Z) (*e.g.* carboxylic acid) that provides a site for covalent attachment of the substrate.
c) have anisotropic group Y (*e.g.* phenyl) which should be able to affect in a selective and recognized way the chemical shifts of substituents L_1/L_2 at the substrate part and strong enough to ensure that the chemical shifts of L_1 and L_2 are different in the two species, and
d) there should exist in both derivatives a significantly more populated conformer where group Y acts strongly on L_1/L_2.

1.2. Common CDA

1.2.1. α-Methoxy-α-phenylacetic acid (MPA)

α-Methoxy-*α*-phenylacetic acid (MPA) or mandelic acid (MA) **1** (Figure 2a) represents a facile approach for analyzing the absolute configuration of chiral secondary

alcohols. The model proposed by Dale and Mosher[5] correlated NMR shifts and absolute stereochemistry of the mandelate ester derivatives of chiral alcohols. It is assumed that the representative conformer in terms of NMR is the one in which the methoxy, carbonyl, and C(1')H groups are situated in the same plane (Figure 2b). In this way, the NMR chemical shift of the substituent which eclipsed the phenyl ring then always appeared upfield, presumably as a result of the shielding effect from the phenyl ring. Derivative (*S*)-MPA ester should show its L_2-proton shift more upfield than that of the corresponding signal in (*R*)-MPA ester and the reverse should be true for the incident of L_1 group (Figure 2b). Consequently, the comparison of both spectra leads to $\Delta\delta^{RS}$ $L_1 < 0$ and $\Delta\delta^{RS}L_2 > 0$ (Figure 2c).

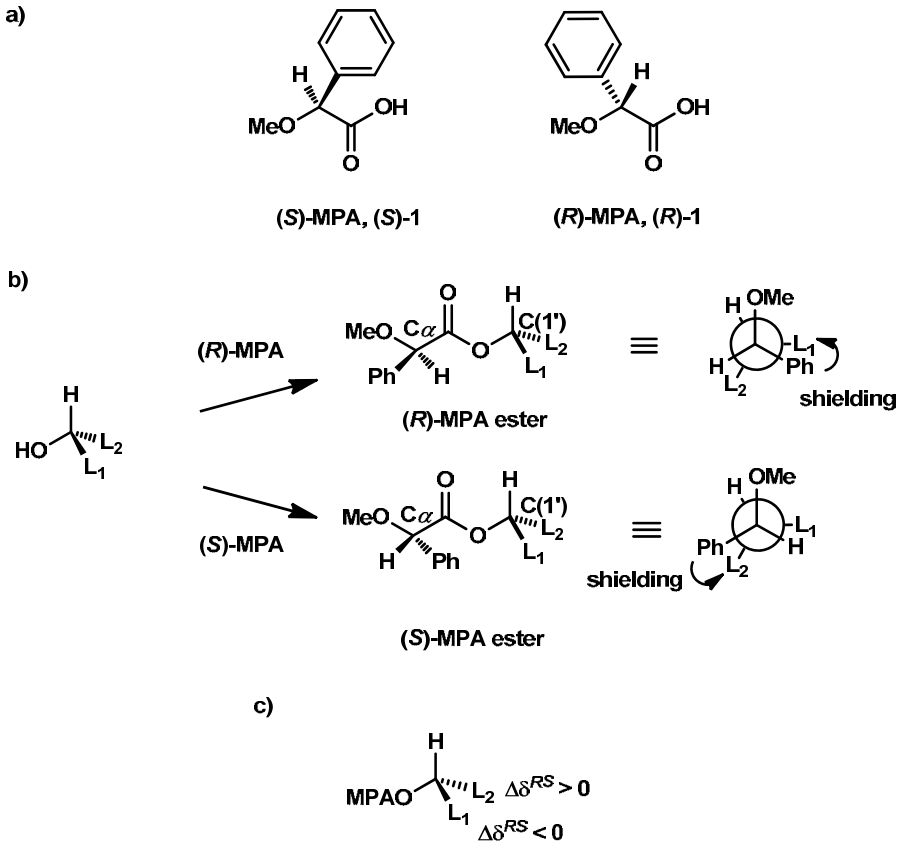

Figure 2. a) *α*-Methoxy-*α*-phenylacetic acid (MPA) or mandalic acid **1**; b) the model for determining of absolute configuration of secondary alcohol; c) the expected signs of $\Delta\delta^{RS}$.

Because of the potential problem with racemization found during esterification,[4] the *α*-methoxy-*α*-phenylacetic acid (MPA) **1** has been less used. This factor led to the design of

new resolving agent to avoid this problem such as methoxy-2-(1-naphthyl)propionic (M*α*NP) acid **2** and Mosher's acid (MTPA) **3** (Figure 3).

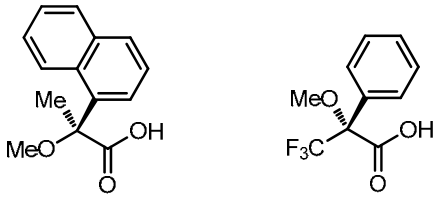

M*α*NP; 2 **MTPA; 3**

Figure 3. The chemical structures of methoxy-2-(1-naphthyl)propionic (M*α*NP) acid **2** and Mosher's acid (MTPA) **3**.

1.2.2. Methoxy-2-(1-naphthyl)propionic (MαNP) acid

Methoxy-2-(1-naphthyl)propionic (M*α*NP) acid **2** is also a powerful tool for determining the absolute configuration of chiral secondary alcohols.[6] This chiral ^{1}H NMR anisotropy reagent is unique in the sense that the diastereomeric M*α*NP esters prepared from enantiopure acid (*S*)-(+)-M*α*NP and racemic alcohols are easily separable by HPLC. In addition, the M*α*NP acid **2** has a chiral quaternary carbon atom, and therefore, does not racemize.

In the (*R*)-M*α*NP ester of the alcohol shown in Figure 4a, substituent L_1 experiences a shielding influence from the naphthyl group, whereas, in the (*S*)-M*α*NP ester, the shielded group is substituent L_2. Therefore, substituent L_1 results in a negative $\Delta\delta^{RS}$ value and substituent L_2 yields a positive $\Delta\delta^{RS}$ value (Figure 4b).

To explain the anisotropy effect of M*α*NP acid esters, the studies of their ^{1}H NMR spectra and those of related carboxylic acid esters suggested that the observed $\Delta\delta$ values are very sensitive to the geometry of the aromatic groups. These results indicate that the *syn-syn* conformation generates a larger $\Delta\delta$ value which is stabilized by a triangular hydrogen-bonding interaction among O-6/ H-8/ O-7 (Figure 4c).

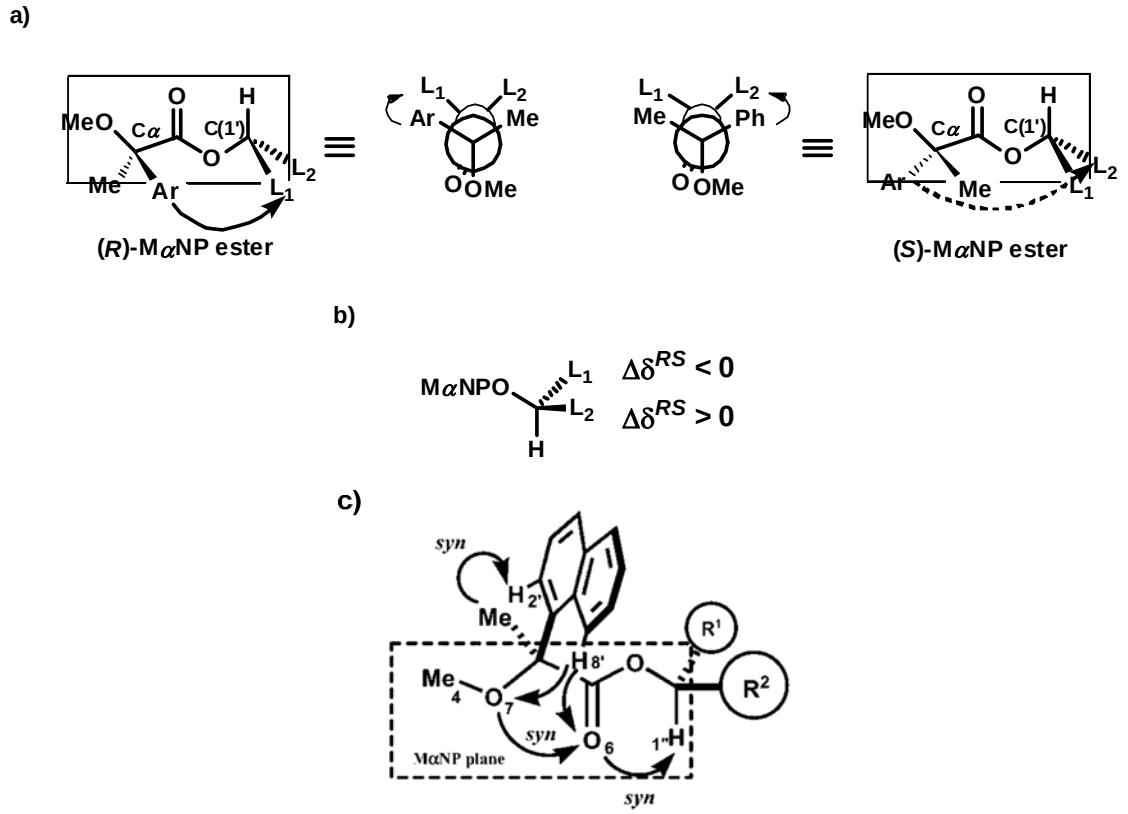

Figure 4. a) Model of methoxy-2-(1-naphthyl)propionic (M*α*NP) acid **2** for determining of the absolute configuration of secondary alcohols; b) the expected signs of $\Delta\delta^{RS}$; c) the proposed conformation of M*α*NP acid esters.

1.2.3. Mosher's acid

In 1991, Kakisawa *et al.*[7] reported the high-field NMR application of Mosher's method[5] to assign the absolute configurations of secondary alcohols. The model was proposed that, in solution, the carbinyl proton, ester carbonyl and the trifluoromethyl group of *α*-methoxy-*α*-trifluoromethylphenylacetic acid (MTPA) moiety lie in the same plane, called MTPA plane (Figure 5a). Similar to the *O*-methylmandelate or MPA's model, due to the diamagnetic effect of the benzene ring, L_2-protons NMR signals of the (*R*)-MTPA ester should appear upfield relative to those of the (*S*)-MTPA ester. The reverse should hold true for L_1-protons. Therefore, when $\Delta\delta^{SR} = \delta_S - \delta_R$, protons on the L_2's side of the MTPA plane must have negative values ($\Delta\delta^{SR}\, L_2 < 0$) and protons on the L_1's side of the plane must have positive values ($\Delta\delta^{SR}\, L_1 > 0$) (Figure 5b). Moreover, the values of $\Delta\delta$ must be proportional to the distance from the anisotropic group of MTPA moiety.

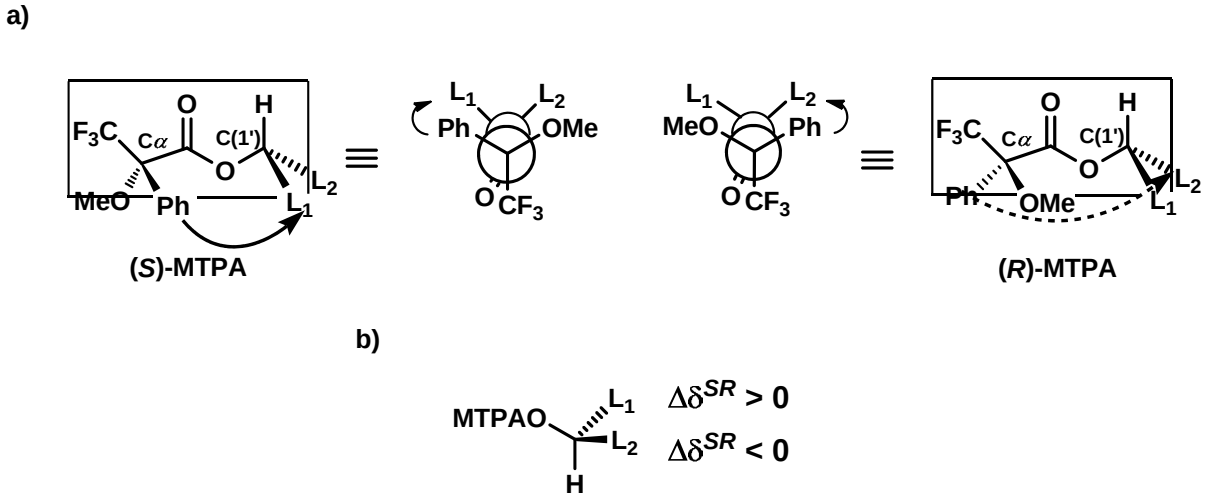

Figure 5. a) Models of MTPA-ester for the assignment of the absolute configuration by ^{1}H NMR and b) the expected sign of Δ^{SR}.

Although MTPA is widely used in determining the absolute configuration of chiral alcohols and amines, its application is sometimes restricted by the conformational limits imposed by the reagent.[8] Three conformations of similar population are presented in Figure 6.[7] Conformer ap_1 is the most stable conformer and has the CF_3 group anti-periplanar, with respect to the carbonyl group; its phenyl ring produces a deshielding effect on the substituent of the alcohol. The next conformer, in terms of energy, is sp_1; it has the CF_3 and carbonyl groups in a *syn*-periplanar disposition, as in the empirical Mosher's model, and its phenyl ring produces a shielding effect on the alcohol part. The third conformer is sp_2, and this conformer also has a *syn*-periplanar disposition that results in deshielding on the alcohol's substituent. The contribution of the three main conformers affects the chemical shift, resulting in the origin of the two most important limitations of this reagent: 1) the small $\Delta\delta^{SR}$ values and 2) irregular sign distributions.

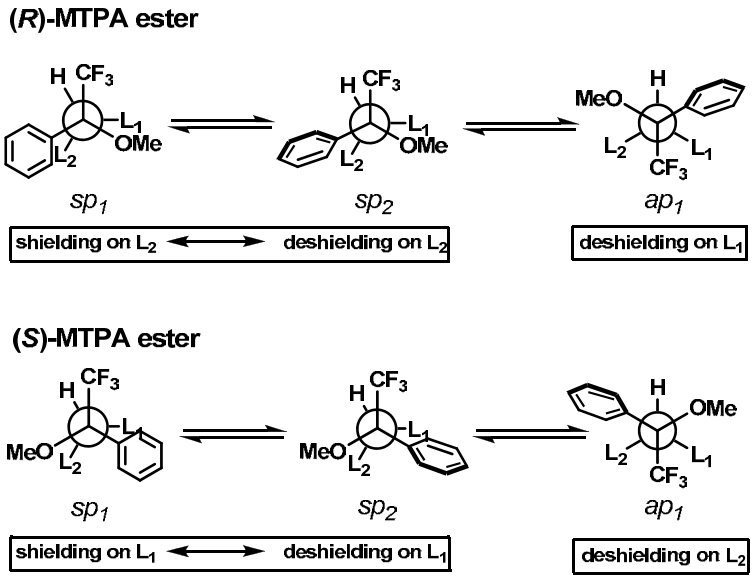

Figure 6. Shielding/deshielding effects in the three most representative conformers of the MTPA esters.

In contrast to the case of MTPA esters, the MPA esters present a simpler conformational composition with only two conformers (*sp*/*ap*) and a clearer preference for one of those (*sp*) (Figure 7), which, in turn, transmits a shielding effect to the substituents to give higher $\Delta\delta^{RS}$ values that are more reliable and with the same trend of sign distribution.

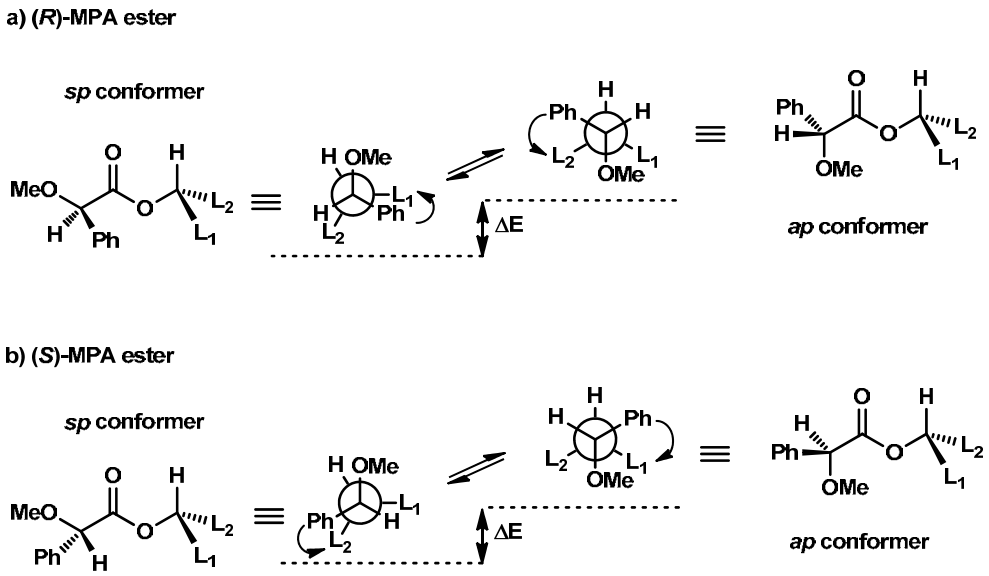

Figure 7. Conformational composition of MPA esters.

To overcome the ambiguousness of those methods concerning the flexible conformation of the anisotropic aromatic group, the design aimed to limit the rotational degree of freedom of the aromatic moiety was conducted through a new CDA for determination of the absolute configuration of chiral secondary alcohols, tetrahydro-1,4-epoxynaphthalene-1-carboxylic acid (THENA) **4** (Figure 8). THENA has the analogous MPA plane as a part of rigid bicyclic system with the merit of chiral quaternary carbon atom to avoid racemization. Moreover, the availability of a proton in the structure which is not influenced by the diastereotopic environment should serve as an internal reference for spectra alignment. Such conformation constraint, along with an internal reference proton, should provide an unambiguous determination of the sign of NMR chemical shift difference, leading to an explicit assignment of the absolute configuration.

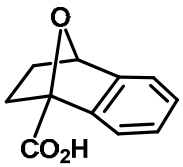

4

Figure 8. Tetrahydro-1,4-epoxynaphthalene-1-carboxylic acid (THENA) **4**.

Results

(±)-Tetrahydro-1,4-epoxynaphthalene-1-carboxylic acid **4** could be synthesized from commercially available and low cost starting materials following a modified Best and Wege's method.[9] The key step for the preparation of **4** was the Diels-Alder reaction of methyl furan-2-carboxylate **5** with benzenediazonium-2-carboxylate **6**, generated from the reaction between anthranilic acid **7** and *iso*-amylnitrite, in boiling dichloroethane to yield (±)-methyl 1,4-dihydro-1,4-epoxynaphthalene-1-carboxylate **8**. The ester **8** was then subjected to hydrogenation and hydrolysis to yield (±)-methyl 1,2,3,4-tetrahydro-1,4-epoxynaphthalene-1-carboxylate **9** and (±)-tetrahydro-1,4-epoxynaphthalene-1-carboxylic acid **4,** respectively. The overall synthetic scheme is shown in Scheme 1.

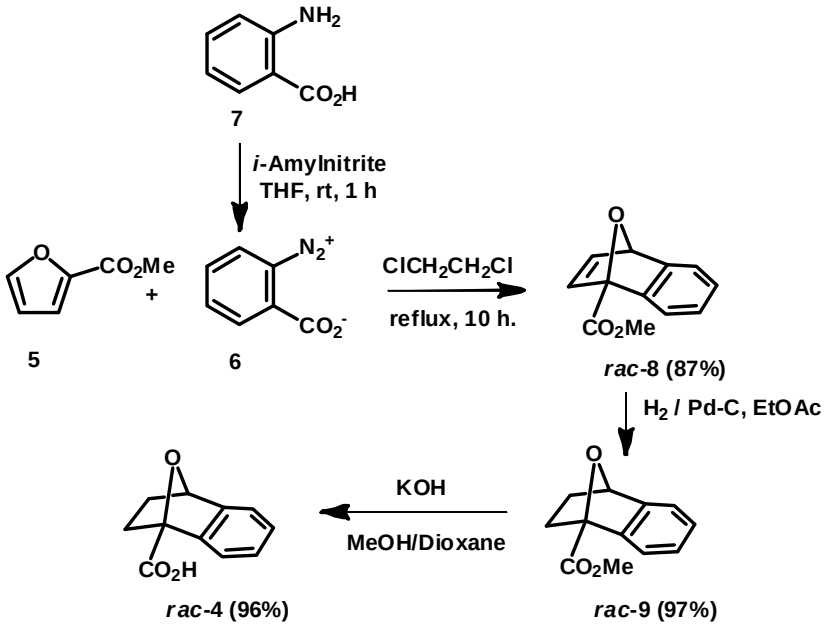

Scheme 1. Preparation of (±)-tetrahydro-1,4-epoxynaphthalene-1-carboxylic acid ***rac* 4**.

The resolution of ***rac*-4** could be affected as follows. Treatment of ***rac*-4** with oxalyl chloride and DMF in dichloromethane at room temperature for 3 h gave acid chloride ***rac*-10** which was then reacted with *D*-(+)-menthol and DMAP (as a catalyst) and then triethylamine in dichloromethane to give the mixture of diasteromers **(*S*,*S*)-11** and **(*R*,*S*)-11** (the absolute configuration assignment derived from the X-ray data as discussed later). The mixture was separated by PLC (Hexane:EtOAc 98:2). The first-eluted ester **(*S*,*S*)-11** (47 %, $[\alpha]_D$ +43.54

(c = 3.85 w/v %, $CHCl_3$) and the second one **(*R*,*S*)-11** (46 %, $[\alpha]_D$ +22.11 (c = 3.99 w/v %, $CHCl_3$) were obtained (Scheme 2).

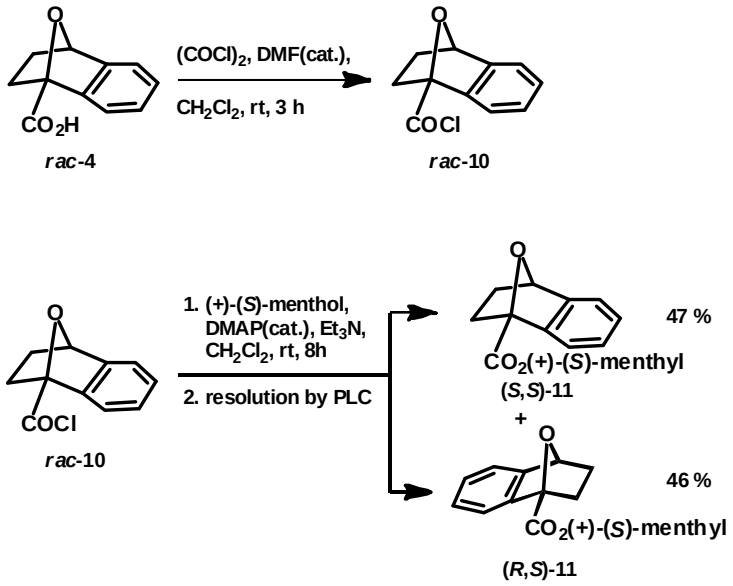

Scheme 2. Resolution of diastereomers **(*S*,*S*)-11** and **(*R*,*S*)-11**.

Because the conformation of the aromatic group was locked by the bicyclic structure, the substituent proton of *D*-(+)-menthol which eclipsed the phenyl ring would be affected by the deshielding anisotropic effect. Therefore, presumably, the *iso*-propyl group situated close to aromatic group should be lower-field shifted than the analogous protons in the other diastereomer. From the ^{1}H NMR spectra of diastereomeric esters **(*S*,*S*)-11** and **(*R*,*S*)-11** (Figure 10), it was found that the protons of *iso*-propyl group in ester **(*S*,*S*)-11** were lower-field shifted than the analogous protons in **(*R*,*S*)-11**. The key ^{1}H NMR chemical shifts of both diastereomers are listed in Figure 9.

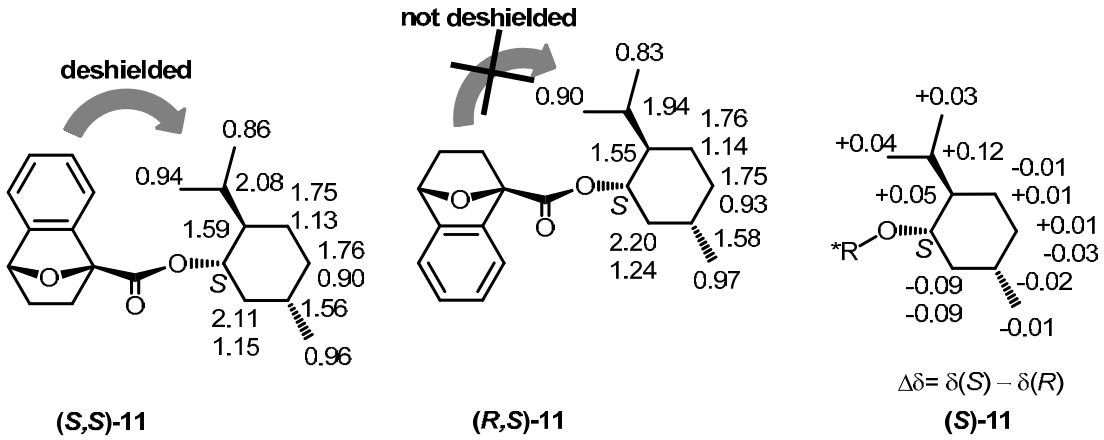

Figure 9. ^{1}H NMR chemical shift data of esters **(*S*,*S*)-11** and **(*R*,*S*)-11** and Δδ values.

Theoretically, THENA **4** should prefer the conformation that the C–O bond, the ester carbonyl and the C(1')H all are in the same plane like *sp* conformer of MPA (Figure 10). It could be postulated that, due to the electronic effect, the σ–π* interaction between the electron rich sigma C–C bond, rather than the C–O bond, and the electron poor π* orbital of the carbonyl carbon stabilize this conformation.

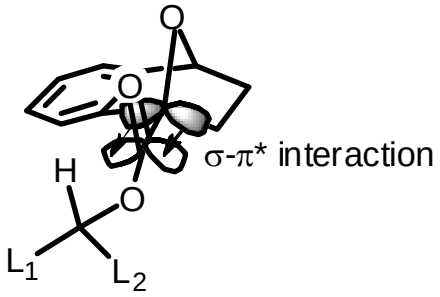

Figure 10. The stable conformation of THENA ester.

The X-ray data (Figure 11)[11] revealed the structure of diastereomeric ester **(*R*,*S*)-11**. The absolute configuration of the THENA moiety could be assigned as '*R*'. The X-ray structure also showed the analogous MPA plan (dotted plane), confirming the preferred confirmation of the THENA moiety as the *syn*-periplanar conformation.

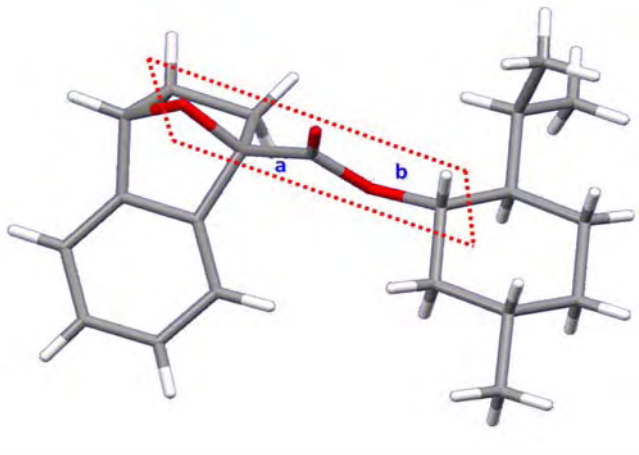

Figure 11. X-ray structure of compound **(*R*,*S*)-11** ; angle **a** is 10° and **b** is 20°.

Finally, (+)-2,3-dihydro-1,4-epoxynaphthalene-1(2H)-carboxylic acid **(*S*)-(+)-4** could be obtained by the hydrolysis of **(*S*,*S*)-11** and (–)-2,3-dihydro-1,4-epoxynaphthalene-1(2H)-carboxylic acid **(*R*)-(–)-4** could be obtained by the hydrolysis of **(*R*,*S*)-11**.

The model for determination of the absolute configuration of chiral secondary alcohols

Due to the diamagnetic deshielding effect of the benzene ring, L^1 's ^{1}H NMR signals of the (*R*)-acid ester should appear downfield relative to those of the (*S*)-acid ester. The reverse should hold true for L^2 's H. Therefore, a model for determining the absolute configuration of chiral secondary alcohols is presented in Figure 12. When $\Delta\delta^{SR} = \delta_S - \delta_R$, protons on the right side of the model should have positive values ($\Delta\delta^{SR} > 0$) and protons on the left side of the model should have negative values ($\Delta\delta^{SR} < 0$). The absolute values of $\Delta\delta$ will be proportional to the distance of the substituents from the aromatic moiety of the CDA. When these conditions were satisfied, the model in Figure 12 would indicate the correct absolute configuration of the compound.

Importantly, the presence of H_{ref} (Figure 10) which is not influenced by the diasteretopic environment should serve as an internal reference for spectra alignment.

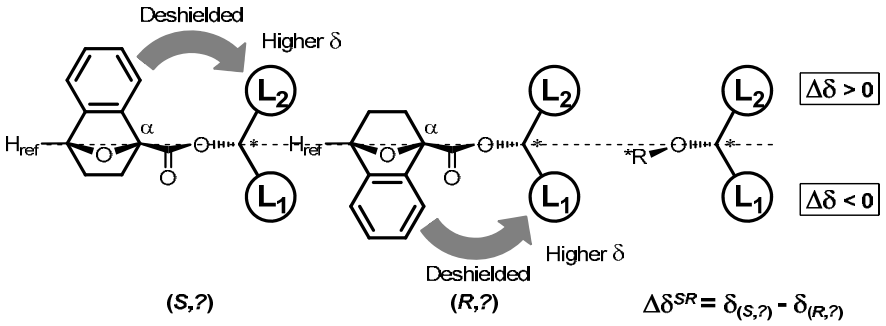

Figure 12. Model for the absolute configuration assignment of chiral secondary alcohols.

Based on the anisotropic data and the proposed model, the chirality of menthol could be reconstructed and was identical to the known absolute configuration of *D*-(+)-menthol. This result implied that each enantiomer of THENA **4** could be used for esterification of chiral alcohol, as a chiral auxiliary, to determine the absolute configuration of alcohols by using ^{1}H NMR anisotropic data.

*The validation of THENA **4** with a variety of chiral secondary alcohols*

The validation of THENA **4** as a chiral derivatizing agent with other cases of chiral secondary alcohols must be performed to assure its reliability.

Firstly, to recover the optically active acids **(*S*)-(+)-4** and **(*R*)-(–)-4**, compounds **(*S*,*S*)-11** and **(*R*,*S*)-11** were subjected to hydrolysis with KOH in 1:1 MeOH : dioxane at room temperature for 3 h to give **(*S*)-(+)-4** and **(*R*)-(–)-4** in 95% yield and 97% yields, respectively (Scheme 3).

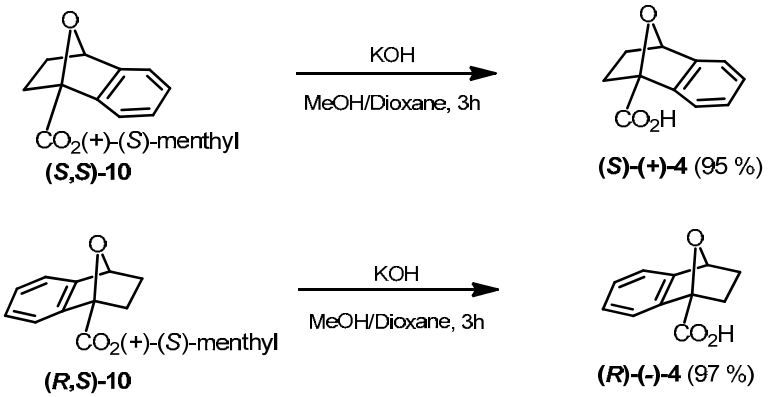

Scheme 3. Preparation of optically active acids (*S*)-(+)-THENA **4** and (*R*)-(–)-THENA **4**.

Then, optically active acids **(*S*)-(+)-4** and **(*R*)-(–)-4** were tested with a varieties of chiral secondary alcohols **12**–**21** of which absolute configuration has already known, as shown in Figure 13.

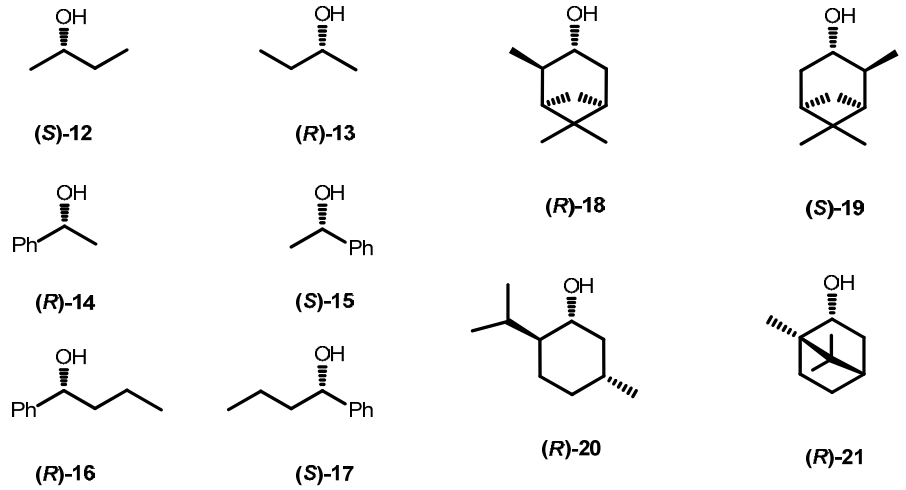

Figure 13. The optically chiral alcohols which are used for tested the anisotropy effect of acid.

Diastereomeric esters of **(*S*)-(+)-4** and **(*R*)-(–)-4** with the optically active alcohols could be prepared as follows. Treatment of optically active acids **(*S*)-(+)-4** and **(*R*)-(–)-4** with oxalyl chloride and DMF (as a catalyst) at room temperature in dichloromethane generated acid chlorides **(*R*)-10** and **(*S*)-10**, respectively. Then, in a separate reaction, both acid chlorides, **(*R*)-10** and **(*S*)-10**, were reacted with the alcohols with DMAP (as a catalyst) at room temperature in CH_2Cl_2 and then triethylamine to give the corresponding diastereomeric pairs which were separated by PLC (Hexane:EtOAc 95:5–90:10) (Scheme 4).

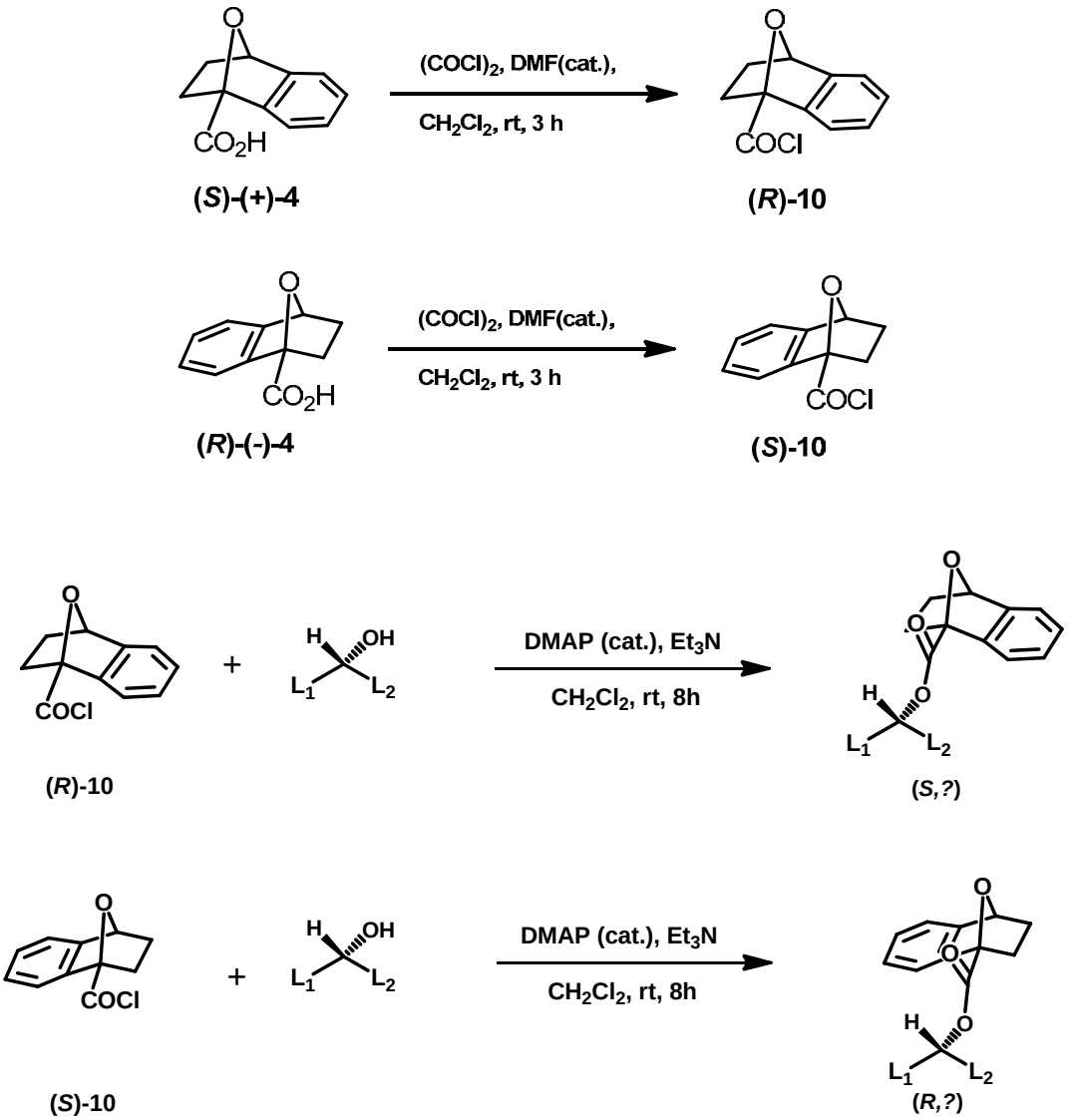

Scheme 4. Preparation of diastereomeric esters of **(*S*)-(+)-4** and **(*R*)-(–)-4** with the optically active alcohols.

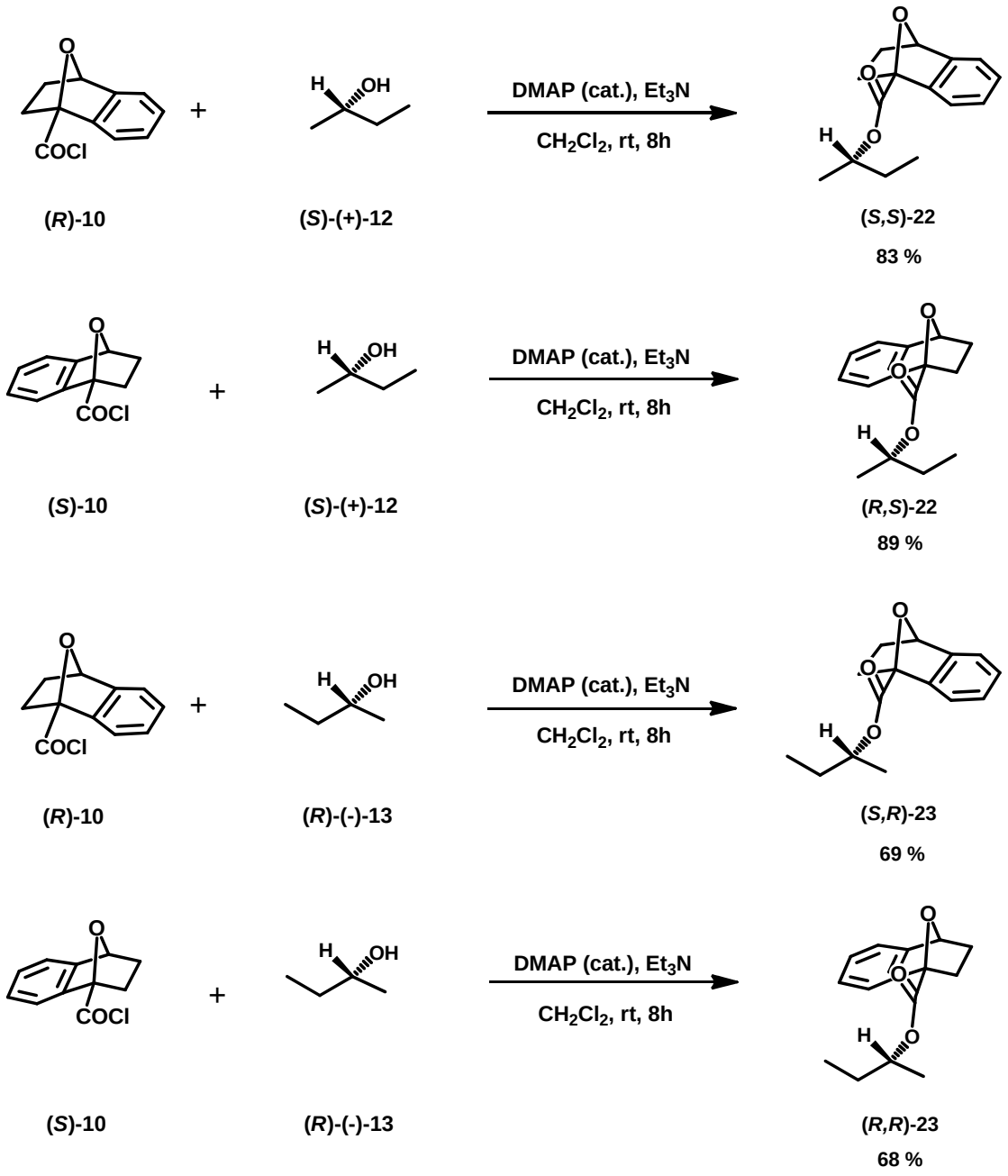

Scheme 4. Preparation of diastereomeric esters of **(*S*)-(+)-4** and **(*R*)-(–)-4** with the optically active alcohols (continued).

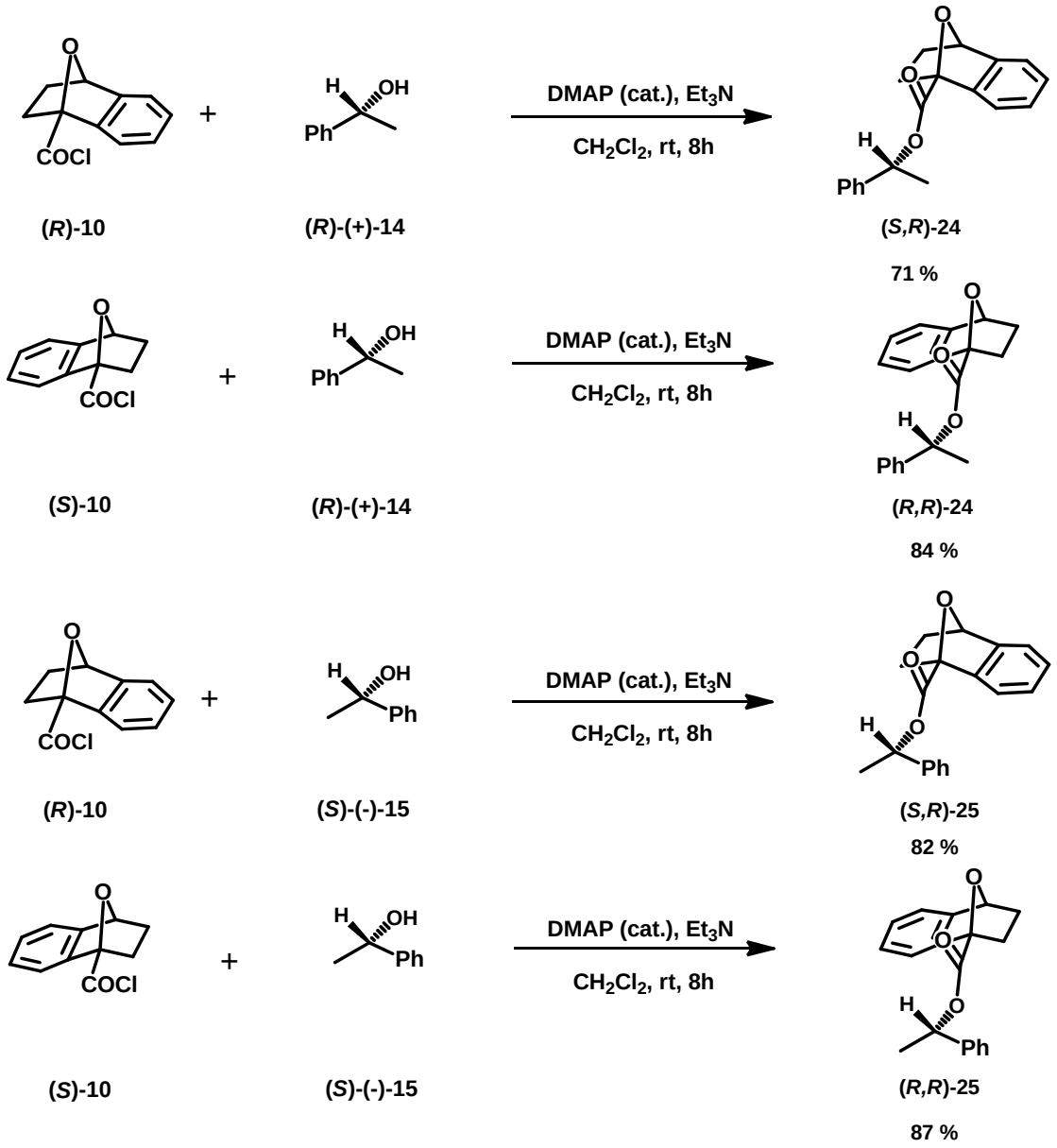

Scheme 4. Preparation of diastereomeric esters of **(*S*)-(+)-4** and **(*R*)-(–)-4** with the optically active alcohols (continued).

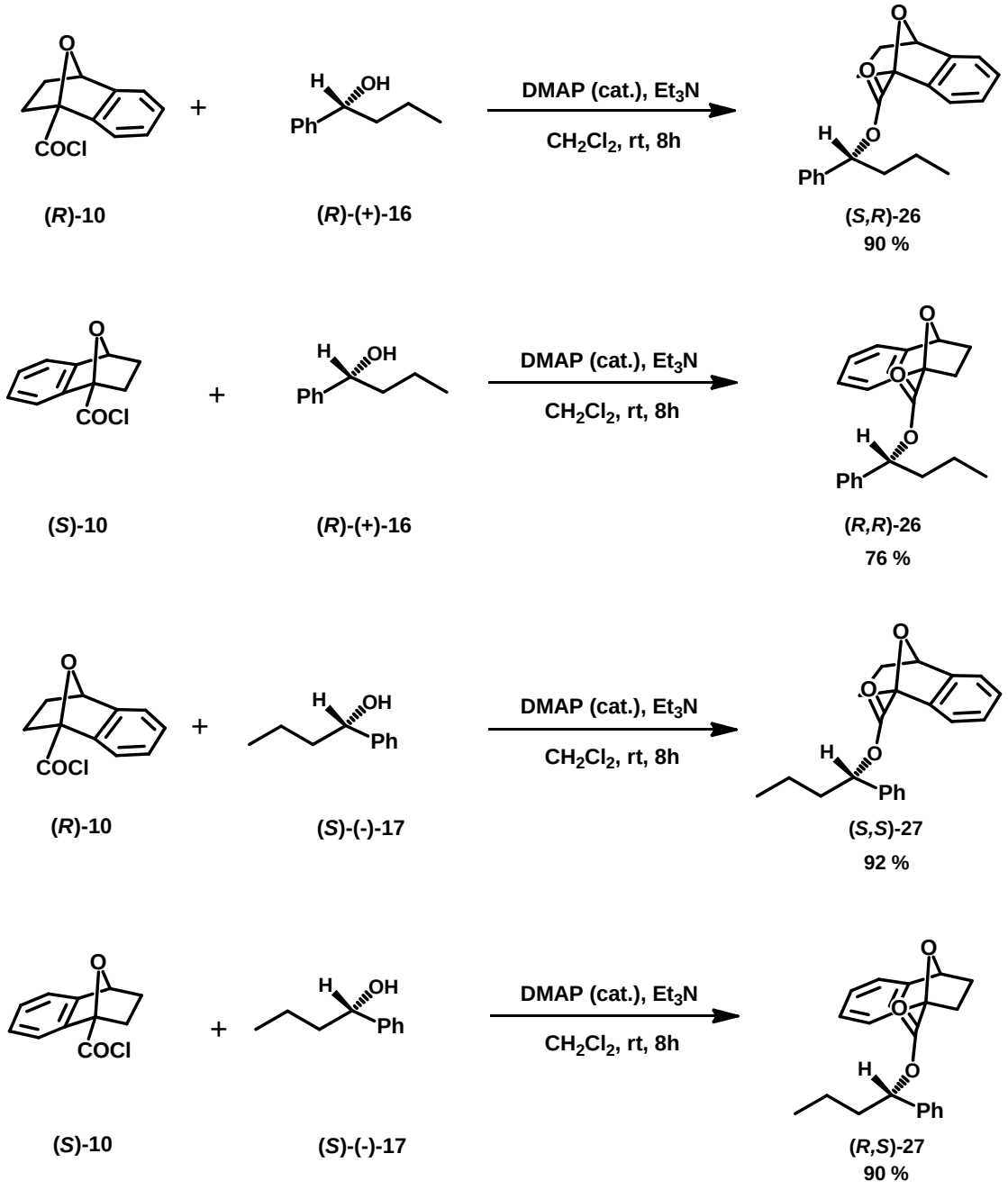

Scheme 4. Preparation of diastereomeric esters of **(*S*)-(+)-4** and **(*R*)-(–)-4** with the optically active alcohols (continued).

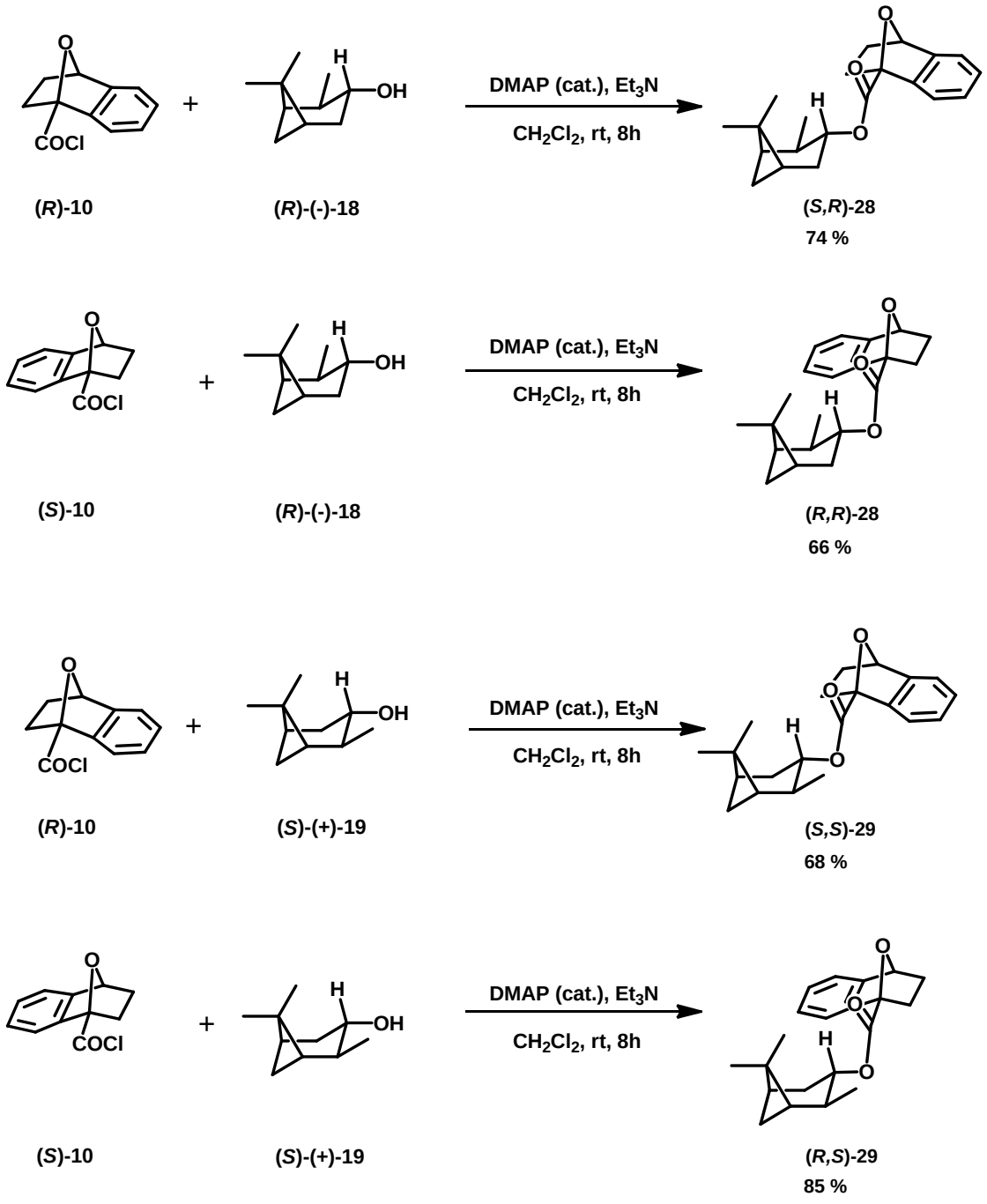

Scheme 4. Preparation of diastereomeric esters of **(*S*)-(+)-4** and **(*R*)-(–)-4** with the optically active alcohols (continued).

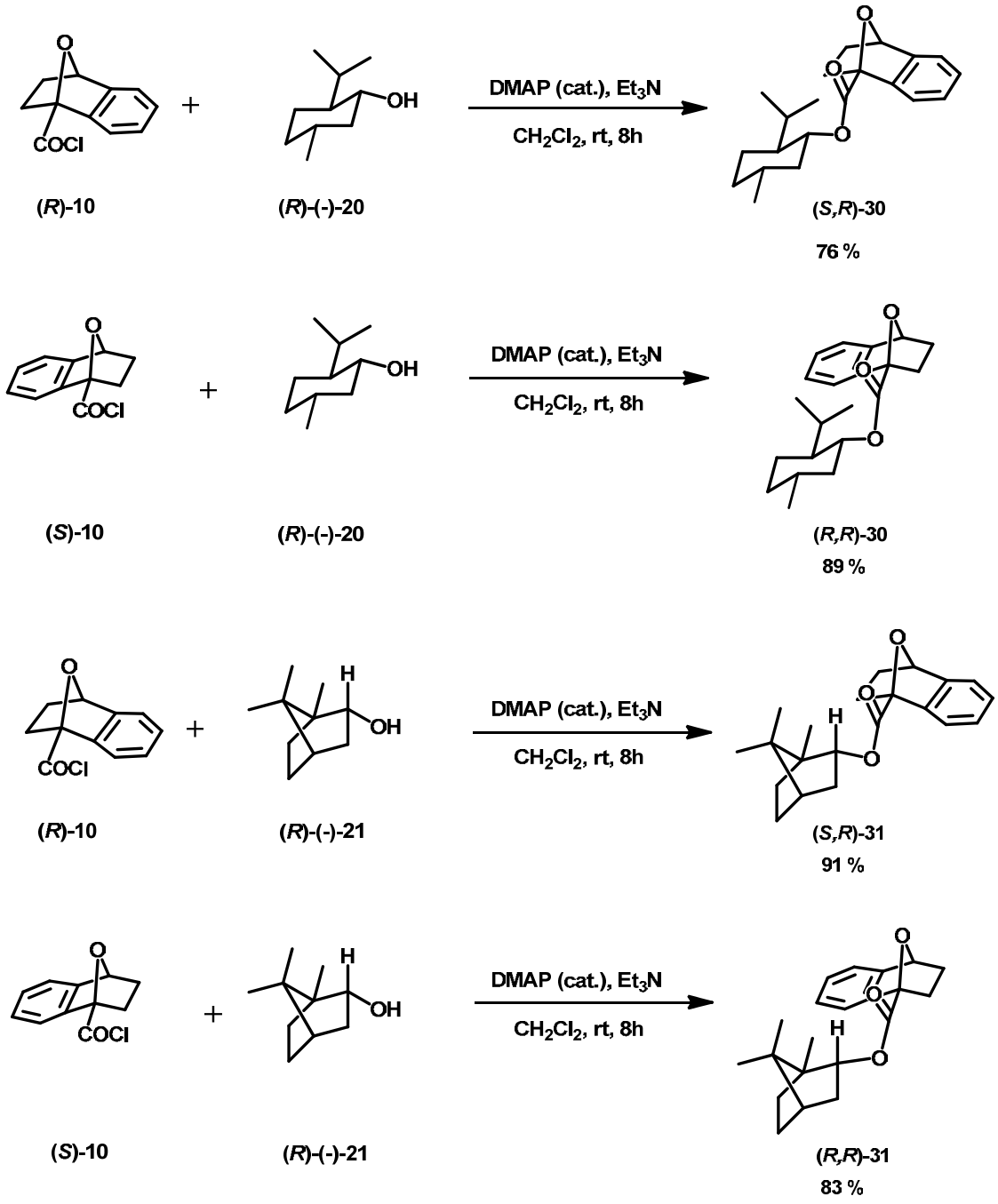

Scheme 4. Preparation of diastereomeric esters of **(*S*)-(+)-4** and **(*R*)-(–)-4** with the optically active alcohols (continued).

The anisotropic effect was observed in all diastereomeric esters **22**–**31**. The chemical shift data of the diastereomeric esters **11**, **22**–**31** were listed in Figure 14 together with the Δδ values (ppm): $\Delta\delta^{SR} = \delta(S) - \delta(R)$ and the results of the Δδ values were concluded in Figure 14. It was found that protons of the alkyl group which were close to aromatic side of acid were downfield shifted by the anisotropy effect of aromatic moiety while the protons of

the alkyl group which were far away from the aromatic ring were not affected. The absolute configuration derived from the experiments all matched well with the known values.

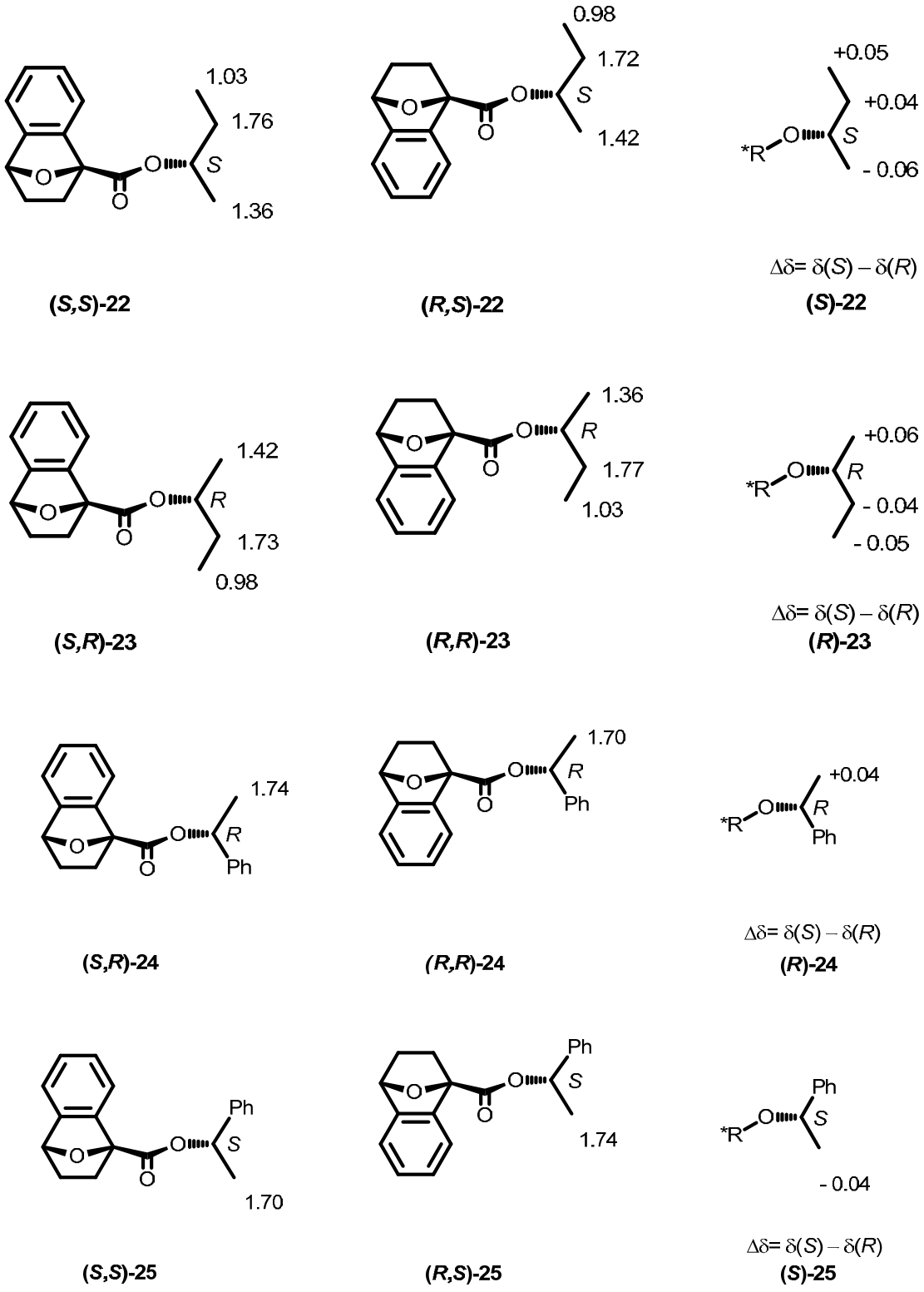

Figure 14. ^{1}H NMR chemical shift data of esters **11**, **22**–**31** and $\Delta\delta^{SR}$ values.

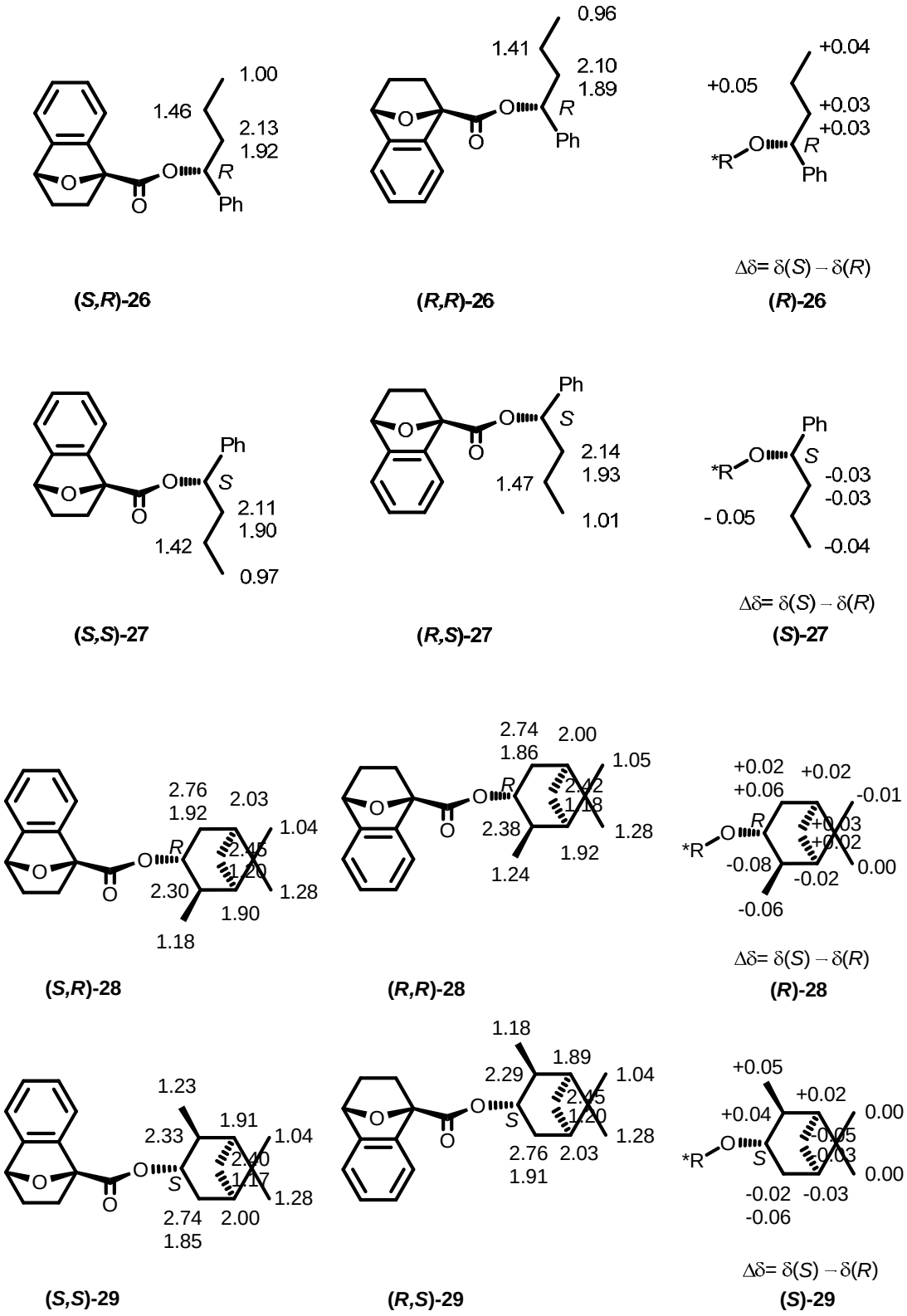

Figure 14. ^{1}H NMR chemical shift data of esters **11**, **22**–**31** and $\Delta\delta^{SR}$ values (continued).

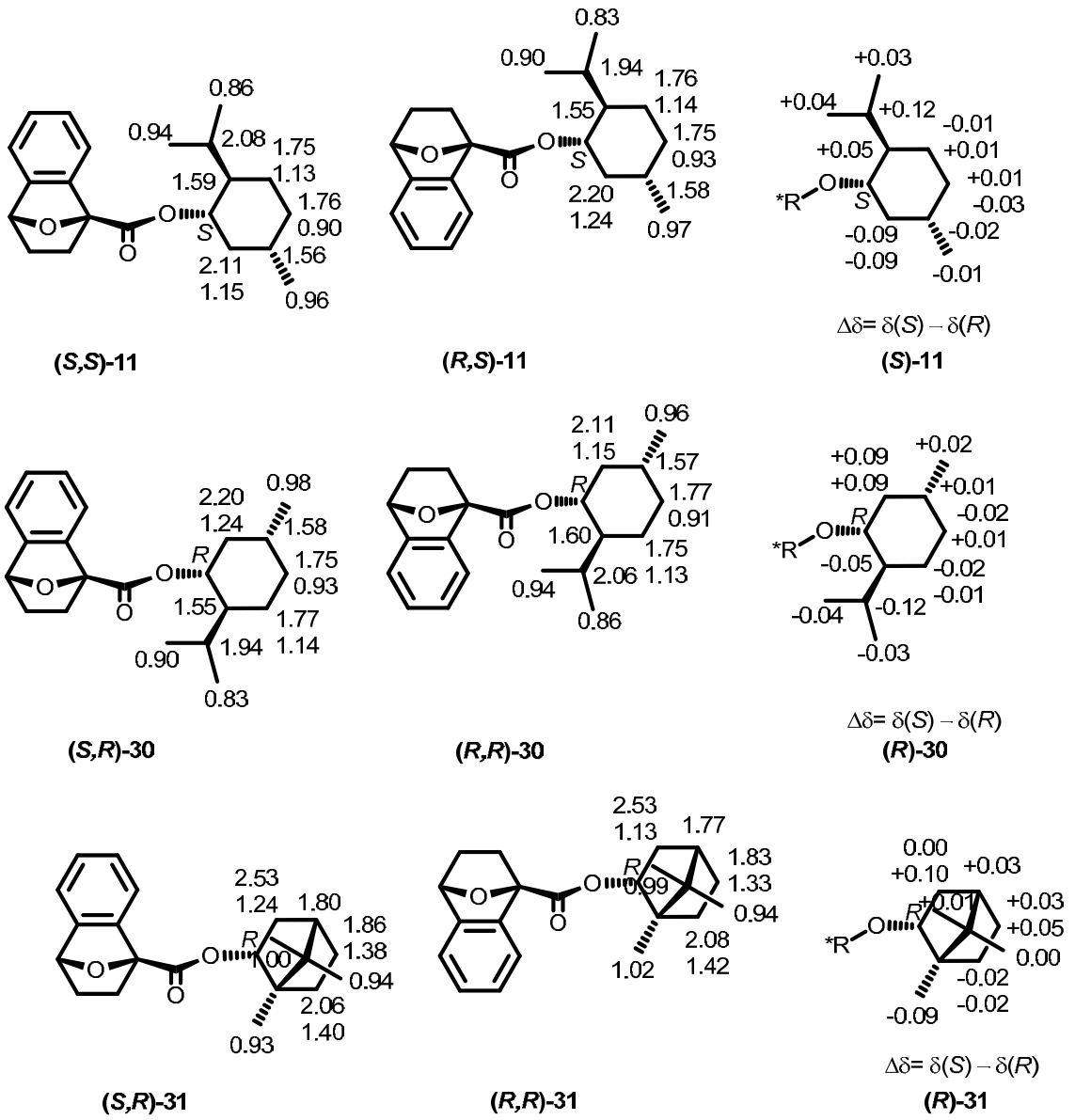

Figure 14. ^{1}H NMR chemical shift data of esters **11**, **22–31** and $\Delta\delta^{SR}$ values (continued).

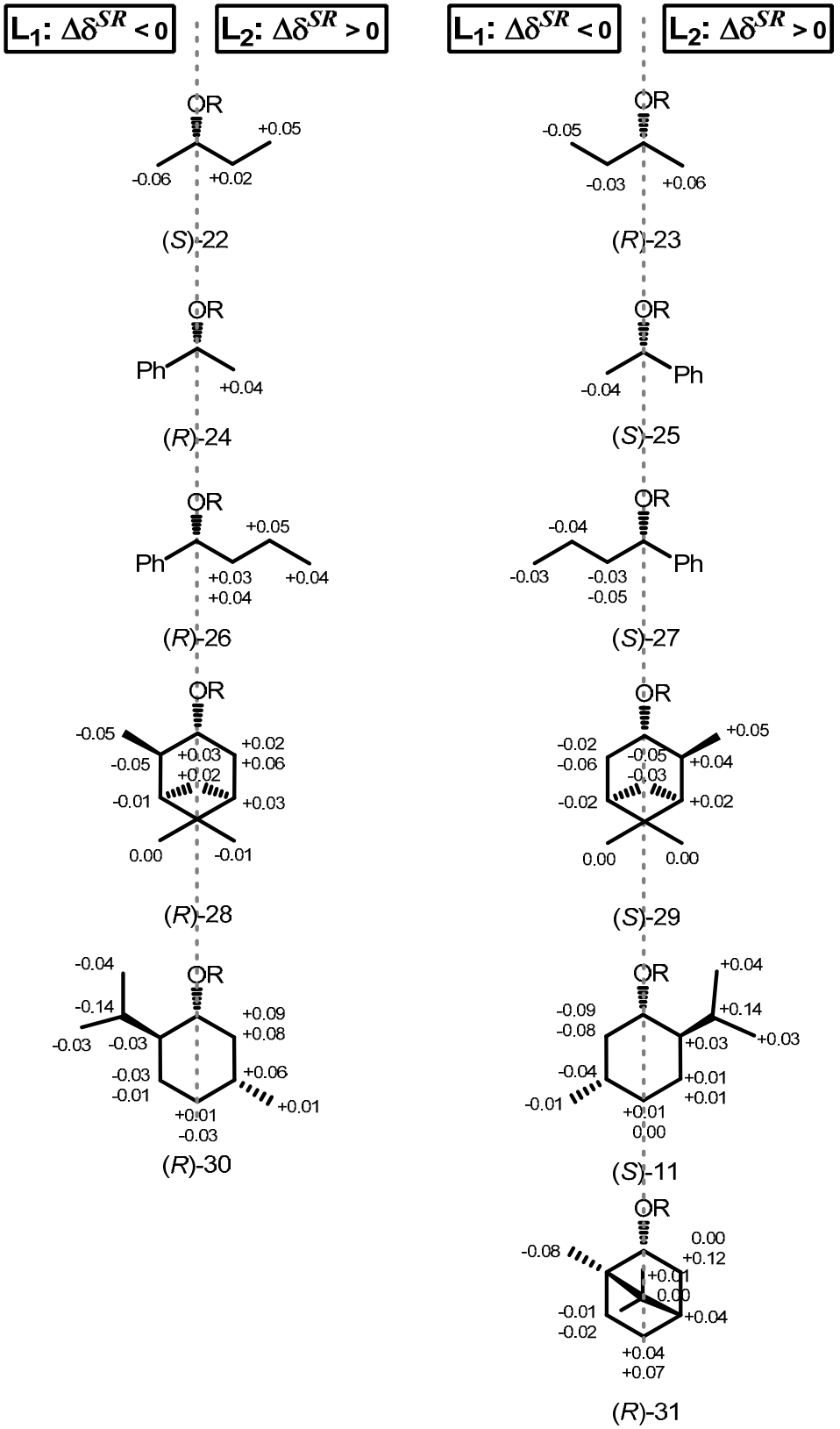

Figure 15. The chemical shift difference values ($\Delta\delta^{SR}$) of tested chiral alcohols with known absolute configuration (dashed line represents the plane).

Further study to improve the effectiveness and convenience in using the bicyclic acid as a chiral derivatizing agent was conducted. The aim was to extend the aromatic moiety to enhance the deshielding effect which would increase the chemical shift difference. Moreover, the methylene group of which the ^{1}H NMR signals were very complicated should be modified to appear with less complicated signals and in the region that did not interfere with other signals.

The α-alkoxa bicyclic acid **32** was then proposed. The naphthalene moiety should provide an extended anisotropic effect while the epoxide should provide a less complicated signal as well as its appearance at lower field which did not interfere much with aliphatic signals. The synthesis of **32** could be accomplished as described in Scheme 5. The Diels-Alder reaction of methyl furan-2-carboxylate **6** with naphthyne, generated from 3-amino-2-naphthoic acid **33** and *i*so-pentylnitrite, provided (±)-methyl 1,4-dihydro-1,4-epoxyanthracene-1-carboxylate ***rac*-34**. The adduct ***rac*-34** was epoxidized to yield compound ***rac*-35**. Then, compound ***rac*-35** was further subjected to hydrolysis to yield (±)-1*a*,2,9,9*a*-tetrahydro-2,9-epoxyanthra[2,3-*b*]oxirene-2-carboxylic acid (±)**-32**.

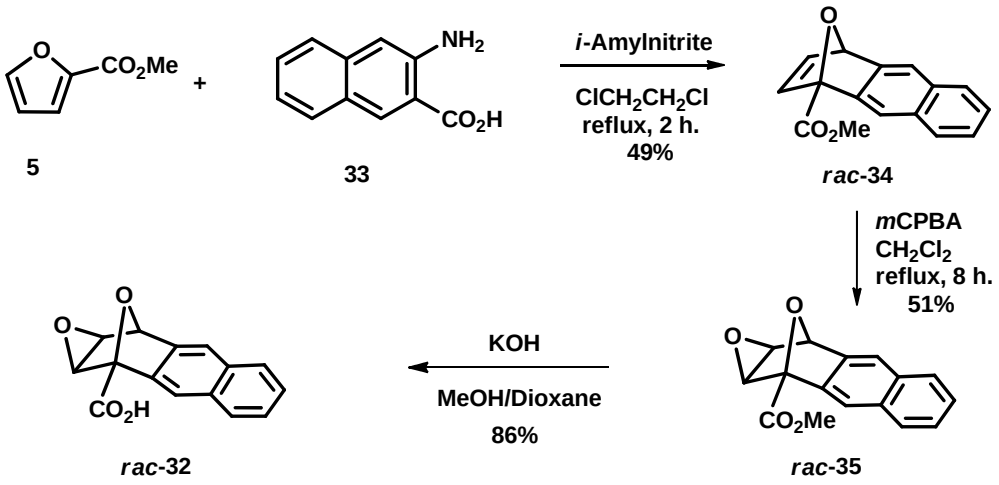

Scheme 5. Preparation of (±)-1*a*,2,9,9*a*-tetrahydro-2,9-epoxyanthra[2,3-*b*]oxirene-2 carboxylic acid ***rac*-32**.

Resolution of ***rac*-32** could be affected as follows. Treatment of ***rac*-32** with *D*-(+)-menthol and DMAP at room temperature in CH_2Cl_2 and then reacted with HBTU, following Pon's method,[12] gave diasteromers **(*S,S*)-36** and **(*R,S*)-36**. The mixture was separated by PLC

(Hexane:EtOAc 91:9). The first-eluted ester **(*S*,*S*)-36** and the second one **(*R*,*S*)-36** were obtained, respectively (Scheme 6).

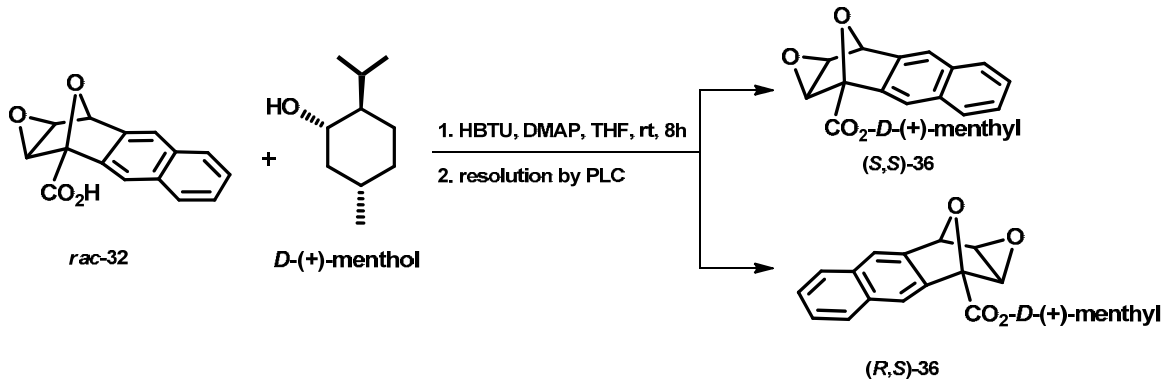

Scheme 6. Preparation of diastereomers **(*S*,*S*)-36** and **(*R*,*S*)-36**.

Similar to the benzene analog, it was proposed that the σ–π* interaction stabilized the conformation of the acid **32** in which the C−O bond, the ester carbonyl and C(1')H are situated in the same plane like *sp* conformer of MPA (Figure 16).

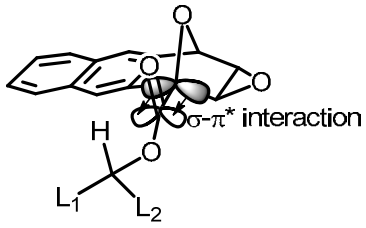

Figure 16. The stable conformation of the ester of compound **5**.

The anisotropic effect in the ^{1}H NMR spectra of diastereomeric esters **(*S*,*S*)-36** and **(*R*,*S*)-36** (Figure 17) showed that the protons of *iso*-propyl group in ester **(*S*,*S*)-36** were lower-field shifted than the analogous protons in **(*R*,*S*)-36**. As a result, the conformation of ester **(*S*,*S*)-36** should align in the way that was *iso*-propyl group situated close to the aromatic group. On the other hand, the *iso*-propyl group of ester **(*R*,*S*)-36** should place away from the aromatic group.

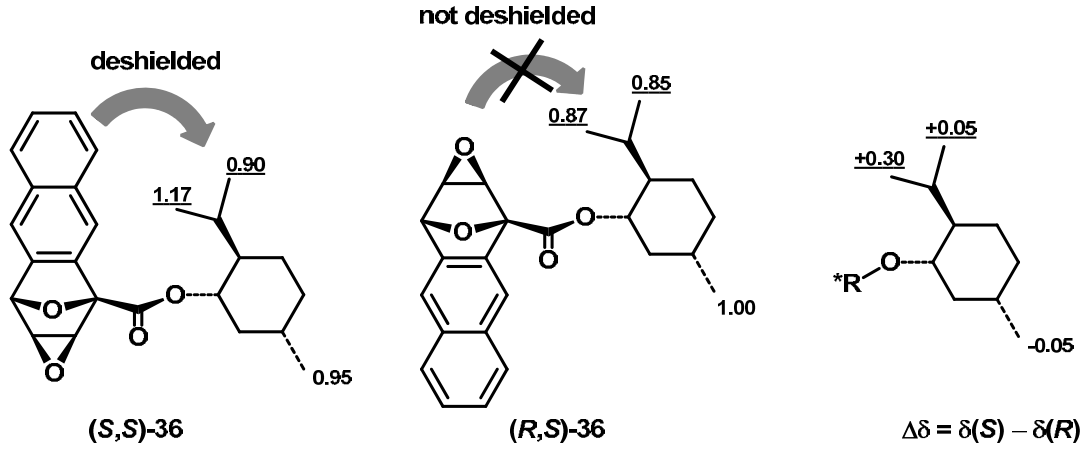

Figure 17. ^{1}H NMR chemical shift data of esters **(*S*,*S*)-36** and **(*R*,*S*)-36** and Δδ values.

Finally, (+)-2,3-dihydro-1,4-epoxynaphthalene-1(2H)-carboxylic acid **(*S*)-(+)-32** could be obtained from the hydrolysis of **(*S*,*S*)-36** while (–)-2,3-dihydro-1,4-epoxynaphthalene-1(2H)-carboxylic acid **(*R*)-(–)-32** could be obtained from the hydrolysis of **(*R*,*S*)-36**.

*The validation of acid **5** with a variety of chiral secondary alcohols*

To obtain optically active acid **(*R*)-(+)-5** and **(*S*)-(–)-5**, compound **(*R*,*S*)-37** and **(*S*,*S*)-37** were subjected to hydrolysis with KOH in 1:1 MeOH:Dioxane at room temperature for 3 h to give **(*R*)-(+)-5** and **(*S*)-(–)-5** in 82% and 95% yields, respectively (Scheme 7).

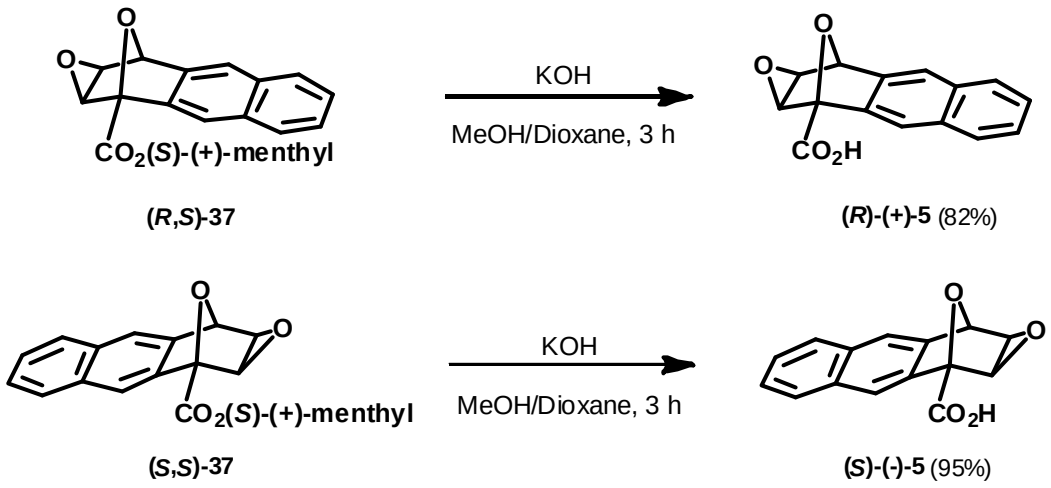

Scheme 7. Preparation of optically active acids **(*R*)-(+)-5** and **(*S*)-(–)-5**.

Then, optically active acids **(*R*)-(+)-5** and **(*S*)-(–)-5** would be tested with a variety of chiral secondary alcohols, **(*S*)-(+)-14, (*R*)-(–)-15, (*S*)-(–)-19, (*R*)-(–)-22** and **(*R*)-(–)-23** of which the absolute configurations were already known, as shown in Figure 18.

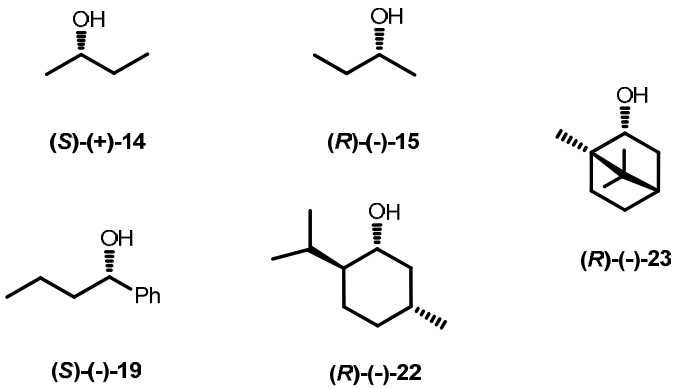

Figure 18. The optically chiral alcohols used for tested the anisotropic effect of acid **5**.

Diastereomeric esters of **(*R*)-(+)-5** and **(*S*)-(–)-5** with the optically active alcohols could be prepared as follows. Treatment of the optically active acids **(*R*)-(+)-5** and **(*S*)-(–)-5** separately with the optically active alcohol of interest and DMAP at room temperature in CH_2Cl_2 and then HBTU gave the corresponding diastereomeric pairs. The products were separated by PLC (Hexane:EtOAc = 95:5–90:10) (Scheme 8).

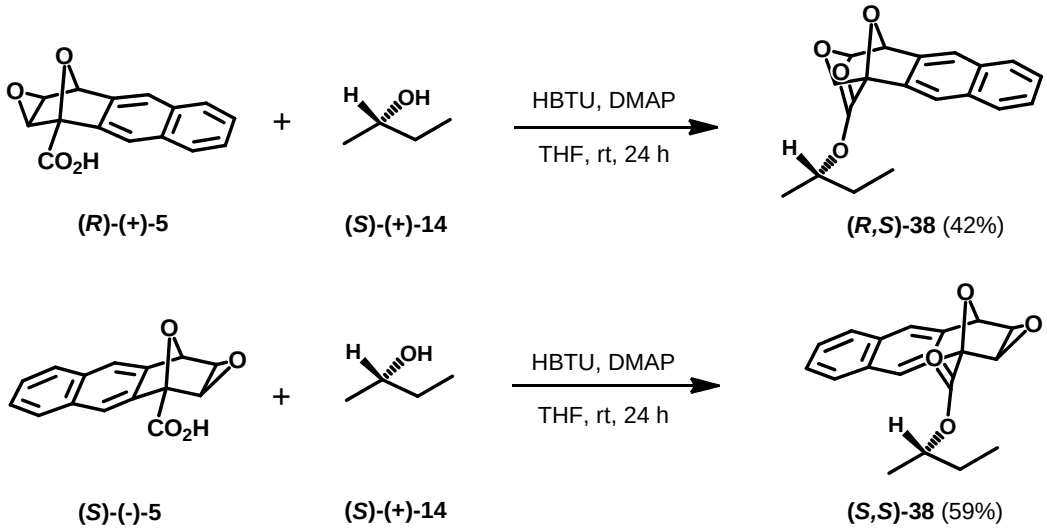

Scheme 8. Preparation of diastereomeric esters of optically active acid **5** with the tested alcohols.

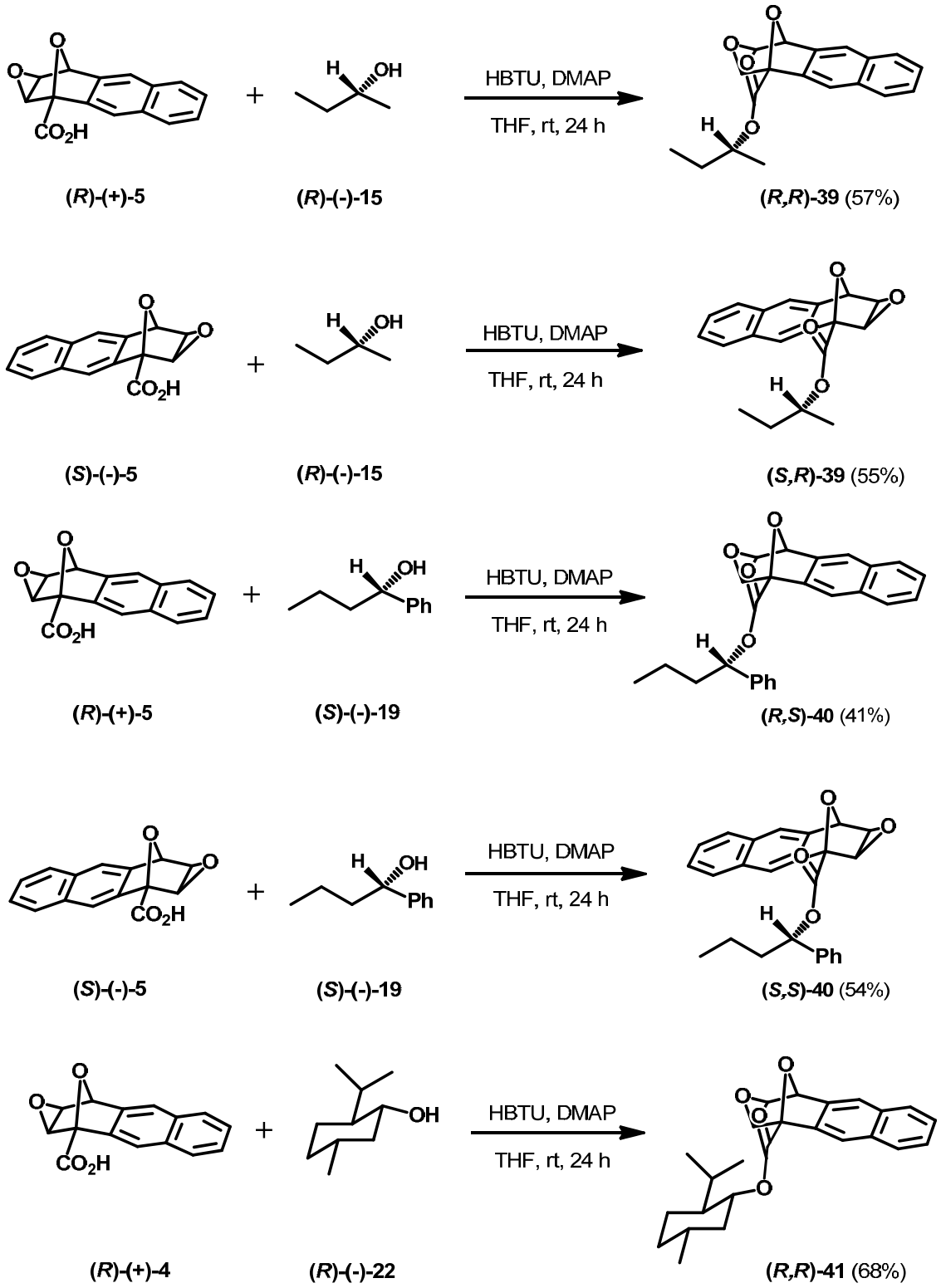

Scheme 8. Preparation of diastereomeric esters of optically active acid **5** with the tested alcohols (continued).

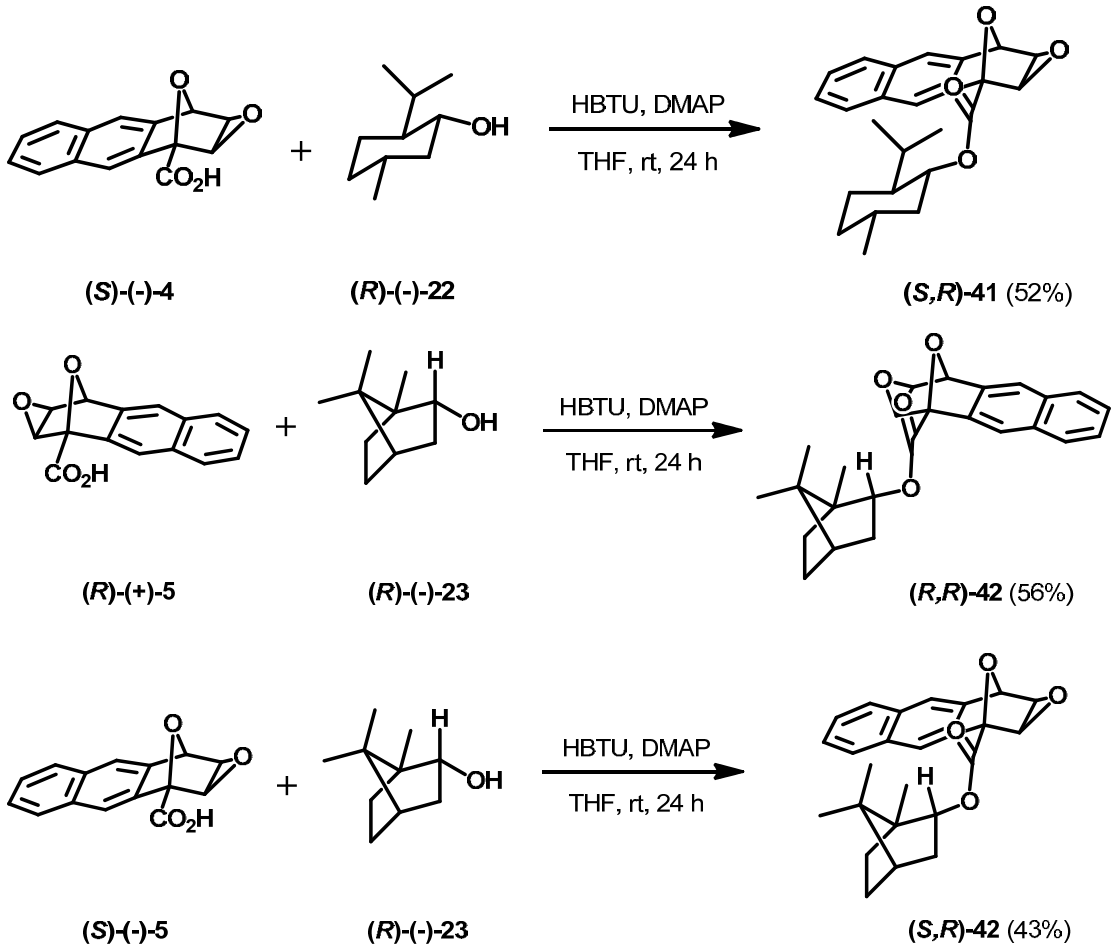

Scheme 8. Preparation of diastereomeric esters of optically active acid **5** with the tested alcohols (continued).

The chemical shift difference data of the diastereomeric esters of the optically active acid **5** with the tested alcohols were listed in Figure 19, and the $\Delta\delta^{RS}$ values (ppm): $\Delta\delta^{RS} = \delta(R) - \delta(S)$ are summarized in Figure 20. Similar to the benzene derivative, it was found that protons of the alkyl group which were close to the aromatic side of the acid residue were downfield shifted by the anisotropic effect while the protons of the alkyl group which were far away from aromatic ring of the acid were not shifted. The resulting signs of $\Delta\delta^{RS}$ values correlated with the model could determine the absolute configuration and all found to be identical to the known configuration of the tested alcohols.

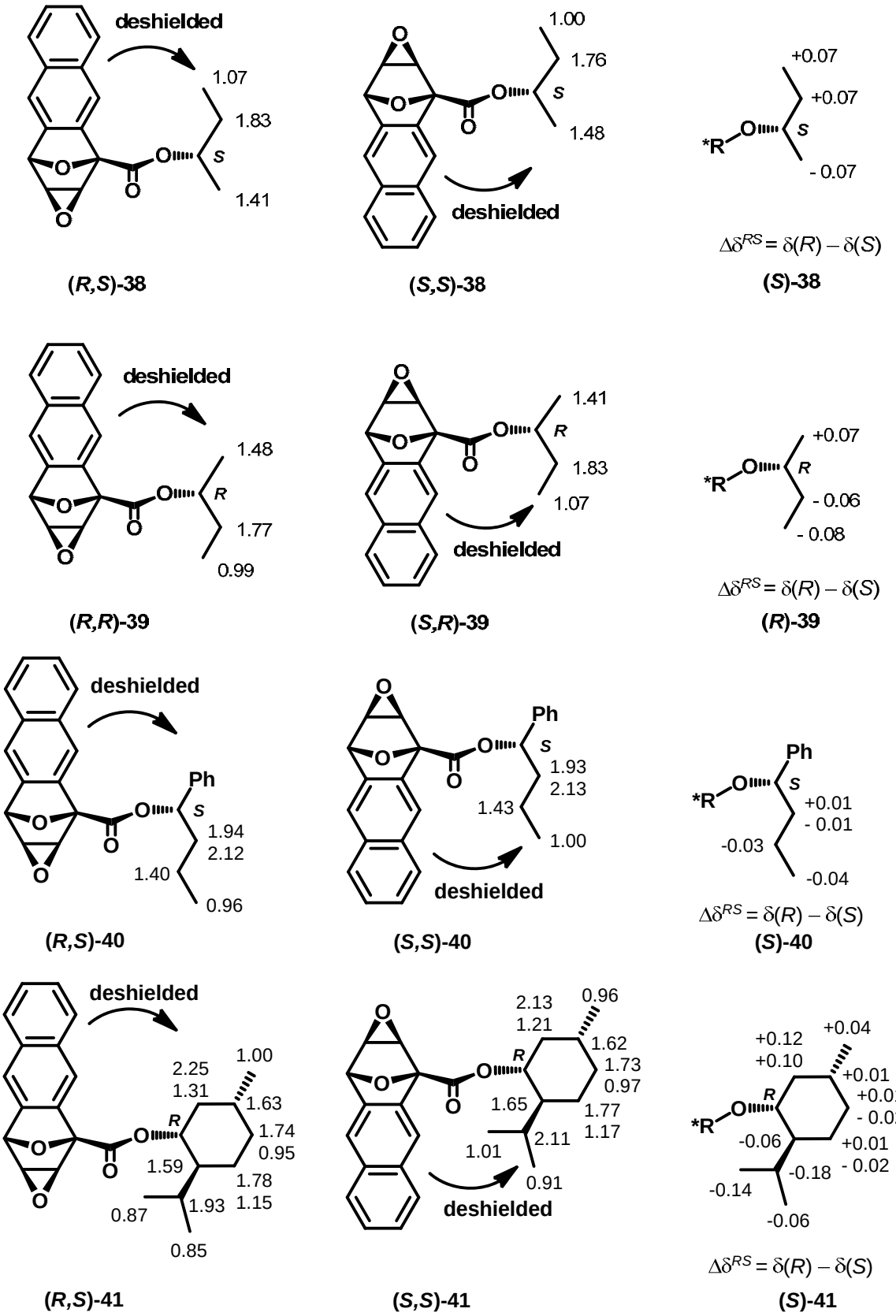

Figure 19. ^{1}H NMR chemical shift data of the esters of optically active acid **5** with the tested alcohols and the corresponding $\Delta\delta^{RS}$ values.

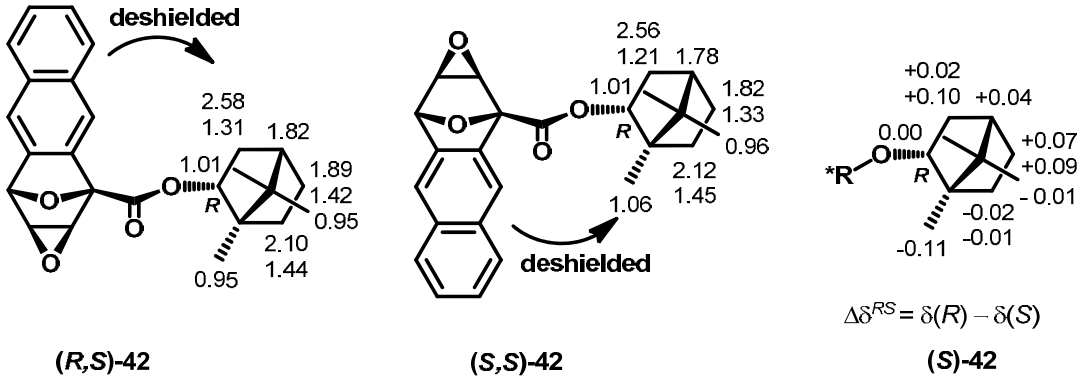

Figure 19. ^{1}H NMR chemical shift data of the esters of optically active acid **5** with the tested alcohols and the corresponding $\Delta\delta^{RS}$ values (continue).

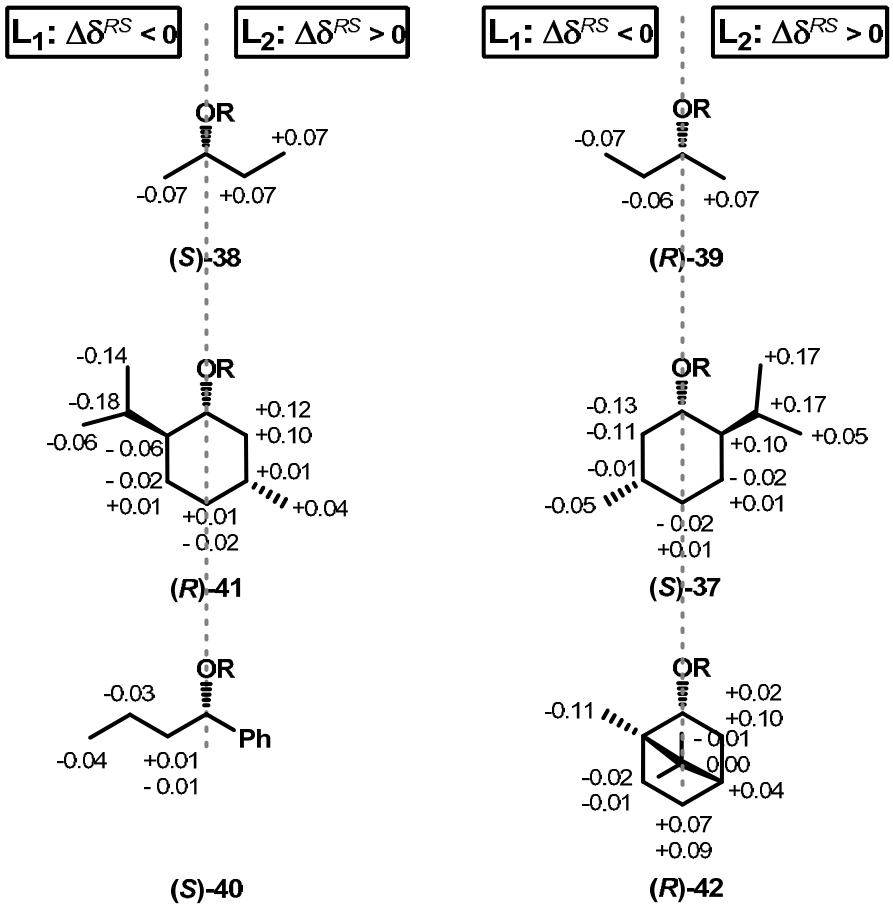

Figure 20. Chemical shift difference values ($\Delta\delta^{RS}$) of tested chiral alcohols with known absolute configuration (dashed line represents the plane).

REFERENCES

1. Allenmark, S.; Gawronski, J. *Chirality* **2008**, *20*, 606-608.
2. Harada, N. *Top. Stereochem.* **2006**, *25*, 177-203.
3. Djerassi, C. Optical Rotatory Dispersion. McGraw-Hill, New York, NY **1960**, 187.
4. Seco, J. M.; Quinoa, E.; Riguera, R. *Chem. Rev.* **2004**, *104*, 17-118.
5. Dale, J. A.; Mosher, H. S. *J. Am. Chem. Soc.* **1973**, *95*, 512-519.
6. Kasai, Y.; Sugio, A.; Sekiguchi, S.; Kuwahara, S.; Matsumoto, T.; Watanabe, M.; Ichikawa, A.; Harada, N. *Eur. J. Org. Chem.* **2007**, 11, 1811-1826.
7. Ohtani, I.; Kusumi, T.; Kashman, Y.; Kakisawa, H. *J. .Am. Chem. Soc.* **1991**, *113*, 4092-4096.
8. Latypov, S. K.; Seco, J. M.; Quinoa, E.; Riguera, R. *J. .Org. Chem.* **1996**, *61*, 8569-8577.
9. Best, W. M.; Collins, P. A.; McCulloch, R. K.; Wege, D. *Aust. J. Chem.* **1982**, *35*, 843-848.
10. Thongpanchang, T.; Paruch, K.; Katz, T. J.; Rheingold, A. L.; Lam, K.-C.; Liable-Sands, L. *J. Org. Chem.* **2000**, *65*, 1850-1856.
11. Ruangsupapichat, N [M.Sc. Thesis in Organic Chemistry]. Bangkok: Facuty of Graduate Studies, Mahidol University; **2006**.
12. Pon, R. T.; Yu, S.; Sanghvi, Y. S. *Bioconj. Chem.* **1999**, *10*, 1051-1057.

APPENDIX

\

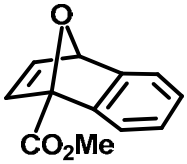

rac-9

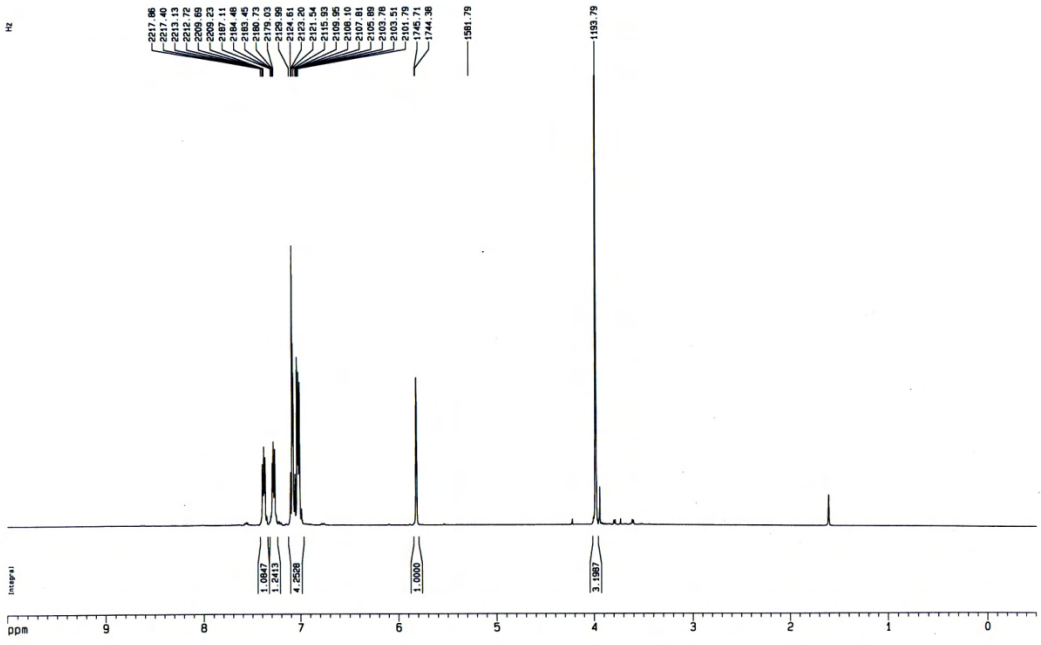

Figure A1. ^{1}H NMR spectrum of compound ***rac*-9.**

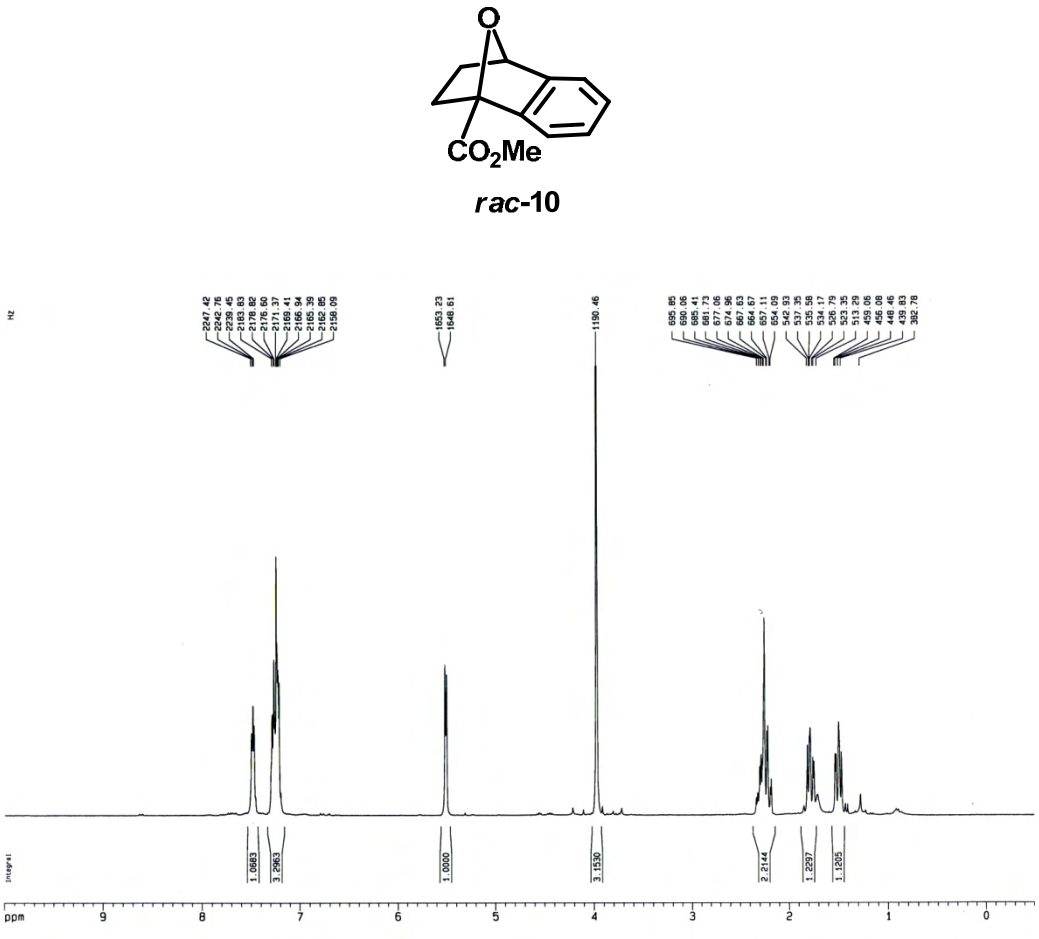

Figure A1. ^{1}H NMR spectrum of compound ***rac*-10**.

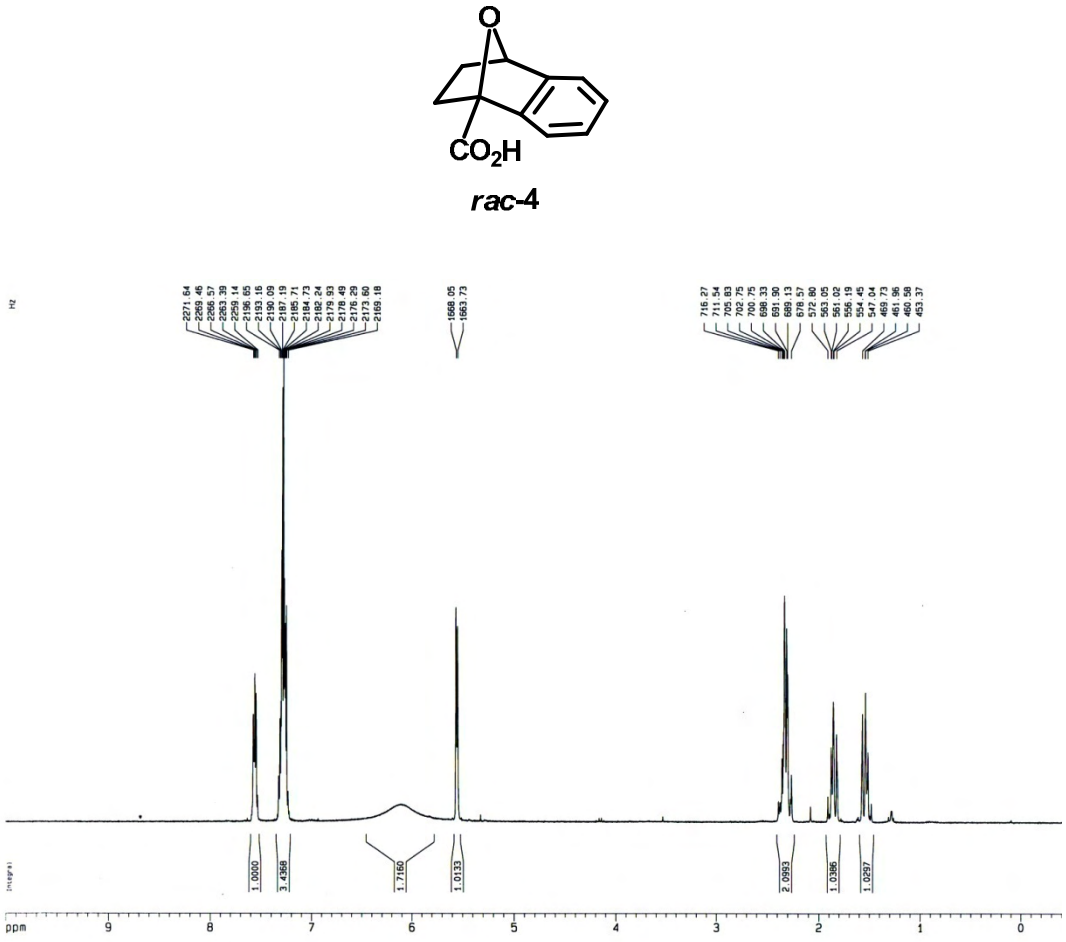

Figure A3. ^{1}H NMR spectrum of compound ***rac*-4**.

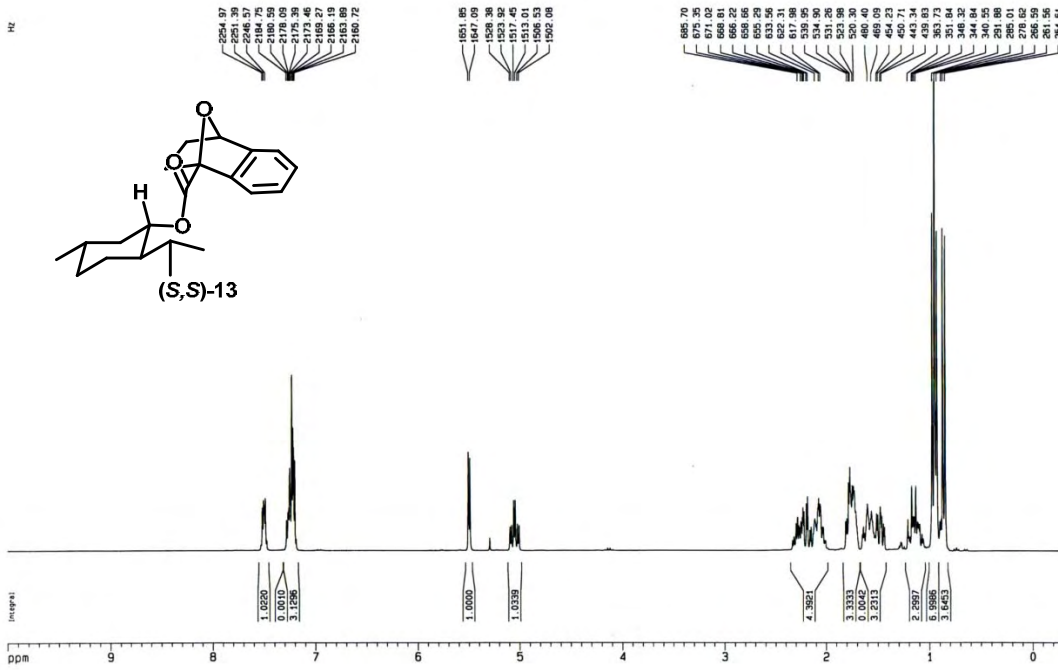

Figure A4. ^{1}H NMR spectrum of compound **(*S*,*S*)-13**.

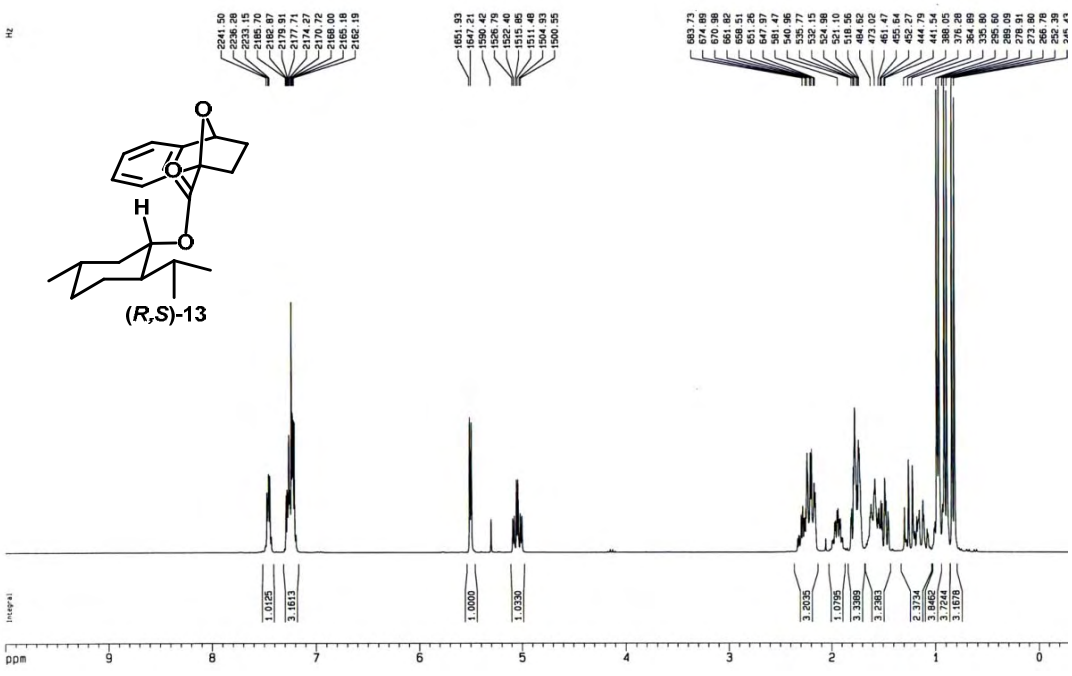

Figure A5. ^{1}H NMR spectrum of compound **(*R*,*S*)-13**.

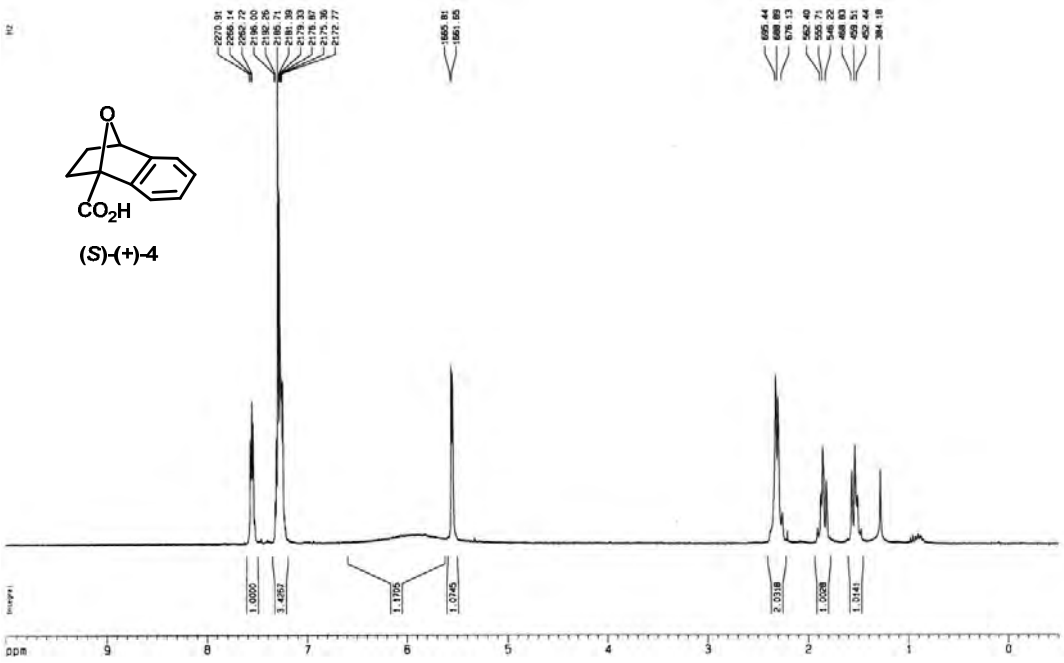

Figure A6. ^{1}H NMR spectrum of compound **(*S*)-(+)-4**.

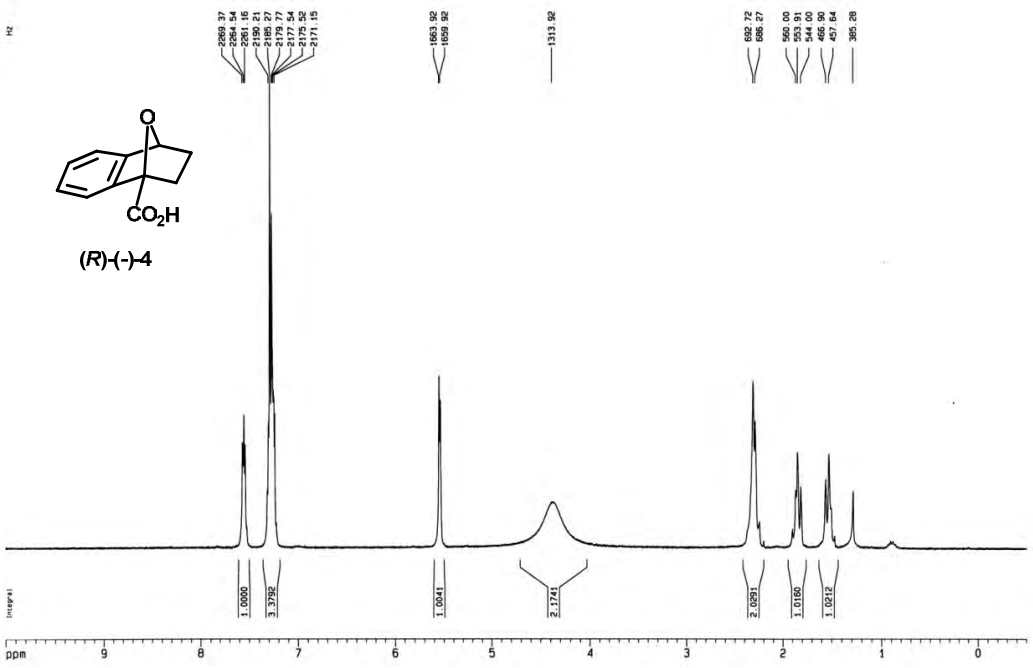

Figure A7. ^{1}H NMR spectrum of compound **(*R*)-(–)-4**.

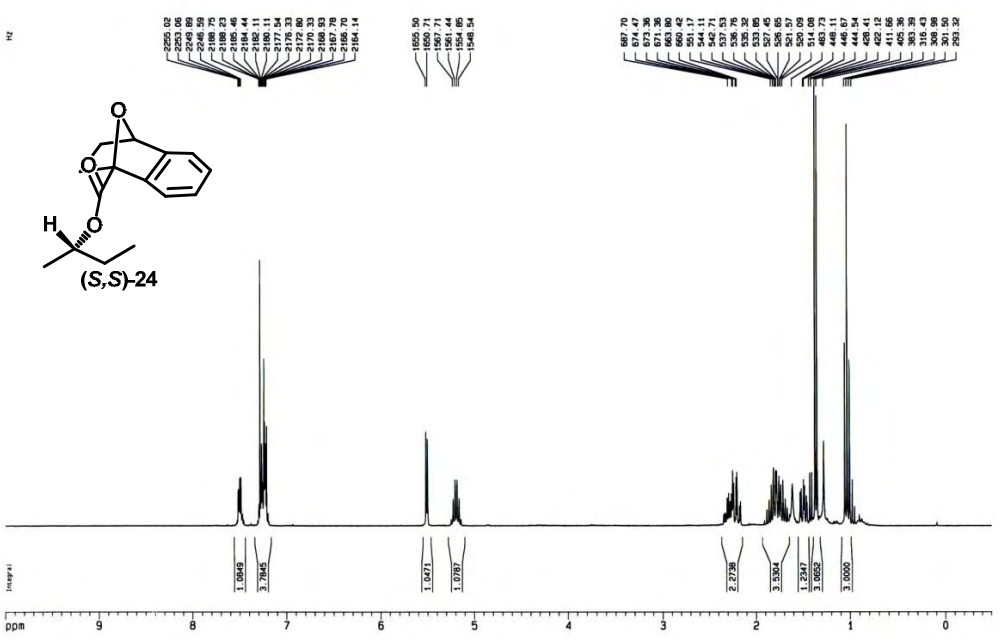

Figure A8. ^{1}H NMR spectrum of compound **(*S*,*S*)-24**.

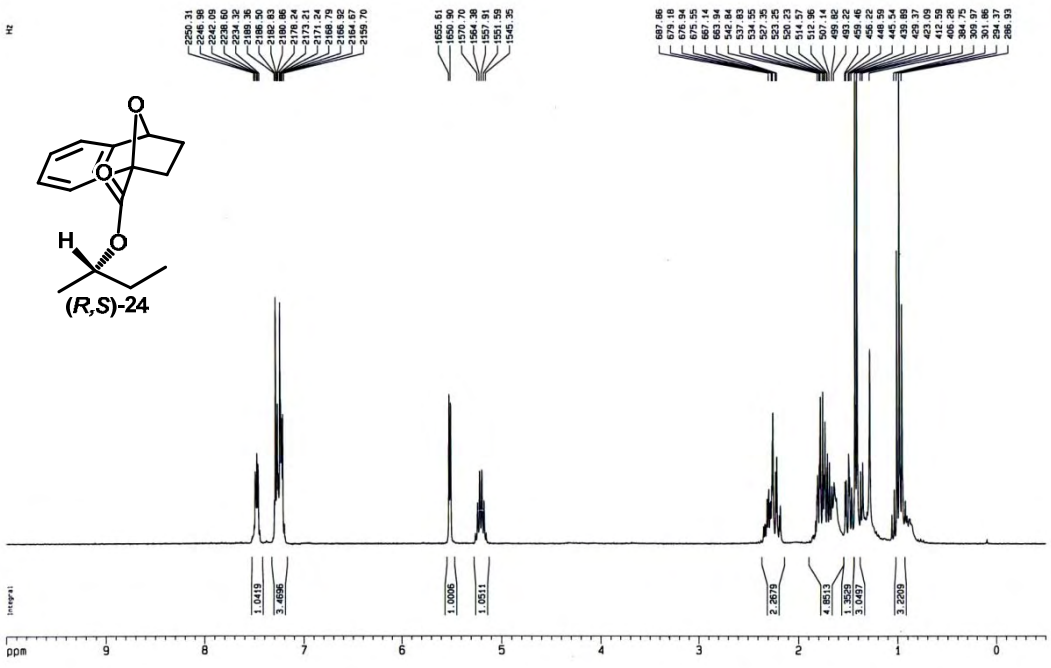

Figure A9. ^{1}H NMR spectrum of compound **(*R*,*S*)-24**.

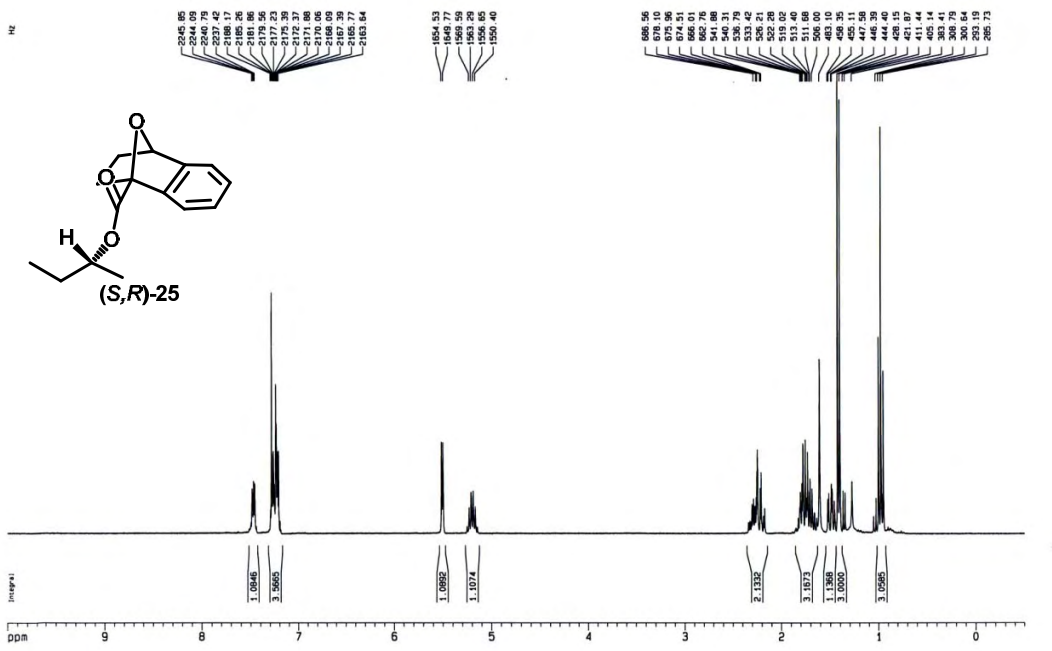

Figure A10. ^{1}H NMR spectrum of compound **(*S*,*R*)-25**.

^{1}H NMR in $CDCl_3$

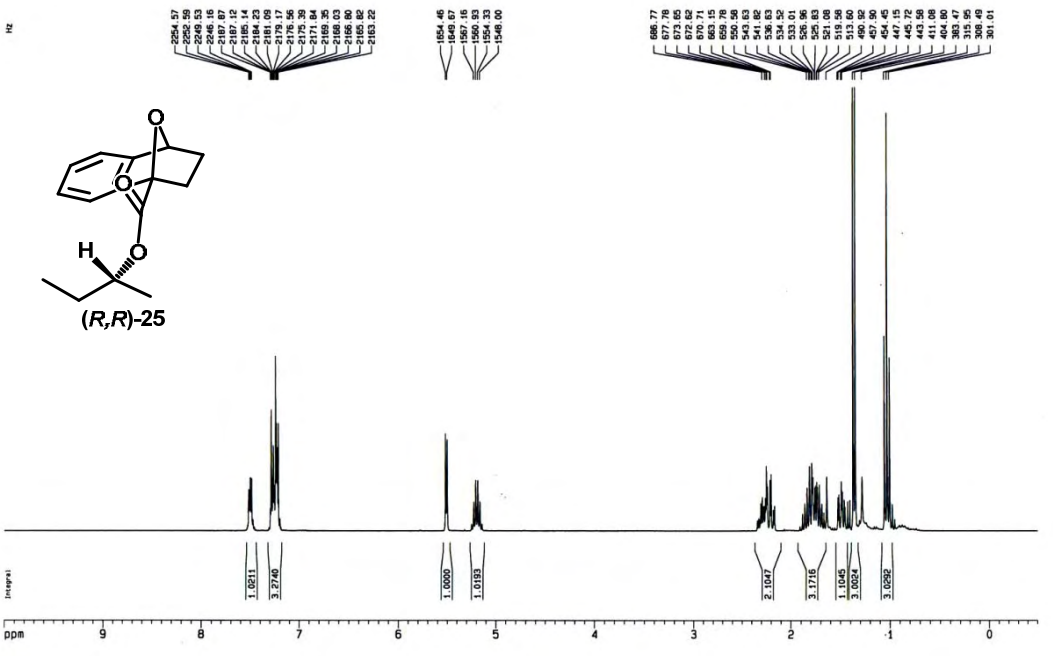

Figure A11. ^{1}H NMR spectrum of compound **(*R*,*R*)-25**.

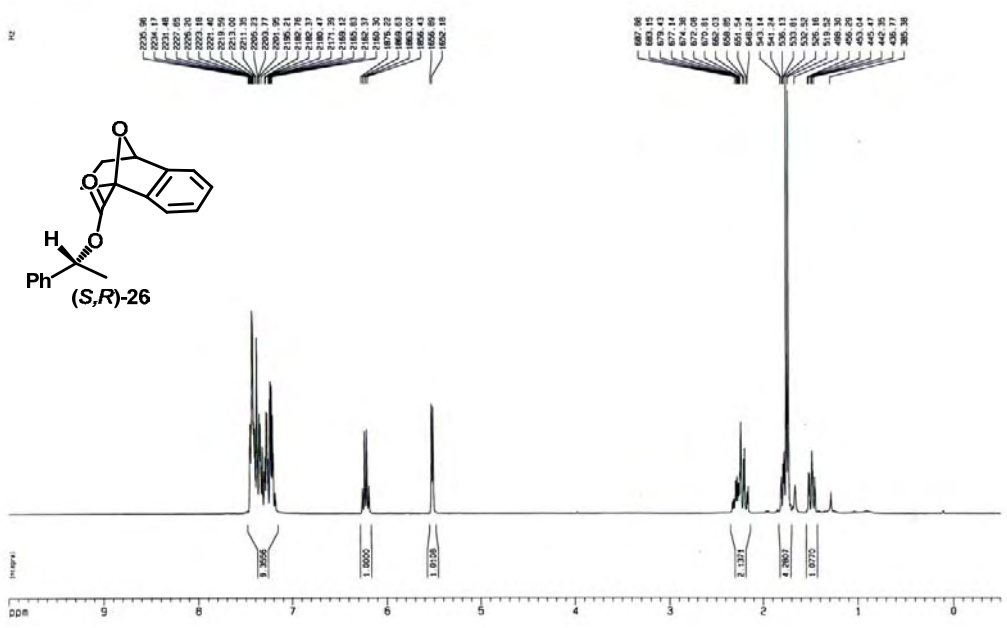

Figure A12. ^{1}H NMR spectrum of compound **(*S*,*R*)-26**.

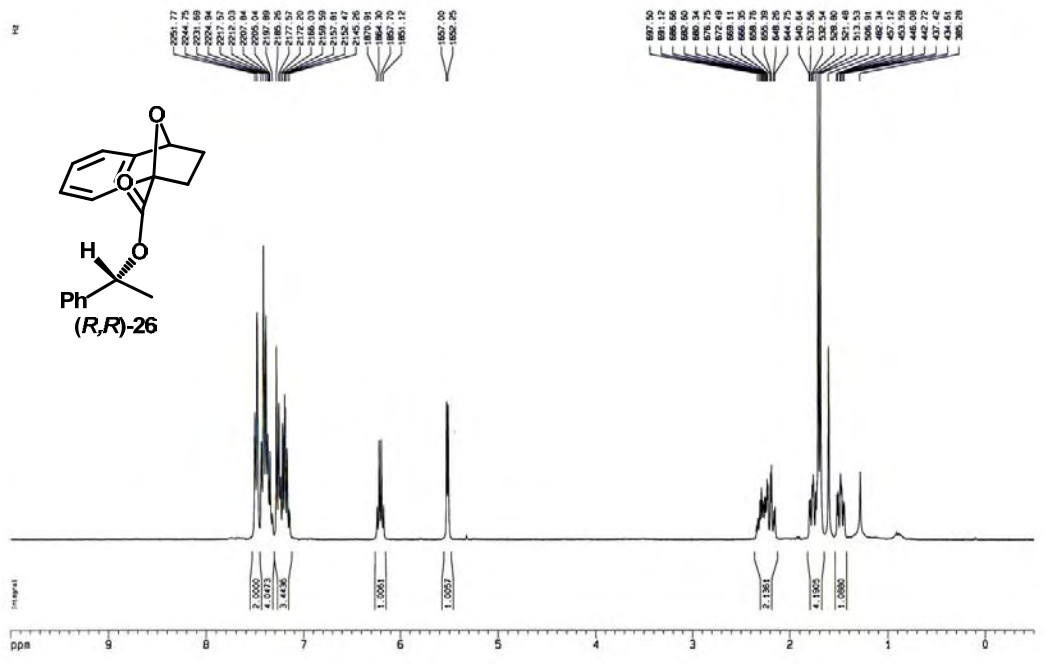

Figure A13. ^{1}H NMR spectrum of compound **(*R*,*R*)-26**.

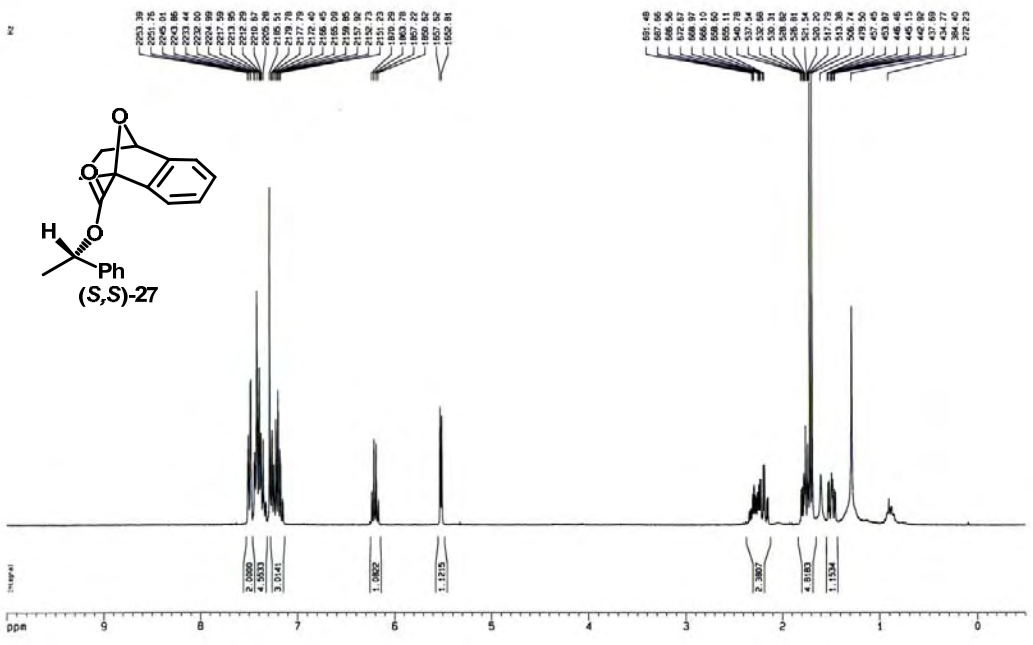

Figure A14. ^{1}H NMR spectrum of compound **(*S*,*S*)-27**.

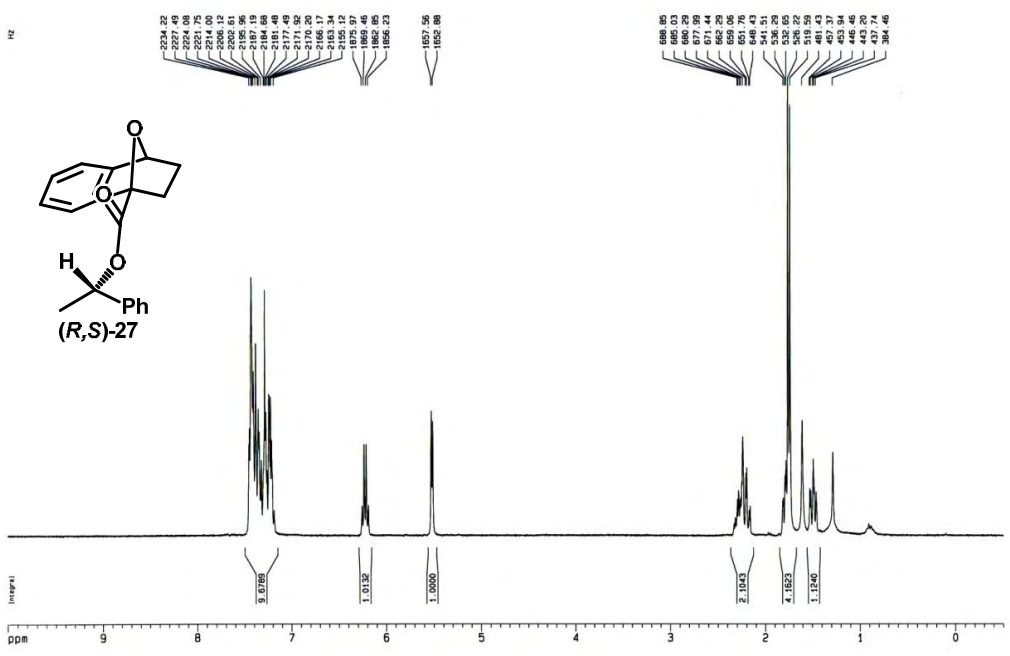

Figure A15. ^{1}H NMR spectrum of compound **(*R*,*S*)-27**.

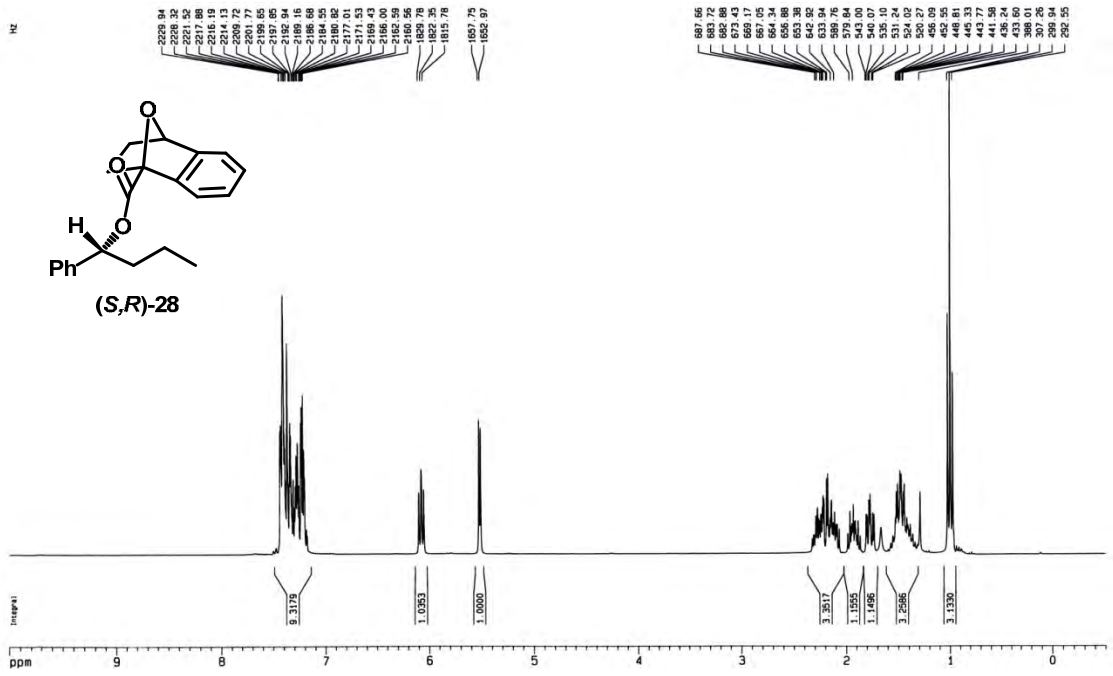

Figure A16. ^{1}H NMR spectrum of compound **(*S*,*R*)-28**.

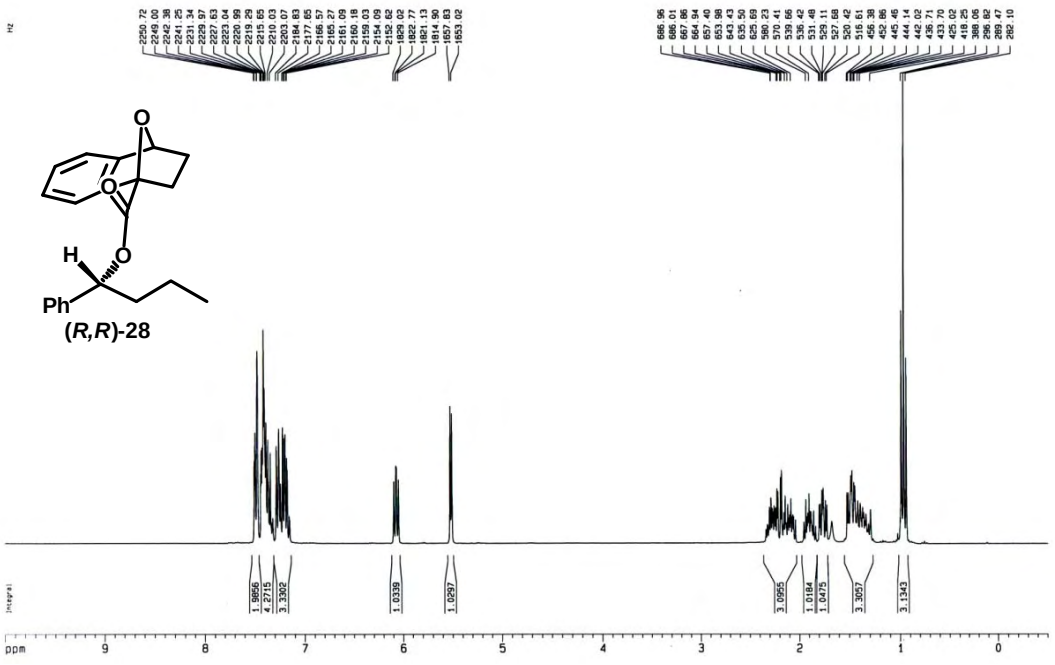

Figure A17. ^{1}H NMR spectrum of compound **(*R*,*R*)-28**.

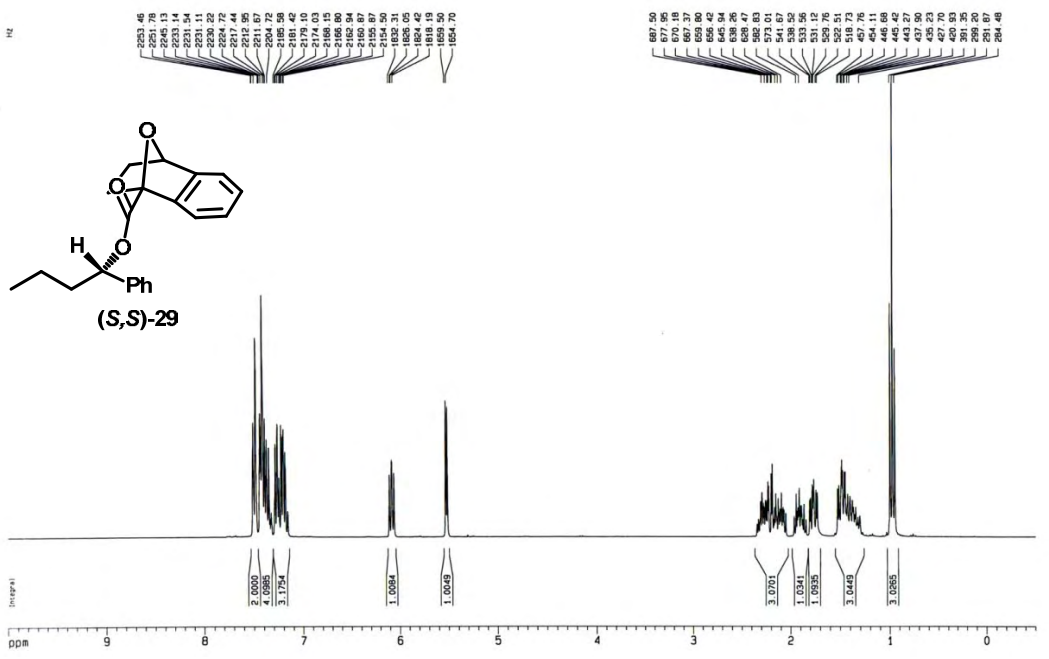

Figure A18. ^{1}H NMR spectrum of compound **(*S*,*S*)-29**.

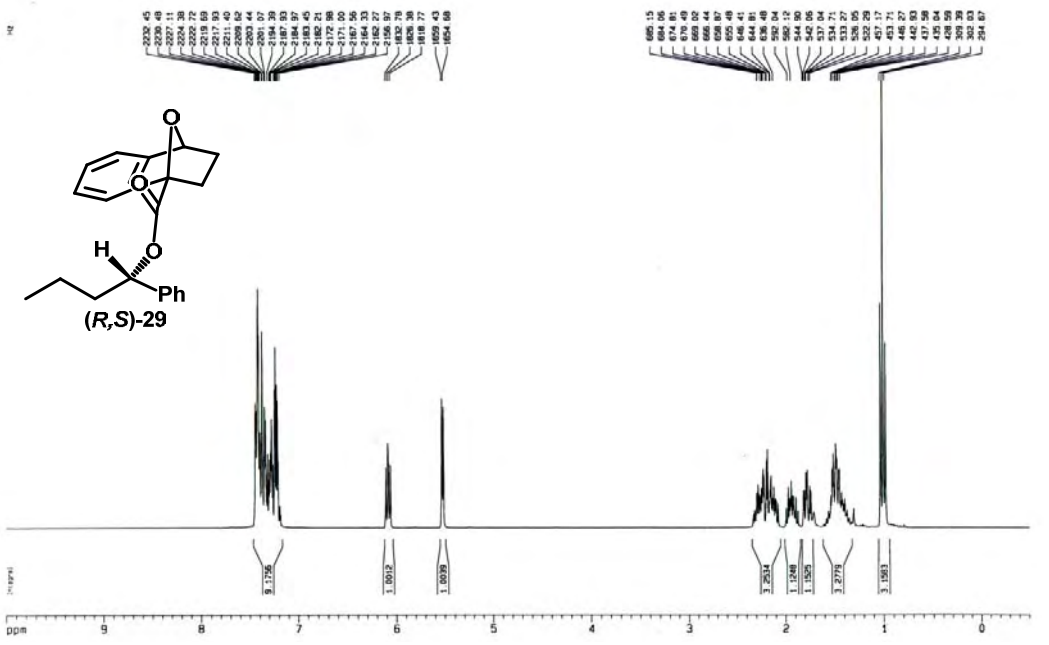

Figure A19. ^{1}H NMR spectrum of compound **(*R*,*S*)-29**.

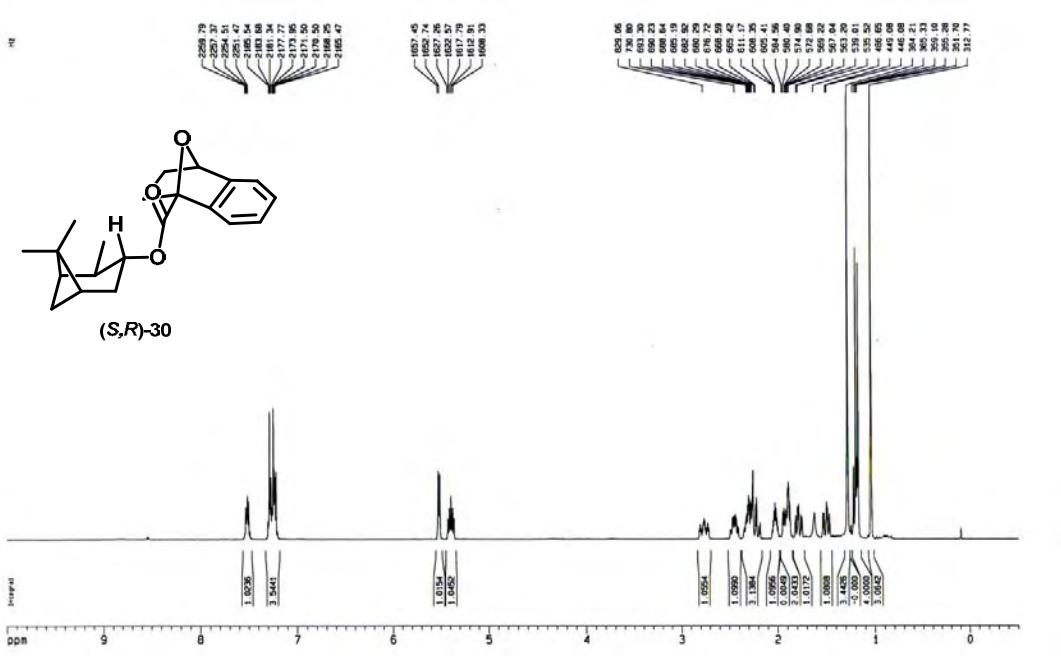

Figure A20. ^{1}H NMR spectrum of compound **(*S*,*R*)-30**.

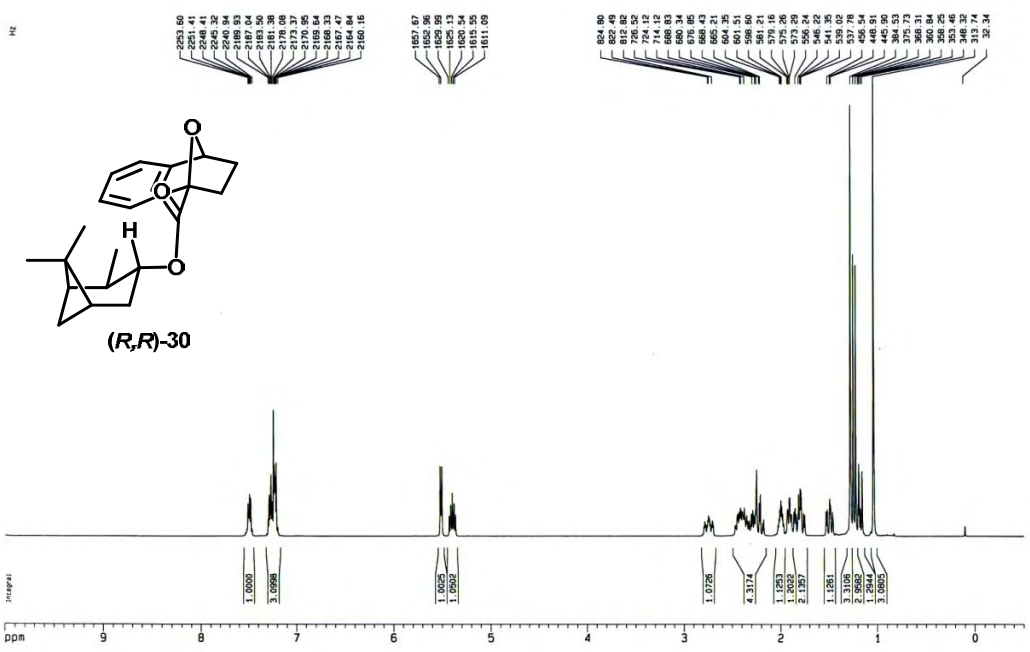

Figure A21. ^{1}H NMR spectrum of compound **(*R*,*R*)-30**.

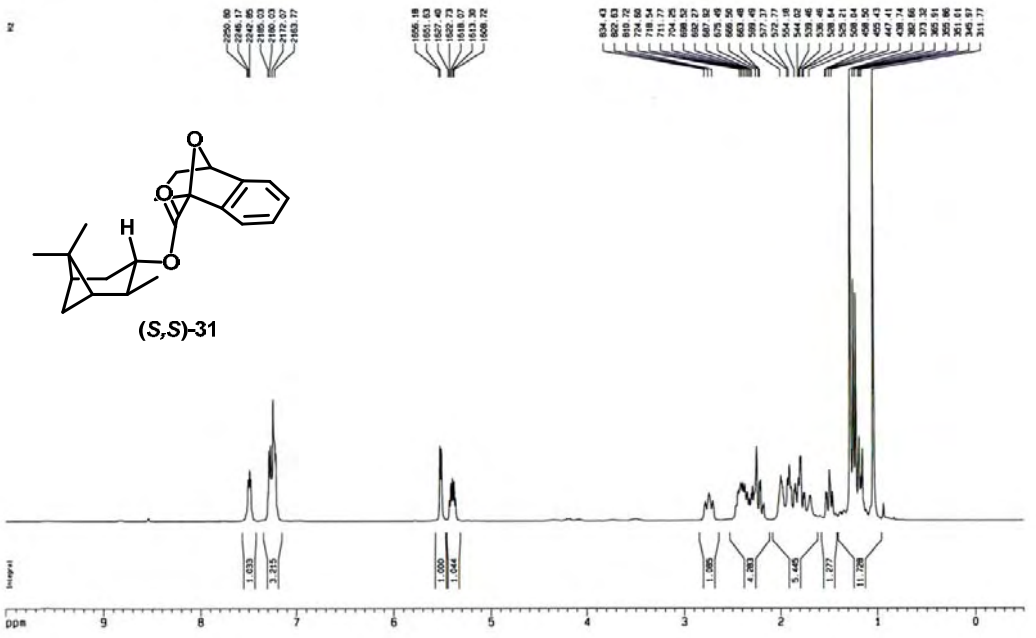

Figure A22. ^{1}H NMR spectrum of compound **(*S*,*S*)-31**.

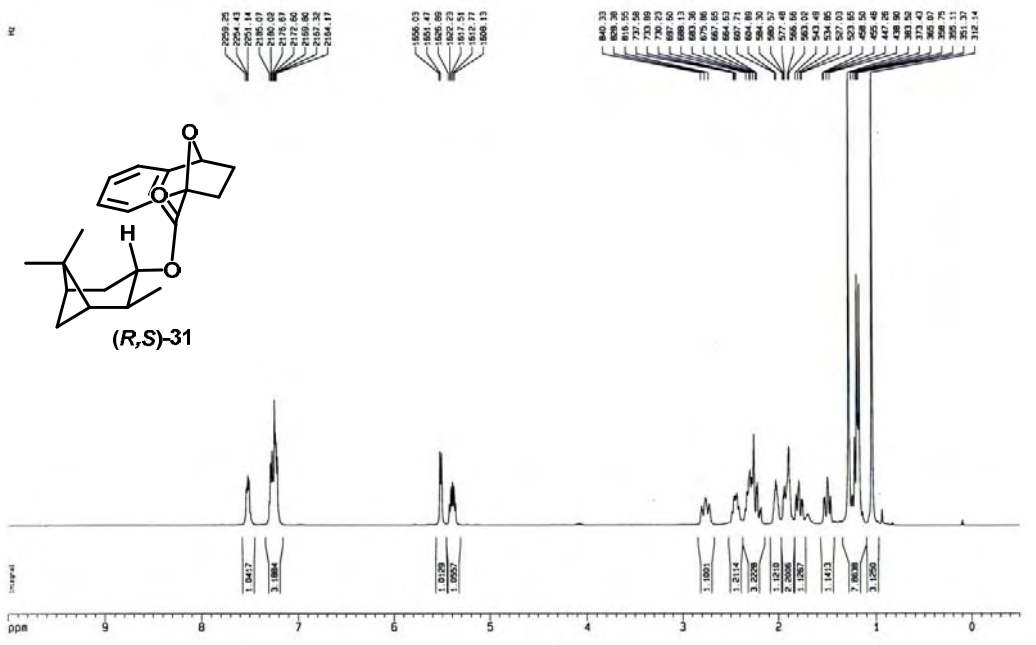

Figure A23. ^{1}H NMR spectrum of compound **(*R*,*S*)-31**.

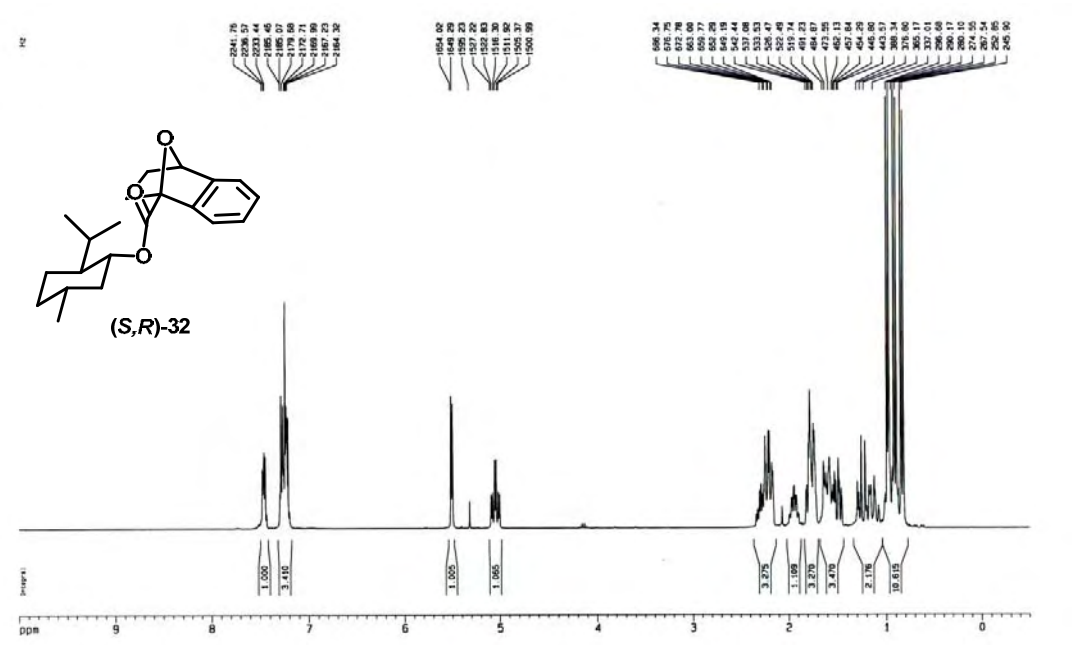

Figure A24. ^{1}H NMR spectrum of compound **(*S*,*R*)-32**.

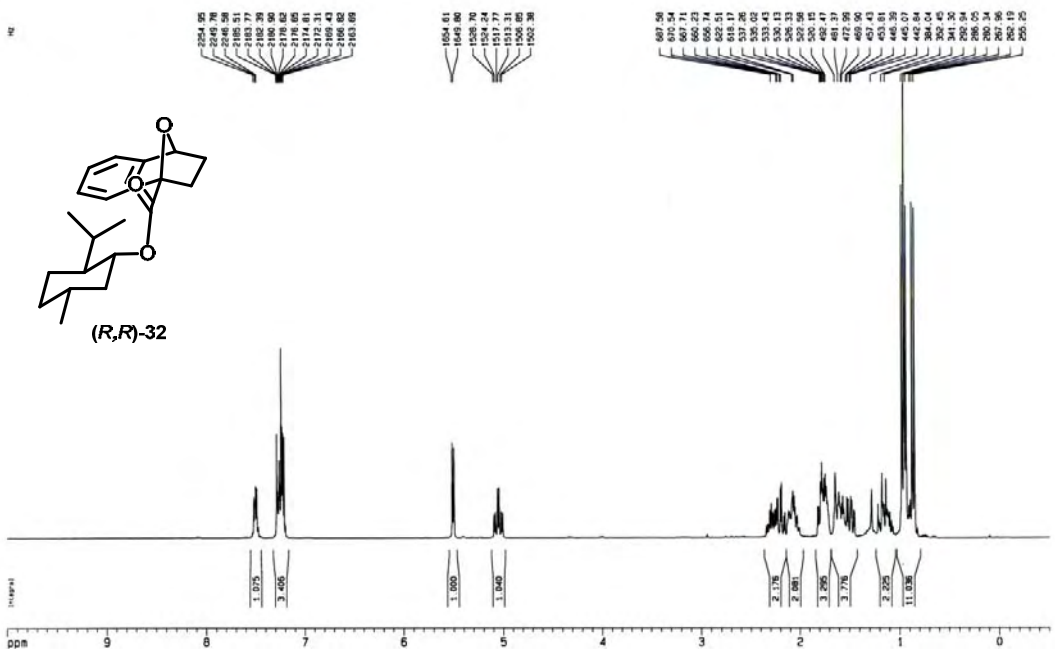

Figure A25. ^{1}H NMR spectrum of compound **(*R*,*R*)-32**.

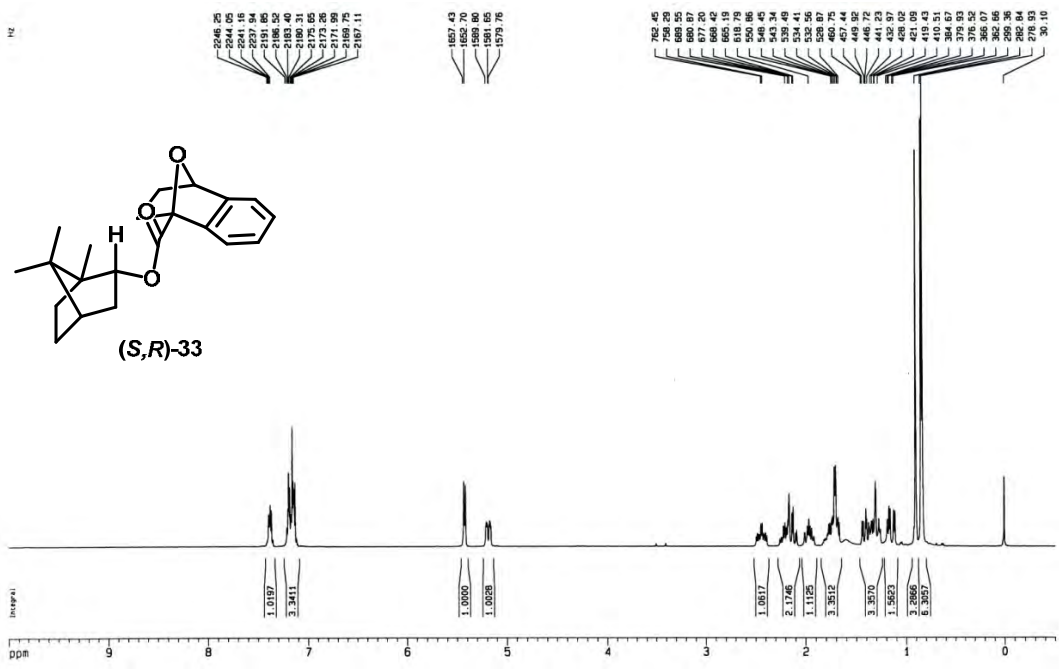

Figure A26. ^{1}H NMR spectrum of compound **(*S*,*R*)-33**.

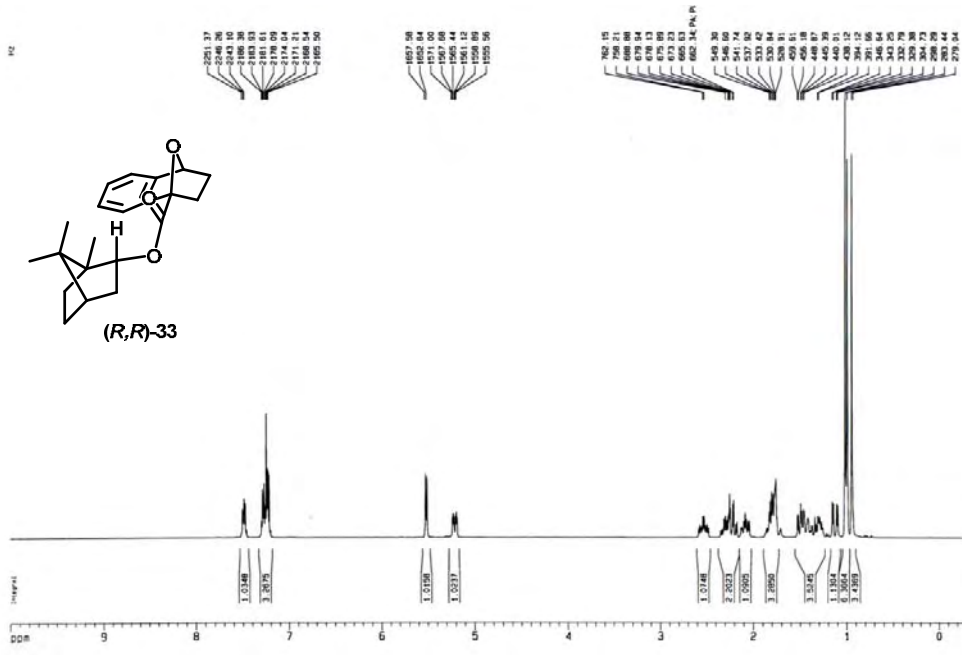

Figure A27. ^{1}H NMR spectrum of compound **(*R*,*R*)-33**.

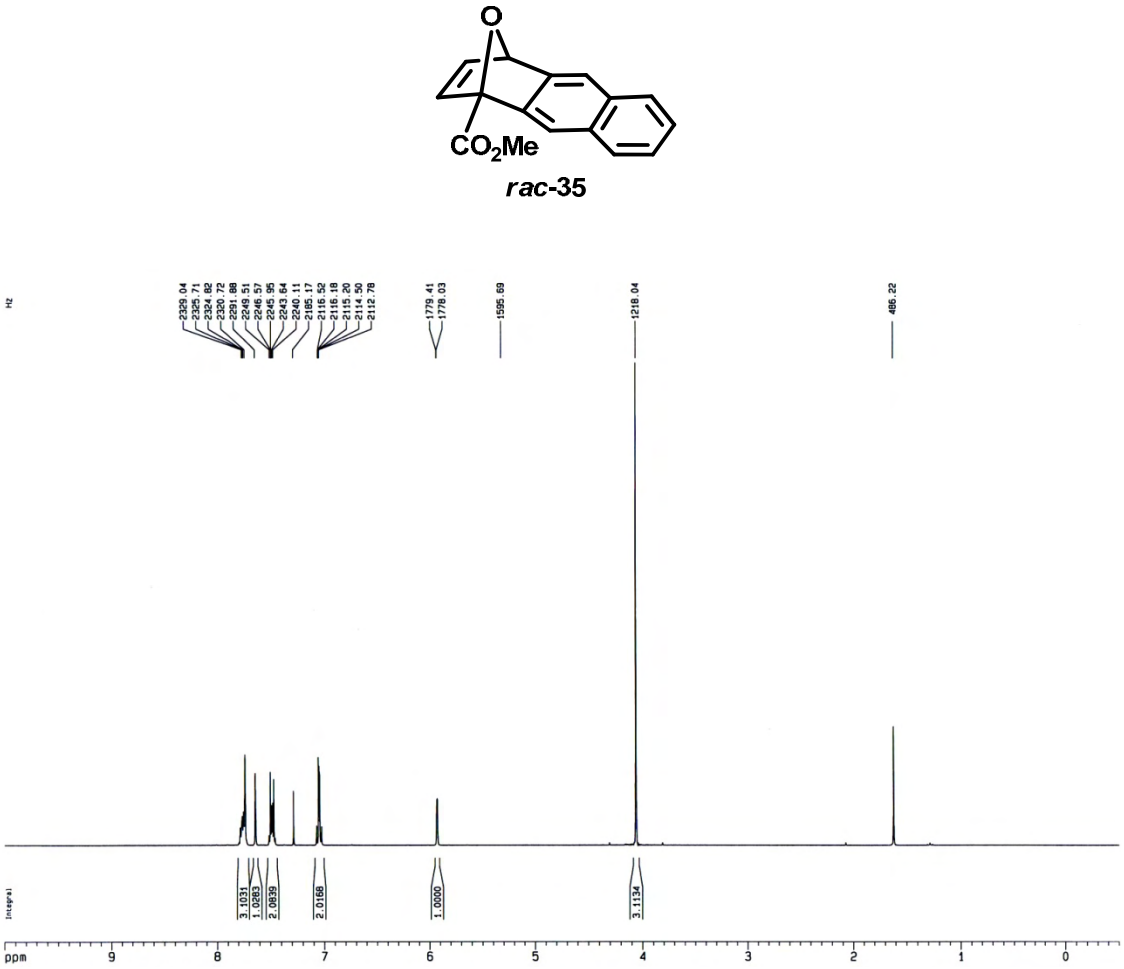

Figure A27. ^{1}H NMR spectrum of compound ***rac*-35**.

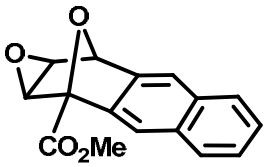

rac-36

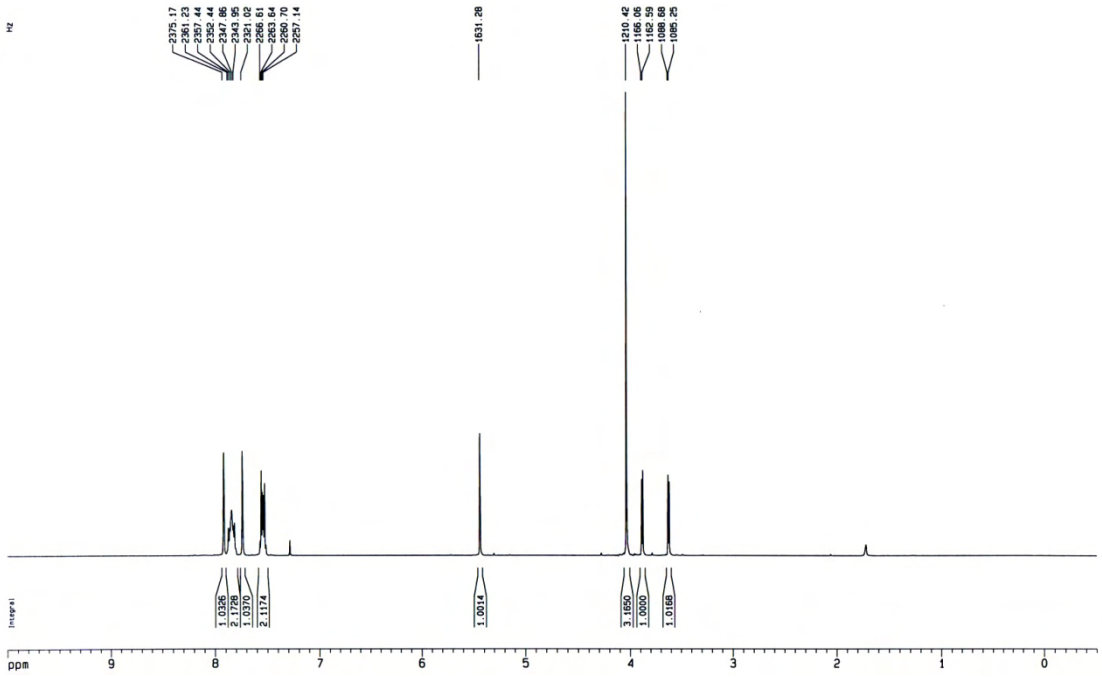

Figure A28. ^{1}H NMR spectrum of compound ***rac*-36**.

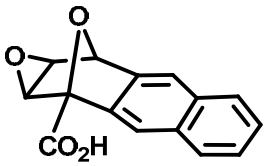

rac-5

^{1}H NMR in Acetone-D$_6$

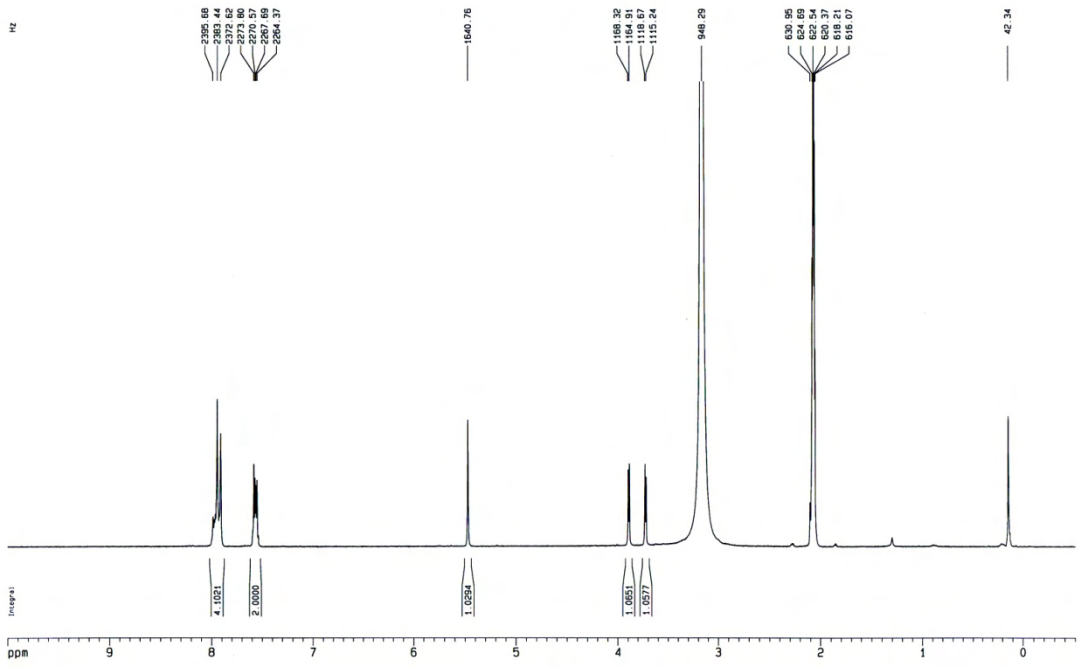

Figure A29. ^{1}H NMR spectrum of compound ***rac*-5**.

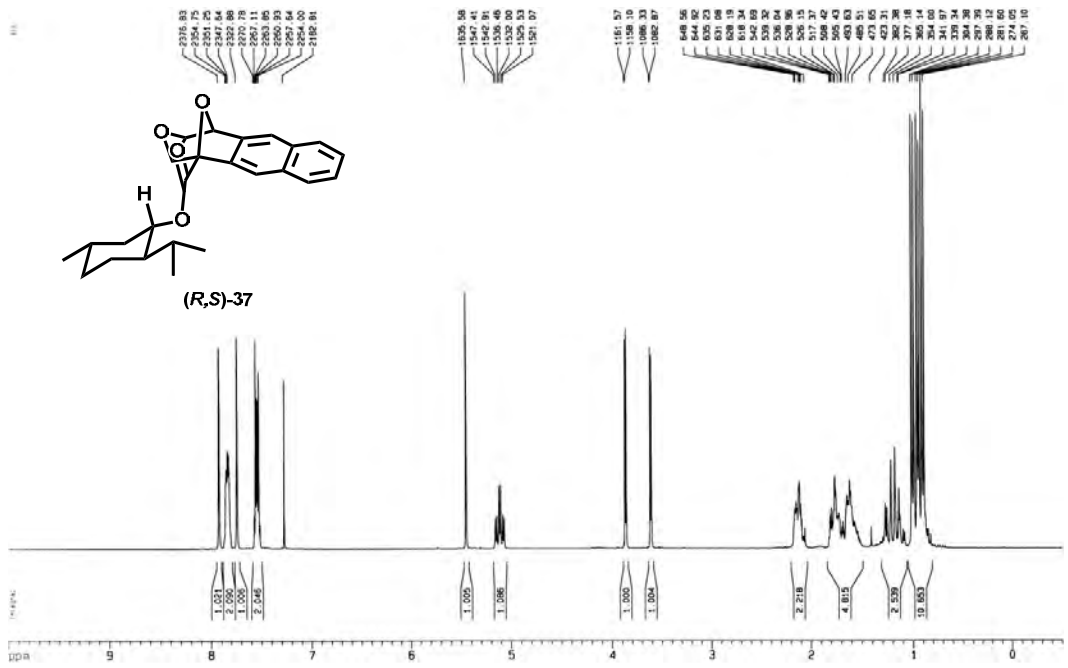

Figure A30. ^{1}H NMR spectrum of compound **(*R*,*S*)-37**.

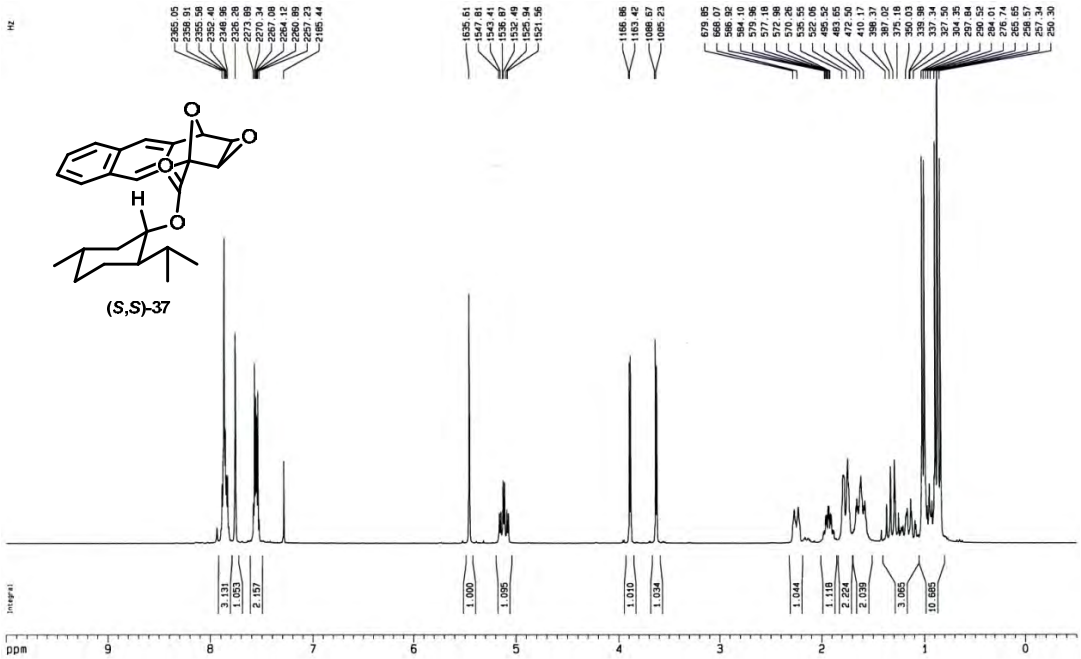

Figure A31. ^{1}H NMR spectrum of compound **(*S*,*S*)-37**.

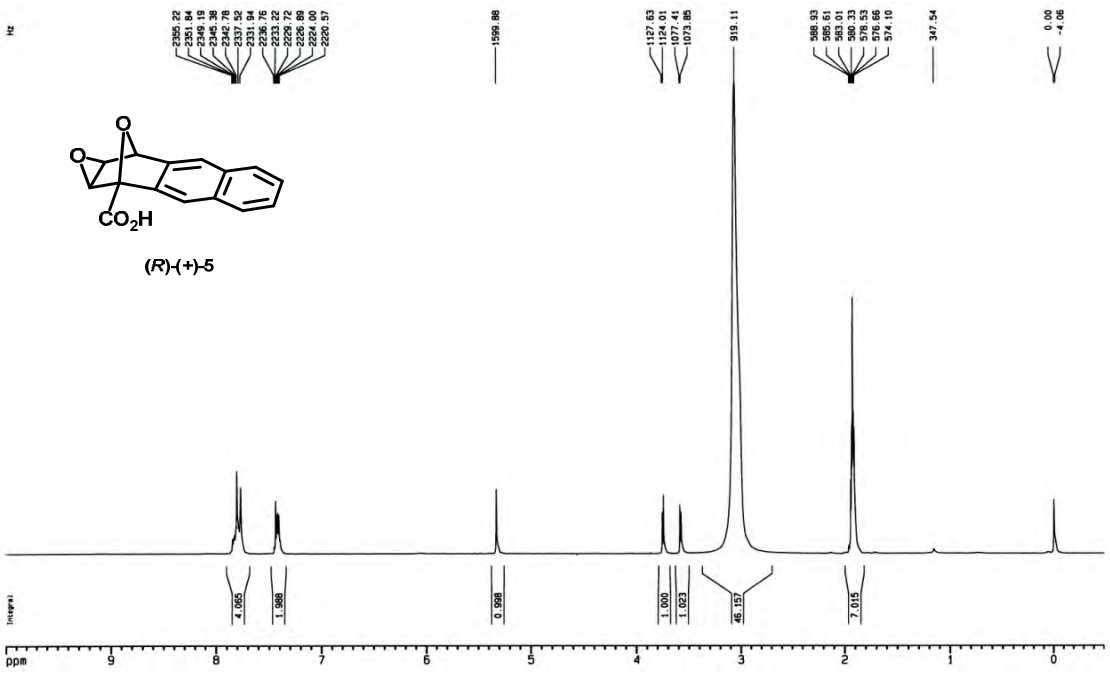

Figure A32. ^{1}H NMR spectrum of compound **(*R*)-(+)-5**.

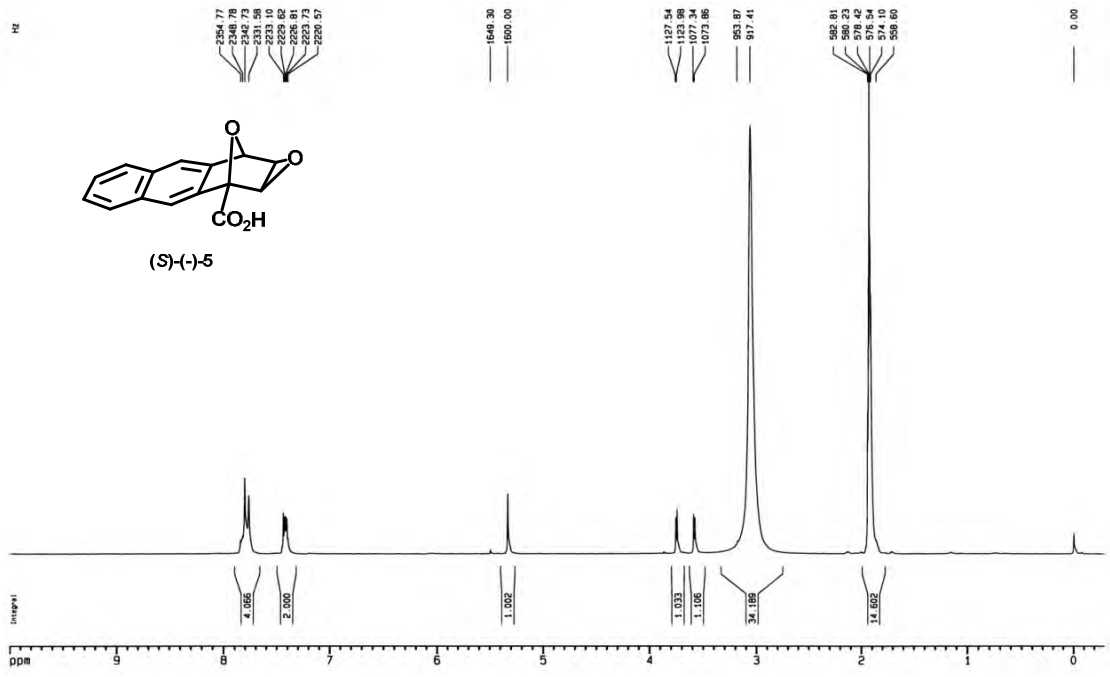

Figure A33. ^{1}H NMR spectrum of compound **(*S*)-(-)-5**.

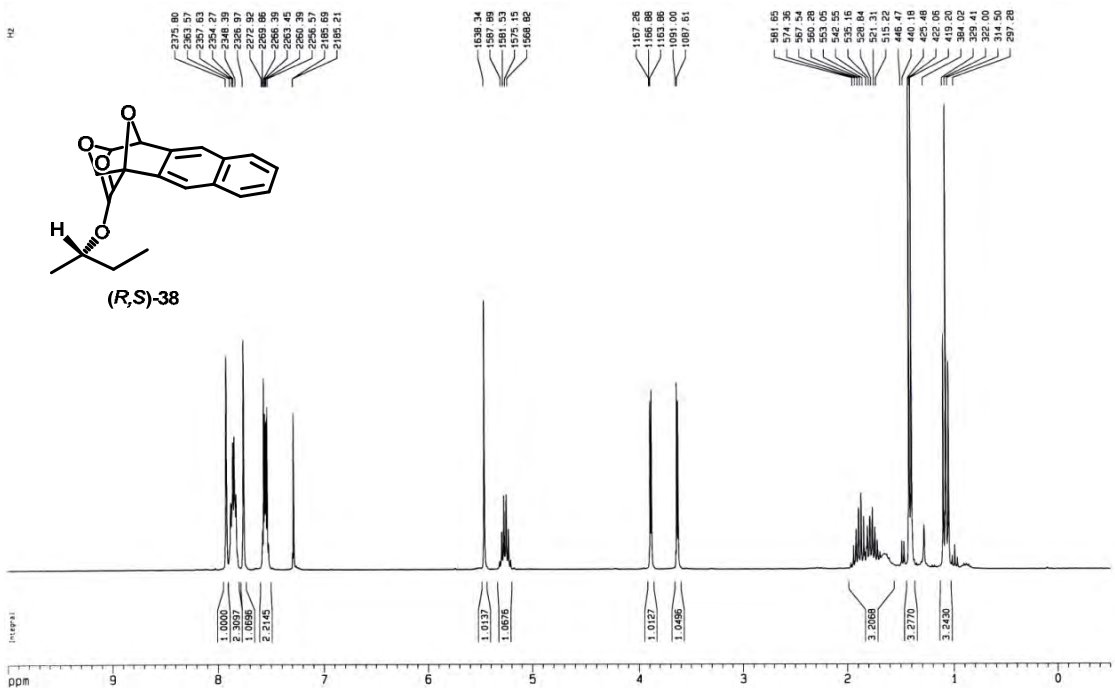

Figure A34. ^{1}H NMR spectrum of compound **(*R*,*S*)-38**.

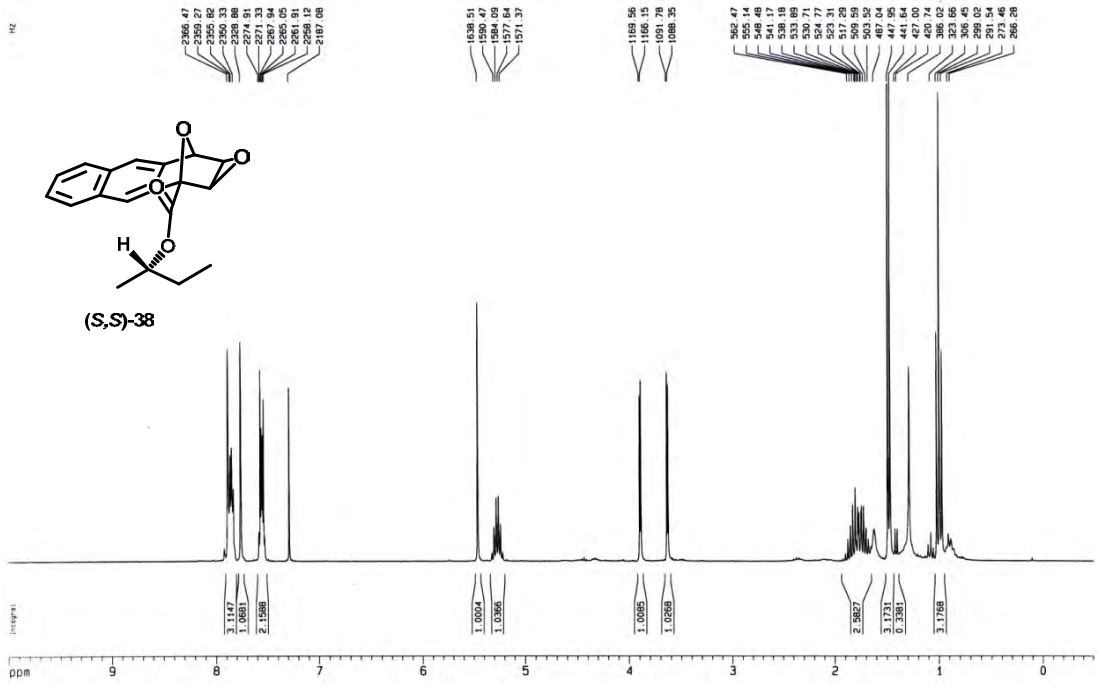

Figure A35. ^{1}H NMR spectrum of compound **(*S*,*S*)-38**.

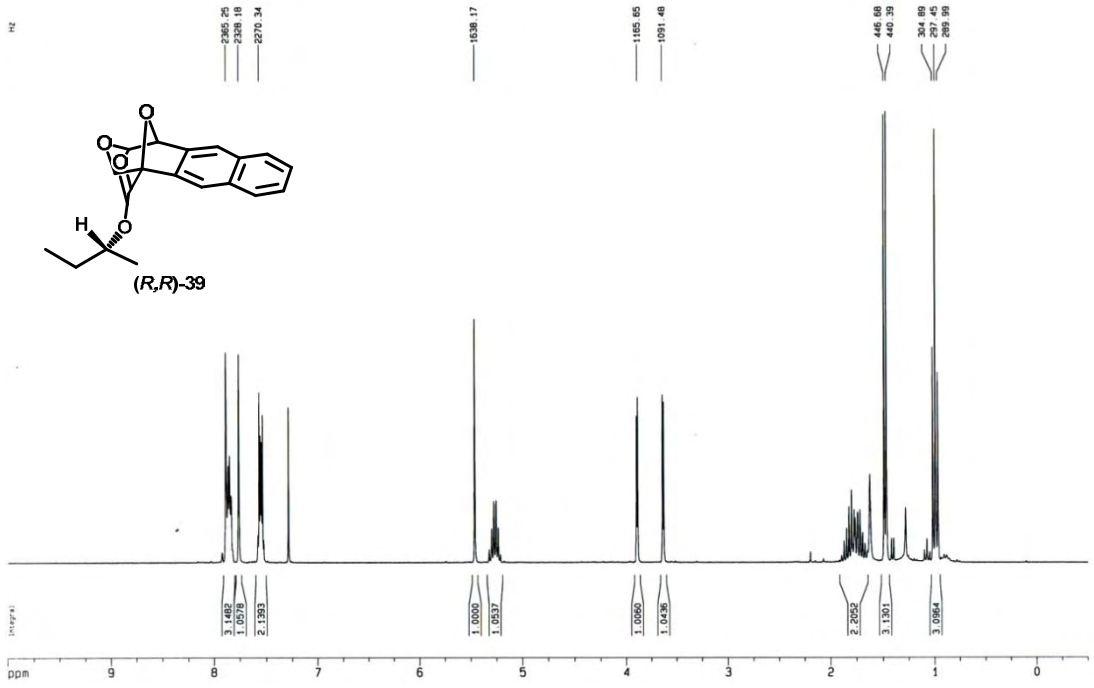

Figure A36. ^{1}H NMR spectrum of compound **(*R*,*R*)-39**.

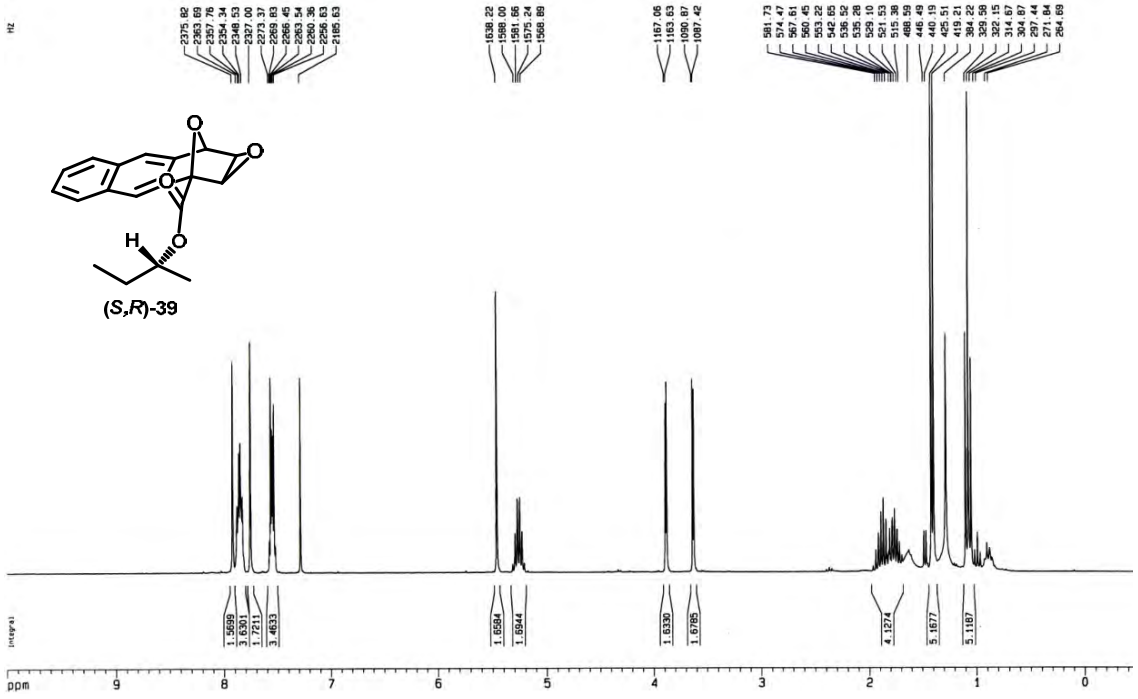

Figure A37. ^{1}H NMR spectrum of compound **(*S*,*R*)-39**.

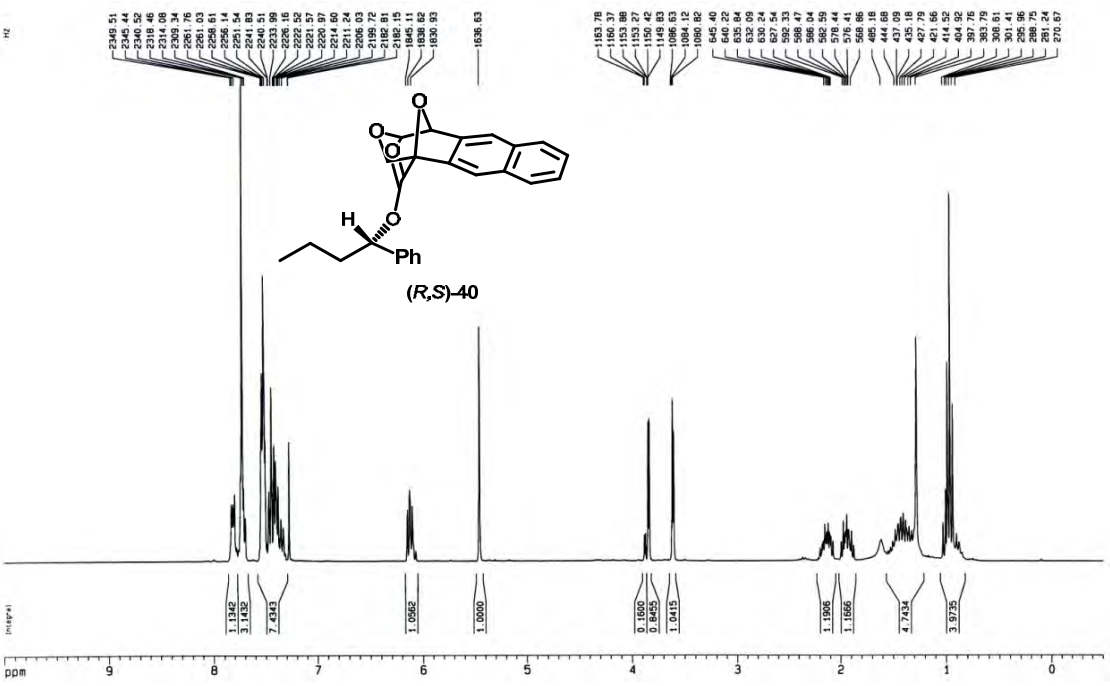

Figure A39. ^{1}H NMR spectrum of compound **(*R*,*S*)-40**.

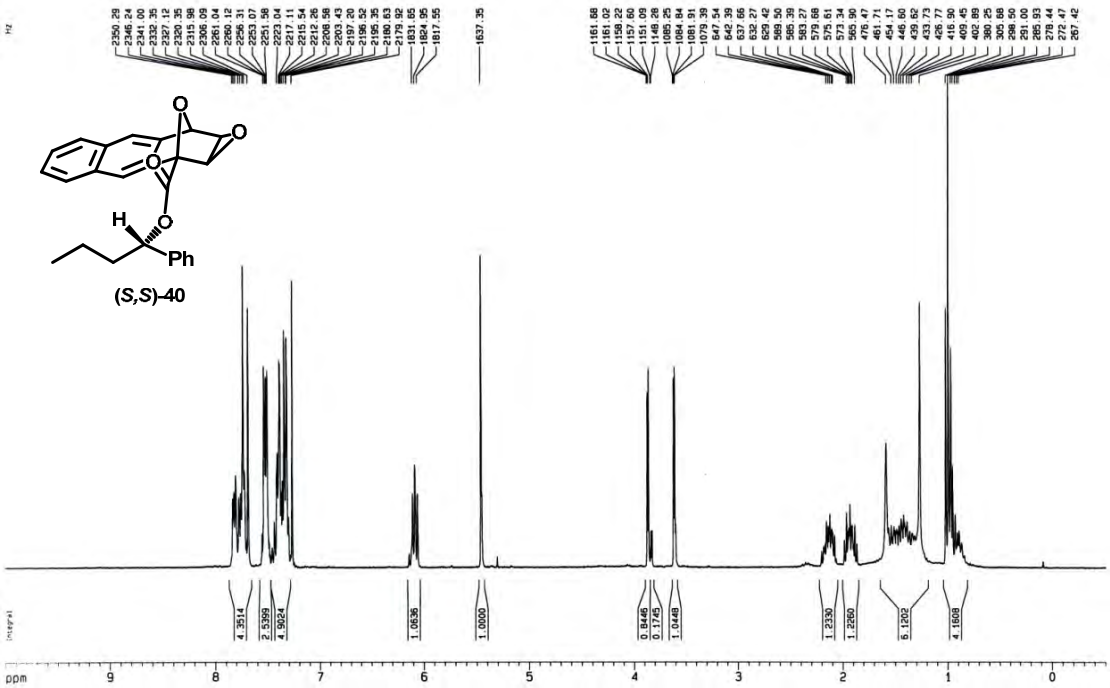

Figure A40. ^{1}H NMR spectrum of compound **(*S*,*S*)-40**.

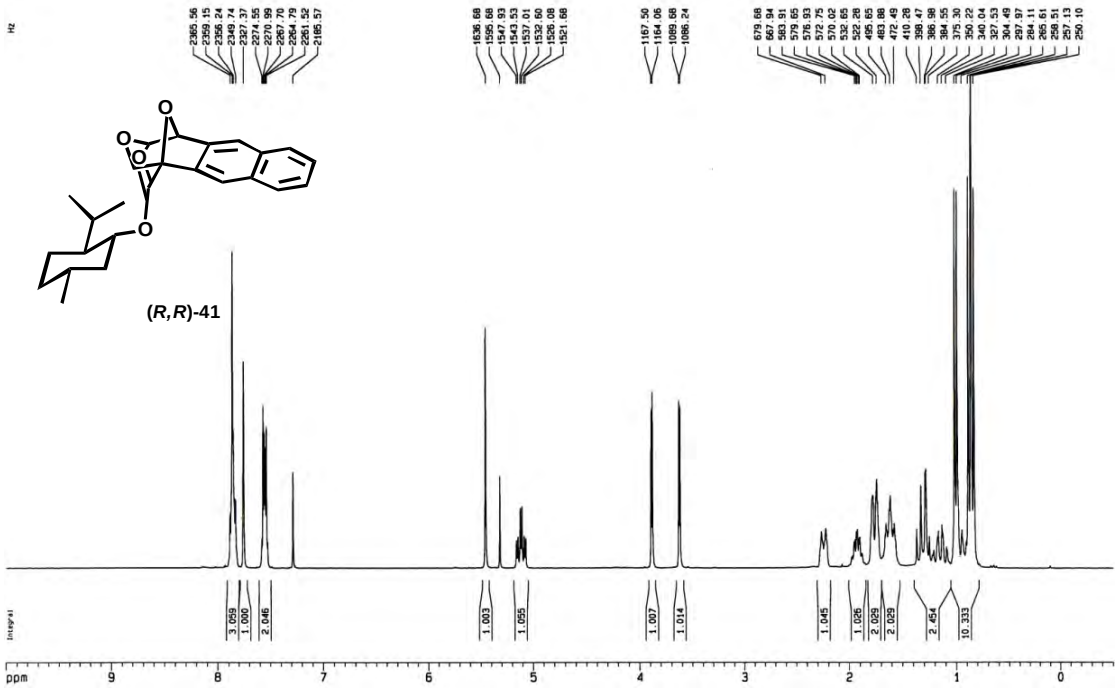

Figure A41. ^{1}H NMR spectrum of compound **(*R*,*R*)-41**.

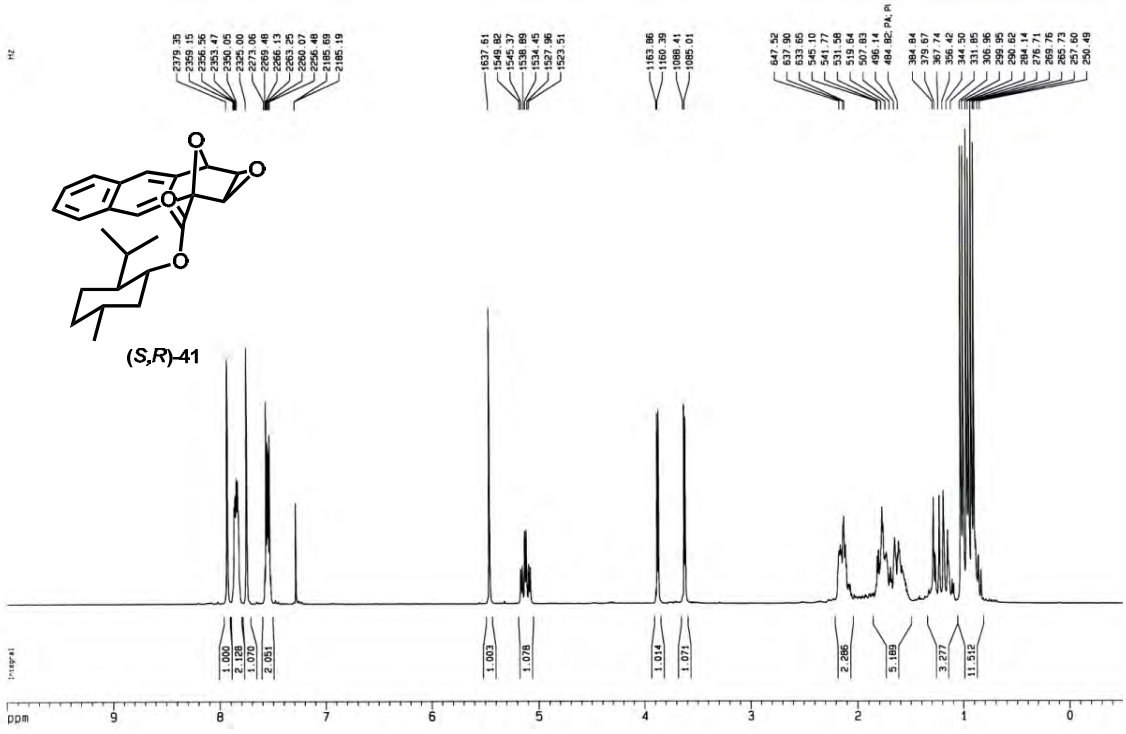

Figure A42. ^{1}H NMR spectrum of compound **(*S*,*R*)-41**.

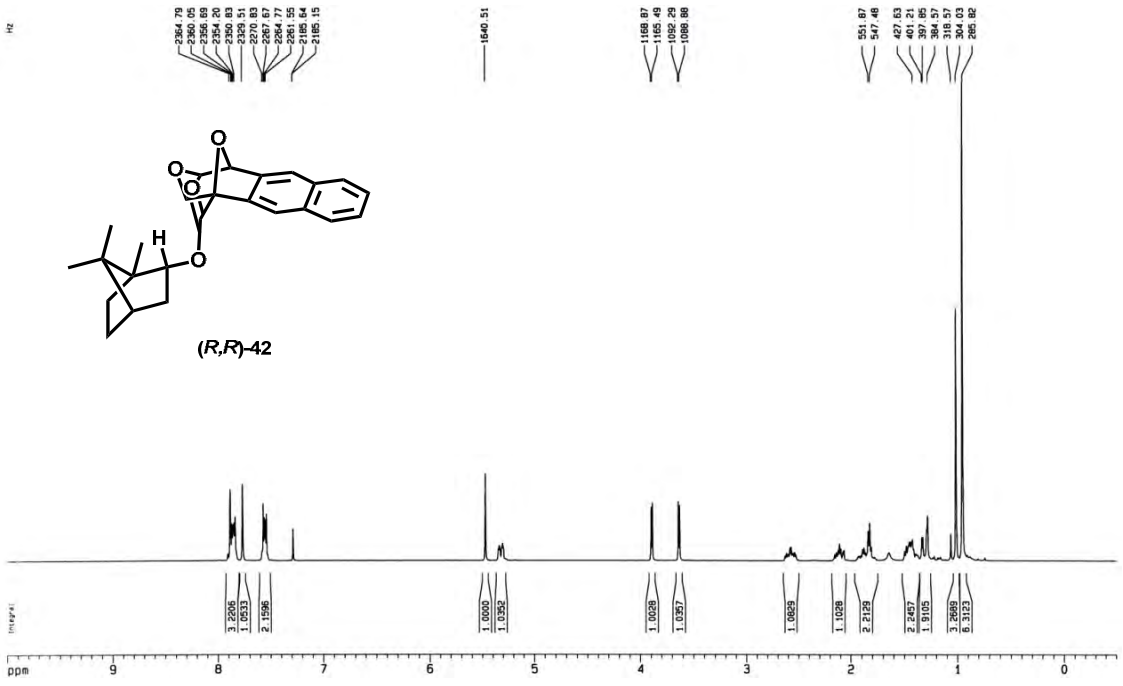

Figure A43. ^{1}H NMR spectrum of compound **(*R*,*R*)-42**.

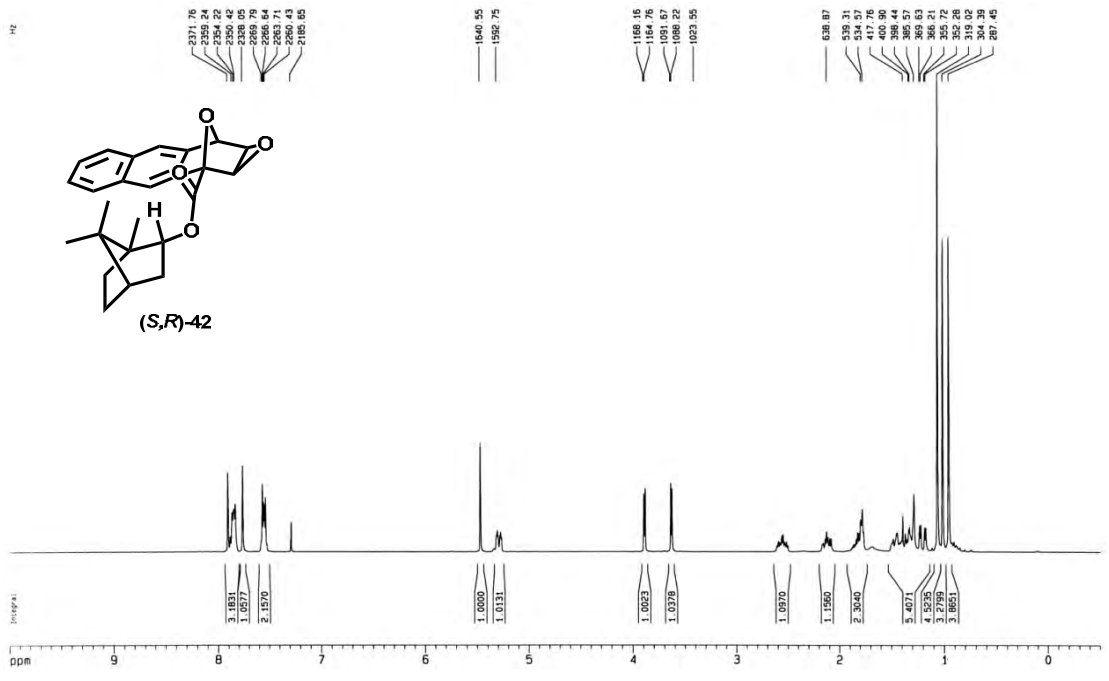

Figure A44. ^{1}H NMR spectrum of compound **(*S*,*R*)-42**.

PART II. Application of THENA for the resolution of binaphthol derivatives

Introduction

Atropisomerism[1,2] is a type of stereoisomerism that arises in systems where free rotation about a single bond is limited so as to allow different optical isomers to be isolated. Typically, atropisomerism appears in *ortho*-substituted biaryls where steric congestion between the substituents restricts free rotation about the sp^2–sp^2 carbon–carbon bond, increasing hindrance to the rotation at the pivotal 1,1'-bond, and thus makes these molecules resolvable into optically pure enantiomers.

One interesting example of such biaryl systems was 1,1'-binaphthyl **3**, reported by Cooke and Harris in 1963.[3] The molecule was found to be optically active and its racemization half-life was 14.5 min at 50 °C (Scheme 1).

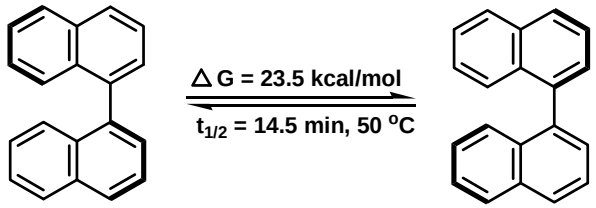

(*S*)-3 (*R*)-3

Scheme 1. Racemization energy of 1,1'-binaphthyl **3**.

When substituents are introduced at 2,2'-position, the chiral configuration of the 1,1'-binaphthyl compounds becomes very stable. For example, the temperature of racemization of (*S*)-1,1'-binaphthyl-2,2'-dicarboxylic acid **5** is as high as 175 ºC (Figure 1).[4]

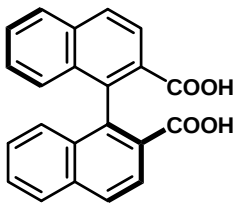

(*S*)-5

Figure 1. Optically active (*S*)-1,1'-binaphthyl-2,2'-dicarboxylic acid **5**.

Absolute configuration of chiral binaphthyl compounds was first proposed by Mislow in 1958 on the basis of their optical properties, *i.e.* CD and ORD, stereochemical mechanism, and thermal analysis. This was later confirmed by Yamada and co-workers in 1971 from the X-ray analysis of (*R*)-(+)-2,2'-dihydroxy-1,1'-binaphthyl-3,3'-dicarboxylate ester **6** and its chemical correlation with other binaphthyl molecules (Figure 2).[5]

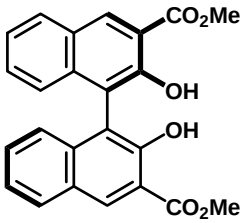

(*R*)-(+)-6

Figure 2. Optically active (*R*)-(+)-2,2'-dihydroxy-1,1'-binaphthyl-3,3'-dicarboxylate ester **6**.

As a result of their highly stable chiral configuration, 2,2'-disubstituted-1,1'-binaphthyls have been used to control many asymmetric processes. Its rigid structure with C_2 symmetry plays an important role in chiral induction. Figure 3 shows examples of binaphthols which have been applied in asymmetric induction and catalysis.[6,7]

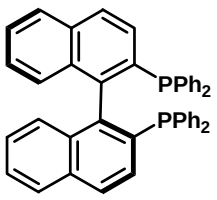

(*S*)-7

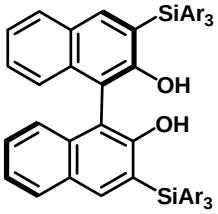

(*R*)-8

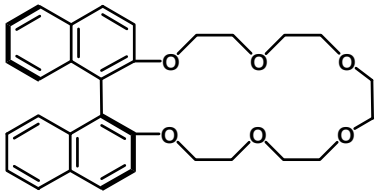

(*S*)-9

Figure 3. Examples of optically active binaphthol derivatives.

Thus it is essential to establish a simple and convenient method for the preparation of binaphthyl derivatives. Many procedures have been developed for the propose.[1] For example, two molecules of 2-naphthol **10** can be coupled by using iron (III) or copper (II) as the oxidizing agent to produce binaphthol **11** as shown in Scheme 2.[8]

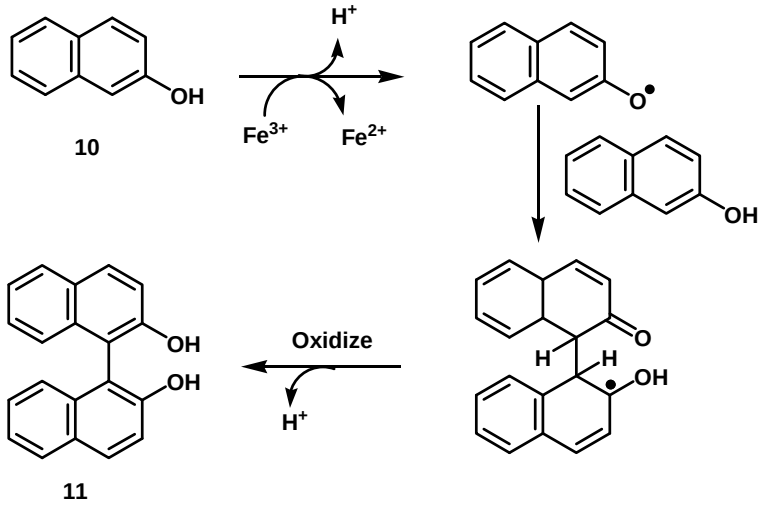

Scheme 2. Oxidative coupling of binaphthol.

Moreover, stereoselective aryl couplings have been reported by employing chiral copper-complex mediated phenolic oxidation. Optically active binaphthol, (*R*)-**12**, could be achieved in good yield with high optical purity (96% ee) (Scheme 3).[9]

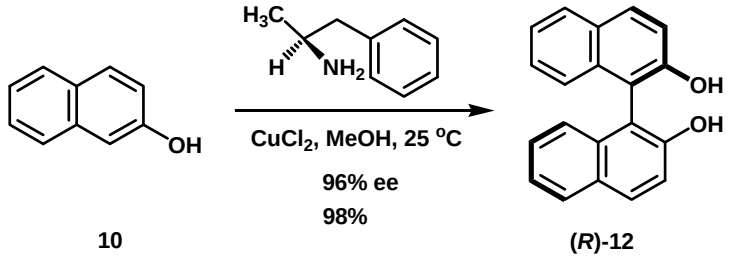

Scheme 3. Asymmetric oxidative coupling of *β*-naphthol.

Meyers *et al*. also reported that (*S*)-oxazoline, when subjected to classical Ullmann conditions, could lead to bis-(oxazoline)-(*S*,*S*)-**14** as a single diastereomer (Scheme 4).[10] The difference in stability between the two diastereoisomers appears to be due to the steric interaction of the *tert*-butyl groups. This result implied that the addition of a steric factor, such as substituents at the 2 and 2' positions of the binaphthyl ring system, could raise the rotational barrier of the BINAP-type ligands and could make it usable as a chiral ligand.

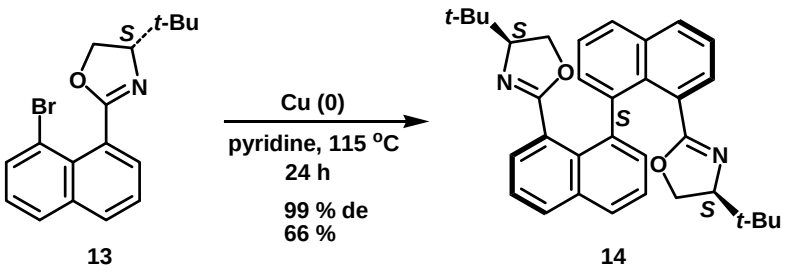

13 14

Scheme 4. Enantioselective oxidative coupling by (*S*)-oxazoline.

Thus Meyers *et al.*[11] later applied this method to prepare binaphthyls with oxazoline substituents at the 2 and 2' positions (Scheme 5).

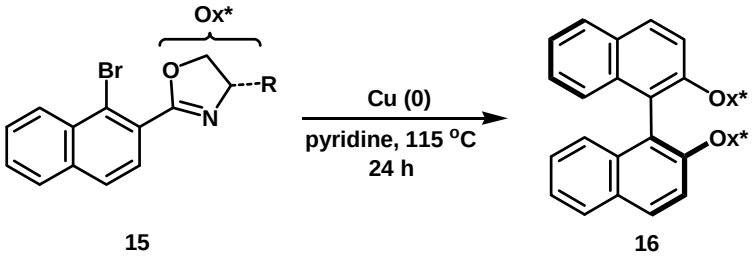

15 16

	(*S*):(*R*)
R= Ph	2: 1
R= *i*-Pr	4: 1
R= *t*-Bu	32: 1

yields > 90 %

Scheme 5. Enantioselective oxidative coupling of binaphthyl by several oxazolines.

The diastereomeric ratio of **16** was found to be sensitive to the size of the substituent (*R*) in the oxazoline ring. Determination of the transition states and copper intermediates revealed that one of the two diastereomeric copper complexes was free of any severe steric interaction caused by the close proximity of the (*R*)-substituents of the two oxazolines.

Besides the asymmetric approach to optically active binaphthyl derivatives, the resolution of racemic binaphthyls is an alternative route which has been proven to be very effective.

For example, an efficient, practical, and inexpensive method was described in 1993 by Brunel *et al.*[12] which involved the application of tricoordinated compound **18**, prepared from phosphorus trichloride and L-menthol (Scheme 6).

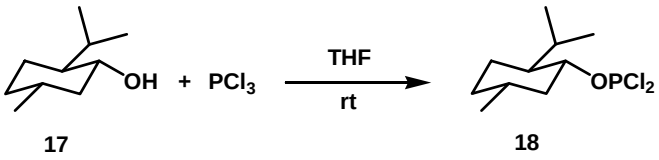

Scheme 6. The preparation of chiral phosphorus tricoordinated compound.

Compound **18** then reacted with *rac*-binaphthol **11** leading to a 1:1 mixture of diastereomers (*R*)-**19** and (*S*)-**20** in quantitative yield. Complete separation of the two diastereomers was achieved in a single recrystallization from diethyl ether. Oxidation with 30% hydrogen peroxide led to the phosphites **21** and **22**, which were reduced with $LiAlH_4$ to afford enantiomerically pure (*R*)-binaphthol **12** and (*S*)-binaphthol **12** in 81% and 85% overall yields, respectively (Scheme 7).

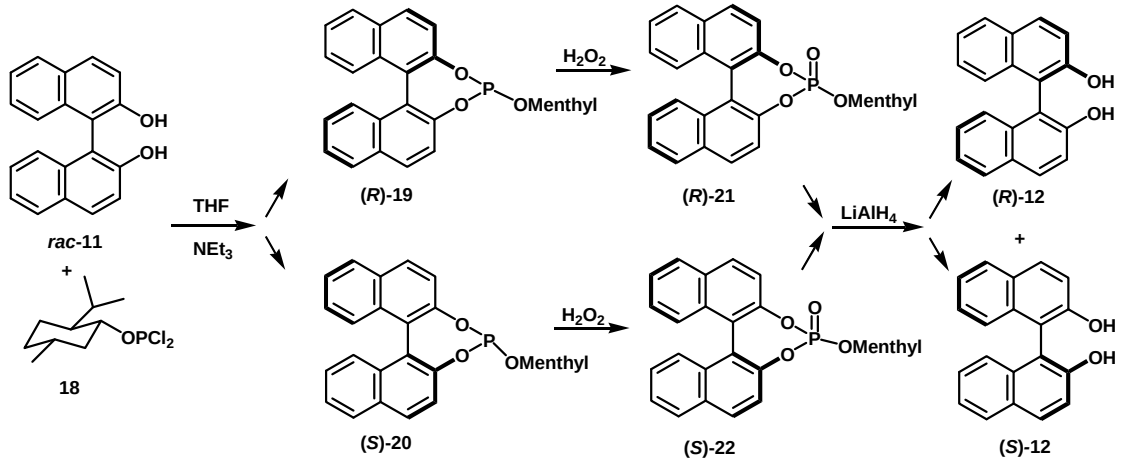

Scheme 7. Reaction of *rac*-binaphthol with chiral phosphorus compound.

Interestingly, Chow *et al*. discovered a versatile method for the resolution of disubstituted-1,1'-binaphthyl-2,2'-diols **23** by using (*1S*)-camphor-10-sulfonyl chloride **24** as a chiral auxiliary (Scheme 8).[13]

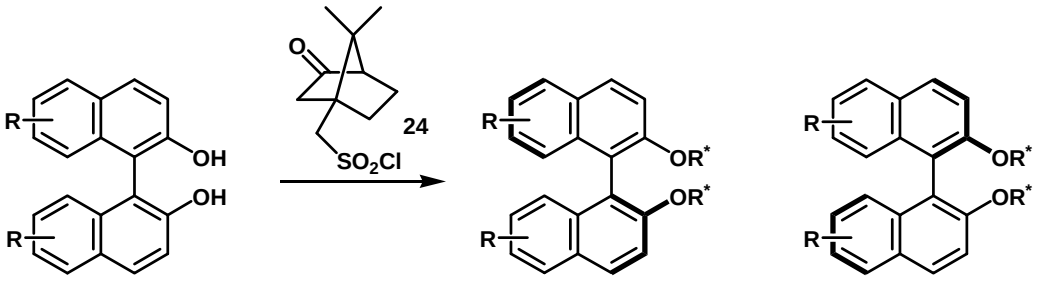

23 25 26

Entry	$[\alpha]_D$	%yield	$[\alpha]_D$	%yield
a) R = 3-Br	+ 97.3	29	- 101.5	29
b) R = 4-Br	+ 15.2	35	- 9.3	34
c) R = 6-OMe	+ 46.6	47	- 41.5	47

R* = (*1s*)-camphor-10-sulfonyl

Scheme 8. The resolution of disubstituted-1,1'-binaphthyl-2,2'-diols.

Not only could the *rac*-**23** be resolved *via* its diastereomeric bis-(*S*)-camphor-10-sulfonates **25** and **26**, but the absolute configurations of the diastereomeric pairs **25** and **26** could also be inferred from their relative chromatographic mobility. In all of the less polar bis-(camphor-10-sulfonate)-**25a**–**c**, the diastereomeric methylene groups adjacent to the sulfonyl moiety appeared as an AX system (J = 15 Hz) with a chemical shift difference of less than 0.5 ppm, while those of the more polar diastereomeric **26 a**–**c** compounds had a significantly larger chemical shift difference of 1 ppm.

Furthermore, circular dichroism (CD) spectra of the hydrolyzed products derived from the less polar diastereoisomers **25a**–**c** all gave a negative first Cotton effect at around 236–240 nm and a positive second Cotton effect at 224–228 nm. The observed Cotton effect pattern is closely parallel to those previously reported by Mason[14] and Harada.[15] In both ^{1}H NMR and CD spectra, the less polar diastereomers **25a**–**c** could be assigned as having an (*S*)-configuration.

Extensive studies of the convenient and highly efficient chromatographic resolution of the *rac*-binaphthol **11** *via* esterification with *N*-protected-*L*-amino acid were reported by Einhorn *et al.* (Scheme 9).[16]

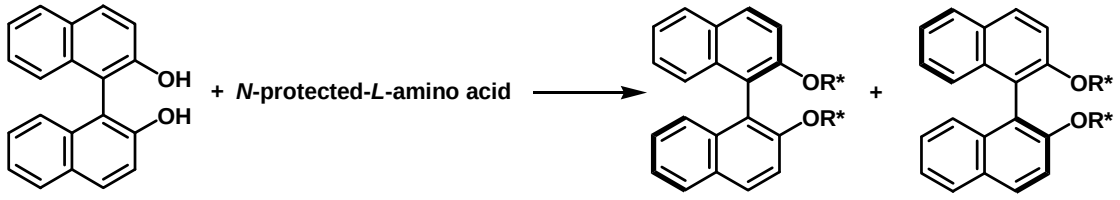

11 (*R*)-27 (*S*)-28

Entry	Amino acid derivative	$R_{f\,27}$	$R_{f\,28}$	α_a
1	*N*-Boc-phenylglyciene	0.76	0.74	1.03
2	*N*-Boc-phenylalanine	0.78	0.70	1.11
3	*N*-Cbz-phenylalanine	0.80	0.74	1.08
4	*N*-(α)-Boc-tryptophan	0.54	0.26	2.15
5	*N*-(α)-Cbz-tryptophan	0.68	0.36	1.89

a) α defined as seperation factor, $\alpha = R_{f27} / R_{f28}$

Scheme 9. TLC data for diester of *rac*-binaphthol and *N*-protected-*L*-amino acid.

R_f values and separation factors (α) were determined by TLC analysis, in order to select the most promising candidates for efficient separation. *N*-(α)-Boc-tryptophan was shown to be an excellent resolving agent for the resolution of binaphthol **11**. After hydrolysis, the less polar isomer, (*R*)-(+)-**11**, was obtained in 91% yield (100% ee) and the more polar isomer, (*S*)-(–)-**11**, was obtained in 93% yield (100% ee). However, the effect of the resolving agents on the different polarities of the diastereomeric pairs was not explained.

The resolution of binaphthol derivatives, using (1*S*)-camphanoyl chloride **29** as a resolving agent was first investigated by Fuji *et al.*[18] in 1998 and it was found the applications in the field of asymmetric synthesis as well as chiral molecular recognition. Chiral recognition of amino acid derivatives by optically active 8,8'-dihydroxy-1,1'-binaphthyl **30** was used as a chiral derivatizing agent for the ^{1}H NMR determination of the absolute configuration of carboxylic acids.[19]

For the resolution of compound **30**, mono-acylation of racemic **30** with (1*S*)-camphanoyl chloride **29** gave a mixture of diastereoisomers **31** and **32** in 32% and 21% yields, respectively (Scheme 10).[20]

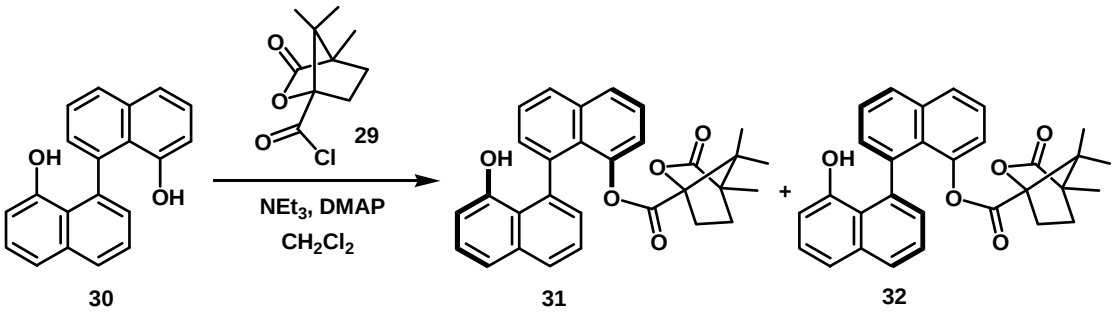

Scheme 10. Resolution of 8,8'-dihydroxy-1,1'-binaphthyl.

Diastereoisomer **31** was reported to have a larger R_f value than its corresponding isomer **32**. After chromatographic separation, the camphanate moieties in **31** and **32** are readily removed in aqueous KOH to give the optically pure (*S*)-**30** and (*R*)-**30**, respectively.

Moreover, a series of 8'-alkoxyl-1,1'-binaphthalen-8-ols was investigated by Hua. Enantiopure 8'-alkoxy-8-hydroxy-1,1'-binaphthyl (*R*)-**36** or (*S*)-**37** were obtained from *rac*-**33** as described in Scheme 11.[21]

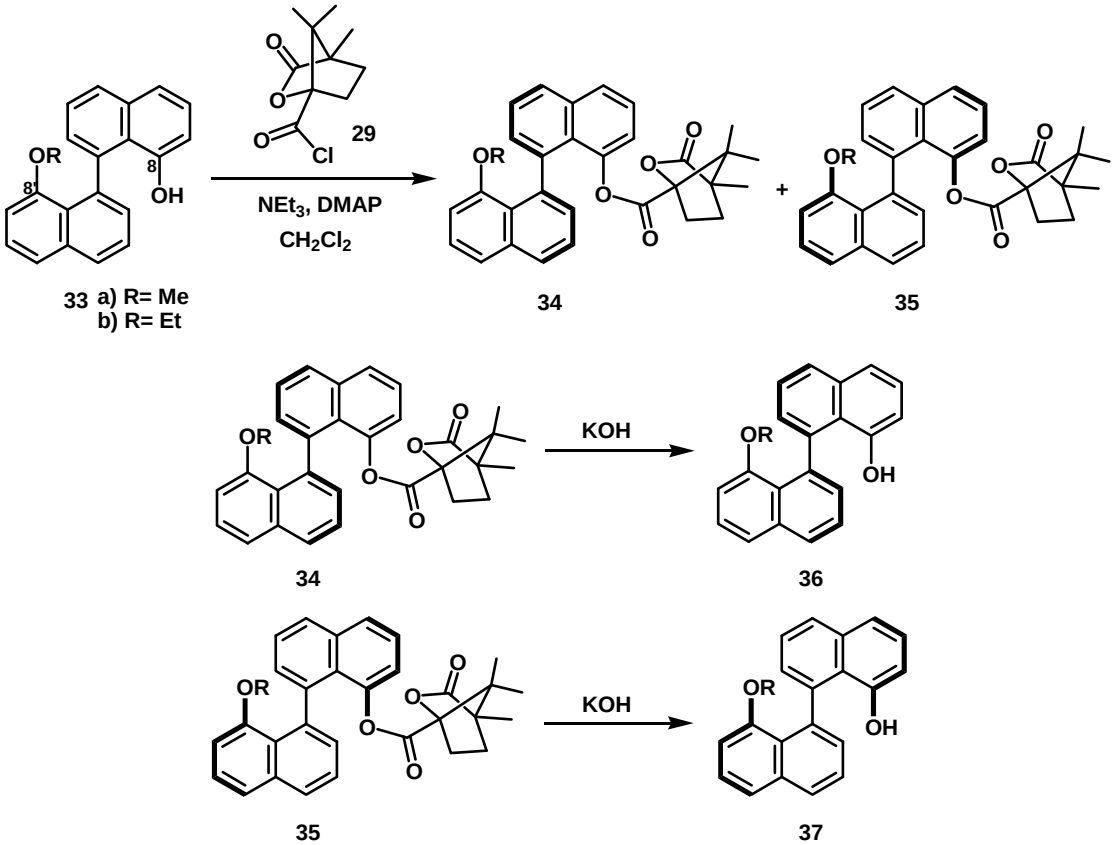

Scheme 11. Resolution of 8'-alkoxyl-1,1'-binaphthalen-8-ols with (1*S*)-camphanate.

Interestingly, all of the faster running isomers **34** had an (*R*)-configuration. These results controverted to those from the resolution of 8,8'-dihydroxy-1,1'-binaphthyl **30** which indicated that the fast running on TLC, less polar isomer had an (*S*)-configuration. Apparently, types of substituted groups at position 8 might affect the different polarity of the diastereomeric pairs of compounds **30** and **33**.

Our interest then focused on the resolution of the binaphthol derivatives which would be derived from the reactions of chiral α-alkoxa bicyclic acid chloride **38** and binaphthols **39**. The resolution of 7,7'-disubstituted binaphthols at the 2,2'-position of binaphthyls **39** (entry 1–5) by using (*R*)-(–)-2,3-dihydro-1,4-epoxynaphthalene-1(2*H*)-carboxylic acid **4** (refer to compound **4** in Scheme 1, PART I) as a new resolving agent was carried out. Treatment of binaphthols **39** with (*R*)-(–)-acid chloride **38** in dichloromethane in the presence of triethylamine and a catalytic amount of DMAP afforded a diastereomeric mixture of (*R*,*R*)-**40** and (*R*,*S*)-**41** in good yields. It was found that the isomers **40** had larger R_f value than their corresponding diastereoisomers **41** (Scheme 12). %Yields, R_f values and separation factors of diastereomers **40** and **41** are summarized in Table 1.

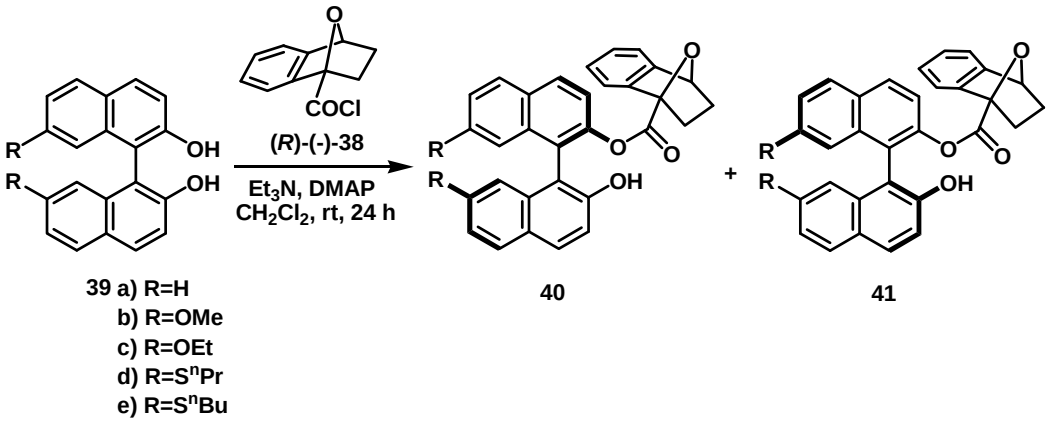

Scheme 12. Resolution of binaphthols with (*R*)-(–)-acid chloride **38**.

Table 1. Separation factors (α), %yields and R_f values of diastereomers **40** and **41**.

Entry	%Yield of (*R*,*R*)-39	R_f of (*R*,*R*)-39	%Yield of (*R*,*S*)-40	R_f of (*R*,*S*)-40	α (R_{f39}/R_{f40})
1. a) R=H	48	0.46	43	0.34	1.35
2. b) R=OMe	45	0.45	42	0.35	1.29
3. c) R=OEt	47	0.60	45	0.49	1.22
4. d) R=S^{n}Pr	24	0.46	25	0.37	1.24
5. e) R=S^{n}Bu	22	0.45	20	0.37	1.21

Careful examination of the ^{1}H NMR spectra of all diastereoisomers revealed an interesting feature. For example, ^{1}H NMR spectra of compound **40b** and **41b**, displayed in Figure 4, showed a significant difference of chemical shifts of their methylene groups on the α-alkoxa bicyclic acid. It could be observed that methylene protons (a) and (b) of compound **41b** were upfield shifted by diamagnetic anisotropic effect of naphthalene moiety when compared to its diastereomer **40b**.

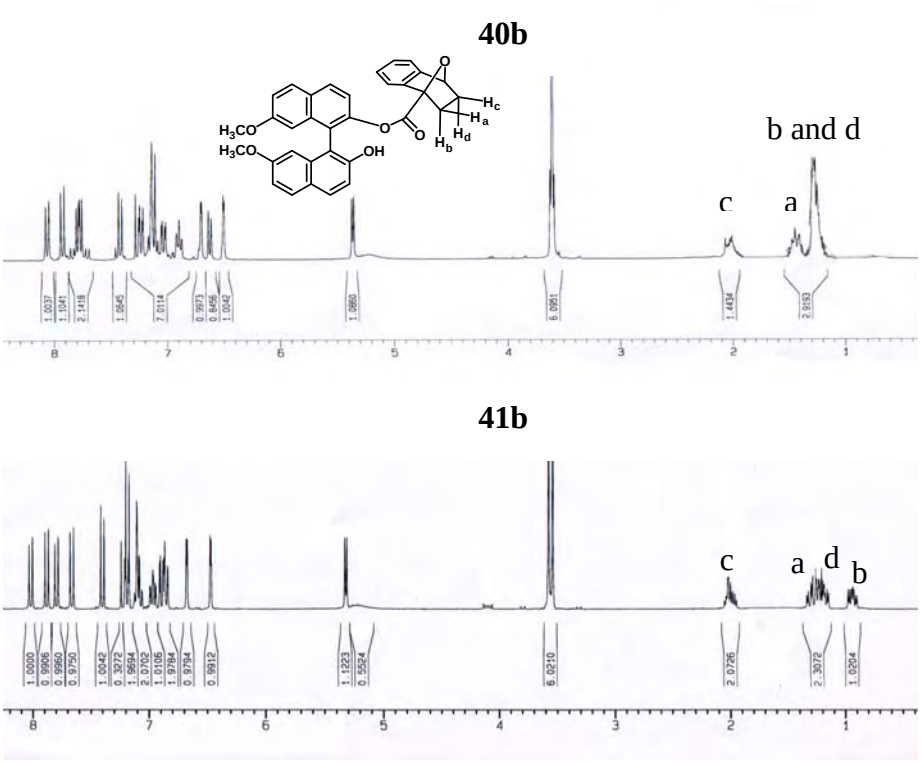

Figure 4. The difference on the ^{1}H NMR spectra of compounds **40b** and **41b**.

Chemical shifts of the methylene protons of the other derivative compounds are summarized in Table 2. In all case, chemical shifts of H_a and H_b of **40** were all shifted lower field than those of **41**.

Table 2. Chemical shifts of methylene protons of compounds **40a–e** and **41a–e**.

Entry	Chemical shift (ppm)							
	Compound 40				Compound 41			
	Ha	Hb	Hc	Hd	Ha	Hb	Hc	Hd
1. a) R=H	1.49	1.29	2.01	1.29	1.33	0.95	2.05	1.22
2. b) R=OMe	1.45	1.30	2.05	1.30	1.35	0.99	2.05	1.25
3. c) R=OEt	1.46	1.25	2.02	1.25	1.31	0.95	2.01	1.20
4. d) R=S^{n}Pr	1.52	1.23	1.97	1.23	1.23	0.70	1.93	1.15
5. e) R=S^{n}Bu	1.64	1.28	2.16	1.28	1.30	0.90	2.02	1.20

*Chiroptical properties of all diastereomers **40a–e** and **41a–e***

Circular dichroism of each diastereomer was then determined. The faster moving isomer **40a** displayed first positive Cotton effect at 278 nm and second negative Cotton effect at 242 nm as demonstrated in Figure 23. On the other hand, ester **40b** showed first negative Cotton effect at 326, 277 nm and strong negative Cotton effect at 249 nm, which was similar in shape to the CD spectra of compound **40c**, which showed negative Cotton effect at 329, 278 nm and strong negative Cotton effect at 251 nm (Figures 5–7). Esters **40d**–**e** showed first negative Cotton effect at 307 nm and a negative second Cotton effect at 264 nm (Figures 8–9).

CD spectra of compounds **41a**–**e** appeared rather like mirror image of those of their corresponding diastereomers **40a**–**e**. For isomer **41a**, it displayed a negative first Cotton effect at 282 nm and a positive second Cotton effect at 239 nm. In contrast, **41b**–**c** showed positive Cotton effect at 326, 278 nm and strong positive Cotton effect at 247 nm. The esters **41d**–**e** similarly exhibited a first positive Cotton effect at 307 nm and a negative second

Cotton effect at 265 nm. The observed bathochromic shift in CD spectra could be from the effect of substituents on binaphthols.

*Circular dichroism (CD) spectra of diastereomeric compounds **40** and **41**.*

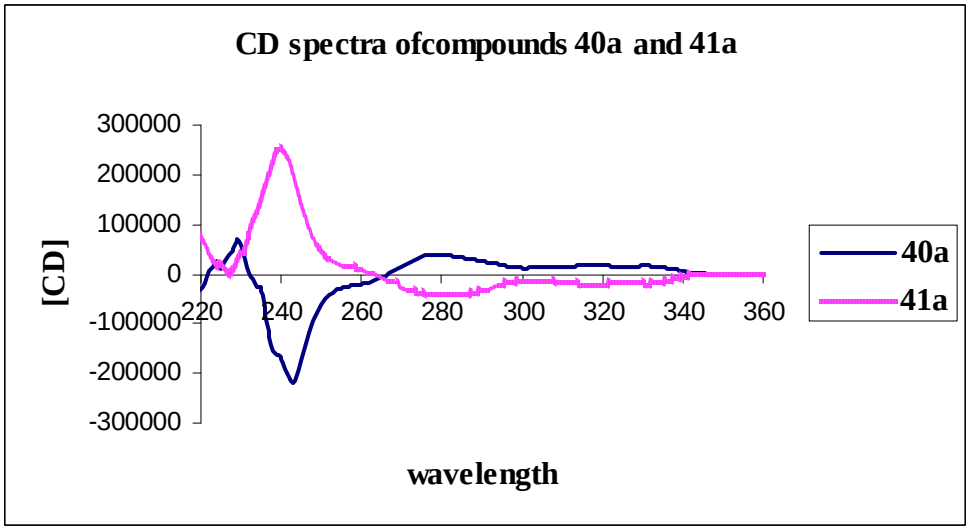

Figure 5. CD spectra of compounds **40a** and **41a**.

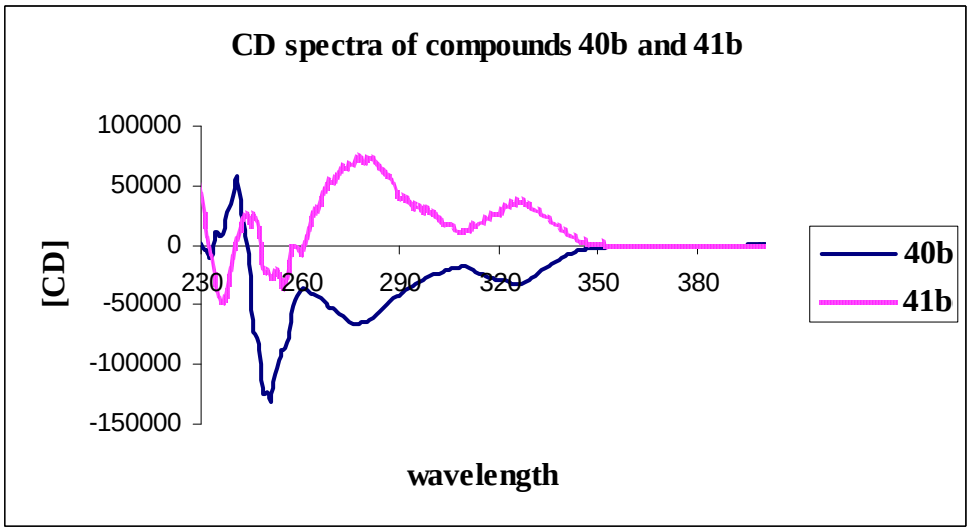

Figure 6. CD spectra of compounds **40b** and **41b**.

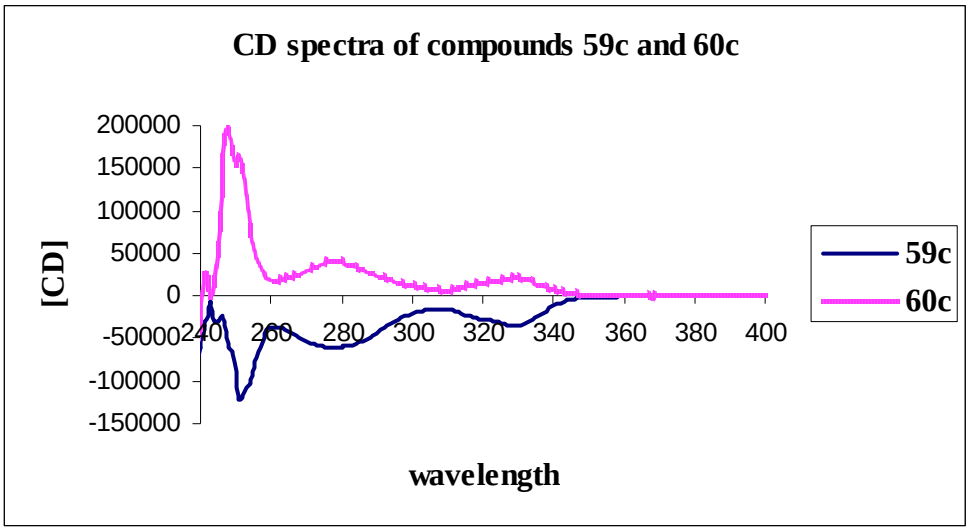

Figure 7. CD spectra of compounds **40c** and **41c**.

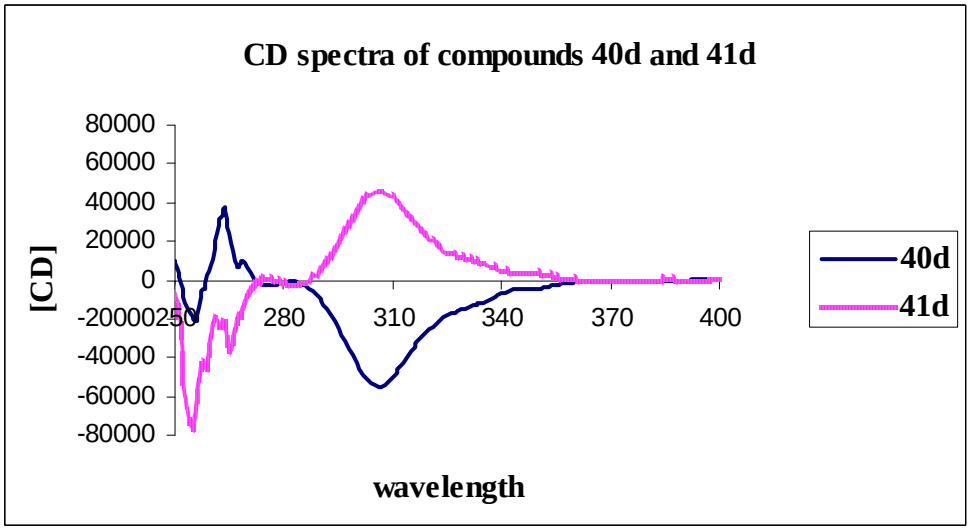

Figure 8. CD spectra of compounds **40d** and **41d**.

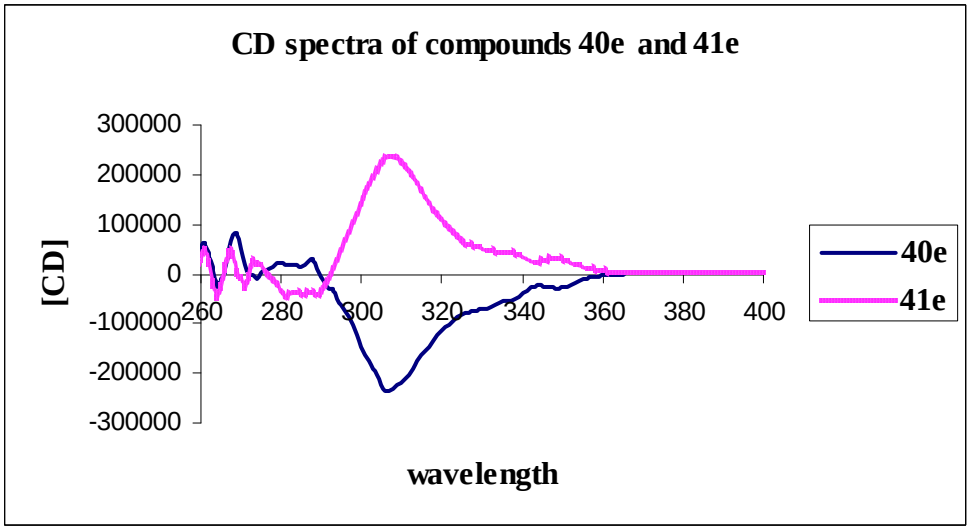

Figure 9. CD spectra of compounds **40e** and **41e**.

Moreover, the specific rotations $[\alpha]_D$ of compounds **40** and **41** were recorded as shown in Table 3.

Table 3. Specific Rotation of diastereomers **40a**–**e** and **41a**–**e** in CH_3CN.

Entry	$[\alpha]_D$ of compound 40	$[\alpha]_D$ of compound 41
1. a) R=H	–48.66	–95.12
2. b) R=OMe	–62.63	–16.98
3. c) R=OEt	–279.76	+10.62
4. d) R=S^{n}Pr	–496.80	–377.57
5. e) R=S^{n}Bu	–497.14	–399.92

Absolute Configuration Assignment

The absolute configurations of each diastereoisomer were determined by converting them to the corresponding binaphthols **42**. To recover the enantiopure (*R*)-and (*S*)-**42**, esters **40a**–**e** and **41a**–**e** were hydrolyzed with KOH in methanol and dioxane to yield binaphthol derivatives (*R*)-**42a**–**e** and (*S*)-**42a**–**e** (Scheme 13).

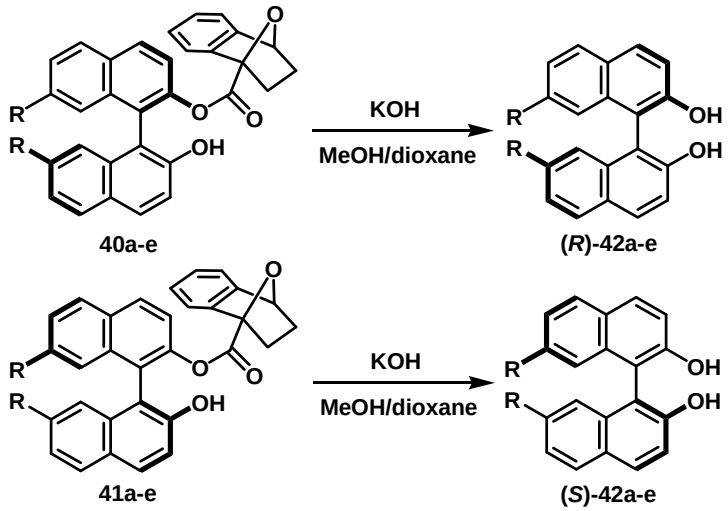

Scheme 13. Formation of the optically active binaphthols **42**.

%Yield and the optical rotation of all hydrolyzed binaphthols (*R*)-**42** and (*S*)-**42** were summarized in Table 4 and 5, respectively.

Table 4. % Yields of compounds (*R*)-**42** and (*S*)-**42**.

Entry	%Yield of (*R*)-42	%Yield of (*S*)-42
1. a) R=H	84	85
2. b) R=OMe	91	87
3. c) R=OEt	87	92
4. d) R=S^{n}Pr	89	79
5. e) R=S^{n}Bu	82	86

Table 5. Specific οπτιχαλ rotations of compounds (*R*)-**42** and (*S*)-**42** in CH_3CN.

Entry	$[\alpha]_D$ of compound (*R*)-42	$[\alpha]_D$ of compound (*S*)-42
1. a) R=H	+45.32[a] at 25.2 ºC, c = 1.00	–43.82 at 25.9 ºC, c = 1.00
2. b) R=OMe	–119.97[b] at 25.9 ºC, c = 1.00	+117.95 at 25.7 ºC, c = 1.15
3. c) R=OEt	–218.50[c] at 25.5 ºC, c = 1.02	+217.12 at 25.8 ºC, c = 1.03
4. d) R=S^{n}Pr	–334.52[c] at 25.8 ºC, c = 0.80	+375.68 at 26.0 ºC, c = 0.60
5. e) R=S^{n}Bu	–132.98 at 26.2 ºC, c = 1.00	+190.63 at 26.1 ºC, c = 0.80

a Ref. 26: (*R*)-**42a**; $[\alpha]_D$= +43.0 (c=0.19, THF) and (*S*)-**42a**; $[\alpha]_D$ = –95.5 (c=1.1, benzene)

b Ref. 13: (*R*)-**42b**; $[\alpha]_D$ = –125.5 (c=0.17, $CHCl_3$) and (*S*)-**42b**; $[\alpha]_D$ = +127.4 (c=0.17, $CHCl_3$)

c Ref. 25: (*R*)-**42c**; $[\alpha]_D$= –196.0 (c=0.27, CH_3CN) and (*S*)-**42c**; $[\alpha]_D$ = +193.6 (c=0.27, CH_3CN)

(*R*)-**42d**; $[\alpha]_D$ = –300.5 (c=0.20, CH_3CN) and (*S*)-**42d**; $[\alpha]_D$ = +300.4 (c=0.20, CH_3CN)

By direct comparison between $[\alpha]_D$ of the samples and values in the literature,[13,24,25] the absolute configurations of both enantiomers of (*R*)-**42a**–**d** and (*S*)-**42a**–**d** could then be assigned. However, more evidences were still required for the stereochemical assignments of (*R*)-**42a**–**e** and (*S*)-**42a**–**e**. Circular dichroism spectra of all (*R*)-**42** and (*S*)-**42** were therefore determined (Figures 10–14). In fact, all compounds assigned as (*S*)-configuration displayed similar CD curves with first negative Cotton effect around 300–350 nm, while compounds assigned as (*R*)-configuration showed the mirror image curves in comparison to the (*S*)-isomer, giving CD curves with the first positive Cotton effect. These results were in good agreement with the results reported by Areephong.[25] Accordingly, the conclusion of the absolute configuration of binaphthol derivatives could be assured and related to the chiral sense of both binaphthols **40** and **41**.

Consequently, the faster moving, less polar, isomers **40a**–**e** consist of (*R*)-binaphthol whereas binaphthols of the slow moving, more polar isomers **41a**–**e**, have an (*S*)-configuration.

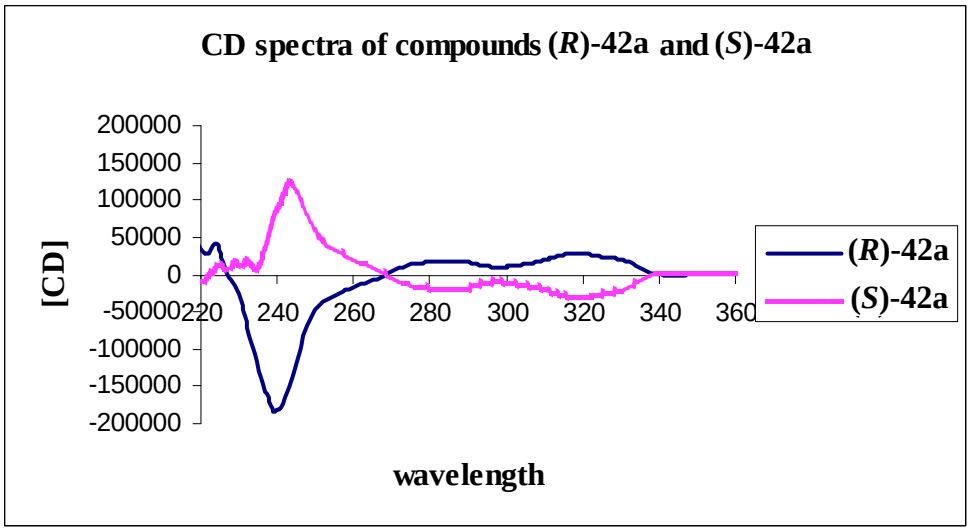

Figure 10. CD spectra of compound (*R*)-**42a** and (*S*)-**42a**.

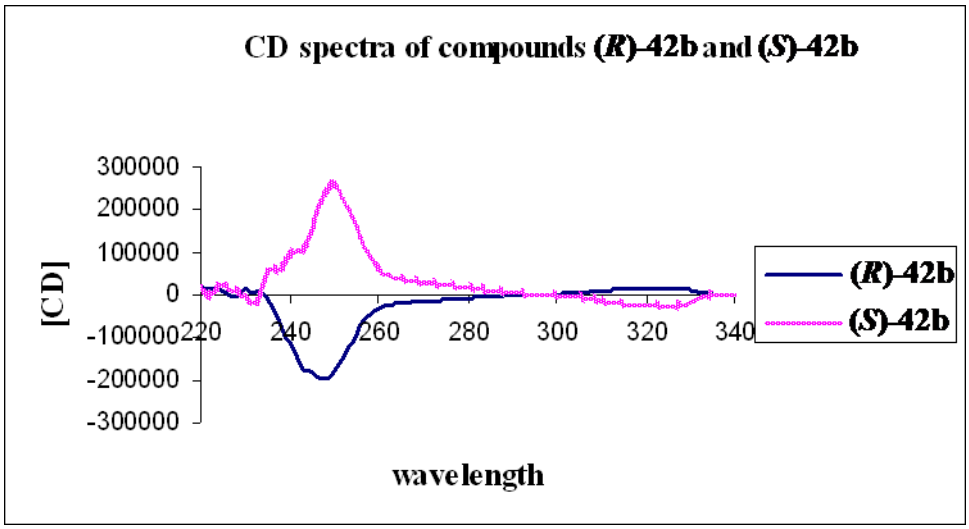

Figure 11. CD spectra of compound (*R*)-**42b** and (*S*)-**42b**.

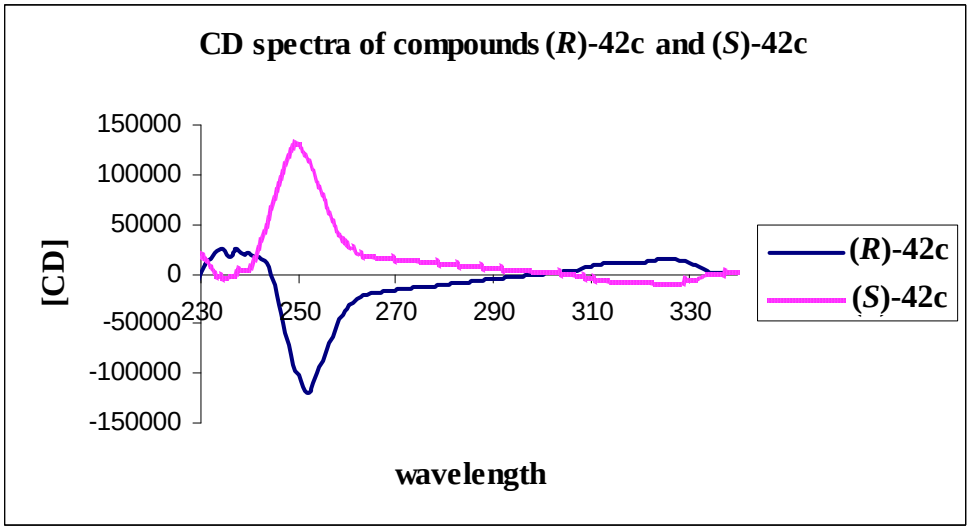

Figure 12. CD spectra of compound (*R*)-**42c** and (*S*)-**42c**.

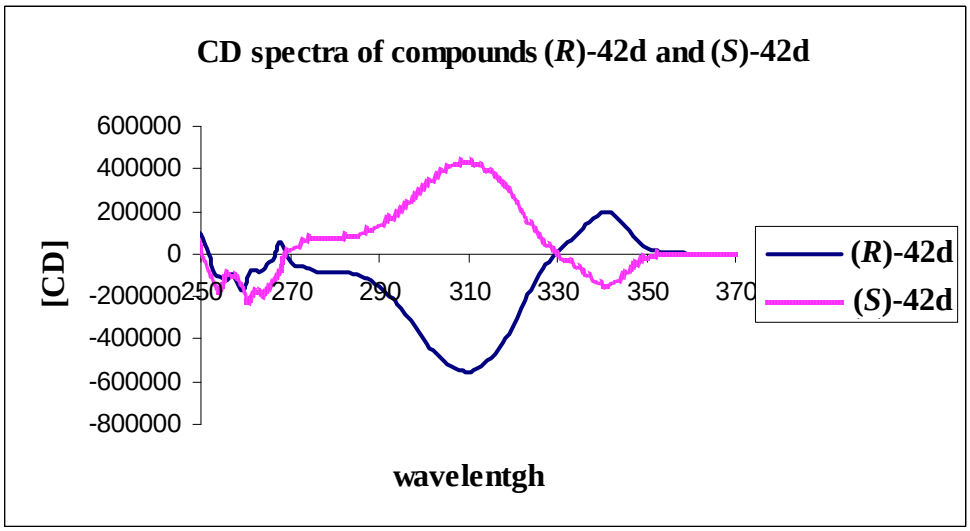

Figure 13. CD spectra of compound (*R*)-**42d** and (*S*)-**42d**.

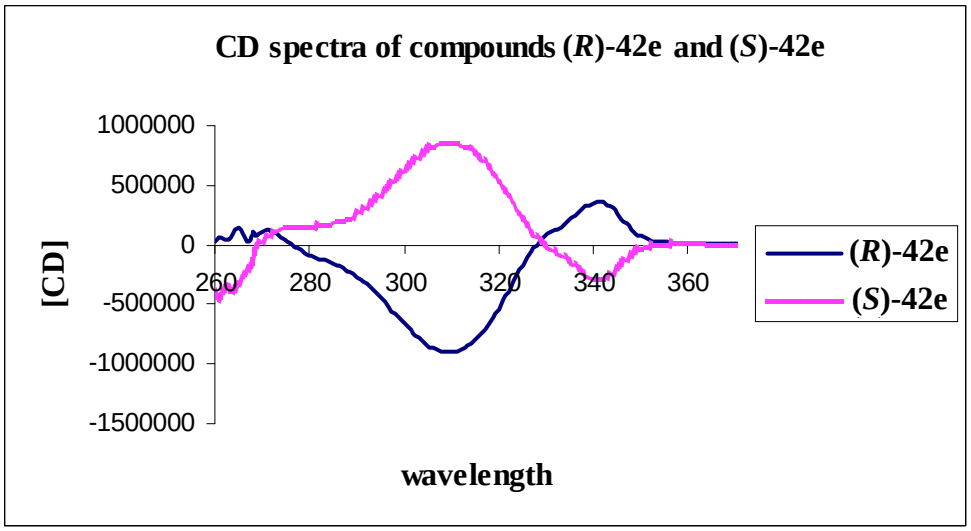

Figure 14. CD spectra of compound (*R*)-**42e** and (*S*)-**42e**.

The extended study of the resolution by using (*S*)-(+)-2,3-dihydro-1,4-epoxynaphthalene-1(2*H*)-carboxylic acid **4** with 7,7'-Dimethoxy-[1,1']-binaphthalenyl-2,2'-diol was also performed to compare the results with those of (*R*)-(–)-acid **4**. A mixture of chiral acid chloride (*S*)-(+)-**38**, *rac*-binaphthol **39b**, NEt_3 and DMAP in CH_2Cl_2 was stirred for 24 h, yielding a diastereomeric mixture of esters. The mixture was separated by PLC on silica gel (hexane: EtOAc 85:15; separation factor α = 1.32) (Scheme 14). The first-eluted ester **43** (46%, $[\alpha]_D$ –3.74 (c = 1.50 w/v, CH_3CN)) and the second one **44** (42%, $[\alpha]_D$ –17.23 (c = 1.50 w/v, CH_3CN)) were obtained.

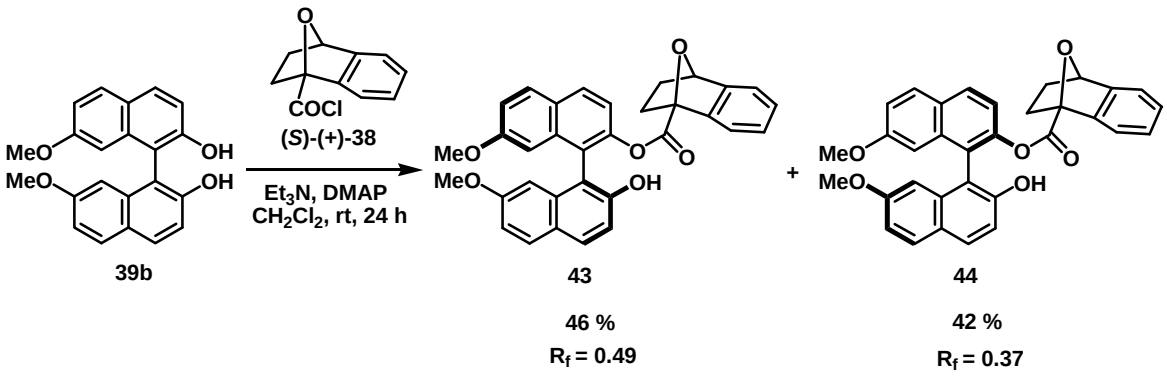

Scheme 14. Resolution of binaphthols **39b** with (*S*)-(+)-acid chloride **38**.

^{1}H NMR signals of esters **43** and **44** similarly showed a significant difference of chemical shifts of their methylene group on the α-oxa acid (Table 3). Chemical shift of methylene protons (H_a = 1.23 and H_b = 0.89) of compound **44** were upfield shifted by diamagnetic anisotropic effect of naphthalene moiety when compared to its diastereomer **43** (H_a = 1.40 and H_b = 1.25).

In addition, CD spectra of the first-eluted ester **43**, was directly opposite to **40b**, *i.e.* it displayed first positive Cotton effect at 326, 277 nm and strong positive Cotton effect at 248 nm. Moreover, CD of ester **44** was opposite to the CD spectra of compound **41b**, displayed first negative Cotton effect at 327, 277 nm and strong positive Cotton effect at 250 nm (Figure 15).

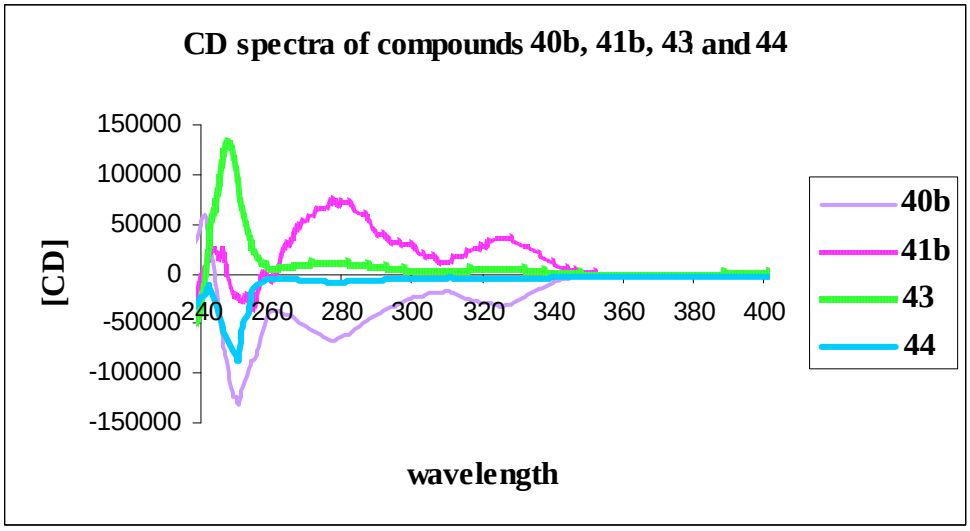

Figure 15. CD spectra of compound **43** and **44** from (*S*)-(+)-acid **4** compared with compound **40b** and **41b** from (*R*)-(–)-acid **4**.

The absolute configuration of each diastereoisomer was determined by converting them to the corresponding binaphthol. Esters **43** and **44** were hydrolyzed with KOH in MeOH and dioxane to give binaphthol derivatives (*S*)-**42b** (79% yield) and (*R*)-**42b** (82% yield), respectively (Scheme 15).

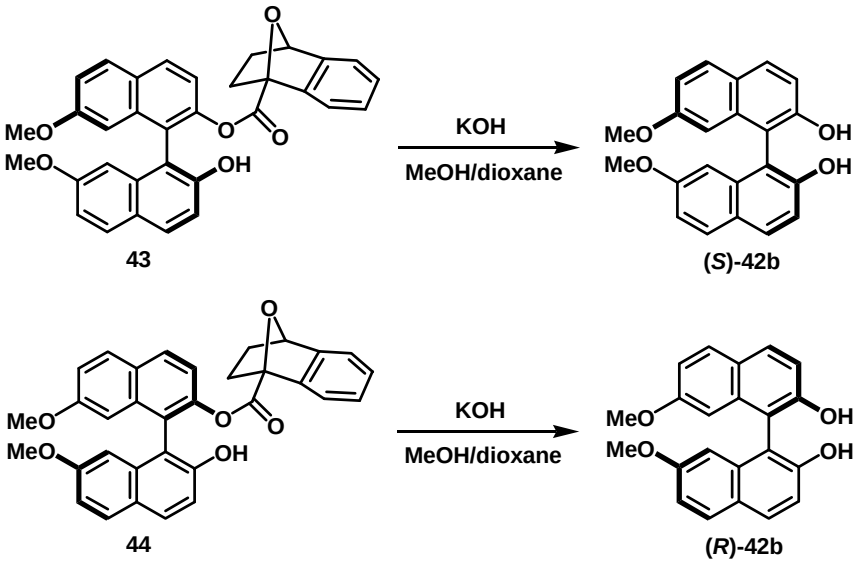

Scheme 15. Formation of optically active binaphthols **42b** from (*S*)-(+)-acid **4**.

The optical rotations of binaphthols (*R*)-**42b** and (*S*)-**42b** from (*R*)-(–)-acid and (*S*)-(+)-acid **4** were also exhibited in Table 6.

Table 6. Specific optical rotations of 7,7'-Dimethoxy-[1,1']-binaphthalenyl-2,2'-diols (*R*)-**42b** and (*S*)-**42b**, hydrolyzed from (*R*)-(–)-acid and (*S*)-(+)-acid **4**.

Entry	$[\alpha]_D$ of binaphthol (*R*)-42b	$[\alpha]_D$ of binaphthol (*S*)-42b
1.From (*R*)-(–)-acid	–119.97 at 25.9 °C, c = 1.00	+117.95 at 25.7 °C, c = 1.15
2.From (*S*)-(+)-acid	–132.44 at 25.6 °C, c = 1.20	+103.57 at 25.7 °C, c = 1.10

Based on the CD analysis, the faster moving, less polar isomer **43**, suggested (*S*)-binaphthol **42b**, while binaphthol of the slow moving, more polar isomer **44**, has an (*R*)-configuration (Figure 16).

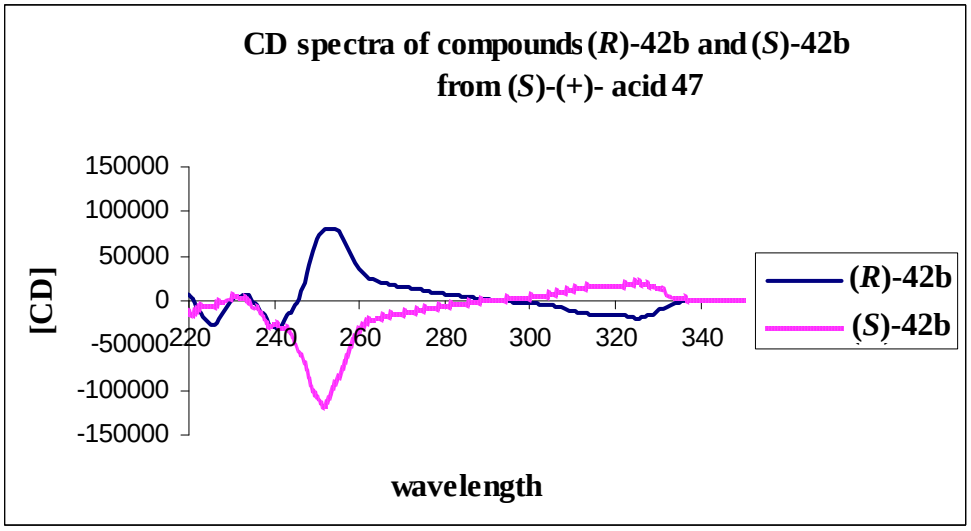

Figure 16. CD spectra of compound (*S*)-**42b** and (*R*)-**42b** from (*S*)-(+)-acid **47**.

It is clear that (*S*)-(+)-acid **47** can be used as a chiral derivatizing agent in the same manner as its corresponding isomer, (*R*)-(–)-acid, does.

In addition to the CD analysis, compounds with good quality crystals, *i.e.* **40a**, **40b**, **40c**, **41b** and **41c**, were then subjected to X-ray diffraction analyses. Molecular structures were as shown in Figures 17–21. X-ray data clearly confirmed the assignment of absolute stereochemistry of binaphthols.

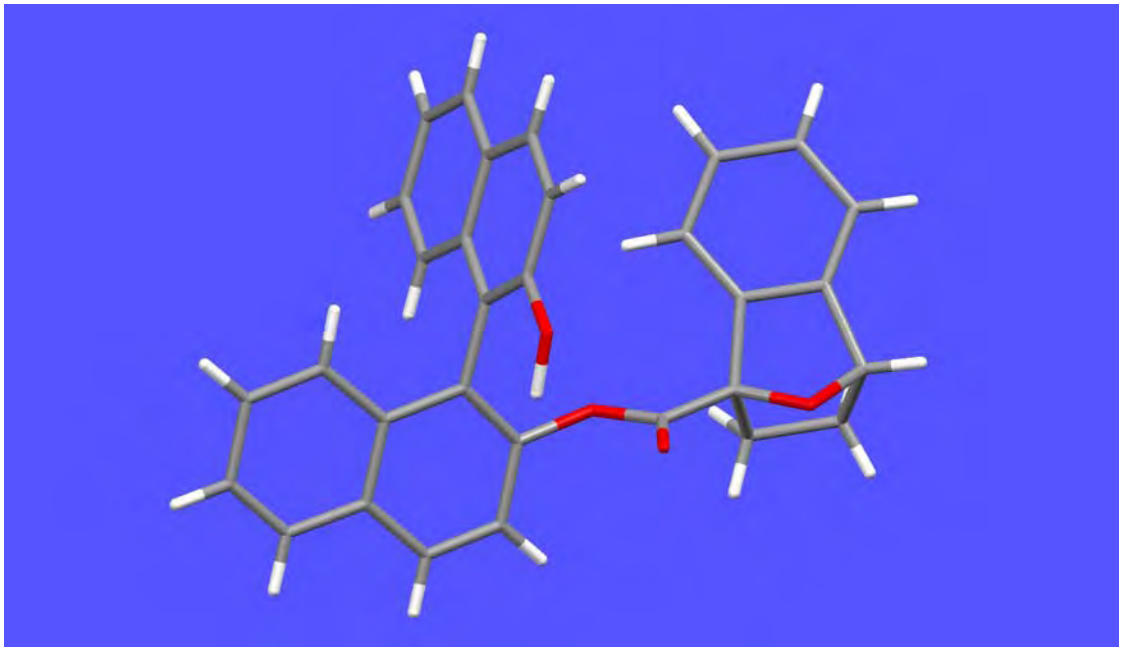

Figure 17. X-ray structure of compound (*R*,*R*)-**40a**.

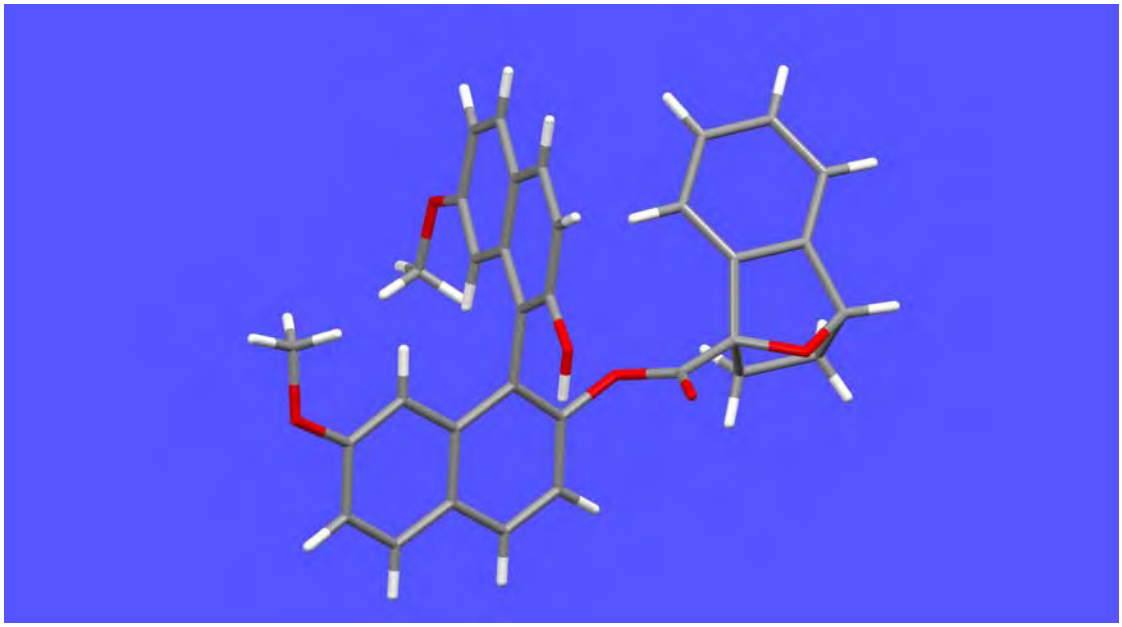

Figure 18. X-ray structure of compound (*R*,*R*)-**40b**.

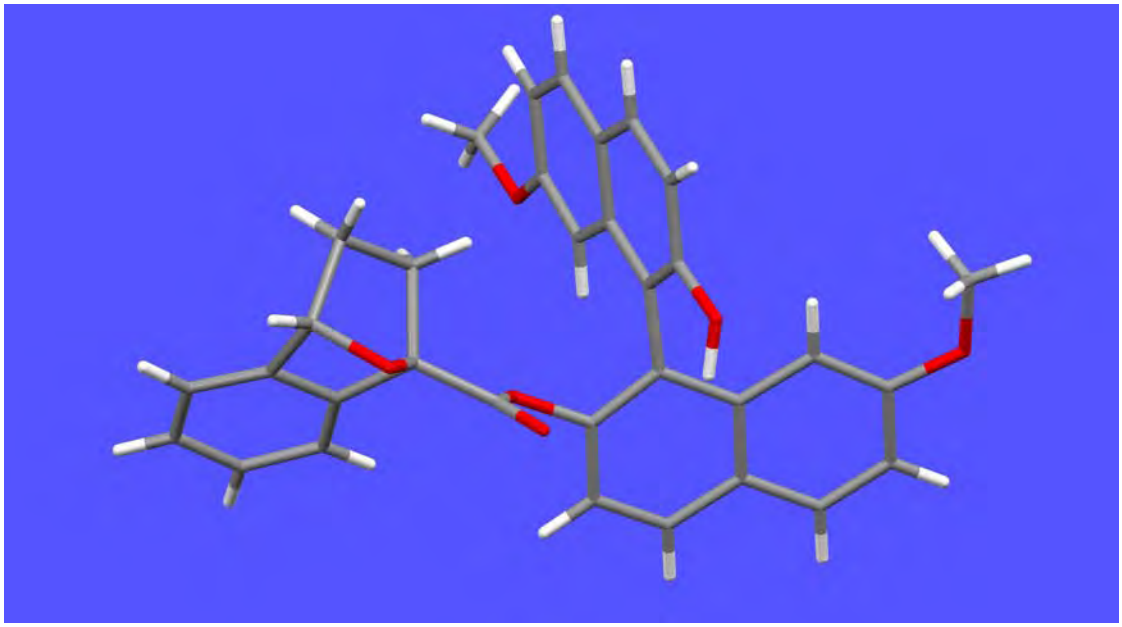

Figure 19. X-ray structure of compound (*R*,*S*)-**41b**.

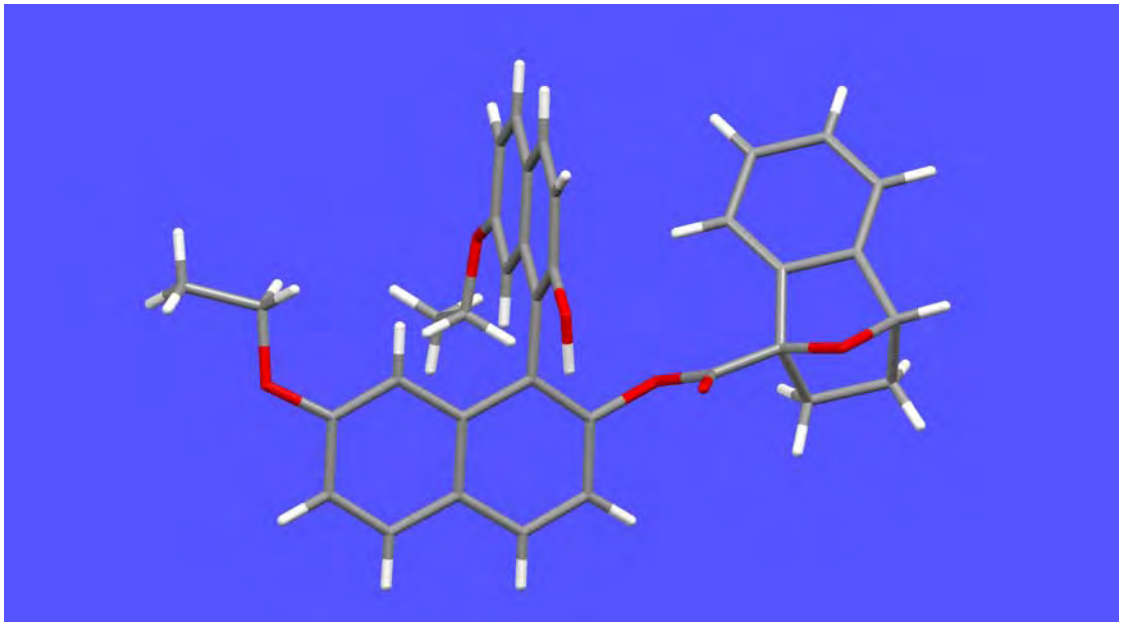

Figure 20. X-ray structure of compound (*R*,*R*)-**40c**.

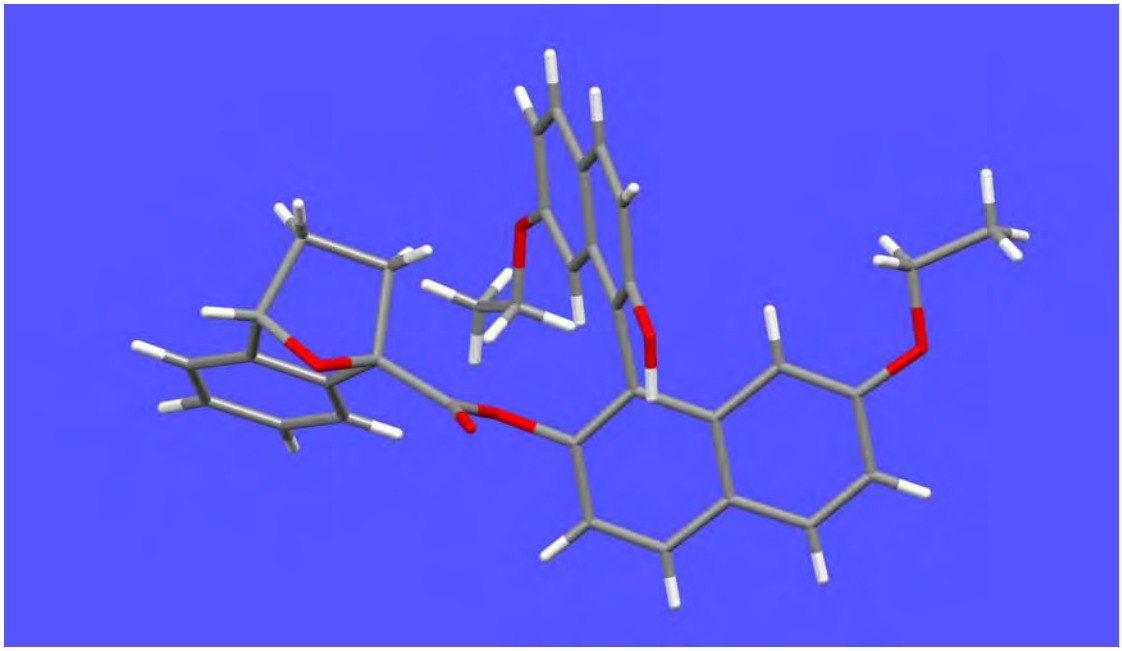

Figure 21. X-ray structure of compound (*R*,*S*)-**41c**.

It is remarkable that all diastereomers with similar chirality display the same chromatographic behavior. Thus, not only that the X-ray data provided the absolute configuration of binaphthol derivatives, but it also displayed the orientation of α-oxa bicyclic acid group over binaphthol moiety. Models to provide rationalization of this observation were then constructed, as analogy to the camphanate-binaphthol system.[25] Considering the structure of α-oxa acid-binaphthol derivatives (Figure 22), the orientation of α-oxa acid with respect to the binaphthol system was determined by the dihedral angles about four single bonds **a**, **b**, **c**, and **d**. The angles could be defined as follows: **a** (O=C–Cα–O), **b** (C2–O–C=O), **c** (C1–C2–O–C), and **d** (C2–C3–C4–C5) and the dihedral angle parameters **a**, **b**, **c**, and **d** were then studied from the X-ray analyses and the results were listed in Table 7.

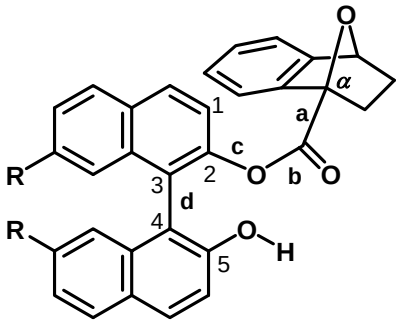

Figure 22. Defined parameters for conformational analysis.

Table 7. Structural parameters for binaphthol-(*R*)-α-oxa bicyclic acid according to X-ray Diffraction Analyses.

Entry	X-ray			
	a	**b**	**c**	**d**
40a	5.29	–6.16	–83.85	–87.19
40b	11.57	–10.35	–88.29	–102.11
40c	6.10	–11.18	–92.57	–96.55
41b	–5.39	–2.59	106.16	109.95
41c	–17.21	–7.86	102.59	110.27

The preferred conformation of bond **a** was proposed by Mosher[22] that the ester carbonyl and methoxy groups of the mandelic acid moiety lie in the same plane (Figure 23). The calculations on this mandelate derivative reveal that the mandelic acid moiety is in the conformation that dihedral angel **a** (O=C–C_{α}–OCH_3) is 0º. Because of the high EN of oxygen, the stereoelectronic effect would present the orientation in the way that the electron poor (C–O) σ bond will align in perpendicular to C–O π* bond. Thus C–OMe bond should either be syn- or antiperiplanar to C=O group.

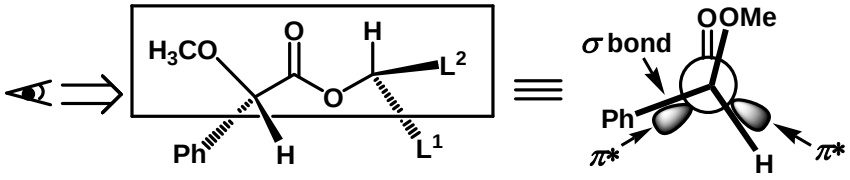

Figure 23. The stable conformation of mandelate model.

As expected, bond **a** in X-ray data shows its angle= 0±17° which greatly resembles the mandelic ester model.

The preferred conformation of bond **c** was clearly reported. The carbonyl group of ester would not lie in the plane of the benzene ring due to the steric repulsion between the carbonyl oxygen and the phenyl's C-1 hydrogen. Thus the C=O of the ester bond, in Figure 40, must point either up, away from the binaphthol moiety (*exo*), or point down, toward the aromatic ring (*endo*). From the X-ray data, the preferred angles of bond **c** would most likely be perpendicular to the aromatic plane, being 90+ 16° or –90±2° (*exo*).

The ester bond **b**, in general, is planar and resumes s-*trans* configuration rather than s-*cis*. This can be attributed to the stereoelectronic effect from the lone pair electron of oxygen ether which is oriented antiperiplanar to the C–O σ bond of the carbonyl group. This orbital can therefore overlap with the antibonding orbital (σ*) of the carbonyl, or in other words, the hyperconjugation between an ether oxygen lone pair and a σ* orbital of the carbonyl group as shown in Figure 24.[27] Thus the dihedral angle **b** in the binaphthol structure should be 0±5°. From the X-ray structures, the C=O bond of diastereomers **40** and **41** would most likely be planar, being 0±11°.

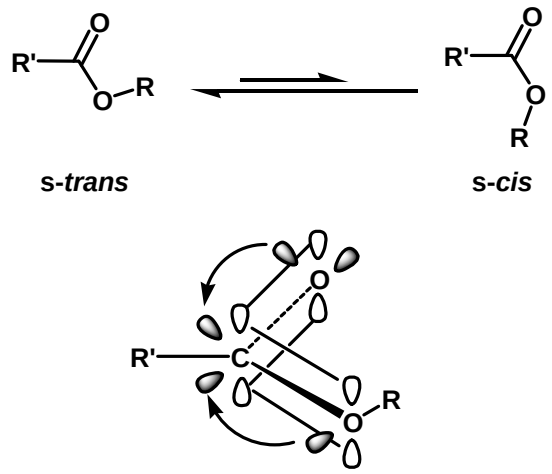

Figure 24. Favored configuration of ester bond.

For binaphthol derivatives, their structures, especially bond **d** are not conformationally rigid. They can therefore exist in both cisoid and transoid conformations.[28] The X-ray crystallographic studies for binaphthol derivatives showed the dihedral angle **d** in the range of 96–110° (transoid) except ester **40a** displayed the dihedral angle **d** = 87° (cisoid).

Apparently X-ray analysis gave information on key dihedral angles on each binaphthol derivatives. Unlike helicene-camphanate system,[17] this analysis did not provide sufficient evidence to explain the difference in polarity of each diastereomeric pair. Detailed molecular structures, derived from the NMR data, implemented with computational chemistry calculations, are still required.

References

1. Eliel, E. L. Stereochemistry of organic compounds. New York: John Wiley and Sons 1994.
2. Moss, G. P. *Pure Appl. Chem* **1996**, *68*, 2193-2222.
3. Cooke, A. S.; Harris, M. M. *J. Chem. Soc.* **1963**, 2365-2373.
4. Hall, D. M.; Turner, E. E. *J. Chem. Soc.* **1995**, 1242-1251.
5. Akimoto, H.; Yamada, S. *Tetrahedron* **1971**, *27*, 5999-6009.
6. Noyori, R. *Acc. Chem. Res.* **1990**, *23*, 345-350.
7. Noyori, R.; Ohta, T.; Takay, H. Catalytic Asymmetric Synthesis. New York: John Wiley and Sons 1993.
8. Ding, K.; Wang, Y.; Zang, L.; Wu, Y.; Matsuura, T. *Tetrahedron* **1996**, *52*, 1005-1010.
9. Kamikawa, K.; Watanabe, T.; Daimon, A.; Uemura, M. *Tetrahedron* **2000**, *56*, 2325-2337.
10. Meyers, A. I.; McKennon, M. J. *Tetrahedron Lett.* **1995**, *36*, 5869-5872.
11. Meyers, A. I.; Nelson, T. D. *J. Org. Chem.* **1994**, *59*, 2655-2658.
12. Brunel, J. M.; Buono, G. *J. Org. Chem.* **1993**, *58*, 7313-7314.
13. Chow, H. F.; Wan, C. W.; Ng, M. K. *J. Org. Chem.* **1996**, *61*, 8712-8714.
14. Mason, S. F.; Seal, R. H.; Roberts, D. R. *Tetrahedron* **1974**, *30*, 1671-1682.
15. Harada, N.; Nakashi, K. Circular dichroic spectroscopy, exciton coupling in organic stereochemistry. Mill Valley, CA; University Science Books 1983, 193-201.
16. Panchal, B. M.; Einhorn, C.; Einhorn, J. *Tetrahadron Lett.* **2002**, *43*, 9245-9248.
17. Thongpanchang, T. ; Paruch, K. ; Katz, T. J. ; Rheingold, A. L. ; Lam, K. C. ; Liable-Sands L. *J. Org. Chem.* **2000**, *65*, 1850-1856.
18. Fuji, K.; Sakurai, M.; Kinoshita, T.; Kawabata, T.; *Tetrahedron Lett.* **1998**, *39*, 6323-6326.
19. Fukushi, Y.; Shigematsu, K.; Mizutani, J.; Tahara, S. *Tetrahedron Lett.* **1996**, *37*, 4737-4740.
20. Fuji, K.; Yang, X. S.; Ohnishi, H.; Hao, X. J.; Obata, Y.; Tanaka, K. *Tetrahedron: Asym.* **1999**, *10*, 3243-3248.
21. Hua, D. H.; Nguyen, T. X. C.; Mcgill, J. W.; Chen, Y.; Robinson, P. D. *Tetrahedron: Asym.* **2001**, *12*, 1999-2004.

22. Dale, J. A.; Mosher, H. S. *J. Am. Chem. Soc.* **1973**, *95*, 512-519.
23. Kakisawa, H.; Ohtani, I.; Kusumi, T.; Kashman, Y. *J. Am. Chem. Soc.* **1991**, *113*, 4092-4096.
24. Best, W. M.; Collins, P. A.; McCulloch, R. K.; Wege, D. *Aust. J. Chem.* **1982**, *35*, 843-848.
25. Areephong, J. [M.Sc. Thesis in Organic Chemistry]. Bangkok: Faculty of Graduate Studies, Mahidol University; 2005.
26. Akimoto, H.; Shioiri, T.; Iitaka, Y. *Tetrahedron Lett.* **1968**, *1*, 97-102.
27. Deslongchamps, P. Stereoelectronic Effects in Organic Chemistry. Pergamon Press: Oxford 1983, *1*.
28. a) Mason S F. Molecular optical activity and the chiral discriminations. New York: Cambridge University Press; **1982**: 73.
    b) Gottarelli, G., Spada, G. P. *J. Org. Chem.* **1986**, *51*, 589-592.

APPENDIX

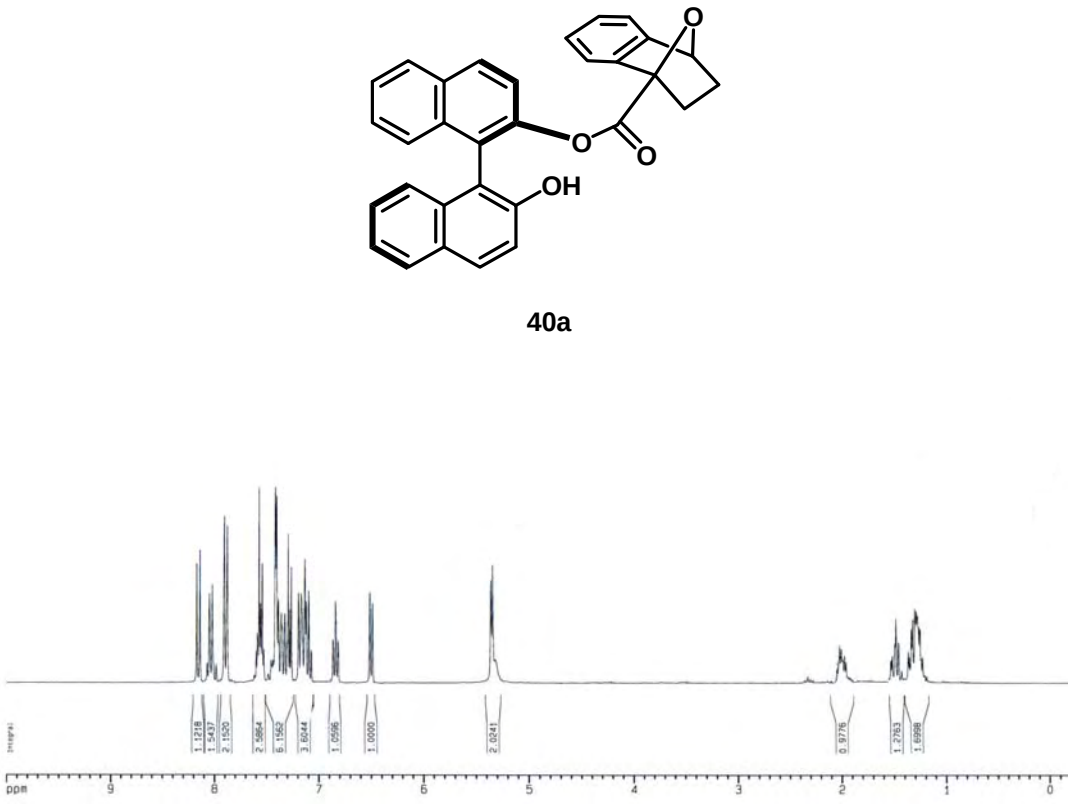

40a

Figure A1. ^{1}H NMR spectrum of compound **40a**.

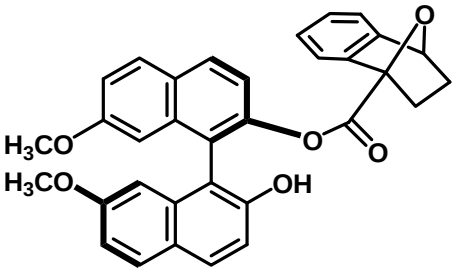

40b

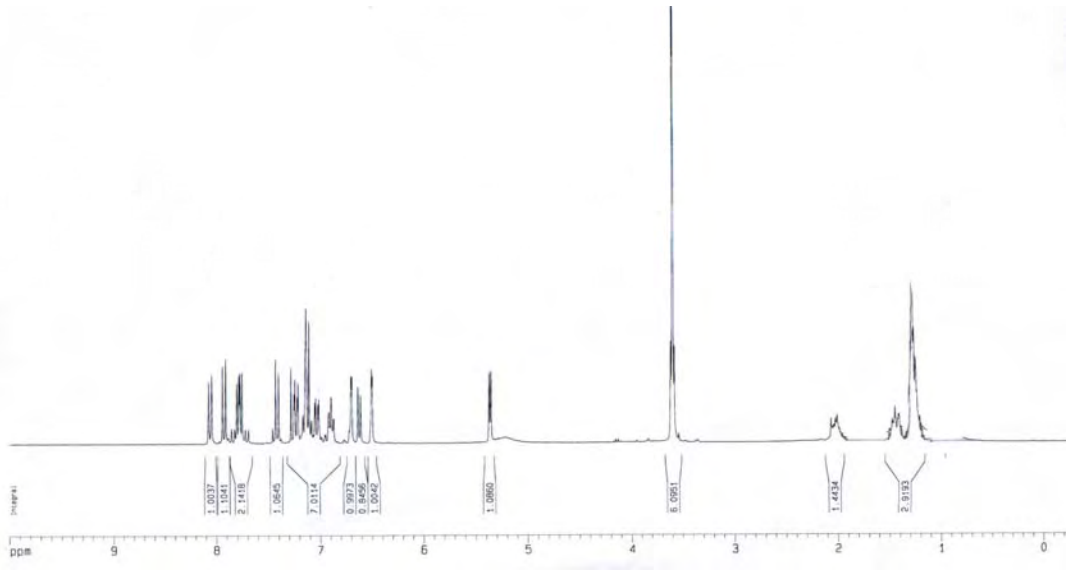

Figure A2. ^{1}H NMR spectrum of compound **40b**.

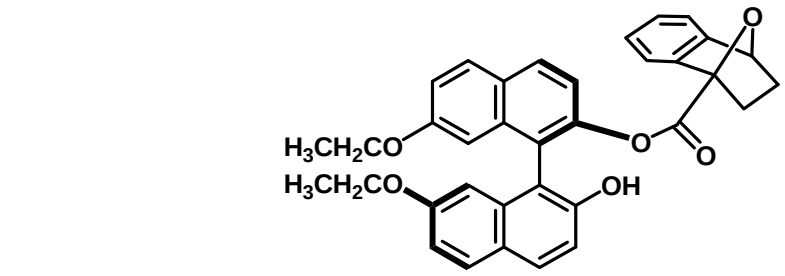

40c

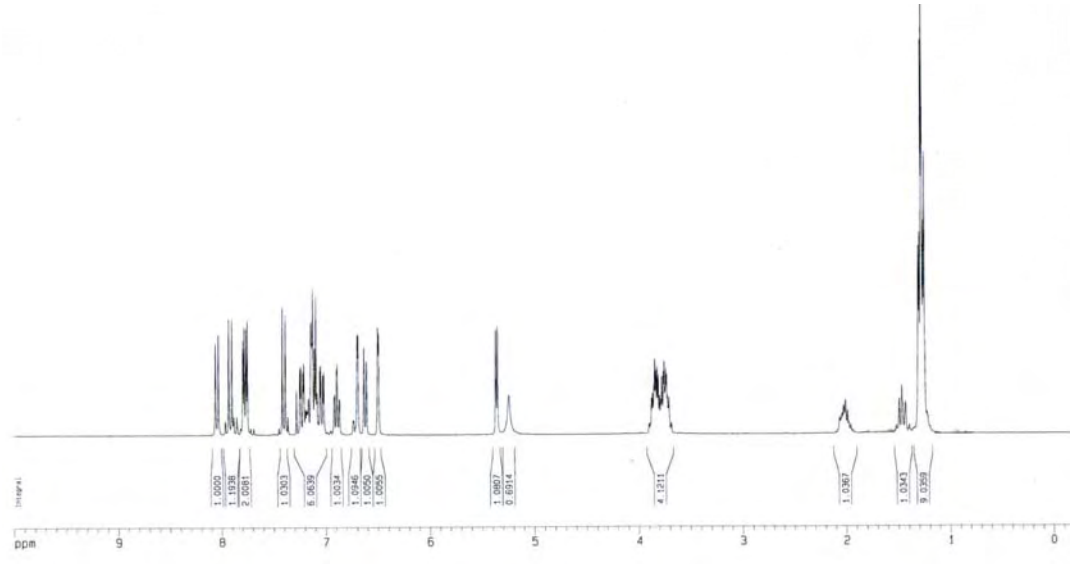

Figure A3. ^{1}H NMR spectrum of compound **40c**.

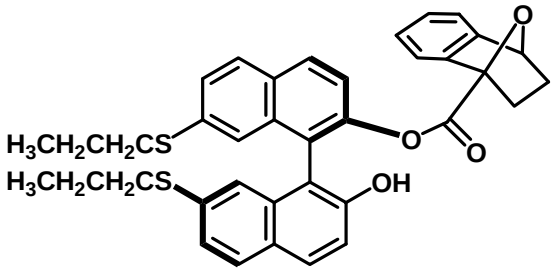

40d

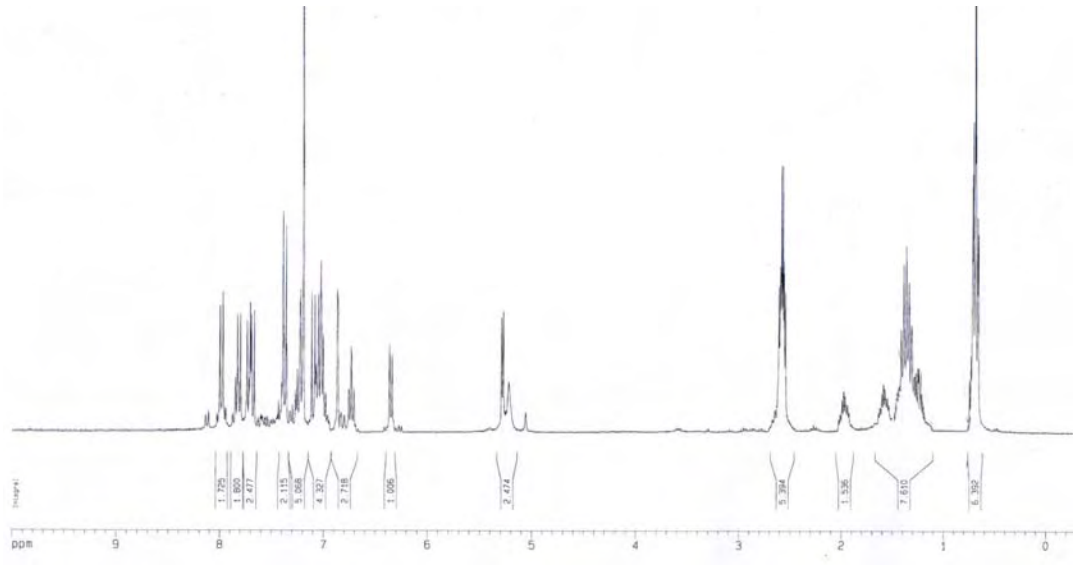

Figure A4. ^{1}H NMR spectrum of compound **40d**.

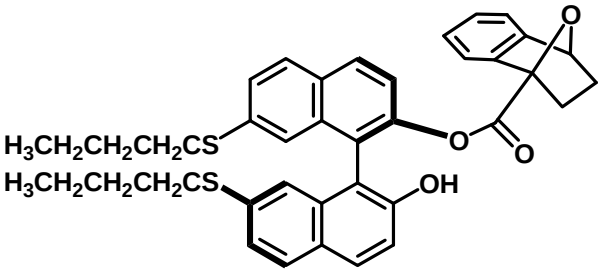

40e

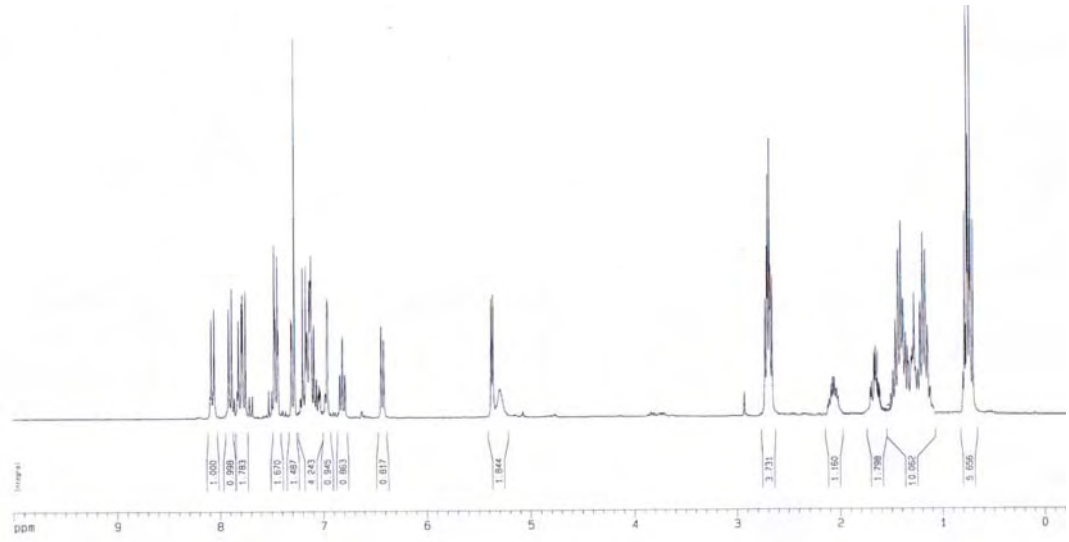

Figure A5. ^{1}H NMR spectrum of compound **40e**.

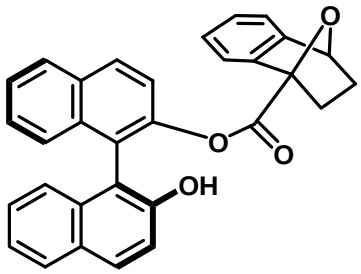

41a

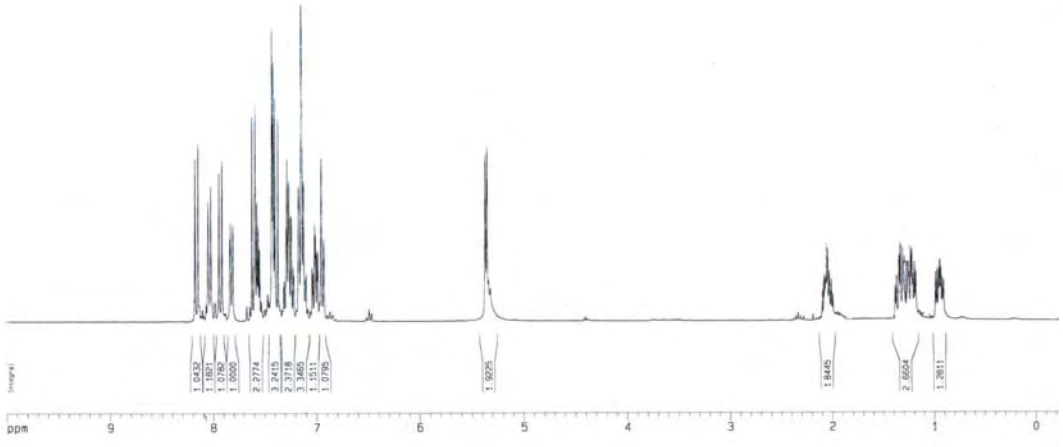

Figure A6. ^{1}H NMR spectrum of compound **41a**.

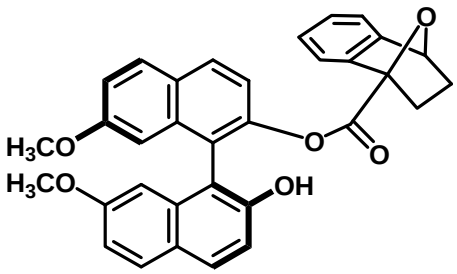

41b

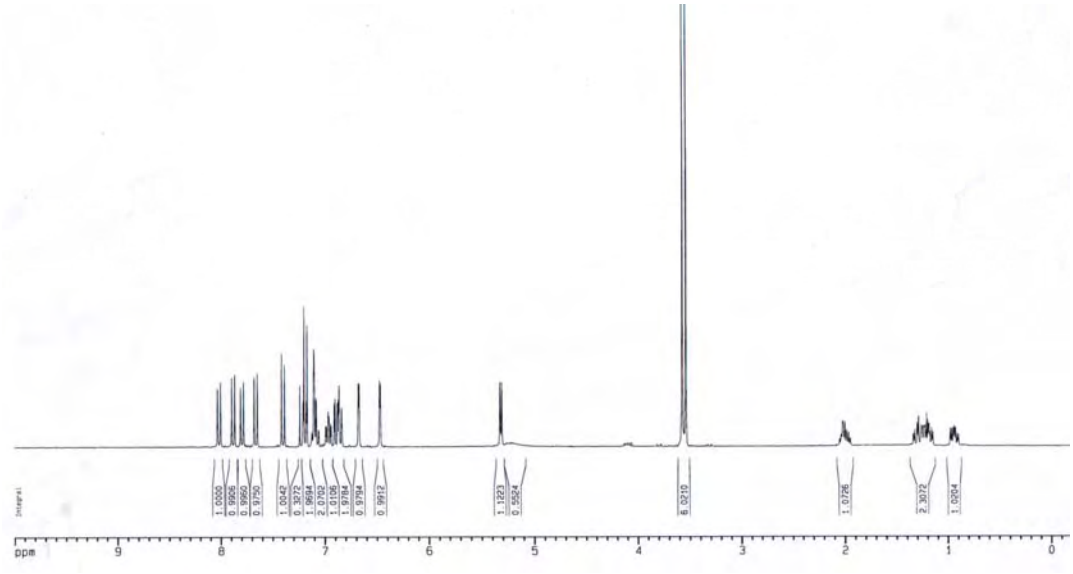

Figure A7. ^{1}H NMR spectrum of compound **41b**.

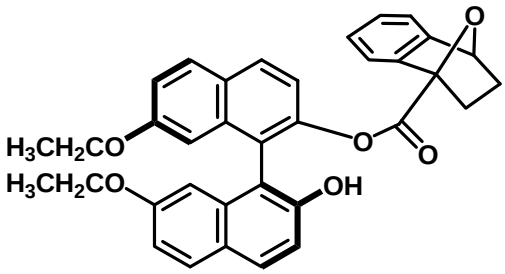

41c

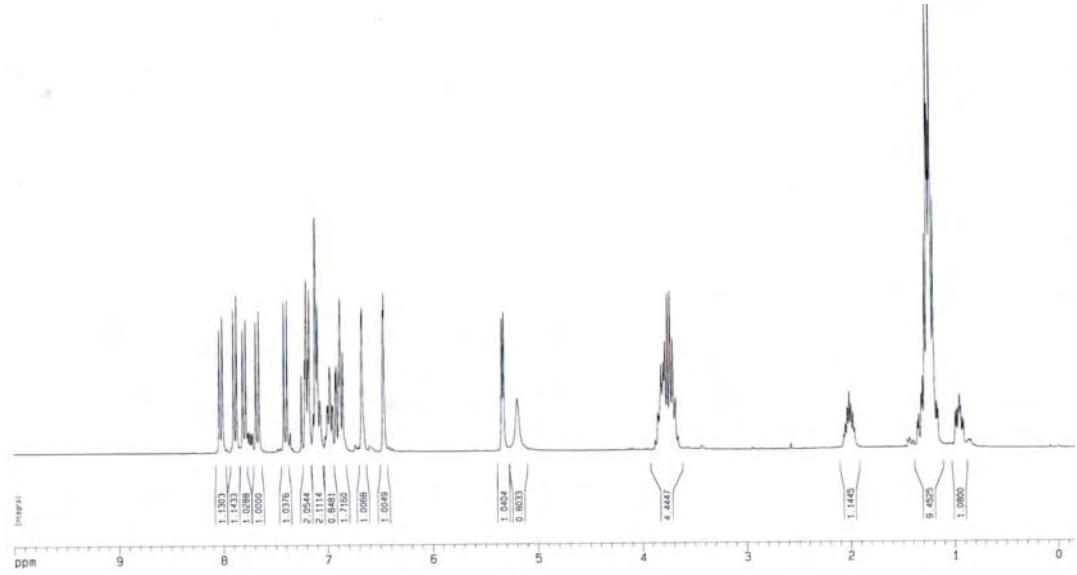

Figure A8. ^{1}H NMR spectrum of compound **41c**.

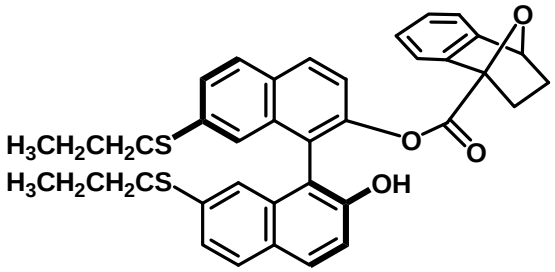

41d

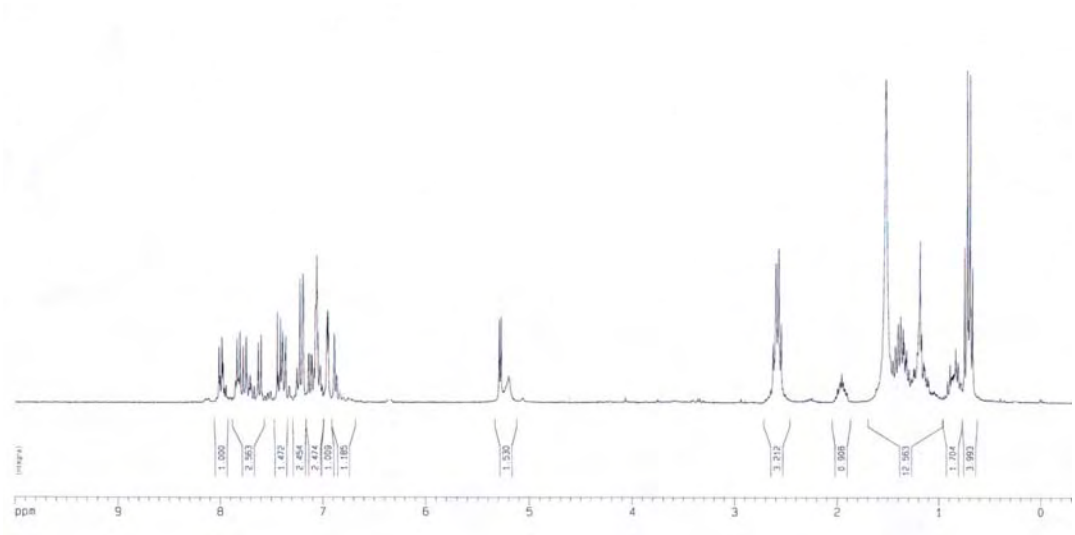

Figure A9. ^{1}H NMR spectrum of compound **41d**.

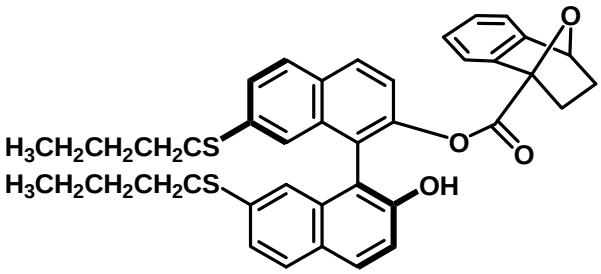

41e

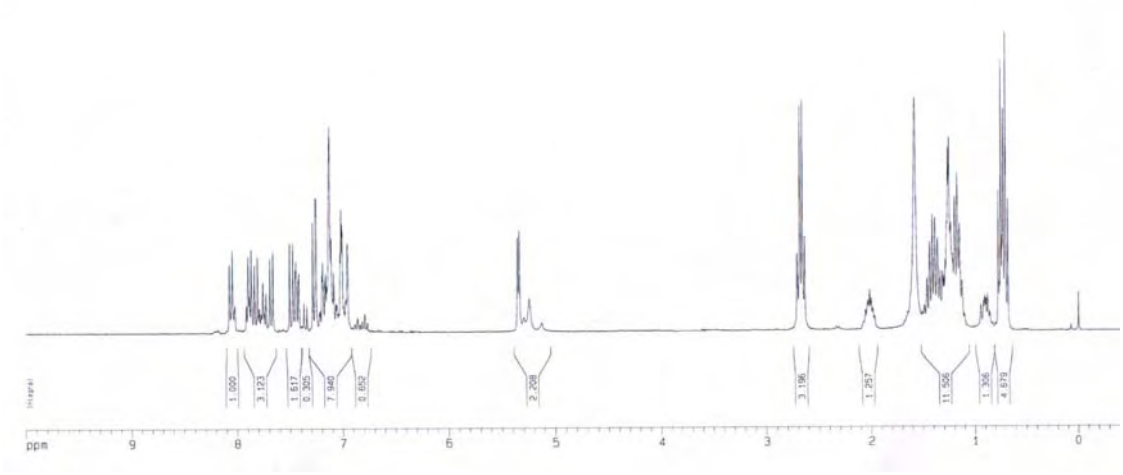

Figure A10. ^{1}H NMR spectrum of compound **41e**.

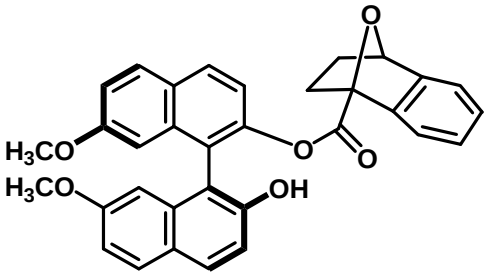

42

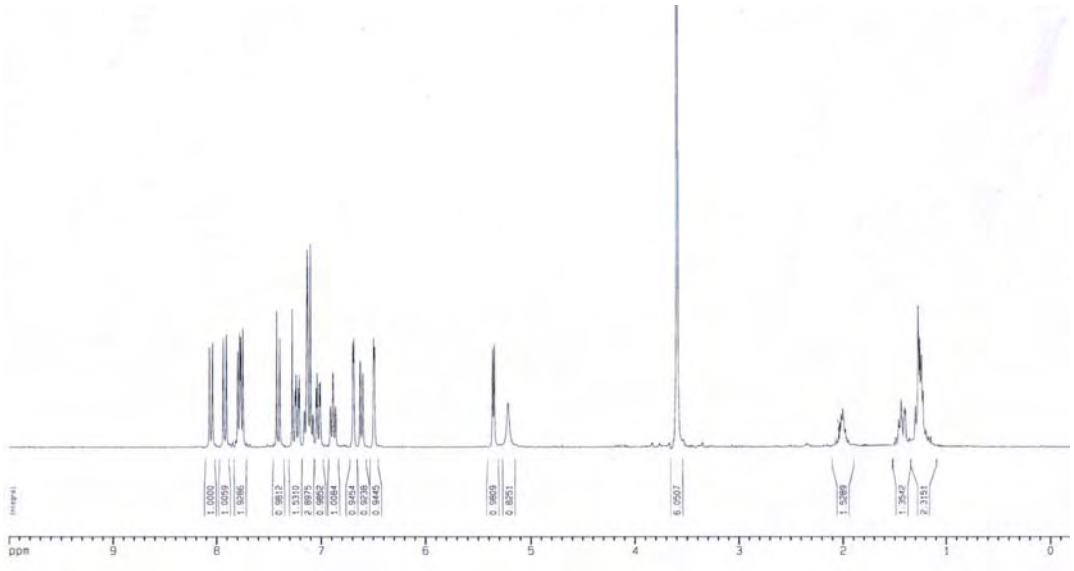

Figure A11. ^{1}H NMR spectrum of compound **42**.

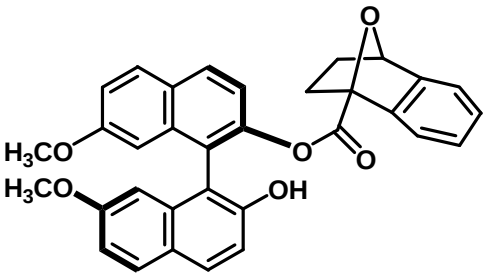

43

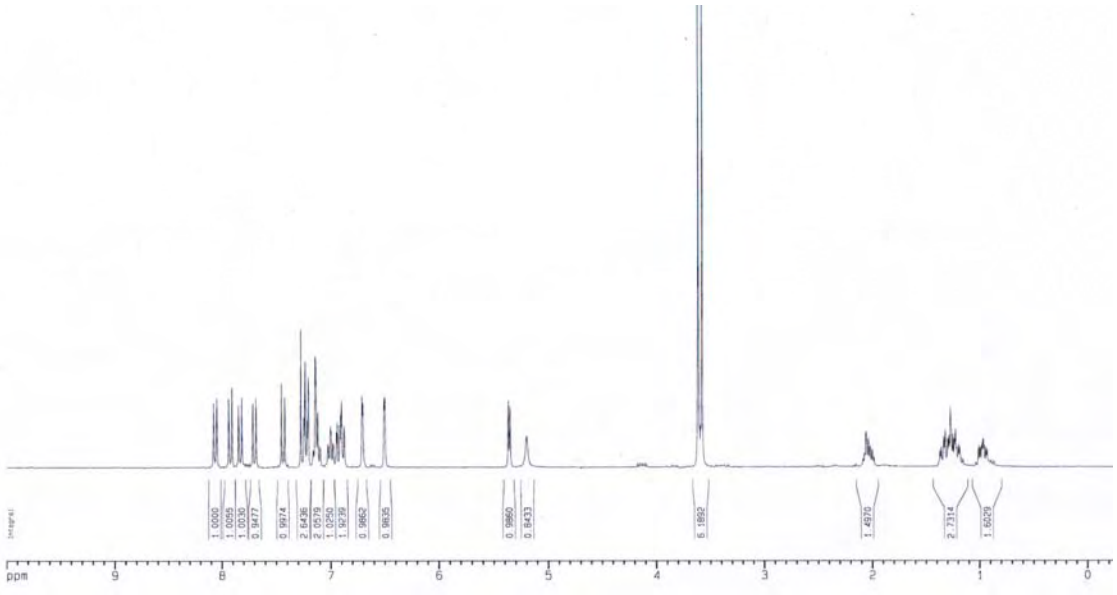

Figure A12. ^{1}H NMR spectrum of compound **43**.

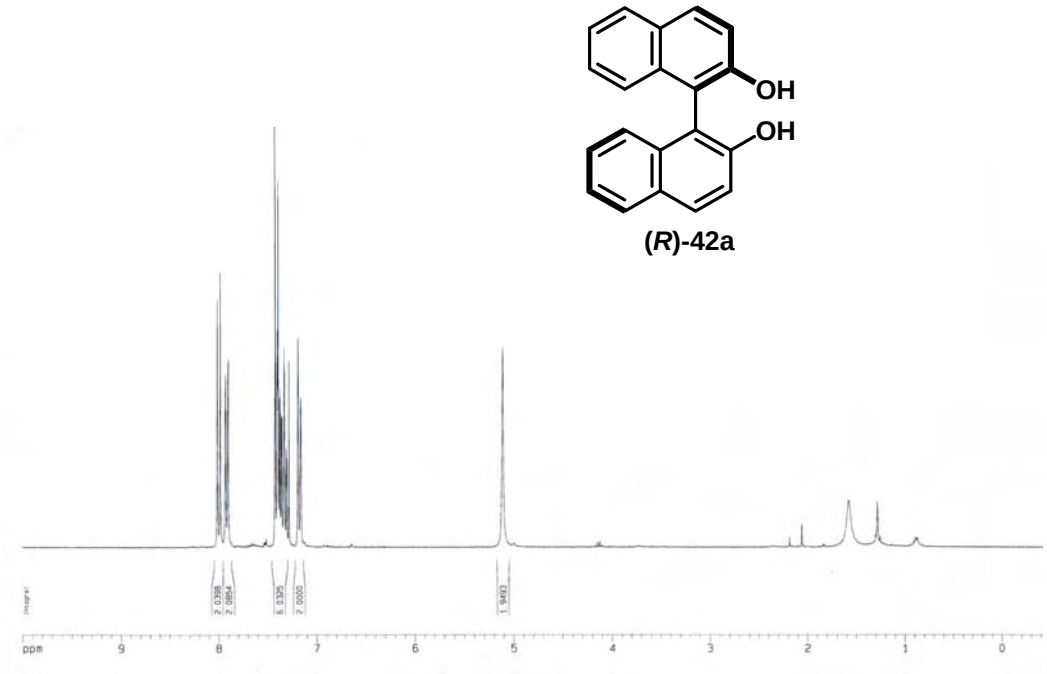

Figure A13. ^{1}H NMR spectrum of compound **(*R*)-42a.**

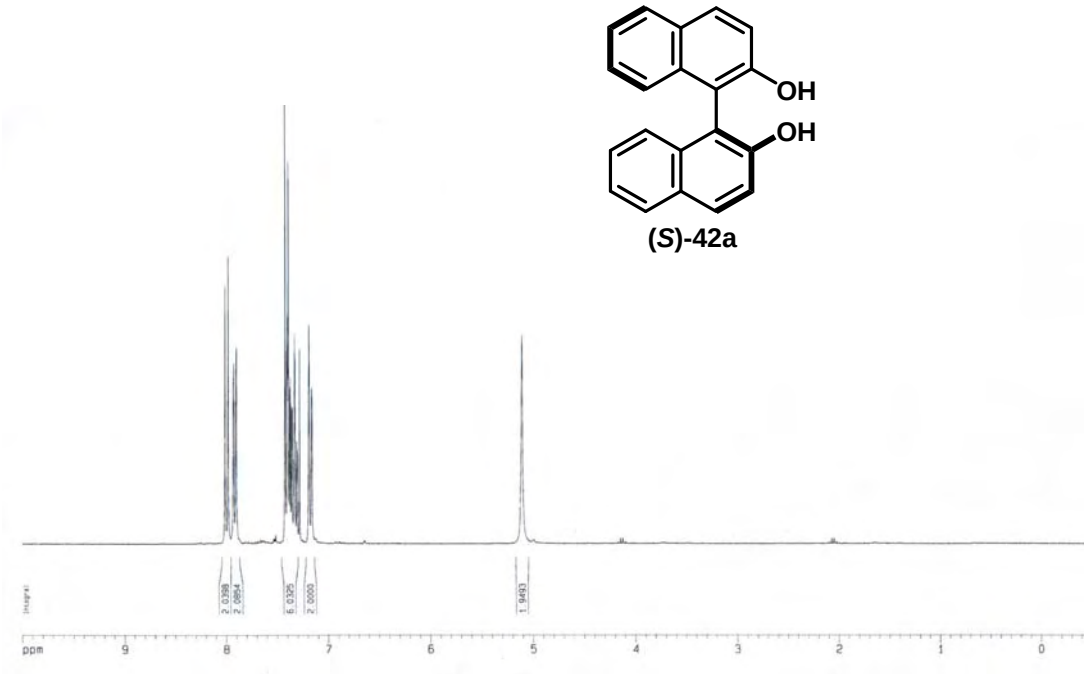

Figure A14. ^{1}H NMR spectrum of compound **(*S*)-42**a.

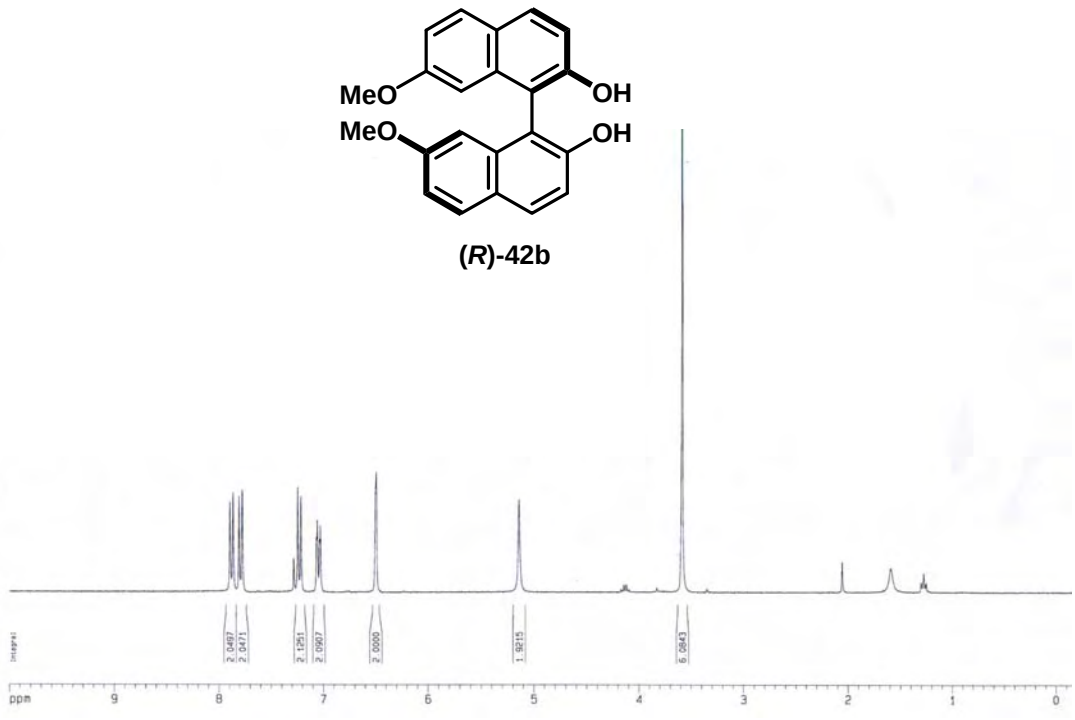

Figure A15. ^{1}H NMR spectrum of compound **(*R*)-42b**.

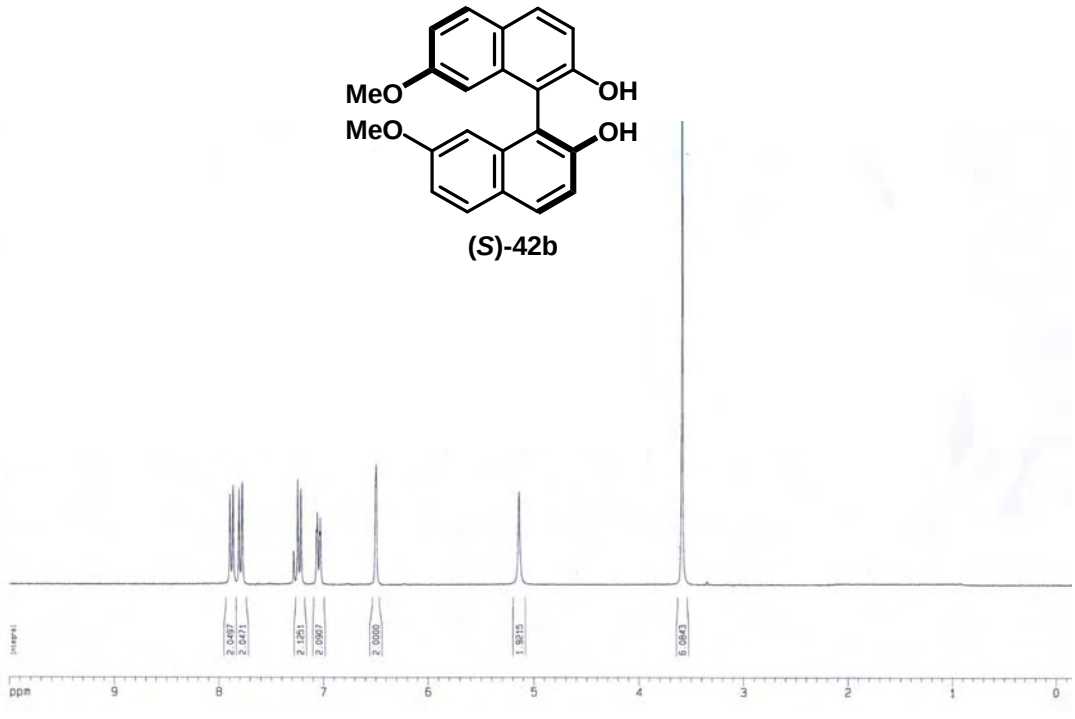

Figure A16. ^{1}H NMR spectrum of compound **(*S*)-42b**.

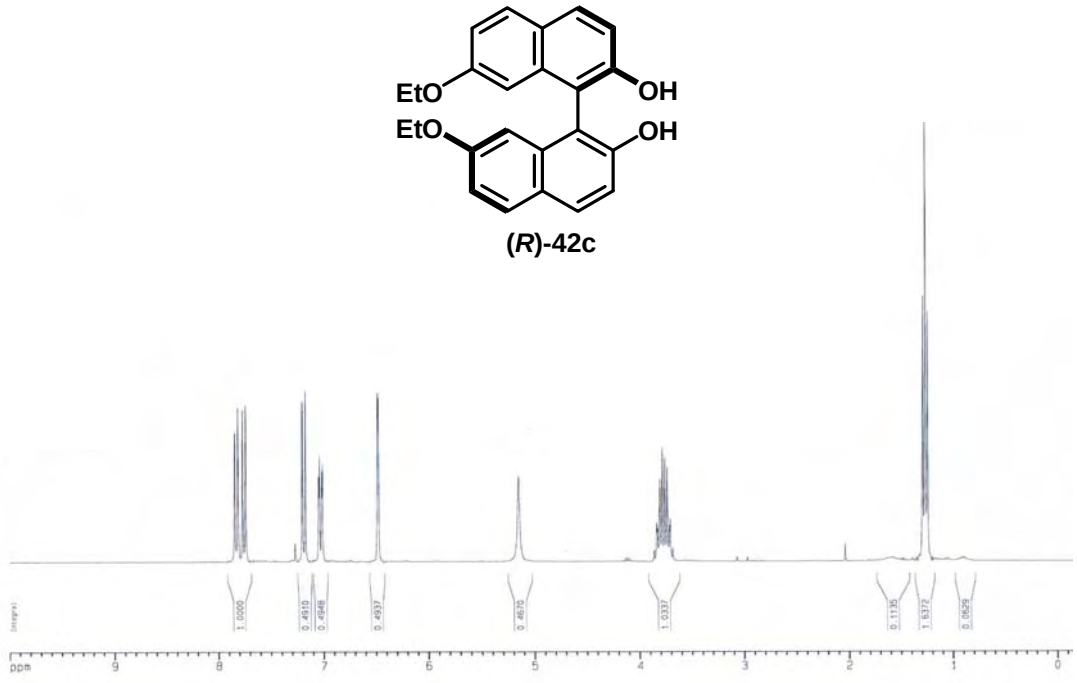

Figure A17. ^{1}H NMR spectrum of compound **(*R*)-42c**.

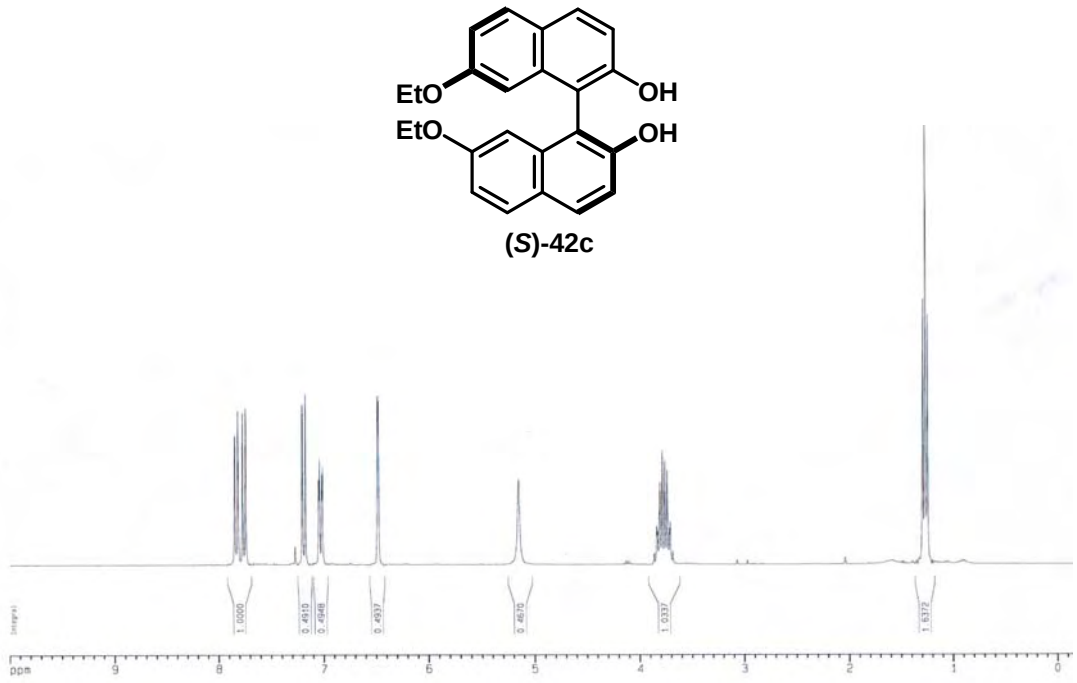

Figure A18. ^{1}H NMR spectrum of compound **(*S*)-42c**.

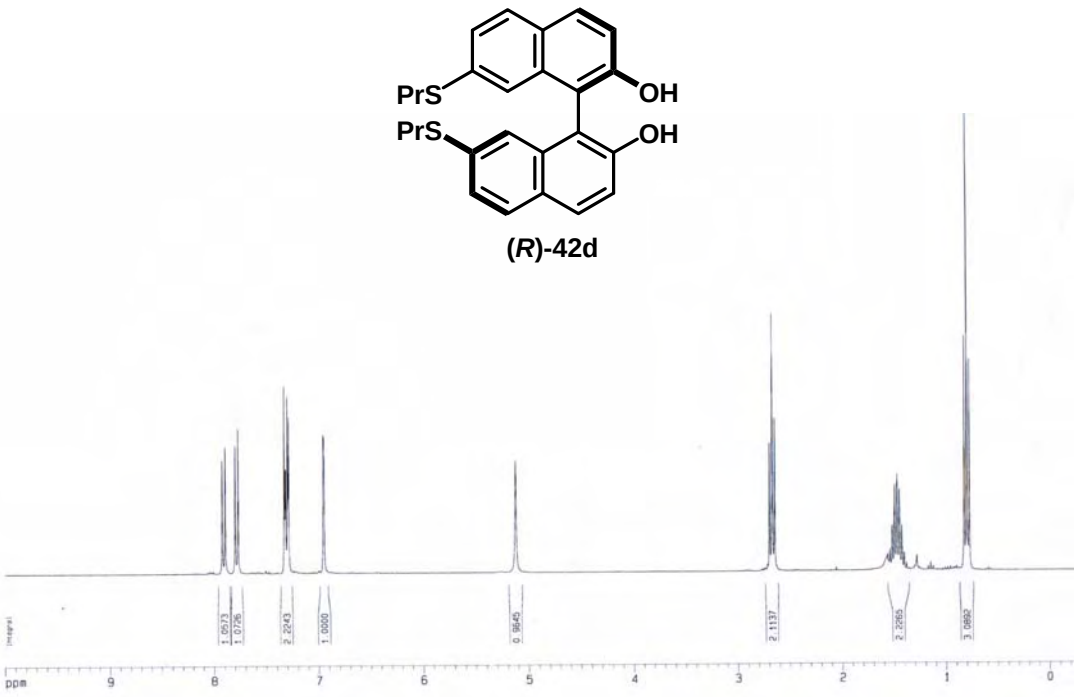

Figure A19. ^{1}H NMR spectrum of compound **(*R*)-42d**.

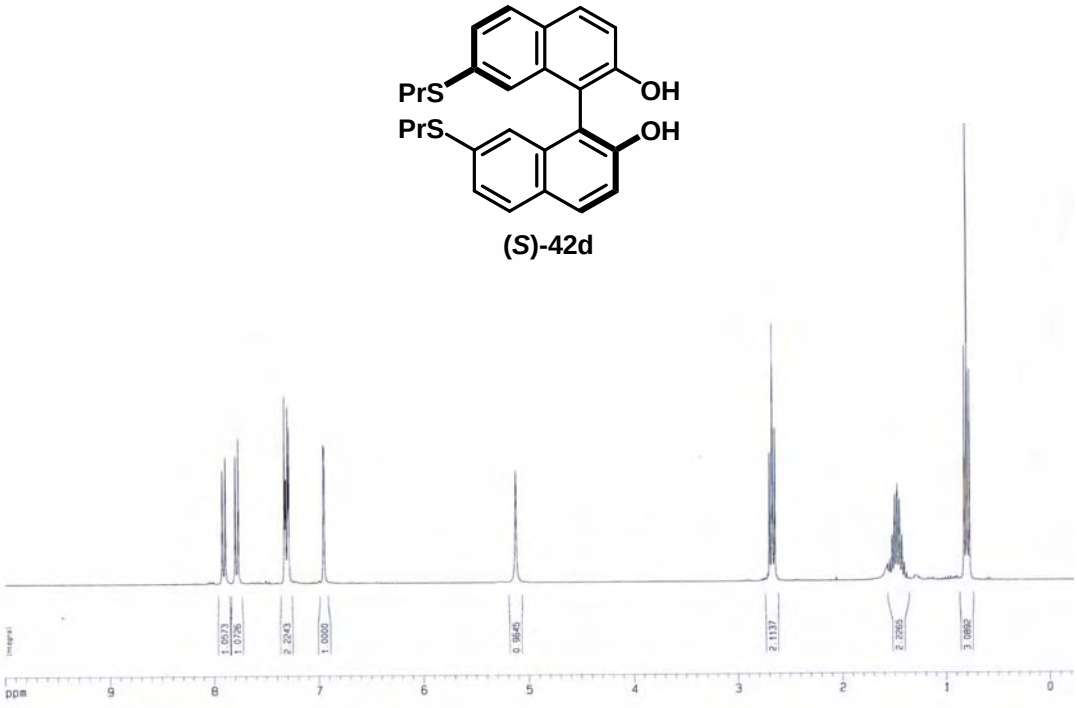

Figure A20. ^{1}H NMR spectrum of compound **(*S*)-42d**.

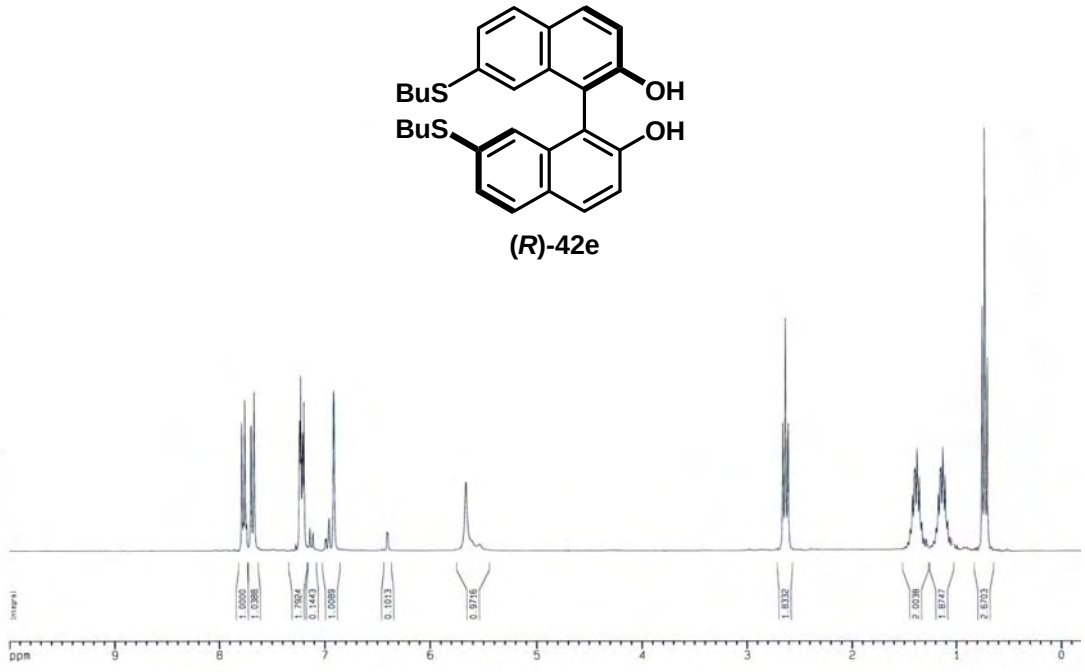

Figure A21. ^{1}H NMR spectrum of compound **(*R*)-42e**.

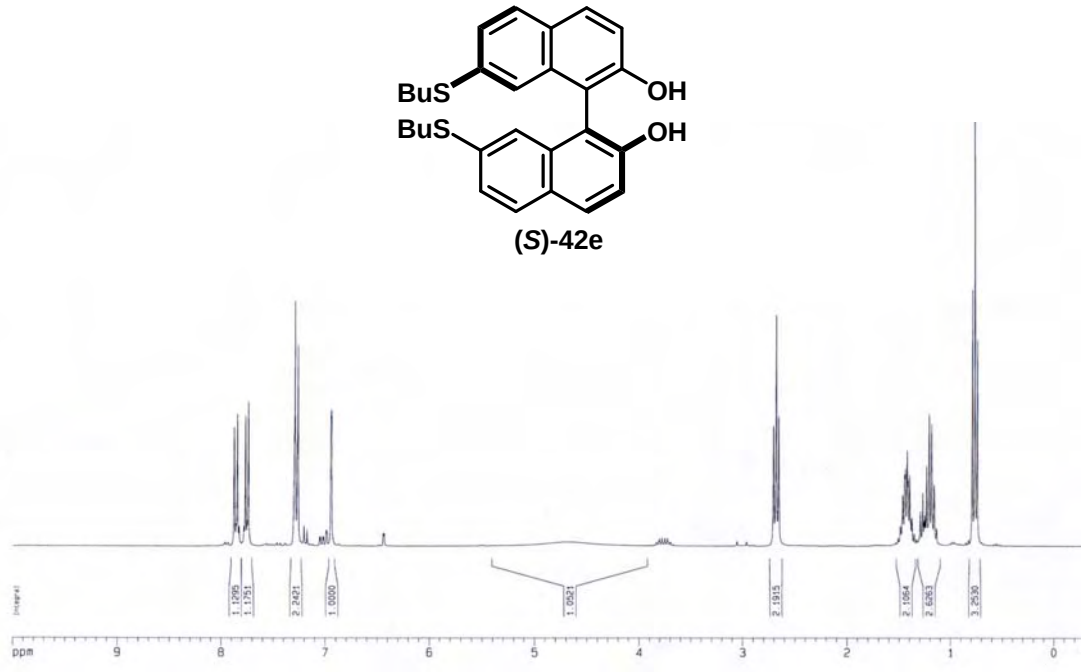

Figure A22. ^{1}H NMR spectrum of compound **(*S*)-42e**.

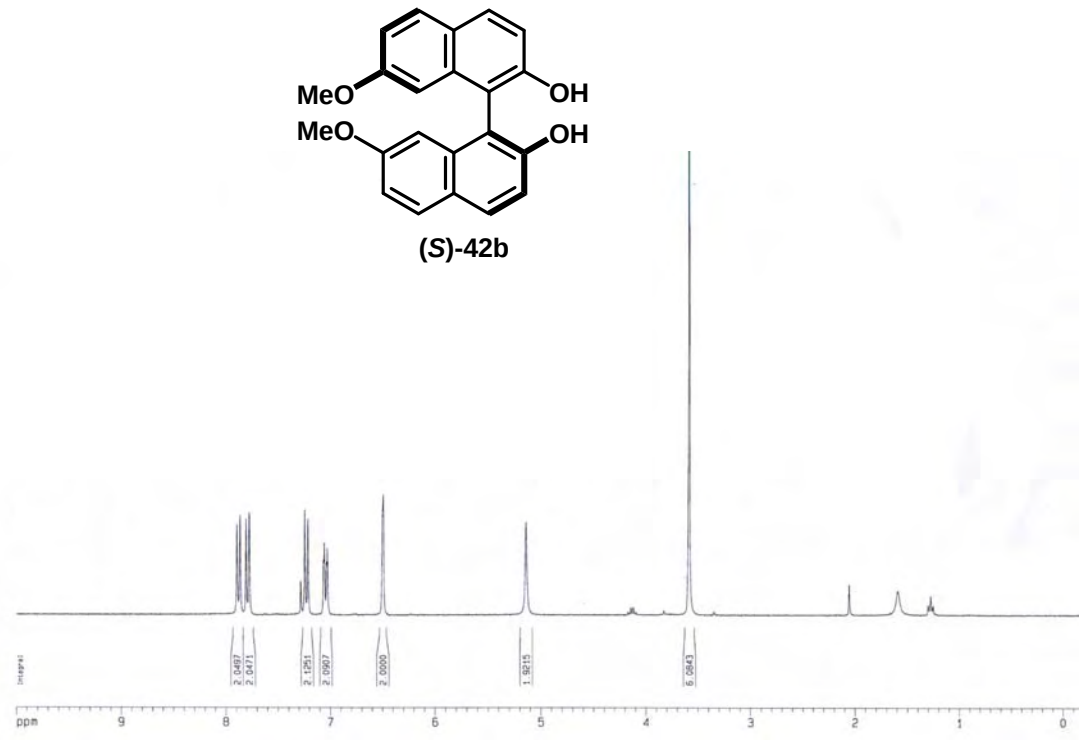

Figure A23. ^{1}H NMR spectrum of compound **(*R*)-42b** from (*S*)-acid.

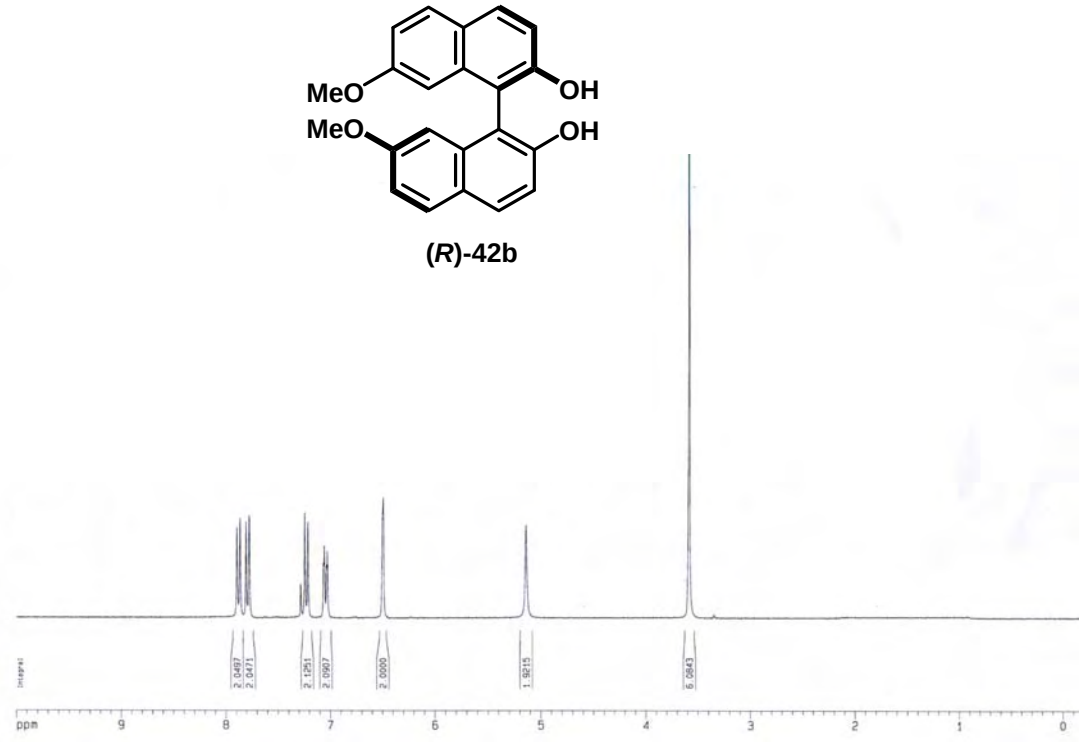

Figure A24. ^{1}H NMR spectrum of compound **(*S*)-42b** from (*S*)-acid.

Part III. Oxidative photocyclization of diaryl sulfides: A new approach towards new thiophene-based organic materials

During the study of the preparation of binaphthol derivatives and the synthesis of oxa-[5]-helicenes, it was found that our chemistry on the acid catalyzed nucleophilic substitution of phenols could lead to the synthesis of dinapthothiophene derivatives. Thus this part of this report then described briefly the investigation of this chemistry.

Introduction

Due to the high polarizability of sulfur electron in the thiophene ring which resulting in the great intermolecular interactions such as Van der Waals interactions, π–π or sulfur–sulfur interaction, sulfur containing heteroaromatic molecules are of great interest due to their potential application for organic light emitting diodes (OLEDs)[1] or organic field-effect transistors (OFETs).[2,3] For example, thieno[3,2-*f*:4,5-*f*']bis[1] benzothiophene (*syn*-**1**) and thieno[2,3-*f*:5,4-*f*']bis[1]benzothiophene (*anti*-**1**) have recently been characterized as new P-type organic semiconducting materials for OFETs (Figure 1).[3]

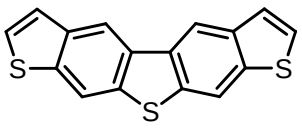

syn-**1**

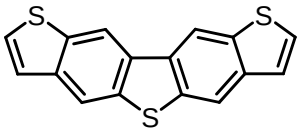

anti-**1**

Figure 1. Thieno[3,2-*f*:4,5-*f* ']bis[1]benzothiophene (*syn*-**1**) and Thieno[2,3-*f*:5,4-*f*']bis[1] benzothiophene (*anti*-**1**).

Furthermore, the applications of the fused ring thiophene derivatives have been found in the asymmetric catalysis. Dinaphtho[2,1-*b*:1',2'-*d*]thiophene **2**, for example, was used as a precursor for the synthesis of axially chiral binaphthyl derivative **3**, a chiral building block for the catalytic asymmetric reactions (Scheme 1).[4-6]

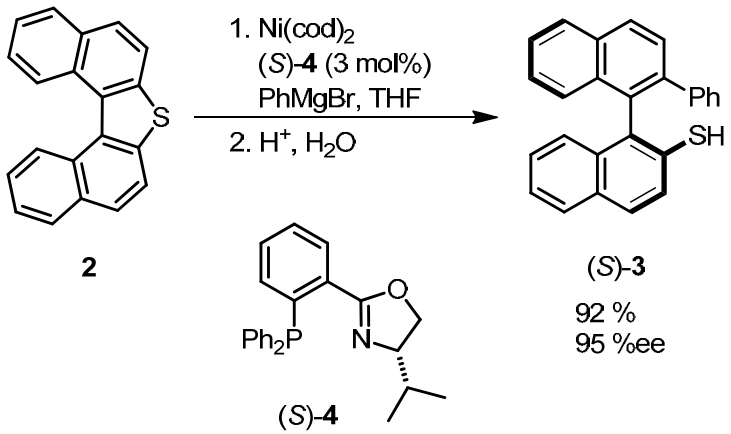

Scheme 1. Dinaphthothiophene **2** and its Nickel-catalyzed asymmetric Grignard cross-coupling to form axially chiral binaphthyl ligand **3**.

Accordingly, it is of great interest to study the synthesis of fused ring thiophene derivatives, such as dinaphthothiophene **2**. Previous reports described many procedures for the synthesis of dinaphthothiophene **2**. For example, Tedjamulia and co-workers reported that iodine-catalyzed oxidative photocyclization of 2-styrylnaphtho[2,1-*b*]thiophene **5** in the presence of iodine in cyclohexane for 4 hours provided dinaphtho[2,1-*b*:1',2'-*d*]-thiophene **2** in 45% yield (Scheme 2).[7]

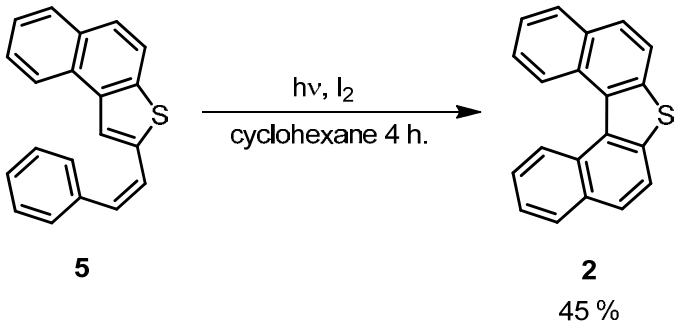

Scheme 2. Iodine-catalyzed oxidative photocyclization of stilbene analogue compound **5**.

Later, Fabbri and co-workers reported the preparation of enantiomerically pure (*R*)-1,1'-binapythyl-2,2'-dithiol **9** from (*R*)-1,1'-binaphthalene-2,2'-diol **6** *via* Newman-Kwart rearrangement (Scheme 3).[8] Thermal rearrangement of (*R*)-thiocarbamate **7** provided the product (*R*)-**8** in 70% yield and also dinaphthothiophene **2** in 20% yield.[8,9]

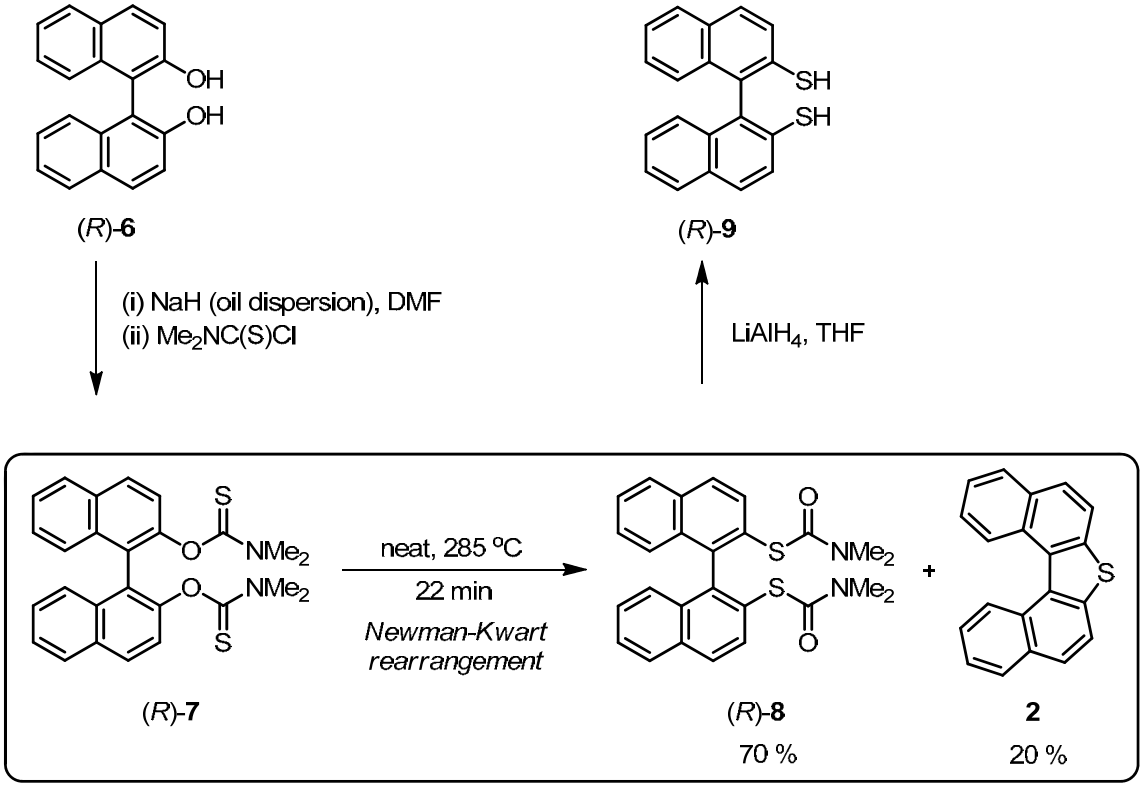

Scheme 3. Newman-Kwart rearrangement of (*R*)-**7**.

In 1999, Imamura and co-workers reported an application of the flash vacuum pyrolysis to synthesize sulfur containing heteroaromatic system.[10] Pyrolysis of bis-ethynyl thiophene **10** could afford not only the desired compound **2** but also the fused compound **11** (Scheme 4).

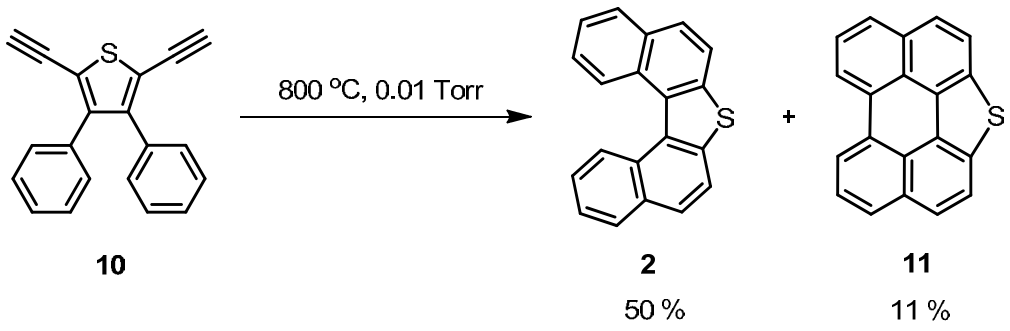

Scheme 4. Flash Vacuum Pyrolysis (FVP) of compound **10.**

The methodology was inspired by the work of Zeller, *et al.* which reported that diphenyl sulfide **12** could undergo oxidative photocyclization in the presence of iodine to

yield dibenzothiophene **13**.[11] The mechanism of this photocyclization was proposed to occur *via* the electrocyclic ring closure of diphenyl sulfide **12** followed by oxidation of cyclic intermediate **14** by iodine to provide dibenzothiophene **13** and hydrogen iodide (HI) as a by-product (Scheme 5).[11]

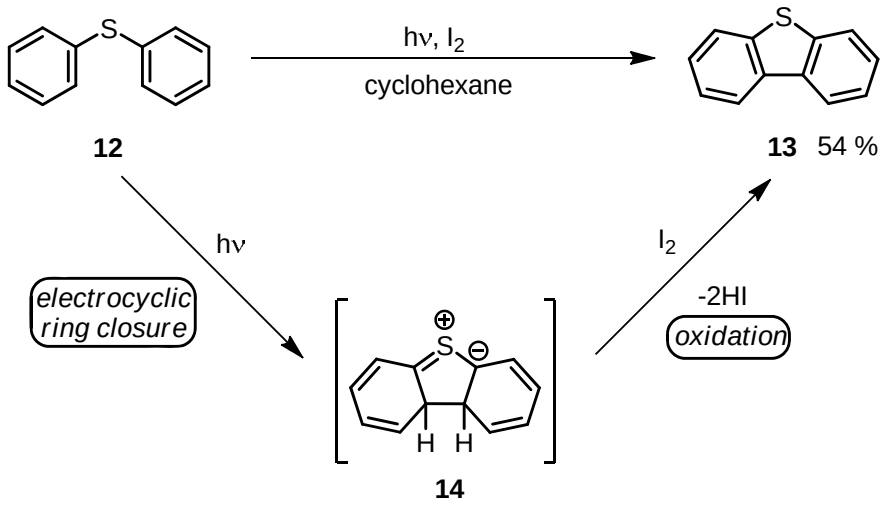

Scheme 5. Iodine-catalyzed oxidative photocyclization of diphenyl sulfide **12**.

Accordingly, this oxidative photocyclization of diphenyl sulfide **12**[11] could be an alternative approach for the synthesis of dinaphthothiophene **2** and its derivatives.

Results

The structure and our retrosynthetic strategy of dinaphtho[2,1-*b*:1',2'-*d*]thiophene **2** is as shown below (Scheme 6).

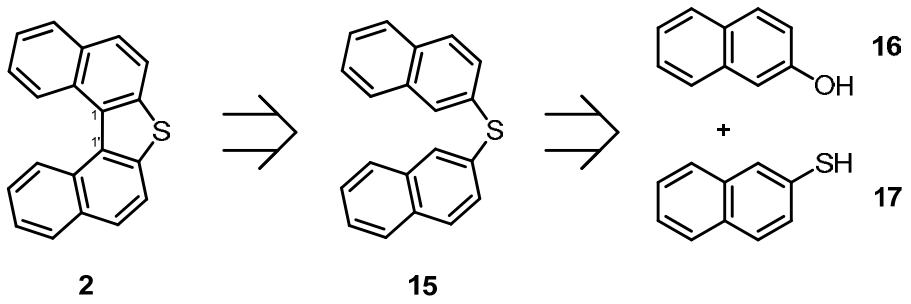

Scheme 6. The structure and retrosynthetic analysis of dinaphthothiophene **2**.

Disconnection at the C1−C1' bond of dinaphthothiophene **2** indicated that the possible precursor for the oxidative photocyclization could be dinaphthyl sulfide **15** which could be synthesized from 2-naphthol **16** and 2-naphthalenethiol **17** through the acid-mediated nucleophilic aromatic substitution.

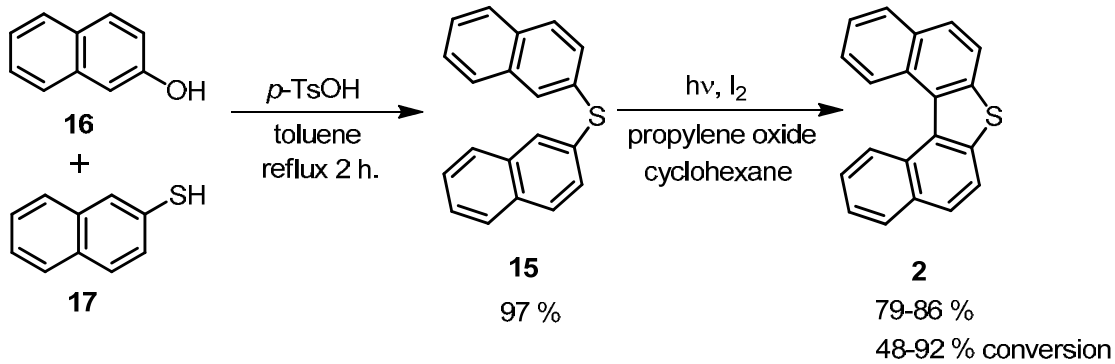

Scheme 7. The novel synthetic route of dinaphthothiophene **2**.

Thus, as shown in Scheme **7**, treatment of 2-naphthol **16** with 2-naphthalenethiol **17** in the presence of *p*-TsOH under refluxing toluene for 2 hours gave the desired dinaphthyl sulfide **15** in 97% yield.[12] The next step of this synthetic route is the iodine-catalyzed

oxidative photocyclization reaction.[11,13] The solution of disulfide **15**, iodine and propylene oxide in cyclohexane was purged with argon gas and irradiated in a photochemical reactor with Hanovia 450 watt medium pressure mercury lamp to provide dinaphthothiophene **2** in 79–86% yield (48–92% conversion). Conditions for the oxidative photocyclization process, %conversions and %yields were as summarized in Table 1.

Table 1. Iodine-catalyzed oxidative photocyclization of dinaphthothiophene **2** in various conditions.

Entry	Time (minutes)	Iodine (equivalent)	Propylene oxide (equivalent to iodine)	%conversion	%yield
1	10	1.0	10.0	48	79
2	20	1.0	10.0	80	83
3	30	1.0	10.0	87	85
4	40	1.0	10.0	89	84
5	60	1.0	10.0	88	86
6	30	0.8	10.0	86	82
7	30	1.2	10.0	91	85
8	30	1.5	10.0	92	84
9	30	1.2	0.0	80	81
10	30	1.2	5.0	90	85

Accordingly, the optimal condition for the iodine-catalyzed oxidative photocyclization of dinaphthyl sulfide **15** could be deduced. The reaction could be carried out in the presence of 1.2 equivalent of iodine and excess propylene oxide in cyclohexane under a stream of argon gas for 30 minutes (Entry 7).

The mechanism of the reaction was assumed to be similar to that reported by Zeller (Scheme 8).[11] Sulfide **15** underwent electrocyclic ring closure to provide the cyclic intermediate **18** which was then oxidized by iodine to give dinaphthothiophene **2** along with

HI as a by-product. Propylene oxide was used to consume hydrogen iodide (HI) that was formed in the reaction.[13]

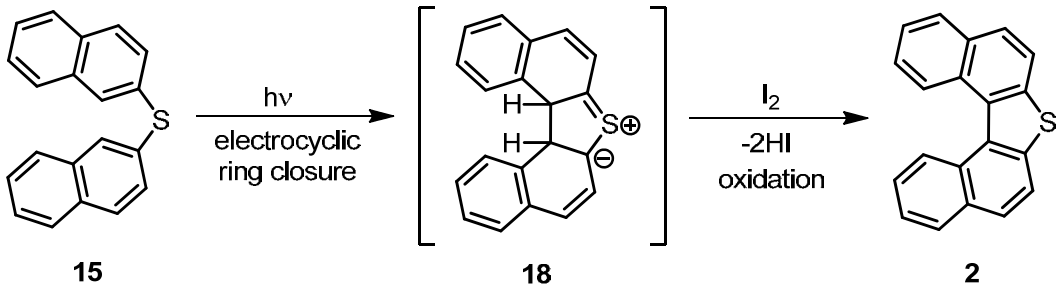

Scheme 8. The mechanism of oxidative photocyclizaion of dinaphthothiophene **2**.

Later, the oxidative photocyclization procedure was applied for the synthesis of other dinaphthothiophene derivatives **19**, **20** and **21** in 84%, 83% and 80% yields, respectively (Figure 2).

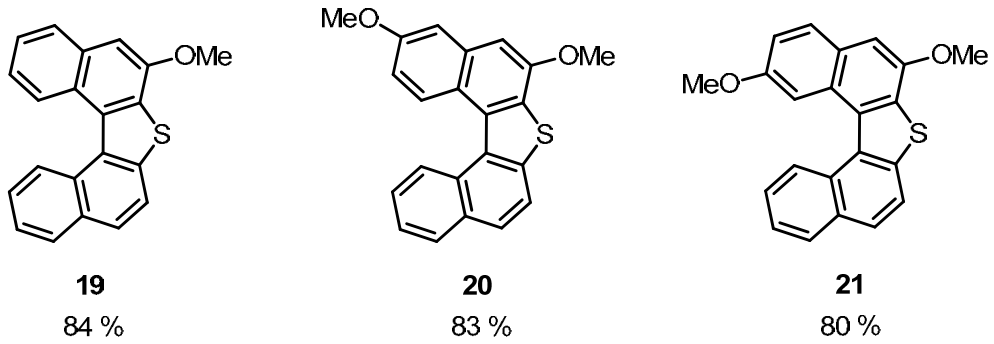

Figure 2. Oxidative photocyclizaion products **19**, **20** and **21**.

Furthermore, the oxidative photocyclization would also be used in the synthesis of a more complex skeleton such as compound **24**. Indeed, the acid-mediated nucleophilic aromatic substitution of 2,3-dihydroxynaphthalene **22** with 2-naphthalenethiol **17** in refluxing toluene provided disulfide compound **23** in 87% yield. The oxidative photocyclization of **23** then yielded compound **24** in 83% yield (Scheme 9).

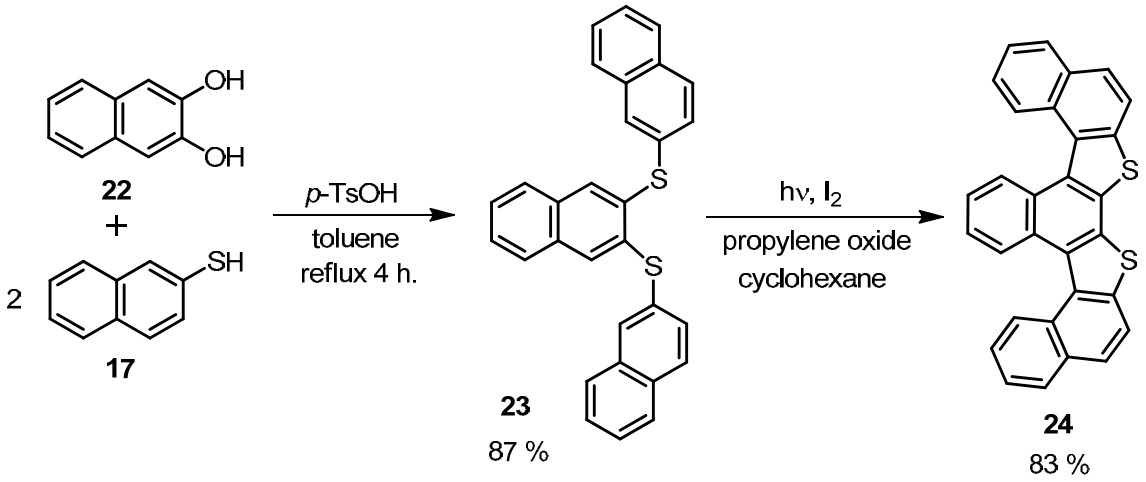

Scheme 9. The synthetic route of M-like molecule **24**.

Structure of **24** could be recrystallized from CH_2Cl_2 : MeOH providing a yellow needle crystal and its X-ray analysis was shown below (Figure 3). Detailed investigation of this molecule as a new type of organic materials is currently in progress.

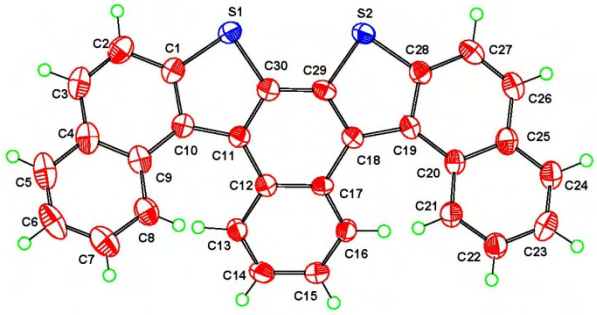

Figure 3. X-ray structure of M-like molecule **24**.

In conclusion, an alternative, highly efficient synthesis of dinaphthothiophene **2** and its analogues was achieved by using the oxidative photocyclization reaction as the key step.[14]

References

1. (a) Burroughes, J. H.; Bradley, D. D.; Brown, A. R.; Mards, R. N.; Mackay, K.; Friend, R.H.; Burns, P. L.; Holmes, A. B. *Nature*, **1990**, *347*, 539-541. (b) Kovac, J.; Peternai, L.; Lengyel, O. *Thin Solid Films*. **2003**, *433*, 22-26.
2. (a) Torrent, M. M.; Hadley, P.; Bromley, S. T.; Ribas, X.; Tarrés, J.; Mas, M.; Molins, E.; Veciana, J.; Rovira, C. *J. Am. Chem. Soc.* **2004**, *126*, 8546-8553. (b) Xia, K.; Liu, Y.; Qi, T.; Zhang, W.; Wang, F.; Gao, J.; Qui, W.; Ma, Y. ; Cui, G.; Chen, S.; Zhan, X.; Yu, G.; Qin, J.; Hu, W.; Zhu, D. *J. Chem. Soc.* **2005**, *127*, 13281-13286. (c) Yamada, H.; Kawamura, E.; Sakamoto, S.; Yamashita, Y.; Okujima, T.; Uno, H.; Ono, N. *Tetrahedron Letters*. **2006**, *47*, 7501-7504. (d) Murphy, A. R.; Frécher, J. M. *Chem. Rev.* **2007**, *107*, 1066-1096.
3. Wex, B.; Kaafarani, B.; Kirschbaum, K.; Neckors, D. C. *J. Org. Chem.* **2005**, *70*, 4502-4505.
4. Shimada, T.; Cho, Y. H.; Hayashi, T. *J. Am. Chem. Soc.* **2002**, *124*, 13396-13397.
5. Cho, Y. H.; Kina, A.; Shimada, T.; Hayashi, T. *J. Org. Chem.* **2004**, *69*, 3811-3823.
6. (a) Kitayama, K.; Uozumi, Y.; Hayashi, T. *J. Chem. Soc., Chem. Commun.* **1995**, 1533-1534. (b) Hayashi, T. *Acc.Chem. Rev.* **2000**, *33*, 354-362. (c) Hayashi, T.; Hirate, S.; Kitayama, K.; Tsuji, H.; Torii, A.; Uozumi, Y. *J. Org. Chem.* **2001**, *66*, 1441-1449.
7. Tedjamulia, M. L.; Tominaga, Y.; Castle, R. N. *J. Heterocyclic. Chem.* **1983**, *20*, 1143-1148.
8. Fabbri, D.; Delogu, G.; Lucchi, O. D. *J. Org. Chem.* **1993**, *58*, 1748-1750.
9. Bandarage, U. K.; Simpson, J.; Smith, A. J.; Weavers, R. T. *Tetrahedron.* **1994**, *50*, 3463-3472.
10. Imamura, K.; Hirayama, D.; Yoshimura, H.; Takimiya, K.; Aso, Y.; Otsubo, T. *Tetrahedron Letters.* **1999**, *40*, 2789-2792.
11. Zeller, K. P.; Petersen, H. *Synthesis.* **1975**, *8*, 532-533.
12. Charoonniyomporn, P.; Karoonnirun, O.; Thongpanchang, T.; Witayakran, S.; Thebtaranonth, Y.; Phillip, K. E. S.; Katz, T. J. *Tetrahedron Letters.* **2004**, *45*, 1343-1346.

13. Liu, L.; Yang, B.; Katz, T. J.; Poindexter, M. K. *J. Org. Chem.* **1991**. *56*, 3769-3775.
14. Sadorn, K.; Sinananwanich, W.; Areephong, J.; Nerungsi, C.; Wongma, C.; Pakawatchai, C.; Thongpanchang *Tetrahedron Lett.* **2008**, *49*, 4519-4521.

Output

งานวิจัยที่เกี่ยวข้องกับโครงการวิจัยนี้ ได้ทำการตีพิมพ์เพื่อเผยแพร่ผลงานในวารสารวิชาการดังนี้

1. Sadorn, K.; Sinananwanich, W.; Areephong, J.; Nerungsi, C.; Wongma, C.; Pakawatchai, C.; Thongpanchang *Tetrahedron Lett.* **2008**, *49*, 4519-4521.
2. Saisaha, P.; Nerungsi, C.; Iamsaard, S.; Thongpanchang, T. *Tetrahedron Lett.* **2009**, *50*, 4217-4220.
3. Sungsuwan, S.; Ruangsupapichart, N.; Prabpai, S.; Kongsaeree, P.; Thongpanchang, T. *Angewandte Chemie International Edition*, submitted for publication.

และได้มีการนำเสนอผลงานในการประชุมวิชาการระดับชาติและนานาชาติได้แก่

Sungsuwan, S.; Ruangsupapichart, N.; Thongpanchang, T. The 4th International Conference on Cutting-Edge Organic Chemistry in Asia. November 29-December 3, 2009 Thailand.

สารเตรียมอนุพันธ์ไครัลที่พัฒนาขึ้นจากโครงการวิจัยนี้ มีศักยภาพที่จะนำไปต่อยอดเพื่อช่วยในการวิจัยทางด้านเคมีผลิตภัณฑ์ธรรมชาติในวงกว้าง และมีแนวโน้มที่จะนำไปใช้ประโยชน์ในเชิงพาณิชย์ต่อไป

ภาคผนวก

Tetrahedron Letters 49 (2008) 4519–4521

Contents lists available at ScienceDirect

Tetrahedron Letters

journal homepage: www.elsevier.com/locate/tetlet

An efficient synthesis of dinaphthothiophene derivatives

Karoon Sadorn [a], Warapon Sinananwanich [a], Jetsuda Areephong [a], Chakkrapan Nerungsi [a], Chalayut Wongma [a], Chaveng Pakawatchai [b], Tienthong Thongpanchang [a,*]

[a] Department of Chemistry, Faculty of Science, Mahidol University, Rama 6 Road, Bangkok 10400, Thailand
[b] Department of Chemistry, Faculty of Science, Prince of Songkla University, Hat Yai, Songkhla 90112, Thailand

ARTICLE INFO

Article history:
Received 10 April 2008
Revised 7 May 2008
Accepted 8 May 2008
Available online 13 May 2008

ABSTRACT

A short and efficient synthesis of dinaphthothiophene and its derivatives was achieved by employing oxidative photocyclization of the corresponding dinaphthyl sulfides as a key step.

1. Introduction

Dinaphthothiophene **1** can be classified as a sulfur-containing heteroaromatic system with a unique structure. Despite its helical structure, the molecule does not exhibit optical activity due to rapid racemization at ambient temperature.[1,2] The molecule has received much attention recently due to its potential as a precursor for the synthesis of axially chiral binaphthyl derivatives, which are effective chiral building blocks in asymmetric reactions.[2,3]

A number of dinaphthothiophene syntheses have been reported in the literature as outlined in Scheme 1. For example, in chronological order, Tominaga and co-workers reported the synthesis of dinaphthothiophene derivatives via the photocyclization of **2**.[4] Later Murata et al. reported that the reaction between the lithiated binaphthyl **3** and sulfur provided dinaphthothiophene **1** in 19% yield.[5] De Lucchi et al.[6] and Smith et al.[7] reported the application of the Newman–Kwart thermal rearrangement of the dimethylthiocarbamate of binaphthol **4** to provide the desired product **1**. This approach was later improved by Hayashi and co-workers and the yield was increased to 68%.[3] In 1999, Otsubo and co-workers[8] reported an approach via the flash vacuum pyrolysis of diethynyl thiophene **5**. Finally, Matzger and co-workers[9] employed a cascade Bergman cyclization of **6** to furnish dinaphthothiophene **1** in trace amount.

Our research focuses on the development of new methodology towards helical conjugated structures.[10] Interestingly, it was reported, by Zeller and Petersen,[11] that the oxidative photocyclization of diphenyl sulfide could lead to dibenzothiophene. It was envisioned that such an approach could be applied for the direct synthesis of dinaphthothiophene **1**. Retrosynthetic disconnection at the C1–C1′ bond of dinaphthothiophene suggested that the precursor for photochemical reaction could be dinaphthyl sulfide **7** which could be derived straightforwardly from the acid-mediated nucleophilic aromatic substitution between 2-naphthol **8** and 2-naphthalenethiol **9** (Scheme 2).[12]

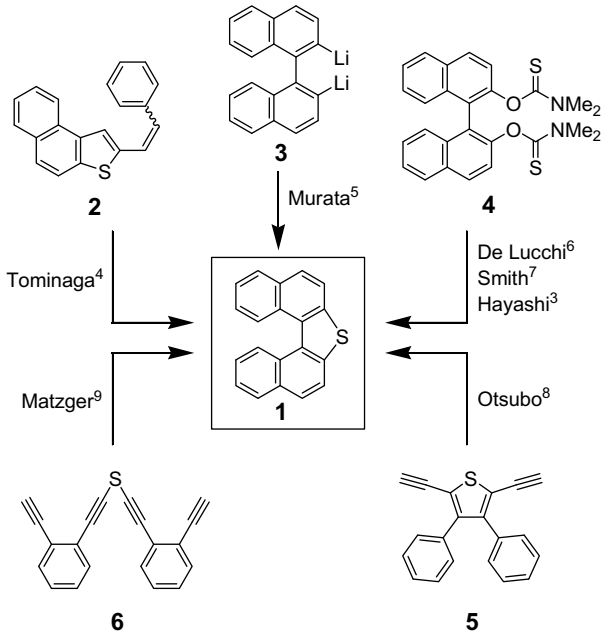

Scheme 1. Reported syntheses of dinaphthothiophene **1**.

2. Result and discussion

The reaction of 2-naphthol **8** and 2-naphthalenethiol **9** was thus carried out in the presence of *p*-TsOH in refluxing toluene for 2 h to provide the desired dinaphthyl sulfide **7** in 97% yield. The sulfide **7** was then subjected to oxidative photocyclization in the presence of I_2 and propylene oxide (PO), Scheme 3.[11,13] Conditions for the oxidative photo-cyclization process and yields are summarized in Table 1.

* Corresponding author. Tel./fax: +66 2 201 5139.
E-mail address: tettp@mahidol.ac.th (T. Thongpanchang).

0040-4039/$ - see front matter © 2008 Elsevier Ltd. All rights reserved.
doi:10.1016/j.tetlet.2008.05.045

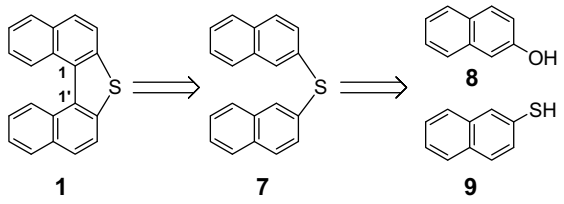

Scheme 2. Retrosynthetic analysis of dinaphthothiophene **1**.

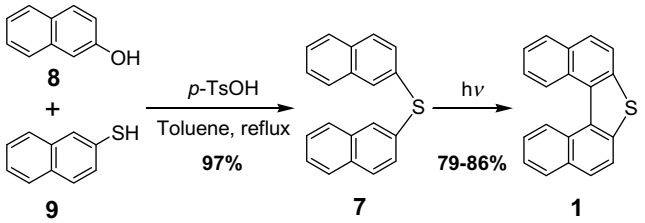

Scheme 3. Synthesis of dinaphthothiophene **1**.

Table 1
Conditions and yields of the oxidative photocyclization reaction of dinaphthyl sulfide **7**[a]

Entry	Time (min)	I_2 (equiv)	PO (equiv to I_2)	Yield % (conversion %)[b]
1	10	1.0	10.0	79 (48)
2	20	1.0	10.0	83 (78)
3	30	1.0	10.0	85 (87)
4	40	1.0	10.0	84 (89)
5	60	1.0	10.0	86 (88)
6	30	0.8	10.0	82 (86)
7	30	1.2	10.0	85 (91)
8	30	1.5	10.0	84 (92)
9	30	1.2	0.0	81 (80)
10	30	1.2	5.0	85 (90)

[a] The reaction was conducted in a 1 L Hanovia 450 W medium pressure Hg lamp photochemical reactor. All experiments were performed on 1 mmol scale at a concentration of 1 mM.
[b] The % conversion refers to the percentage of reacted starting material; the % yield refers to the percentage of the product from the reacted starting material.

It was found that a stoichiometric amount of I_2 was required for the reaction. On 1 mmol scale, the appropriate reaction time was 30 min. A shorter reaction time led to a decreased percent conversion whilst prolonged irradiation did not increase the yield and % conversion, but did result in the formation of a brownish stain on the surface of the quartz tube and reactor. Addition of propylene oxide did not significantly improve the percent yield and conversion, but it did influence the purity of the crude product.

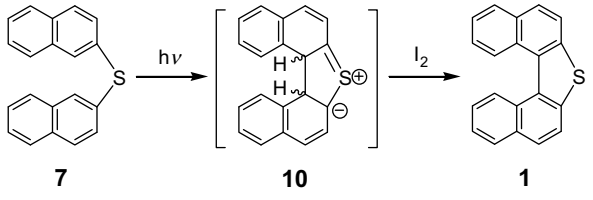

Scheme 4. Mechanism of the oxidative photocyclization.

The mechanism of the reaction is proposed to be similar to that reported by Zeller and Petersen[11] (Scheme 4). Electrocyclic ring closure of dinaphthyl sulfide **7** provided the cyclic intermediate **10** which, upon reaction with I_2, yielded the dinaphthothiophene **1**. Propylene oxide served as a HI-quencher.[13] The decreased extent of aromatic energy in naphthalene is believed to facilitate the photo-electrocyclic process and this provides a rationalization for the better yield and higher conversion when compared to the reaction of diphenyl sulfide.

This oxidative photocyclization was a very efficient and convenient procedure for the construction of other dinaphthothiophene derivatives. For example, compounds **11**, **12** and **13** could be prepared by photocyclization of their corresponding dinaphthyl sulfides in 84%, 83% and 80% yields, respectively.

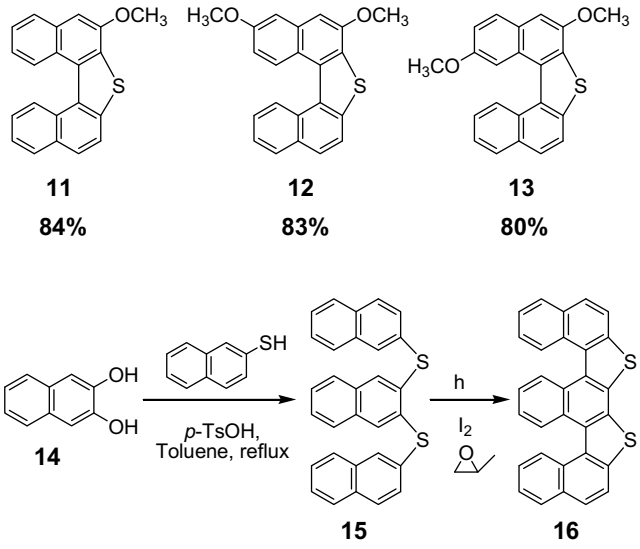

Scheme 5. Two-step synthesis of **16**.

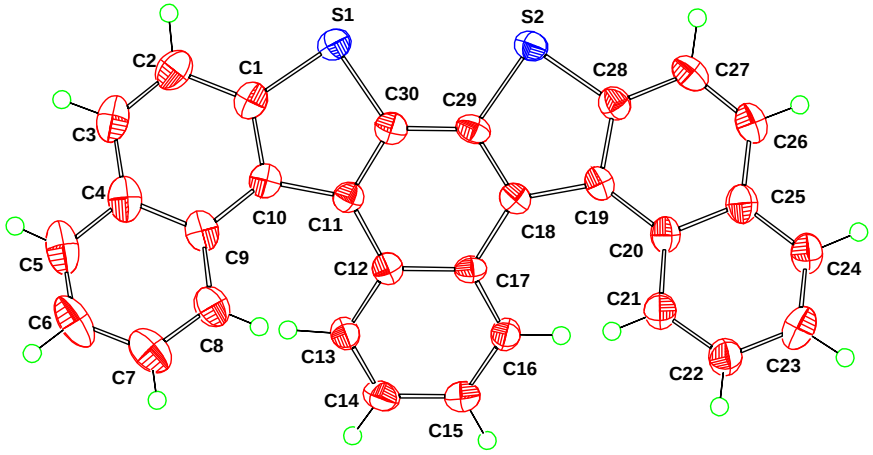

Figure 1. ORTEP diagram of compound **16**.

Compounds with complicated skeletons, such as **16**, could also be accessed via this oxidative photocyclization method. Indeed, treatment of 2,3-naphthalenediol **14** with 2-naphthalenethiol **9** in refluxing toluene in the presence of *p*-TsOH yielded **15** (87%), which upon oxidative photocyclization by the aforementioned procedure provided **16** in 83% yield (Scheme 5).

X-ray analysis of compound **16**[14] (Fig. 1) revealed an interesting structural feature where the product adopted a conformation that possessed a plane of symmetry, rather than a C_2-axis. A detailed investigation of this molecule as a new type of organic material is currently in progress.

In conclusion, an alternative synthesis of dinaphthothiophene has been described. The method is highly efficient and can be applied to the synthesis of a variety of dinaphthothiophene derivatives.

3. General procedures[15]

3.1. Synthesis of dinaphthyl sulfide 7

A solution of 2-naphthol **8** (1.24 g, 8.60 mmol) and 2-naphthalenethiol **9** (2.07 g, 12.90 mmol) in the presence of *p*-TsOH (1.64 g, 8.60 mmol) was refluxed in toluene for 2 h. The reaction was cooled down and then quenched with saturated $NaHCO_3$ solution. The mixture was then extracted with CH_2Cl_2 (3 times), and the combined organic extracts were washed with H_2O, dried over Na_2SO_4 and then evaporated to dryness. The crude product was purified by column chromatography (SiO_2, hexane as eluent) to yield dinaphthyl sulfide **7** (2.39 g, 97% yield).

3.2. Oxidative photocyclization of diaryl sulfide: synthesis of dinaphthothiophene 1

A solution of dinaphthyl sulfide **7** (300 mg, 1.05 mmol) and I_2 (320 mg, 1.26 mmol) in cyclohexane (1000 mL) was charged into a 1 L Hanovia photochemical reactor equipped with a 450 W medium pressure Hg lamp. The solution was purged with argon for 20 min. Then, propylene oxide (366 mg, 0.44 mL, 6.30 mmol) was added and the solution was irradiated for 30 min. Upon completion, the solution was evaporated to dryness and the crude product was subjected to column chromatography (SiO_2, hexane as eluent) to yield dinaphthothiophene **1** (228 mg, 85% yield, 90% conversion).

Acknowledgements

Financial support from the Thailand Research Fund (TRF-RMU4980021) and National Synchrotron Research Center (Grant 2-2549/PS01) for T.T. is gratefully acknowledged. K.S., C.N. and C.W. thank the Center for Innovation in Chemistry: Postgraduate Education and Research Program in Chemistry (PERCH-CIC), the Development and Promotion of Science and Technology Talents (DPST) program and the Royal Golden Jubilee (RGJ) program for their scholarships.

Supplementary data

Supplementary data (^1H and ^{13}C NMR spectra of compounds **1**, **7**, **11**, **12**, **13**, **15** and **16**) associated with this article can be found, in the online version, at doi:10.1016/j.tetlet.2008.05.045.

References and notes

1. Fabbri, D.; Dore, A.; Gladiali, S.; De Lucchi, O.; Valle, G. *Gazz. Chim. Ital.* **1996**, *126*, 11.
2. Shimada, T.; Cho, Y.-H.; Hayashi, T. *J. Am. Chem. Soc.* **2002**, *124*, 13396.
3. Cho, Y.-H.; Kina, A.; Shimada, T.; Hayashi, T. *J. Org. Chem.* **2004**, *69*, 3811.
4. Tedjamulia, M. L.; Tominaga, Y.; Castle, R. N.; Lee, M. L. *J. Heterocycl. Chem.* **1983**, *20*, 1143.
5. Murata, S.; Suzuki, T.; Yanagisawa, A.; Suga, S. *J. Heterocycl. Chem.* **1991**, *28*, 433.
6. Fabbri, D.; Delogu, G.; De Lucchi, O. *J. Org. Chem.* **1993**, *58*, 1748.
7. Bandarage, U. K.; Simpson, J.; Smith, R. A. J.; Weavers, R. T. *Tetrahedron* **1994**, *50*, 3463.
8. Imamura, K.; Hirayama, D.; Yoshimura, H.; Takimiya, K.; Aso, Y.; Otsubo, T. *Tetrahedron Lett.* **1999**, *40*, 2789.
9. Lewis, K. D.; Rowe, M. P.; Matzger, A. J. *Tetrahedron* **2004**, *60*, 7191.
10. Areephong, J.; Ruangsupapichart, N.; Thongpanchang, T. *Tetrahedron Lett.* **2004**, *60*, 3067.
11. Zeller, K.-P.; Petersen, H. *Synthesis* **1975**, 532.
12. Charoonniyomporn, P.; Thongpanchang, T.; Witayakran, S.; Thebtaranonth, Y.; Phillips, K. E. S.; Katz, T. J. *Tetrahedron Lett.* **2004**, *45*, 457.
13. Liu, L.; Yang, B.; Katz, T. J.; Poindexter, M. K. *J. Org. Chem.* **1991**, *56*, 3769.
14. Crystallographic data for compound **16** have been deposited with the Cambridge Crystallographic Data Centre as supplementary publication no. CCDC 680516. Copies of the data can be obtained, free of charge, on application to CCDC, 12 Union Road, Cambridge CB2 1EZ, UK (fax: +44 1223 336033; e-mail: deposit@ccdc.cam.ac.uk or via www.ccdc.cam.ac.uk/data_request/cif).
15. *Compound characterization*: *Dinaphthyl sulfide* **7**: ^1H NMR (300 MHz, $CDCl_3$, δ/ppm): 7.48–7.55 (m, 6H, Ar–H); 7.76–7.78 (m, 6H, Ar–H); 7.94 (br s, 2H, Ar–H). ^{13}C NMR (75 MHz, $CDCl_3$, δ/ppm): 133.8, 133.1, 132.3, 129.8, 128.9, 128.7, 127.7, 127.4, 126.6, 126.2. MS (EI [70 eV], *m*/*z* (%)): 286 (100) [M^+]; 252 (34) [{M−H_2S}$^+$]. CHN: Required for $C_{20}H_{14}S$: C, 83.88; H, 4.93. Found: C, 83.72; H, 4.53. Melting point 157–160 °C.
Dinaphthothiophene **1**: ^1H NMR (300 MHz, $CDCl_3$, δ/ppm): 7.60 (m, 4H, Ar–H); 7.95 (d, *J* = 8.6 Hz, 2H, Ar–H); 7.99 (d, *J* = 8.6 Hz, 2H, Ar–H); 8.06 (m, 2H, Ar–H); 8.90 (m, 2H, Ar–H). ^{13}C NMR (75 MHz, $CDCl_3$, δ/ppm): 138.5, 132.1, 131.4, 129.9, 128.6, 127.4, 126.1, 125.2, 124.8, 120.8. MS (EI [70 eV], *m*/*z* (%)): 284 (72) [M^+]. CHN: Required for $C_{20}H_{12}S$: C, 84.47; H, 4.25. Found: C, 84.92; H, 4.18. Melting point 213–216 °C.
6-Methoxy-dinaphthothiophene **11**: ^1H NMR (300 MHz, $CDCl_3$, δ/ppm): 4.20 (s, 3H, OCH_3); 7.26 (s, 1H, Ar–H); 7.47 (m, 1H, Ar–H); 7.54–7.62 (m, 3H, Ar–H); 7.93–8.07 (m, 4H, Ar–H); 8.85–8.94 (m, 2H, Ar–H). ^{13}C NMR (75 MHz, $CDCl_3$, δ/ppm): 152.5, 139.0, 134.1, 133.4, 132.2, 131.7, 131.6, 130.0, 128.6, 127.6, 127.4, 126.2, 126.0, 125.9, 125.5, 125.2, 124.8, 122.5, 121.1, 103.5, 55.9. MS (EI [70 eV], *m*/*z* (%)): 314 (100) [M^+]; 282 (60) [{M–CH_3OH}$^+$]. CHN: Required for $C_{21}H_{14}OS$: C, 80.22; H, 4.49. Found: C, 80.57; H, 4.41. Melting point 190–192 °C.
3,6-Dimethoxy-dinaphthothiophene **12**: ^1H NMR (300 MHz, $CDCl_3$, δ/ppm): 4.02 (s, 3H, OCH_3); 4.17 (s, 3H, OCH_3); 7.12 (dd, *J* = 2.69, 9.21 Hz, 1H, Ar–H); 7.18 (s, 1H, Ar–H); 7.33 (d, *J* = 2.65, 1H, Ar–H); 7.56–7.62 (m, 2H, Ar–H); 7.93 (d, *J* = 8.65 Hz, 1H, Ar–H); 7.98 (d, *J* = 8.64 Hz, 1H, Ar–H); 8.04 (m, 1H, Ar–H); 8.77 (d, *J* = 9.21 Hz, 1H, Ar–H); 8.89 (m, 1H, Ar–H). ^{13}C NMR (75 MHz, $CDCl_3$, δ/ppm): 157.4, 153.1, 139.0, 135.7, 133.5, 132.1, 131.5, 130.3, 129.2, 128.6, 127.5, 127.3, 126.0, 125.1, 124.8, 121.1, 120.9, 113.4, 107.2, 103.1, 55.9, 55.4. MS (EI [70 eV], *m*/*z* (%)): 344 (100) [M^+]; 312 (20) [{M–H_3OH}$^+$]. CHN: Required for $C_{22}H_{16}O_2S$: C,76.72; H,4.68. Found: C, 76.97; H, 4.65. Melting point 213–216 °C.
2,6-Dimethoxy-dinaphthothiophene **13**: ^1H NMR (300 MHz, $CDCl_3$, δ/ppm): 3.89 (s, 3H, OCH_3); 4.17 (s, 3H, OCH_3); 7.23–7.26 (m, 2H, Ar–H); 7.58–7.62 (m, 2H, Ar–H); 7.87 (d, *J* = 8.88 Hz, 1H, Ar–H); 7.94–8.08 (m, 3H, Ar–H); 8.18 (d, *J* = 2.27 Hz, 1H, Ar–H); 8.92 (m, 1H, Ar–H). ^{13}C NMR (75 MHz, $CDCl_3$, δ/ppm): 155.4, 151.0, 138.9, 132.5, 132.2, 132.0, 131.6, 129.7, 129.0, 128.7 (2C), 127.2, 126.7, 126.6, 125.2, 124.3, 121.1, 117.3, 106.6, 103.6, 55.9, 55.4. MS (EI [70 eV], *m*/*z* (%)): 344 (100) [M^+]. CHN: Required for $C_{22}H_{16}O_2S$: C, 76.72; H, 4.68. Found: C, 76.38; H, 4.57. Melting point 184–186 °C.
2,3-Dinaphthyl disulfide **15**: ^1H NMR (300 MHz, $CDCl_3$, δ/ppm): 7.43 (m, 2H, Ar–H); 7.48–7.55 (m, 6H, Ar–H); 7.64 (m, 2H, Ar–H); 7.74–7.80 (m, 4H, Ar–H); 7.83–7.88 (m, 4H, Ar–H); 7.93 (br s, 2H, Ar–H). ^{13}C NMR (75 MHz, $CDCl_3$, δ/ppm): 135.3, 134.0, 132.8, 132.5, 132.2, 130.9, 130.6, 129.0, 128.9, 127.8, 127.5, 127.1, 126.5, 126.3. MS (EI [70 eV], *m*/*z* (%)): 444 (75) [M^+]; 284 (100) [{M–$C_{10}H_8S$}$^+$]. CHN: Required for $C_{30}H_{20}S_2$: C, 81.04; H, 4.53. Found: C, 80.46; H, 4.52. Melting point 122–125 °C.
Compound **16**: ^1H NMR (300 MHz, $CDCl_3$, δ/ppm): 7.57 (m, 2H, Ar–H); 7.65 (m, 4H, Ar–H); 7.98 (d, *J* = 8.68 Hz, 2H, Ar–H); 8.03 (d, *J* = 8.63 Hz, 2H, Ar–H); 8.09 (m, 2H, Ar–H); 8.98 (m, 2H, Ar–H); 9.05 (m, 2H, Ar–H). ^{13}C NMR (75 MHz, $CDCl_3$, δ/ppm): 137.9, 133.3, 132.3, 131.7, 131.6, 129.7, 129.3, 128.8, 127.5, 126.4, 126.1, 125.5, 125.3, 124.7, 120.9. MS (EI [70 eV], *m*/*z* (%)): 440 (100) [M^+]. CHN: Required for $C_{30}H_{16}S_2$: C, 81.78; H, 3.66. Found: C, 81.91; H, 3.55. Melting point 316–318 °C.

Tetrahedron Letters 50 (2009) 4217–4220

Contents lists available at ScienceDirect

Tetrahedron Letters

journal homepage: www.elsevier.com/locate/tetlet

Pyridine stabilized oxiranyl remote anions

Pattama Saisaha [a], Chakkrapan Nerungsi [a], Supitchaya Iamsaard [a], Tienthong Thongpanchang [a,b,*]

[a] Department of Chemistry and Center for Innovation in Chemistry, Faculty of Science, Mahidol University, Rama 6 Road, Bangkok 10400, Thailand
[b] National Center for Genetic Engineering and Biotechnology, Thailand Science Park, Klong Luang, Patumthani 12130, Thailand

ARTICLE INFO

Article history:
Received 18 February 2009
Revised 10 April 2009
Accepted 28 April 2009
Available online 3 May 2009

ABSTRACT

The chemistry of oxiranyl remote anions derived from α,β-epoxypyridines is investigated. Deprotonation of α,β-epoxy pyridines at the β-position and reactions of the corresponding anions with a variety of electrophiles are found to be highly regioselective, possibly as a consequence of stabilization from the chelation between lithium and the pyridine moiety in the form of a five-membered cyclic intermediate.

The chemistry of oxiranyl remote anions, although in its early stage, has received significant attention due to unique and fascinating chemical characteristics and its high potential as a new approach towards substituted epoxides, which are key precursors in natural products synthesis.[1,2] As revealed in the literature, the generation of oxiranyl remote anions and their reactions can be exemplified as shown in Scheme 1. It was suggested that the stability of the anions could be promoted by chelation between lithium and the carbonyl oxygen of ketone **2**,[3] ester **4**,[1] lactone or imide **6**,[4] or the nitrogen of oxazoline **8**.[2] These groups apparently used lone pair electrons to promote anion stabilization via chelation.

Pyridine is a fundamentally important heterocyclic aromatic compound which has been used as a directing group in coordination chemistry.[5] In principle, the pyridyl group attached to an epoxide would also serve as a lithium-chelator and thus stabilize the oxiranyl remote anion **10** (Scheme 1). To further extend the chemistry and synthetic utility of the oxiranyl remote anion intermediates, we report here our investigations on the pyridine stabilized oxiranyl remote anion and its reactions with electrophiles.

In analogy to compound **1**, epoxypyridine **9** in which the stabilizing group is pyridine instead of a ketone was prepared following the reaction summarized in Scheme 2. Treatment of 2-picoline **11** with *n*-BuLi then with PhCHO gave, after dehydration, alkene **13**. Two-step epoxidation of **13** with NBS in dioxane-H_2O (2:1), followed by base-induced epoxide ring closure gave the desired product **9**.

Treatment of epoxypyridine **9** with lithium 2,2,6,6-tetramethylpiperidide (LTMP) in the presence of a variety of electrophiles, including TMSCl, EtI, MeCOMe, $MeCONMe_2$ and cyclohexanone, gave the substituted products **14a–e** in moderate[6] to good yields as shown in Table 1. The regiochemistry of the substituted products **14**, wherein H_x was abstracted and replaced by an electrophile, could be deduced by HMBC in which the key correlations were those between H_y and pyridine carbons C3, C4 and C5 (Fig. 1).

In principle, two major factors that govern the regioselectivity of the deprotonation could be envisioned; (i) α-stabilization from the phenyl group[7] and/or (ii) β-stabilization through coordination between the pyridine nitrogen and lithium in the form of a five-membered cyclic chelate (intermediate **10**, Scheme 1). To substantiate the significance of each factor, the chemistry of the oxiranyl remote anion derived from epoxypyridine **15** of which the phenyl group was relocated to the α-position of the epoxypyridine was investigated.

Epoxypyridine **15** could be prepared straightforwardly via the Corey-Chaykovsky reaction between 2-benzoylpyridine and trimethylsulfoxonium iodide.[8] Treatment of epoxy-pyridine **15** with LTMP in the presence of a variety of electrophiles including TMSCl, PhCOPh, MeCOMe and $ClCO_2Et$ yielded substituted products **16a–d** as summarized in Table 2.

Interestingly, the reaction provided the products in which the substituents were oriented regioselectively *syn* to the pyridine group as confirmed by NOESY experiments (Fig. 2). For example, in the case of **16a**, correlations between a methyl of the TMS group and H_a and H_b of the pyridine ring as well as between H_y and H_A of the phenyl ring were observed. Moreover, the observation of the disubstituted product **16d**, entry 4, could be rationalized considering that the first deprotonation–substitution occurred at H_x (via the β-anion, governed by the pyridine moiety), followed by deprotonation–substitution at H_y (via the α-anion of the ester group).

The regiochemical outcomes of the aforementioned reactions unambiguously demonstrate the significance of the chelation effect from pyridine in the induction of the regioselectivity of β-deprotonation. However, the decrease in yield compared between the reaction of compounds **9** (Table 1) and **15** (Table 2) also alludes to participation in anion stabilization of the phenyl group.

To establish that the regioselectivity of deprotonation in **9** was indeed a consequence of the stabilization effect from pyridine through chelation, *cis*-epoxide **20** was prepared. As shown in

* Corresponding author. Tel./fax:+66 2 201 5139.
E-mail address: tettp@mahidol.ac.th (T. Thongpanchang).

0040-4039/$ - see front matter © 2009 Elsevier Ltd. All rights reserved.
doi:10.1016/j.tetlet.2009.04.106

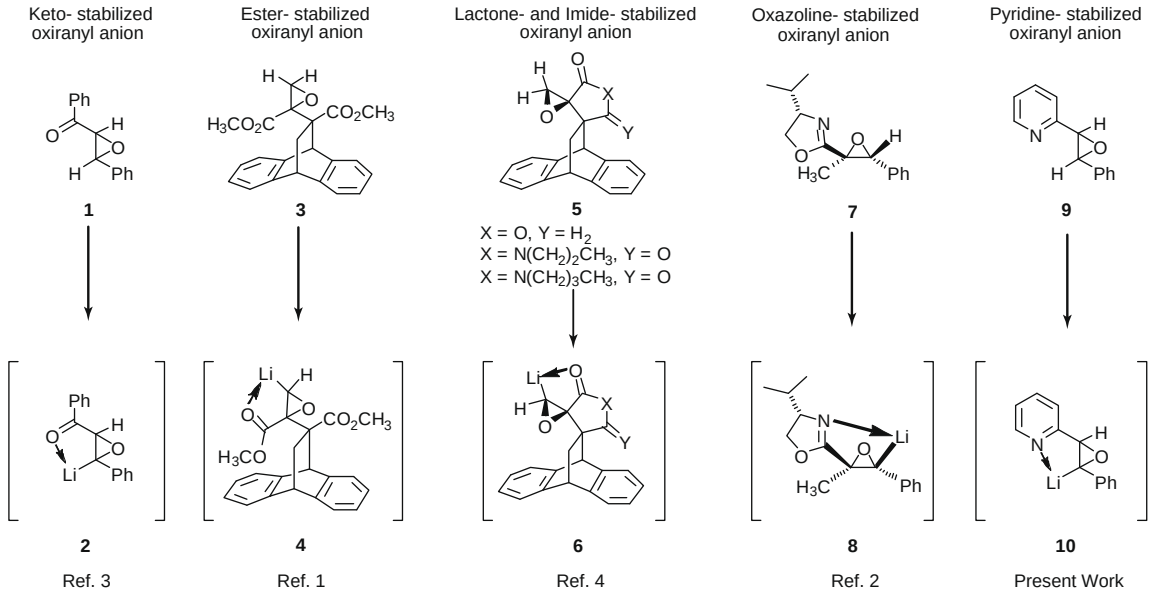

Scheme 1. Formation of remote stabilized oxiranyl anions.

Scheme 3, Wittig reaction of **18** with 2-pyridinecarboxaldehyde yielded *cis*-adduct **19** in 64% yield. Alkene **19** was then subjected to epoxidation with NBS, dioxane-H_2O (2:1) and finally, base-catalyzed epoxide ring closure, to afford the desired product **20** in 33% yield.

Treatment of epoxide **20** with LTMP and then quenching with CD_3OD yielded ketone **21** exclusively, without any deuterium incorporation (Scheme 4). The regiochemistry of the product was assigned by HMBC experiments of which correlations between the α-methylene proton and the phenyl carbons were observed exclusively (Fig. 3).

Formation of **21** could take place via a mechanism similar to that reported by Hodgson et al.,[9] as shown in Scheme 5. In this case, due to the diminishing chelation by the pyridine moiety, the regioselectivity of the deprotonation was thus influenced by the acidity of protons H_x and H_y. Because of its greater acidity,[10] proton abstraction from epoxide **20** occurred at the α-position to the pyridine group (H_y-abstraction). The lithiated species then directed the addition of LTMP to the epoxide regioselectively at the carbon adjacent to the pyridine group, leading to the epoxide ring opening to afford dianion **22**. Elimination of Li_2O from dianion **22** gave enamine **23**. Upon normal work-up, ketone **21**, in which the carbonyl group is adjacent to the pyridine group was thus obtained. This finding confirmed that the highly regioselective deprotonation at H_x of epoxypyridine **9** was the result of the chelation effect from the pyridine and lithium in the form of five-membered cyclic intermediate, instead of the acidity of protons H_x or H_y.

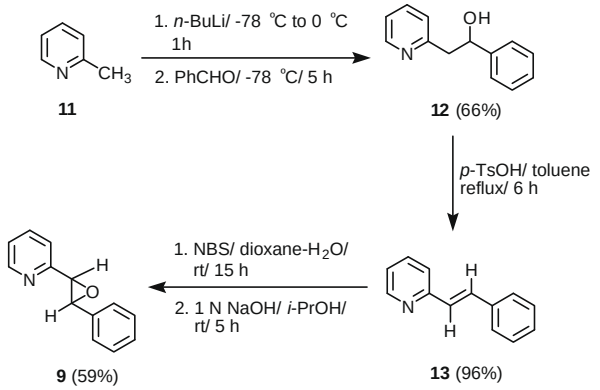

Scheme 2. Preparation of epoxypyridine **9**.

Table 1
Lithiation and substitution reactions of α,β-epoxypyridine **9**

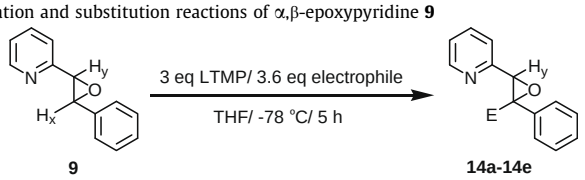

Entry	Electrophile	Product (%yield)	
1	TMSCl	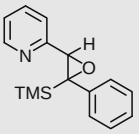	**14a** (94)
2	EtI	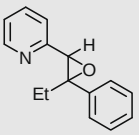	**14b** (44)
3	MeCOMe	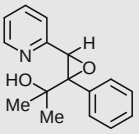	**14c** (55)
4	$MeCONMe_2$	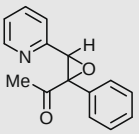	**14d** (56)
5	Cyclohexanone	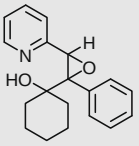	**14e** (67)

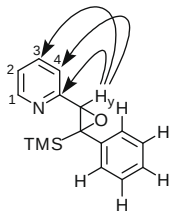

14a

Figure 1. Key HMBC correlations in compound **14a**.

Table 2
Lithiation and substitution reactions of α,β-epoxypyridine **15**

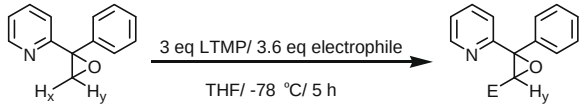

15 **16a-16d**

Entry	Electrophile	Product (%yield)		
1	TMSCl	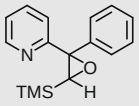	**16a**	(73)
2	PhCOPh	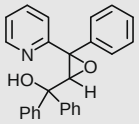	**16b**	(77)
3	MeCOMe	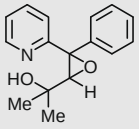	**16c**	(29)
4	$ClCO_2Et$	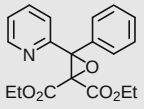	**16d**	(16)

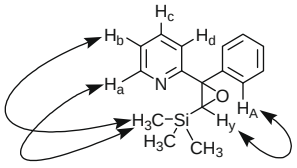

16a

Figure 2. Key NOE correlations in compound **16a**.

In conclusion, this investigation has described the highly regioselective formation of oxiranyl remote anions derived from α,β-epoxypyridines. It was also found that the stabilization from the chelation between the lithium and the pyridine moiety in the form of a five-membered cyclic intermediate played a key role in the regioselectivity. In addition, the phenyl group at the β-position of the α,β-epoxypyridine could also facilitate the formation of the oxiranyl anion, thus enhancing the yields of the substituted products.

General procedure for lithiation and substitution reactions of α,β-epoxypyridine **9**. To a solution of LTMP (1.52 mmol, generated in situ from *n*-BuLi (1.33 N in hexanes, 1.14 mL, 1.52 mmol) and

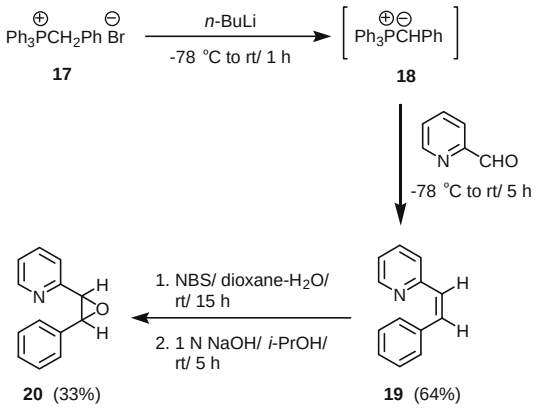

17 **18** **20** (33%) **19** (64%)

Scheme 3. Preparation of epoxypyridine **20**.

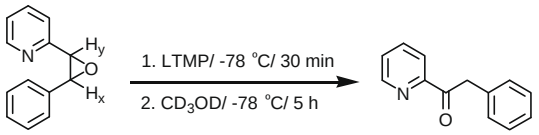

20 **21** (75%)

Scheme 4. Deprotonation of epoxypyridine **20** with LTMP.

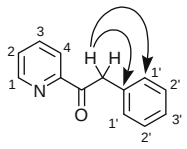

21

Figure 3. Key HMBC correlations in ketone **21**.

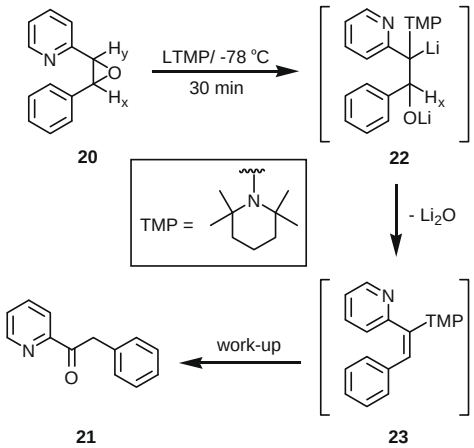

20 **22** **21** **23**

Scheme 5. Proposed mechanism for the generation of ketone **21**.

2,2,6,6-tetramethylpiperidine (0.32 mL, 1.90 mmol) in THF (7 mL)) was added a solution of *trans*-2-(3-phenyloxiran-2-yl)pyridine **9** (100.0 mg, 0.51 mmol) and freshly distilled trimethylsilyl chloride (0.23 mL, 1.82 mmol) in THF (3 mL) at −78 °C. The reaction mixture was stirred at −78 °C for 5 h before quenching with saturated ammonium chloride solution. The crude mixture was extracted with 20 mL CH_2Cl_2 thrice and the combined organic layer was washed with H_2O, dried over Na_2SO_4 and the mixture was

evaporated to dryness. Purification by preparative thin layer chromatography (SiO_2; 5% EtOAc/hexane) gave 2-(3-phenyl-3-(trimethylsilyl)oxiran-2-yl)pyridine **14a** (129.5 mg, 0.48 mmol, 94% yield) as a white solid. mp 48–51 °C. ^{1}H NMR (300 MHz, $CDCl_3$): δ −0.10 (s, 9H, $Si(CH_3)_3$), 4.24 (s, 1H, H_x), 7.32–7.39 (m, 2H, 1ArH, H_b), 7.42–7.47 (m, 2H, 2ArH), 7.53–7.59 (m, 3H, 2ArH, H_d), 7.80 (td, J = 7.68, 1.46 Hz, 1H, H_c), 8.74 (d, J = 4.87 Hz, 1H, H_a); ^{13}C NMR (75 MHz, $CDCl_3$): δ −2.0, 63.2, 65.5, 121.6, 122.6, 126.0, 126.5, 128.0, 136.1, 142.7, 148.9, 156.9; IR (cm^{-1}): 3057, 3023, 2900, 1590, 1568, 1494, 1471, 1446, 1432, 1247, 839, 776, 755, 703; exact mass: m/z [M+H$^+$] found 270.1141.

Acknowledgements

Fellowships from the Development and Promotion of Science and Technology Talents program (DPST), the Royal Golden Jubilee (RGJ) Scholarship and Post-Graduate Education and Research in Chemistry (PERCH-CIC) for P.S., C.N. and S.I. and research support from the Thailand Research Fund (RMU4980021) and from the Commission on Higher Education, Ministry of Education are gratefully acknowledged.

Supplementary data

Supplementary data (^{1}H and ^{13}C NMR spectra of compounds **9**, **14a**–**e**, **15**, **16a**–**d**, **20** and **21** are available) associated with this article can be found, in the online version, at doi:10.1016/j.tetlet.2009.04.106.

References and notes

1. Lertvorachon, J.; Thebtaranonth, Y.; Thongpanchang, T.; Thongyoo, P. *J. Org. Chem.* **2001**, *66*, 4692–4694.
2. (a) Capriati, V.; Degennaro, L.; Flavia, R.; Florio, S.; Luisi, R. *Org. Lett.* **2002**, *4*, 1551–1554; (b) Capriati, V.; Degennaro, L.; Florio, S.; Luisi, R.; Punzi, P. *Org. Lett.* **2006**, *8*, 4803–4806; (c) Florio, S.; Perna, F. M.; Luisi, R.; Barluenga, J.; Fananas, F. J.; Rodriguez, F. *J. Org. Chem.* **2004**, *69*, 9204–9207.
3. Baramee, A.; Clardy, J.; Kongsaeree, P.; Rajviroongit, S.; Suteerachanon, C.; Thebtaranonth, Y. *Chem. Commun.* **1996**, 1511–1512.
4. Chaiyanurakkul, A.; Jitchati, R.; Kaewpet, M.; Rajviroongit, S.; Thebtaranonth, Y.; Thongyoo, P.; Watcharin, W. *Tetrahedron* **2003**, *59*, 9825–9837.
5. (a) Itami, K.; Nokami, T.; Ishimura, Y.; Mitsudo, K.; Kamei, T.; Yoshida, J. *J. Am. Chem. Soc.* **2001**, *123*, 11577–11585; (b) Fort, Y.; Rodriguez, A. L. *J. Org. Chem.* **2003**, *68*, 4918–4922.
6. Aside from TMSCl, the decrease in yield could also reflect the low-compatibility nature of electrophiles with LTMP.
7. For selected references on phenyl stabilized oxiranyl anions, see: (a) Capriati, V.; Florio, S.; Luisi, R. *Chem. Rev.* **2008**, *108*, 1918–1942. and references cited therein; (b) Capriati, V.; Florio, S.; Luisi, R. *Synlett* **2005**, 1359–1369; (c) Hodgson, D. M.; Gras, E. *Synthesis* **2002**, 1625–1642; (d) Capriati, V.; Florio, S.; Luisi, R.; Salomone, A. *Org. Lett.* **2002**, *4*, 2445–2448.
8. (a) Corey, E. J.; Chaykovsky, M. *J. Am. Chem. Soc.* **1962**, *84*, 867–868; (b). *Synth. Commun.* **2003**, *33*, 2135–2143.
9. (a) Hodgson, D. M.; Bray, C. D.; Kindon, N. D.; Reynolds, N. J.; Coote, S. J.; Um, J. M.; Houk, K. N. *J. Org. Chem.* **2009**, *74*, 1019–1028; (b) Hodgson, D. M.; Bray, C. D.; Kindon, N. D. *J. Am. Chem. Soc.* **2004**, *126*, 6870–6871.
10. Although the pK_a of both H_x and H_y in this particular system has not been reported, it could be postulated, based on the pK_a of 2-methylpyridine and toluene, that H_y is more acidic than H_x Fraser, R. R.; Mansour, T. S.; Savard, S. *J. Org. Chem.* **1985**, *50*, 3232–3234.